

Understanding the nutrient sensing branch upstream of mTORC1

by

Rachel L. Wolfson

B.S. Biology  
Stanford University

Submitted to the Department of Biology in Partial Fulfillment  
of the Requirements for the Degree of

Doctor of Philosophy

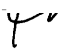
at the  
Massachusetts Institute of Technology

June 2017

© 2017 Rachel L. Wolfson. All rights reserved.

The author hereby grants to MIT permission to reproduce and to distribute publicly  
paper and electronic copies of this thesis document in whole or in part in any medium  
now known or hereafter created.

Signature redacted

Signature of Author: 

Department of Biology  
February 28, 2017

Signature redacted

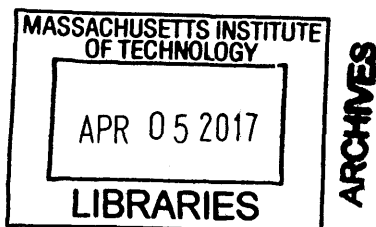
Certified by: \_\_\_\_\_

David M. Sabatini  
Member, Whitehead Institute  
Associate Professor of Biology  
Thesis Supervisor

Signature redacted

Accepted by: \_\_\_\_\_

 Amy Keating  
Professor of Biology  
Chairman, Committee for Graduate Students





# Understanding the nutrient sensing branch upstream of mTORC1

by

Rachel L. Wolfson

Submitted to the Department of Biology on April 1, 2017 in Partial Fulfillment of the Requirements for the Degree of Doctor of Philosophy at the Massachusetts Institute of Technology

## Abstract:

mTORC1 is a master regulator of cell growth that responds to diverse environmental inputs and is deregulated in human diseases, such as cancer and epilepsy. One important input to this system is amino acids, such as leucine, which require the Rag GTPases and its regulators, including GATOR1 and GATOR2, to modulate mTORC1 activity. How amino acids, specifically leucine, are directly sensed, however, was elusive for many years.

In this thesis, we first characterize the role of the Rag GTPases in follicular lymphoma. We identify recurrent, mTORC1-activating mutations in *RRAGC*, the gene that encodes RagC, in a large portion of follicular lymphoma samples (17%). These variants in RagC increase raptor binding and render cells partially insensitive to amino deprivation, implying that mTOR inhibitors may be effective therapies for these patients.

In addition, we identify Sestrin2 as the long-sought leucine sensor for the mTORC1 pathway. Sestrin2 acts as a negative regulator of the pathway that binds GATOR2 only under leucine deprivation. We find that Sestrin2 directly binds leucine at concentrations consistent with those sensed by the pathway. Further, we find that the leucine-binding capacity of Sestrin2 is required for leucine to activate mTORC1 in cells, establishing Sestrin2 as a leucine sensor for the pathway.

Finally, we identify a four-membered complex, KICSTOR (for KPTN, ITFG2, C12orf66, and SZT2-containing regulator of mTORC1), which is necessary for targeting GATOR1 to the lysosomal surface and for its interaction with its substrates, the Rag GTPases, and its potential regulator, GATOR2. Mutations in three of the components of KICSTOR are found in patients with epilepsy or brain malformation disorders, suggesting that rapalogs or other mTOR inhibitors could have some efficacy in these patients.

Thesis supervisor: David M. Sabatini

Title: Member, Whitehead Institute; Professor of Biology, MIT

## Acknowledgements

I feel incredibly fortunate to have spent the past four years surrounded by some of the most intelligent and analytical people I've ever met, spearheaded by my advisor, David Sabatini. Seeing the way that David thinks about scientific problems has inspired me to try to be more critical and think about problems more clearly. His passion for understanding the regulation of mTORC1 is evident – and encourages us all to find what motivates us. The rigor with which he approaches everything in lab and in life – from experiments to writing and beyond – has set a very high standard for the scientist that I hope to someday become. I cannot be more thankful for having had such a fabulous advisor and role model.

While David sets the tone for the lab, on a day-to-day basis it has been the incredible group of students and post-docs around me that have motivated and challenged me. I am very thankful to Alejo Efeyan, who trained me during my rotation, and to Lynne Chantranupong, my long-time collaborator and bay mate, who exemplified what it is to work hard. The two members of the lab that have had the biggest impact on me have been my other bay mates, first Zhi Tsun and then Greg Wyant. Zhi was incredibly generous in sharing his enthusiasm and his cynicism about science and everything else with me – and had a profound impact on my views. Beyond the laughter, Greg is one of the most thoughtful and humble scientists that I've ever met – I feel very fortunate that he's become one of my closest friends.

Over my time in the lab, I've had the pleasure of working with a number of talented rotation students who then went on to be my collaborators, colleagues, and good friends in the lab, including Bobby Saxton, Jose Orozco, Xin Gu, and Kendall Condon. I am also very thankful to Shuyu Wang, Kuang Shen, Tim Wang, and Hank Adelman, who, along with all those previously mentioned, set the tone for an incredibly fun and stimulating place to do science in “the first two rooms” of the Sabatini lab. We would not, however, have been able to be so productive without Kathleen Ottina keeping us in line or Edie Valeri and Danica Rili keeping us organized.

Outside of the lab, I have been supported by many other scientists and programs. I am very thankful to the members of my thesis committee, Iain Cheeseman and Bob Sauer, for their helpful insight over the years, and to Brendan Manning for serving on my thesis defense committee. I am also thankful to my various programs (MIT Biology, HST, and the MD/PhD program) for their support over the years. My classmates from these programs – specifically those from HST and the MD/PhD program – are almost like siblings to me. Without their support, our constant text messaging streams, or our Monday “Science Lunches” I would not have made it through the program as quickly or happily.

Without the encouragement and constant love from my group of best friends, I cannot imagine where I would be. Allison McCann, Meg Hostage, Morgan Redman, Ashley Aruffo, and Leslie Foard have been there for me at every turn – whether by text, google hangout, or for a quick trip, they have listened to my complaints, celebrated my achievements, read my papers, and even listened to my practice talks. Beyond that, we have simply had a lot of fun times; spending time with them was the perfect distraction from hard times in the lab.



I would also like to thank my in laws, Zhibao Mi and Xiaoli Lu, for welcoming me into their family and supporting Mike and I in our new life together.

For my entire life, I have been incredibly lucky to be supported and inspired by my family. My sister, Anna Wolfson, has served as my role model since I was young. Almost everything I do today, from running to medicine, is in large part because of her and to this day Anna inspires me to be a better version of myself. She and Scott Allen have also been great role models for Mike and me, and we couldn't be more thankful to have them living here in Boston with us. We are the most fortunate that they live here, though, because of all the time we've been able to spend with our amazing niece, Claire, whose smiles have brightened our lives.

Of course, along with my sister, my parents have supported me throughout every stage of my training (and life!). My mom's endless patience and understanding have, over many phone calls, gotten me through the difficult times that inevitably occur during the PhD. My dad has always inspired me to tackle more difficult questions and to hold myself to the highest standard. They both have worked so hard to set me up for the best life possible and have inspired me in their dedication to our family and to their careers.

Finally, I am very lucky to have met and married Mike Mi over the course of my time in the MD/PhD program. Mike has shown endless patience for the long days in lab and as acting as a sounding board throughout my PhD. He challenges me to think more critically about how the world works, and our conversations have led to many epiphanies (and laughs!). I cannot imagine having gone through this without his support and love.

## Table of Contents

|                        |   |
|------------------------|---|
| Abstract .....         | 3 |
| Acknowledgements ..... | 4 |

### CHAPTER 1: Introduction

|                                                                                             |    |
|---------------------------------------------------------------------------------------------|----|
| Introduction.....                                                                           | 8  |
| The discovery of mTOR.....                                                                  | 8  |
| mTORC1 and mTORC2.....                                                                      | 9  |
| mTORC2.....                                                                                 | 9  |
| mTORC1.....                                                                                 | 10 |
| mTORC1 signaling <i>in vivo</i> .....                                                       | 17 |
| Deregulation of mTORC1 signaling in disease .....                                           | 19 |
| mTOR pathway component mutations in cancer .....                                            | 19 |
| mTOR inhibitors as cancer therapy .....                                                     | 20 |
| mTORC1 pathway component mutations in epilepsy and other brain malformation disorders ..... | 22 |
| Rapalogs for tuberous sclerosis therapy .....                                               | 24 |
| Preface for work presented in this thesis .....                                             | 25 |
| References .....                                                                            | 28 |

### CHAPTER 1 APPENDIX: Nutrient Sensing Mechanisms Across Evolution

|                                                    |    |
|----------------------------------------------------|----|
| Nutrient Sensing Mechanisms Across Evolution ..... | 35 |
| Abstract .....                                     | 36 |
| Introduction .....                                 | 37 |
| Prokaryotes .....                                  | 39 |
| Eukaryotes .....                                   | 46 |
| Perspectives .....                                 | 68 |
| References .....                                   | 70 |

### CHAPTER 2: Recurrent mTORC1-activating *RRAGC* mutations in follicular lymphoma

|                  |     |
|------------------|-----|
| Abstract .....   | 95  |
| Results.....     | 96  |
| References ..... | 121 |
| Methods.....     | 124 |
| References ..... | 130 |

### CHAPTER 3: The Sestrins interact with GATOR2 to negatively regulate the amino acid sensing pathway upstream of mTORC1

|                   |     |
|-------------------|-----|
| Abstract .....    | 132 |
| Introduction..... | 133 |
| Results.....      | 134 |

|                                            |     |
|--------------------------------------------|-----|
| Discussion .....                           | 152 |
| Experimental Procedures .....              | 154 |
| References .....                           | 158 |
| Supplemental Experimental Procedures ..... | 162 |
| Supplemental References .....              | 165 |

**CHAPTER 4: Sestrin2 is a leucine sensor for the mTORC1 pathway**

|                             |     |
|-----------------------------|-----|
| Abstract .....              | 167 |
| Introduction .....          | 168 |
| Results .....               | 169 |
| Conclusions .....           | 184 |
| References .....            | 187 |
| Materials and Methods ..... | 190 |

**CHAPTER 5: KICSTOR recruits GATOR1 to the lysosome and is necessary for nutrients to regulate mTORC1**

|                  |     |
|------------------|-----|
| Abstract .....   | 200 |
| Results .....    | 201 |
| References ..... | 227 |
| Methods .....    | 230 |

**CHAPTER 6: Future Directions and Discussion**

|                                                                             |     |
|-----------------------------------------------------------------------------|-----|
| The role of RagC mutations in follicular lymphoma tumorigenesis .....       | 243 |
| Amino acid sensing by the mTORC1 pathway .....                              | 244 |
| Understanding the mechanism through which the Sestrins inhibit GATOR2 ..... | 246 |
| Regulation and function of the KICSTOR complex .....                        | 246 |
| mTOR inhibitors as therapy for epilepsy patients .....                      | 247 |
| References .....                                                            | 248 |

## CHAPTER 1

### Introduction

Cell growth is an energy and resource dependent process that is highly regulated. Cells must only grow in the presence of ample nutrients and growth factors and in the absence of any cellular stresses. This process is controlled, at least in part, by the mechanistic target of rapamycin complex 1 (mTORC1). mTORC1 is serine threonine kinase that responds to a diverse set of environmental inputs. Under the correct environmental conditions, mTORC1 phosphorylates substrates that potentiate anabolic processes, such as mRNA translation, and inhibit catabolic ones, such as autophagy. This pathway is deregulated in a variety of diseases, including cancer, epilepsy, and diabetes, and thus understanding the molecular underpinnings of this pathway will be essential for potential therapeutic intervention for these and other illnesses.

### The discovery of mTOR

mTORC1 was originally identified as the target of rapamycin, a potent, lipophilic macrolide. Rapamycin was isolated from a strain of *Streptomyces hygroscopicus* found in a soil sample on Easter Island, also known as Rapa Nui, in the 1970s. Subsequent antibiotic screening at Ayerst Research Laboratories revealed that rapamycin is a potent antifungal growth agent, but does not inhibit bacterial growth (Abraham and Wiederrecht, 1996). Upon further testing it was found that rapamycin also has antigrowth properties in mammalian cells, specifically human cancer and immune cells (Eng et al., 1984), establishing it as an important antigrowth agent from yeast to mammals.

Given the potent antiproliferative effects of rapamycin, many sought to identify its molecular target. Rapamycin exhibits its antiproliferative effects in complex with FK506-binding protein 12 (FKBP12), a peptidylprolyl cis-trans isomerase (PPIase). Two groups used screens in yeast to find that mutations in the genes TOR1 and TOR2 participate in sensitivity to rapamycin (named for Target of Rapamycin) (Heitman et al., 1991; Koltin

et al., 1991). Biochemical studies were performed to identify the mammalian protein target of the FKBP12-rapamycin complex, named mTOR (mammalian target of rapamycin) (Brown et al., 1994; Sabatini et al., 1994; Sabers et al., 1995). mTOR is the only homologue of the two TOR1 and TOR2 genes in *S. cerevisiae*.

## **mTORC1 and mTORC2**

mTOR is a serine-threonine kinase that nucleates two separate complexes in mammalian cells – mTORC1 and mTORC2. These two complexes have different drug sensitivities, regulators, and downstream effectors.

### **mTORC2**

mTORC2 is the largely rapamycin-resistant mTOR-containing complex. It has seven components, four of which are shared between the two mTOR complexes: mTOR, mammalian lethal with sec-13 protein 8 (mLST8, also known as GβL), DEP domain containing mTOR-interacting protein (DEPTOR), and the Tti1/Tel2 complex. Three of its subunits, rapamycin-insensitive companion of mTOR (riCTOR), mammalian stress-activated map kinase-interacting protein 1 (mSin1), and protein observed with rictor 1 and 2 (protor1/2), are specific to mTORC2 (Laplante and Sabatini, 2012). mTORC2 is the mammalian counterpart of the complex nucleated by yeast TOR2, named TORC2. TORC2 contains, along with TOR2, AVO1 (homologous to mSin1), AVO2, and AVO3 (homologous to rictor) (Loewith et al., 2002). Depletion of TORC2 or mTORC2 components leads to defects in the cytoskeleton (Jacinto et al., 2004).

mTORC2 acts as a serine threonine kinase for at least three distinct substrates: protein kinase B (PKB, also known as Akt), serum- and glucocorticoid-induced protein kinase 1 (SGK1), and protein kinase C-α (PKC-α). Akt is a serine-threonine kinase that controls multiple aspects of cellular metabolism, notably growth-factor responsiveness upstream of mTORC1. For years, it was known that Akt needed to be phosphorylated on two sites, threonine 308 and serine 478, to fully induce its kinase activity.

Phosphoinositide-dependent kinase 1 (PDK1) phosphorylates Akt at threonine 308 in

response to growth factor availability downstream of phosphoinositide 3-kinase (PI3K), while mTORC2 is the kinase responsible for phosphorylating Akt at serine 478. This finding established mTORC2 as an important growth-regulatory kinase, although how PI3K signaling activates mTORC2 remains unclear (Sarbasov et al., 2005). Recent work has shed insight into this question, and suggests that phosphatidylinositol-3,4,5-trisphosphate (PIP<sub>3</sub>), the product of PI3K activity, binds to mSin1 and thereby releases its inhibition of mTORC2 (Liu et al, 2015). In addition to Akt, mTORC2 phosphorylates and activates SGK1, a kinase involved in ion transport and growth (García-Martínez and Alessi, 2008), and PKC- $\alpha$ , a kinase involved in cytoskeletal organization (Jacinto et al., 2004; Sarbasov et al., 2004).

## **mTORC1**

In comparison to mTORC2, the regulation and outputs of mTORC1 are much better understood. Along with the four shared components with mTORC2, mTORC1 also contains regulatory-associated protein of mammalian target of rapamycin (raptor) and proline-rich Akt substrate 40 kDa (PRAS40) (Laplante and Sabatini, 2012). mTORC1 is a master regulator of cell growth that controls a variety of downstream outputs that lead to cell growth. mTORC1 controls translation through phosphorylating and activating eukaryotic translation initiation factor 4E (eIF4E)-binding protein 1 (4E-BP1) and S6 kinase 1 (S6K1). The phosphorylation of 4E-BP1 blocks its ability to bind to and inhibit the cap-binding protein eIF4E. This frees eIF4E to form the eIF4F complex and initiate translation. Phosphorylation of S6K1 stimulates it to phosphorylate its substrate, the ribosomal protein S6, thereby promoting translation initiation and elongation (Laplante and Sabatini, 2012).

Another key process downstream of mTORC1 is the control of lipid synthesis, which is important for proliferating cells to make membranes. mTORC1 controls this process primarily through the transcription factors sterol regulatory element-binding protein 1/2 (SREBP1/2), which control the expression of fatty acid and cholesterol synthesis genes. SREBP1/2 reside on the ER membrane in an inactive form, and with certain stimuli are proteolytically cleaved such that an active form of the transcription

factors can travel into the nucleus to stimulate transcription of target genes. Inhibition of mTORC1, such as low growth factor availability, leads to decreased expression and proteolytic processing of SREBP1/2, thereby decreasing the expression of genes involved in lipid synthesis (Laplante and Sabatini, 2009).

In addition to stimulating protein and lipid synthesis, mTORC1 also suppresses autophagy, the lysosomal-based degradative process required for recycling of cellular components. mTORC1 directly phosphorylates and inhibits the kinase responsible for initiating autophagy, ULK1/Atg13/FIP200 (unc-51-like kinase 1/mammalian autophagy-related gene 13/focal adhesion kinase family-interacting protein of 200 kDa) (Ganley et al., 2009; Hosokawa et al., 2009; Jung et al., 2009). In this way, when nutrients and growth factors are abundant, mTORC1 inhibits the recycling of cellular materials. Conversely, under nutrient deprivation, mTORC1 is inhibited, which stimulates autophagy and allows for the reuse of old organelles and other cellular materials under these conditions.

Finally, inhibition of mTORC1 also stimulates lysosomal biogenesis, along with autophagy. mTORC1 controls the production of lysosomes by phosphorylating the transcription factor EB (TFEB), which controls the expression of genes involved in lysosomal function. This phosphorylation prevents TFEB entry into the nucleus, thereby inhibiting lysosomal biogenesis when mTORC1 is active (Settembre et al., 2012).

Through phosphorylating substrates that potentiate anabolic processes, such as mRNA translation and lipid synthesis, and inhibit catabolic ones, such as autophagy and lysosomal biogenesis, mTORC1 acts as a central controller of cell growth. Its activity, however, must be coordinated in response to a variety of environmental inputs such that cell growth only occurs under the proper conditions.

### **Upstream inputs to mTORC1**

A variety of environmental signals, including nutrient levels, growth factor availability, and cellular stresses, impinge on mTORC1 to coordinate its activity. Most of these, including growth factors and stresses, funnel through the tuberous sclerosis complex (the TSC complex), which is composed of TSC1, TSC2, and TBC1D7 (Dibble

et al., 2012). The TSC complex acts as a GTPase activating protein (GAP) for the small GTPase Ras homologue enriched in brain (Rheb), which resides on the lysosomal surface and acts as an essential kinase activator for mTORC1 (Inoki et al., 2002; Manning et al., 2002; Potter et al., 2002). How activity of the TSC complex is controlled is most clear in the case of growth factor availability, but a variety of stresses appear to feed in upstream of this complex as well.

Growth factors, such as insulin, first bind their receptors, which are receptor tyrosine kinases, on the outside of the cell. This binding triggers the recruitment of insulin receptor substrate 1 (IRS1), which activates PI3K, a heterotrimeric lipid kinase, to the plasma membrane, where it comes into contact with its substrate, phospholipid phosphatidylinositol-4,5- bisphosphate (PI-4,5-P<sub>2</sub>). PI3K catalyzes the phosphorylation of its substrate to form phosphatidylinositol-3,4,5-trisphosphate (PIP<sub>3</sub>). An important negative regulator of the pathway, phosphatase and tensin homolog deleted on chromosome 10 (PTEN), reverses this reaction and therefore resets the PI3K signaling pathway (Sengupta et al., 2010).

PIP<sub>3</sub> on the inside of the plasma membrane recruits Akt to this subcellular localization through binding its pleckstrin homology (PH) domain. Akt is activated by two separate phosphorylation events mentioned previously. One of these events, at threonine 308, is catalyzed by PDK1, another PH-domain containing kinase that is also concentrated at the plasma membrane by PIP<sub>3</sub> (Sengupta et al., 2010). Additionally, Akt is phosphorylated at serine 478 by mTORC2 (Sarbasov et al., 2005). Both of these events are necessary for full activation of Akt. As mentioned previously, how mTORC2 is regulated downstream of PI3K is unclear.

Activation of Akt stimulates its kinase activity, and it phosphorylates its substrate, TSC2, part of the TSC complex, which stimulates its translocation off the lysosomal surface (Menon et al., 2014). With its GAP no longer localized to the lysosomal surface, Rheb, which resides in this compartment, becomes GTP-loaded and, under this conformation, can act as an essential kinase activator of mTORC1, but only if mTORC1 is properly localized to the lysosomal surface (**Figure 1**).

Beyond growth factors via the PI3K/Akt pathway, multiple other inputs control mTORC1 activity upstream of the TSC complex. For example, growth factors also feed



in via the Ras-Raf-MEK (Mitogen-activated protein kinase kinase) pathway to activate extracellular signal-regulated kinase (ERK) and ribosomal s6 kinase (RSK) to directly phosphorylate and inactivate the TSC complex (Shaw and Cantley, 2006). In addition, energy stress (i.e. imbalances in the ATP:ADP ratio caused by glucose deprivation or mitochondrial inhibition) directly stimulate 5' AMP-activated protein kinase (AMPK) and GSK3 to phosphorylate and activate TSC2, thereby inhibiting Rheb (Zoncu et al., 2011). Other stresses, such as hypoxia and DNA damage, are thought to inhibit the pathway upstream of the TSC complex, but the exact mechanisms are unknown. Unlike phosphorylation of TSC2 by Akt in response to growth factors, how these other phosphorylation events regulate the TSC complex is not entirely clear, and may not be by controlling its subcellular localization.

Most of the environmental signals to mTORC1, such as growth factors and cellular stresses, impinge on the TSC complex and thus control the nucleotide loading state of Rheb, the essential kinase activator of mTORC1. However, Rheb can only activate mTORC1 if mTORC1 is properly localized to the lysosomal surface, and this localization is controlled by the availability of nutrients through the Ras-related GTPases (Rags) (Sancak et al., 2008).

The Rags are unique GTPases that function as a heterodimer of the highly related and functionally redundant RagA or B bound to RagC or D, which are also very similar. The presence of nutrients, such as amino acids and glucose, renders RagA/B in a GTP-loaded conformation, while RagC/D becomes GDP-loaded. This conformation of the Rags stimulates mTORC1 translocation to the lysosomal surface, where it can come into contact with its activator, Rheb. In this way, the Rag and Rheb GTPases establish an elegant “coincidence detector” system, such that only in the presence of both nutrients and growth factors is mTORC1 active, thereby stimulating cell growth (Sancak et al., 2008) (**Figure 1**).

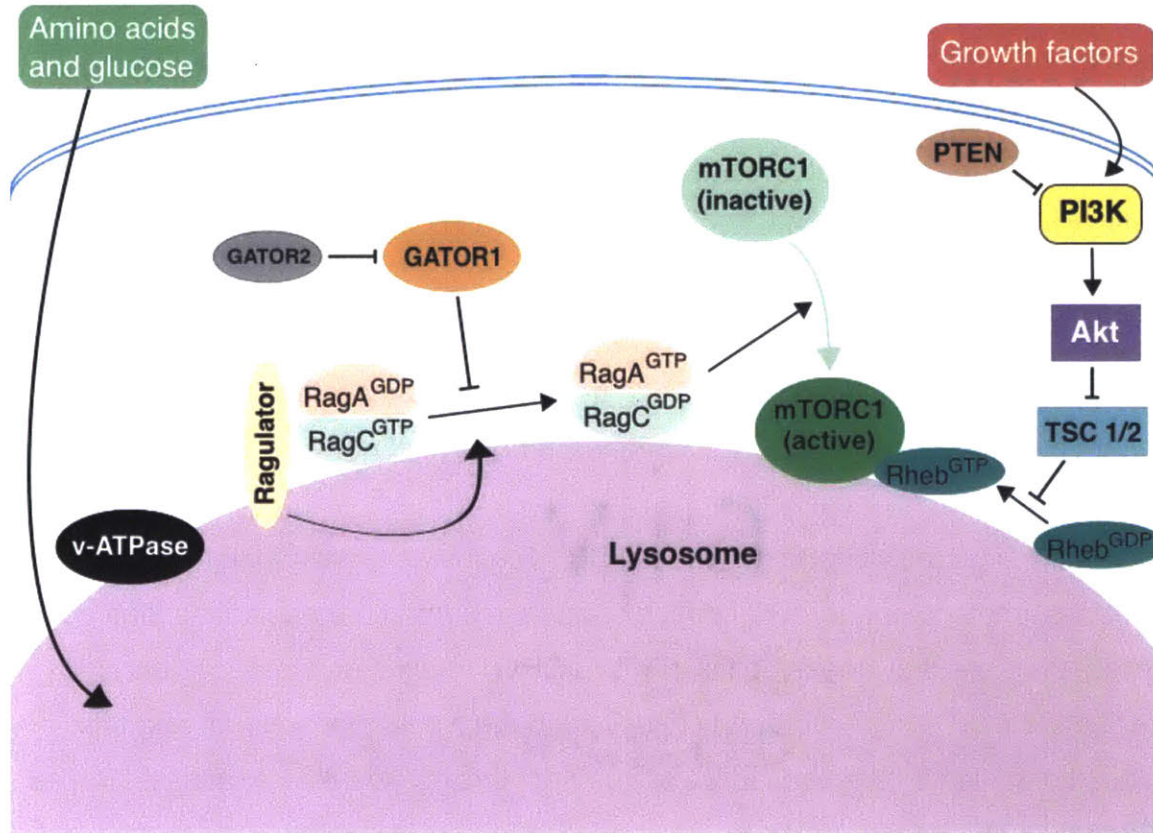


**Figure 1: Model for amino acid and growth factor induced stimulation of mTORC1.** Growth factors activate mTORC1 through a signaling pathway that involves PI3K, Akt, and the TSC complex. Amino acids and glucose activate mTORC1 through a pathway that impinges on the Rag GTPases. When amino acids are present, RagA/B is in a GTP-bound state and (in combination with RagC/D) recruits mTORC1 to the lysosomal surface, where it can come into contact with its activator Rheb. GATOR1 acts as a GAP for RagA/B.

### The nutrient sensing pathway upstream of mTORC1

How nutrients, specifically amino acids, control mTORC1 activity upstream of the Rag GTPases has been an area of intense interest for the past decade. Immunoprecipitation followed by mass spectrometry (IP/MS) by our lab and others has

allowed for the identification of a number of regulators of the Rag GTPases. The pentameric Ragulator complex, composed of p18, p14, HBXIP, C7orf59, and MP1, was the first of these regulators identified (Sancak et al., 2010). The p18 component of Ragulator has a lipidation modification that is necessary for docking the Rag GTPases on the lysosomal surface (Sancak et al., 2010). In addition, Ragulator modulates the nucleotide loading of the Rags, by acting as a guanine exchange factor (GEF) for the Rag GTPases (Bar-Peled et al., 2012).

Ragulator also interacts with two transmembrane components, the vacuolar H<sup>+</sup>-adenosine triphosphate ATPase (v-ATPase) and SLC38A9, both of which, like Ragulator, act as positive regulators of the pathway (Wang et al., 2015; Zoncu et al., 2011). The discovery of a lysosomal transmembrane complex, namely the v-ATPase, as a positive regulator of the pathway led to the hypothesis that amino acids within the lysosome may stimulate mTORC1 activity. Indeed, this is the case, as isolated lysosomes can be loaded with amino acids and this is sufficient for recruitment of mTORC1 *in vitro* (Zoncu et al., 2011). Although it is clear that the ATPase activity of the v-ATPase is necessary for mTORC1 activation by intra-lysosomal amino acids, the molecular mechanism through which the v-ATPase controls mTORC1 activity remains unknown (Zoncu et al., 2011) (**Figure 1**).

More clarity into how amino acids within the lysosome are sensed by the mTORC1 machinery on the cytosolic side of this organelle came with the identification of SLC38A9 as a putative arginine sensor for the pathway (Wang et al., 2015). SLC38A9 was a previously uncharacterized protein with weak homology to amino acid transporters that localizes specifically to lysosomal membranes. Unlike other transporters in its class, SLC38A9 is unique in that it has a 119 amino acid extension on its N-terminus, through which it interacts with Ragulator. Overexpression of full length SLC38A9 or simply this 119 amino acid Ragulator binding domain is sufficient to render cells insensitive to amino acid deprivation, establishing SLC38A9 as a positive regulator of the pathway that likely controls mTORC1 signaling through this extension on its N-terminus. Cells lacking SLC38A9 are defective in their activation of mTORC1 signaling in response to amino acids, specifically arginine. This led to the hypothesis that SLC38A9 may function as an arginine sensor for the pathway. Indeed, SLC38A9 binds

and transports arginine with a Michaelis constant ( $K_m$ ) of ~39 mM, and has some selectivity for arginine (and similar amino acids) over others (Wang et al., 2015). However, the arginine binding capacity of SLC38A9 has not been connected to its effects on mTORC1 signaling, and thus, it remains a putative arginine sensor for the pathway.

In addition to Ragulator, multiple other components have been identified that modulate the nucleotide loading state of the Rag GTPases. Folliculin (FLCN), along with its binding partners folliculin interacting protein 1/2 (FNIP1/2), have GAP activity for RagC/D and therefore act as positive regulators of the pathway (Tsun et al., 2013). In addition, the trimeric GATOR1 complex (which stands for GAP activity toward Rags), composed of DEP domain containing protein 5 (DEPDC5) and nitrogen permease-like regulator 2 and 3 (Npr12 and 3), acts as a GAP for RagA/B and important negative regulator of the pathway (Bar-Peled et al., 2013). Finally, GATOR2 is a GATOR1-interacting, pentameric complex composed of missing in oocytes (Mios), WD-repeat containing protein 24 (WDR24), WDR59, Seh1L, and Sec13. GATOR2 acts a positive regulator of the pathway in a manner that is epistatic to GATOR1, indicating that it acts upstream or parallel to its interacting partner (Bar-Peled et al., 2013). The molecular function of GATOR2, however, is unknown.

For many years, a variety of regulators of this pathway were identified, but none of these, with the exception of SLC38A9, had any amino acid binding capacity. Additionally, although not all amino acids modulate the pathway to the same extent, along with arginine, leucine was known to be of particular importance. The identity of the leucine sensor, however, remained elusive.

### **Leucine sensing upstream of mTORC1**

The connection between amino acids and mTORC1 has long been appreciated. Early work was performed using single amino acid dropouts across multiple cell types and, through monitoring S6K1 or 4E-BP1 phosphorylation, defined leucine and arginine as being particularly important to the pathway (Blommaert et al., 1995; Hara et al., 1998). Restimulation of adipocytes with various leucine analogues lead to the

conclusion that leucine activated the pathway in a dose-dependent manner, that similar amino acids such as isoleucine and valine did not have the same effects, and that the stimulation by leucine was stereospecific (Fox et al., 1998). Interestingly, it was noted that  $\alpha$ -ketoisocaproate ( $\alpha$ -KIC), a metabolite of leucine, could substitute for it, but only in the presence of the enzyme that converts  $\alpha$ -KIC to leucine, indicating that leucine may indeed be the metabolite that is directly sensed by the pathway (Fox et al., 1998). Further work identifying how leucine analogues activate the mTORC1 pathway helped rule out the theory that leucyl-tRNA synthetase (LRS) was the elusive leucine sensor for the pathway, as the mTORC1 pathway was responsive to leucine analogues that do not bind LRS (Lynch et al., 2000). Thus, while it was clear for years the mTORC1 pathway senses leucine, the molecular identity of the leucine sensor remained elusive.

### **Effects of leucine *in vivo***

Leucine and the other branched chain amino acids are unique in that the liver lacks branched-chain aminotransferase (BCAT), the enzyme responsible for metabolizing this group of amino acids, so blood levels of leucine fluctuate in response to dietary intake of protein (Layman and Walker, 2006). Leucine is further known to have a variety of physiological effects beyond simply acting as a proteogenic amino acid. For example, dietary leucine supplementation has been shown to increase satiety and decrease caloric intake (Potier et al., 2009). Further, leucine can directly stimulate insulin release from pancreatic beta cells (Panten et al., 1974) and skeletal muscle anabolism (Greiwe et al., 2001; Nair et al., 1992). Many of the physiological effects of leucine are mediated through the mTORC1 pathway, and thus understanding how leucine is directly sensed has been of great interest in the field.

### **mTORC1 signaling *in vivo***

Rapamycin has now been used in the clinic under a variety of therapeutic settings because it affects a number of organs. To better understand how mTOR

impacts physiology, multiple mouse models have been created (Howell and Manning, 2011).

To explore the importance of mTORC1 *in vivo*, some of the first mouse models created that modulated the pathway were mTOR or raptor knockouts. Disruption of either mTOR or raptor led to embryonic lethality at E5.5, immediately after implantation (Gangloff et al., 2004; Guertin et al., 2006; Murakami et al., 2004). The *MTOR*<sup>-/-</sup> embryos were developmentally delayed at E5.5 (Gangloff et al., 2004), and cells from both embryonic and extraembryonic tissues displayed a proliferation defect *in vitro* (Gangloff et al., 2004; Murakami et al., 2004).

Disruption of the mTORC1 pathway upstream of mTORC1 itself also leads to severe phenotypes. Loss of the Rag GTPases, specifically RagA, leads to embryonic lethality at E10.5 (Efeyan et al., 2014), and loss of Rheb results in embryonic lethality at midgestation (E11.5-12.5) (Goorden et al., 2011). The similar phenotypes between the Rag-null and Rheb-null mice highlight the importance of both the nutrient and growth factor sensing pathways upstream of mTORC1.

Disruption of negative regulators upstream of mTORC1, which lead to hyperactive or constitutively active mTORC1 signaling, also display severe phenotypes *in vivo*. Homozygous null alleles of TSC1 or TSC2 lead to embryonic lethality around E9.5-11.5, and these embryos often display neurological developmental delays such as open neural tubes (Kobayashi et al., 2001; Rennebeck et al., 1998). Constitutive activation of the nutrient sensing pathway *in vivo*, using mutant alleles of RagA that are GTPase defective (*RagA*<sup>GTP/GTP</sup>), leads to perinatal lethality (Efeyan et al., 2013). This phenotype mimics those seen with autophagy deficiency, in which there is a defect in responding to the decreased nutrient supply during the perinatal period due to separation from the placenta (Komatsu, 2005; Kuma et al., 2004). In wild-type embryos, this period of glucose and amino acid starvation stimulates autophagy via the mTORC1 nutrient sensing pathway, which provides amino acids to stimulate gluconeogenesis. However, *RagA*<sup>GTP/GTP</sup> or autophagy defective neonates cannot respond appropriately to this sudden decrease in nutrients, leading to accelerated neonatal death (Efeyan et al., 2013). These mouse models established the importance of mTORC1 signaling in development and in response to fasting during the perinatal period.

## **Deregulation of mTORC1 signaling in disease**

The mTORC1 signaling pathway is deregulated in a variety of human diseases, from cancer to epilepsy. Evidence for this deregulation has come from germline mutations in pathway components that lead to familial syndromes, sporadic mutations leading to disease, and disease phenotypes in mouse models, as discussed below.

### **mTOR pathway component mutations in cancer**

Many upstream regulators of mTOR are mutated in both sporadic cancers and familial cancer syndromes. Regulators of the growth factor sensing branch, such as PI3K and Akt, are well-established oncogenes that are mutated in a variety of malignancies. PTEN, which acts as an important negative regulator of PI3K signaling, is a tumor suppressor that is commonly mutated or lost in sporadic cancers. In addition, germline mutations in Akt, PI3K, and PTEN are associated with familial overgrowth syndromes (Proteus syndrome, PIK3CA Related Overgrowth Spectrum, and Cowden Syndrome, respectively) (Keppler-Noreuil et al., 2016). Further, the Ras-Raf-MEK pathway, which feeds in to activate mTORC1 signaling upstream of the TSC complex, is one of the most frequently perturbed pathways in tumorigenesis (Xu et al., 2014).

Downstream of these commonly mutated components, TSC1/2 have long been recognized to be tumor suppressor genes due to their association with the familial tumor syndrome tuberous sclerosis (Keppler-Noreuil et al., 2016). Tuberous sclerosis is an autosomal dominant syndrome in which patients inherit one mutated allele of either TSC1 or TSC2. The syndrome then results in overgrowth phenotypes in various organs, classically including renal angiomyolipomas, subependymal giant cell astrocytomas, and cardiac rhabdomyomas. These tumors are associated with loss of heterozygosity, and thus inactivating mutations are found in the wild-type allele of the disease-causing gene in the tumor cells (Keppler-Noreuil et al., 2016). Tuberous sclerosis is also associated with epilepsy, as discussed below.

Mouse models of tuberous sclerosis have been critical for validating the role of TSC1/2 as tumor suppressors. As mentioned previously, homozygous loss of expression of either TSC1 or 2 is lethal in mice. However, heterozygotes are viable. A significant portion of *TSC1*<sup>+/-</sup> mice develop renal and liver tumors by 15-18 months, while *TSC2*<sup>+/-</sup> mice develop lung and liver tumors by around this time (Xu et al., 2014). A number of mouse models have been generated in which TSC1/2 are conditionally deleted in certain organs, which, in tissues such as liver and kidney, stimulates tumorigenesis, further validating the role of the TSC complex as a tumor suppressor (Xu et al., 2014).

Apart from upstream regulators that feed in to control mTORC1 activity in response to growth factors, a few other components of the pathway are mutated in cancer. Recurrent, sporadic mutations in the gene *MTOR*, which encodes the mTOR kinase itself, have been found in a subset of cancers, and these have been found to activate mTORC1 signaling in cell culture (Grabiner et al., 2014). In addition, on the nutrient sensing side of the pathway, loss of GATOR1 components occurs in a low percentage of sporadic ovarian cancers and glioblastomas (Bar-Peled et al., 2013). Cancer cell lines derived from these tumors have constitutive mTORC1 signaling in the absence of amino acids (Bar-Peled et al., 2013), but whether loss of GATOR1 components are “driver” events in these cancers is unknown.

### **mTOR inhibitors as cancer therapy**

Given the central role of the mTORC1 pathway in tumorigenesis, there has been a lot of promise over targeting this pathway for therapy. Rapamycin and its analogs (rapalogs) have, however, been effective only in a subset of cancers. The first of these to enter clinic use was temsirolimus, which, in 2007, was approved for the treatment of metastatic renal cell carcinoma (Chiarini et al., 2015). Another rapalog, everolimus, is also approved for the treatment of advanced renal cell carcinoma, along with subependymal giant cell astrocytomas in tuberous sclerosis patients and neuroendocrine pancreatic tumors (Chiarini et al., 2015). These are the only FDA-approved uses for rapalogs as cancer therapy, however, and given how commonly



mutated the PI3K-mTOR pathway is in cancer, the limited effectiveness of rapalogs for treatment of cancer patients has been surprising. There are, however, a few explanations for why this may be the case.

First, patients are often not screened for mutations in the pathway before being given the treatment, especially in large trials. Thus, it may be the case that patients that harbor mTORC1 pathway mutations would be particularly responsive. Recently, for example, a small trial of everolimus in solid tumors uncovered a patient with uroepithelial cancer who displayed an exquisite response to this drug. Targeted sequencing revealed the patient's tumor harbored two mutations in the mTOR kinase gene which, based on cellular studies, led to activated mTORC1 signaling *in vitro*, perhaps explaining the sensitivity of the tumor to mTOR inhibition (Wagle et al., 2014b). The limitations of this treatment were displayed, however, in a separate patient who suffered from a metastatic thyroid carcinoma. The patient also had an exquisite response to everolimus, likely due to an inactivating mutation in *TSC2*. After 18 months of response to the therapy, however, the patient relapsed with a tumor that was found, in addition to the *TSC2* mutation, to also harbor a mutation in the *MTOR* gene. This mTOR mutant kinase was shown, in cell culture studies, to be resistant to allosteric mTOR inhibitors, such as everolimus (Wagle et al., 2014a). These studies emphasize the need for individual sequencing data on patients in order to better understand therapies that will be effective for those patients.

A number of other reasons for why rapalogs have not been effective for the treatment of cancers exist. First, mTOR inhibitors are cytostatic, rather than pro-apoptotic, limiting their ability to kill cancer cells (Chiarini et al., 2015). In addition, rapamycin in particular inhibits phosphorylation on some mTORC1 substrates less than others, specifically having less of an effect on 4E-BP1 phosphorylation than on other substrates (Kang et al., 2013). The effects of mTORC1 on translation, specifically through 4E-BP1, are thought to be crucial to its role in tumorigenesis, and thus having less of an effect on this substrate may limit the effectiveness of these inhibitors (Tamburini et al., 2009). Beyond these limitations, there are also a variety of negative feedback loops controlled downstream of S6K1, an mTORC1 substrate, and thus mTORC1 inhibition may paradoxically increase upstream signaling, such as through Akt

(Chiarini et al., 2015). Finally, rapalogs have been shown to be relatively specific for mTORC1, having effects only on mTORC2 under long-term treatment (Lamming et al., 2012). Thus, ATP-competitive mTOR kinase inhibitors, such as Torin, may prove more effective for the treatment of cancer as a means for inhibiting both mTORC1 and mTORC2 (and therefore Akt, as well) (Thoreen et al., 2009).

To circumvent the issue of feedback loops leading to activation of the mTORC1 signaling pathway upstream of Akt with rapalogs, dual PI3K/mTOR inhibitors have sparked interest. These inhibitors are currently in Phase I or II trials and are showing some promise for the treatment of both solid and hematological malignancies. Similarly, ATP-competitive mTOR kinase inhibitors are being used to target both mTORC1 and 2 in cancer patients (Chiarini et al., 2015). As with all single therapy treatments, acquired resistance has emerged relatively quickly, but many trials are currently underway to combine these treatments with other chemotherapeutics.

### **mTORC1 pathway component mutations in epilepsy and other brain malformation disorders**

As mentioned previously, many of the genetic disorders caused by mutations in components in the mTOR signaling pathway are not only associated with tumor syndromes, but also associated with brain malformation disorders or epilepsy (**Figure 2**). For example, in patients with tuberous sclerosis, a genetic disease due to heterozygous inactivating mutations in *TSC1/2*, cortical tubers form, likely due to loss of heterozygosity in neurons during development and subsequent overgrowth (Keppler-Noreuil et al., 2016). These cortical tubers, or perhaps intrinsic hyper-excitability of neurons lacking the TSC complex (Bateup et al., 2013), trigger the epilepsy observed in tuberous sclerosis patients.

Much excitement came over the recent discovery of TBC1D7 as the third member of the TSC complex, perhaps explaining the cause of tuberous sclerosis in patients without mutations in *TSC1/2*. However, comprehensive sequencing efforts did not reveal any mutations in TBC1D7 in patients with tuberous sclerosis (Dibble et al., 2012). Despite this, two families were found that harbor homozygous mutations in

TBC1D7 leading to macrocephaly, intellectual disability, and neuropsychological disorders – phenotypes that are very reminiscent of deregulation of other mTORC1 pathway components (Alfaiz et al., 2014; Capo-Chichi et al., 2013).

Neurodevelopment malformation disorders, like macrocephaly, are a common feature of syndromes linked to mutations in this pathway. For example, hemimegalencephaly, in which one hemisphere of the brain is overgrown in development, has been associated with Proteus syndrome (mutations in Akt) and tuberous sclerosis (Keppler-Noreuil et al., 2016). Further, somatic activating mutations in the *MTOR*, *AKT3*, and *PI3KCA* genes have been found in sporadic hemimegalencephaly in the affected brain region (Conti et al., 2015; Lee et al., 2012; Mirzaa et al., 2016). Cowden syndrome (heterozygous inactivating mutations in *PTEN*) patients often suffer from macrocephaly as well (Granados et al., 2013).

Finally, the components of GATOR1, specifically DEPDC5, are mutated in patients with focal epilepsy or focal cortical dysplasia (FCD) (D'Gama et al., 2015). FCD is another brain malformation disorder in which an area of the cortex overgrows during development. Again, heterozygous, likely inactivating mutations in *DEPDC5*, *NPRL2*, or *NPRL3* have been found in families with these disorders (Baulac, 2016), establishing that deregulation of either the growth factor or nutrient sensing branches upstream of mTORC1 are sufficient to induce these diseases.

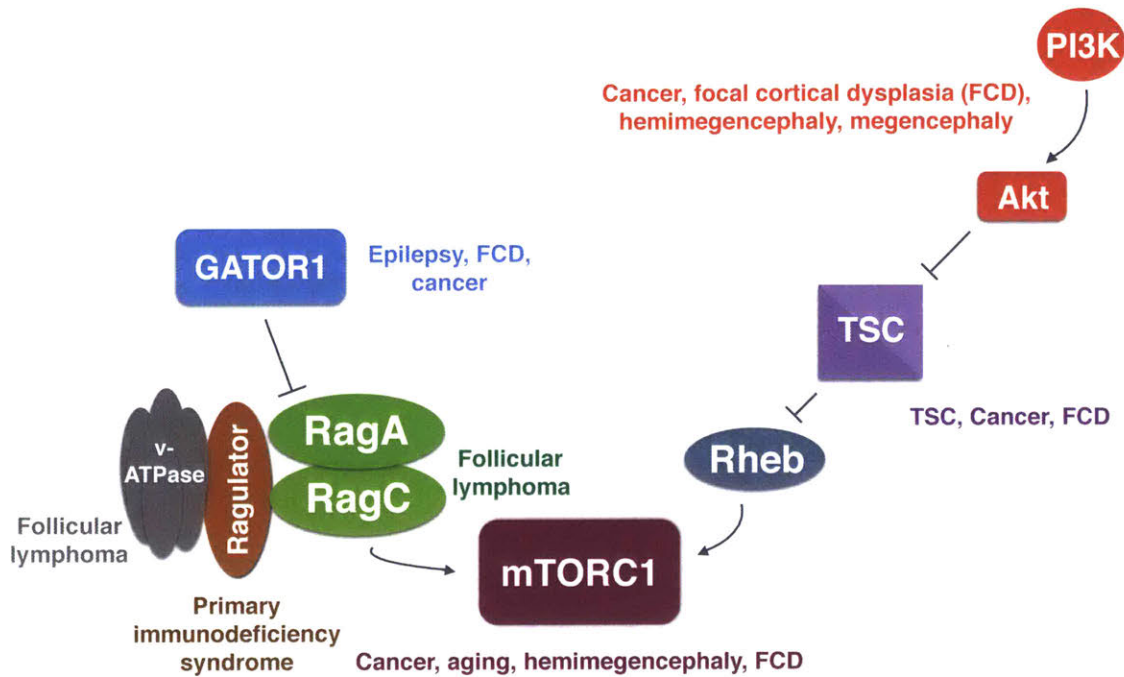


**Figure 2: mTORC1 pathway component mutations in human disease.**

Schematic showing mTORC1 pathway components, mutations of which lead to the human diseases indicated in the corresponding colors.

### Rapalogs for tuberous sclerosis therapy

Rapalogs are the only mTOR inhibitors that have been tested for the treatment of any patients with familial syndromes associated with mutations in mTOR pathway components. Specifically, as was previously mentioned, rapalogs are approved therapy for renal carcinomas and subependymal giant cell astrocytomas, both of which are commonly associated with tuberous sclerosis (Keppler-Noreuil et al., 2016). In addition, rapalogs have shown some success in early clinical trials for the treatment of refractory epilepsy in these patients (Saxena and Sampson, 2015). Unfortunately, the long-term developmental and cognitive effects of treating pediatric patients with mTOR inhibitors is still unclear, limiting the promise behind these therapies (Jeong and Wong, 2016).

## **Preface for work presented in this thesis**

It has become clear that deregulation of the mTORC1 signaling pathway occurs in a number of human diseases. Further, intense investigation into the architecture of this pathway has identified many of the key players involved in transmitting amino acid availability to the Rag GTPases. However, many open questions remain in the field, and the work presented in this thesis will help address some of these issues.

### **1. Are mutations in components of the nutrient sensing machinery found in cancer?**

As mentioned previously, deregulation of mTORC1 signaling plays an important role in tumorigenesis. Many regulators of the growth factor sensing branch upstream of mTORC1, including PI3K, PTEN, and Akt, are mutated in a number of human cancers (Xu et al., 2014). On the nutrient sensing side of the pathway, however, recurrent mutations in tumor samples have only been found in the components of GATOR1, and these occur in a very low percentage of ovarian cancers and glioblastomas (Bar-Peled et al., 2013). Thus, it is of great interest to understand if other components of the nutrient sensing machinery are associated with human cancer.

To this end, we discovered that mutations in *RRAGC*, the gene that encodes RagC, occur recurrently in follicular lymphoma samples, at a frequency of 17%. The RagC mutant GTPases increased raptor binding and rendered cells unable to fully inhibit mTORC1 in the absence of amino acids. The presence of these mutations in the dominant clone, their stability throughout disease progression, and their activation of mTORC1 signaling *in vitro* implies that RagC may be acting as an oncogene in follicular lymphoma. These exciting results may help identify another population of cancer patients in which rapalogs or other mTOR inhibitors could be effective therapy, and further establish that deregulation of the nutrient sensing pathway upstream of mTORC1 may play a role in tumorigenesis.

### **2. What is the identity of the leucine sensor for the mTORC1 pathway?**

To identify novel regulators of the amino sensing pathway, we employed an IP/MS approach using GATOR2 as the bait and identified the Sestrins, a family of three previously poorly characterized growth regulators, Sestrin1-3, as GATOR2-interacting proteins. We found that these proteins act as negative regulators of mTORC1 signaling that interact with GATOR2 under leucine deprivation. Because leucine *in vitro* was sufficient to disrupt the GATOR2-Sestrin2 interaction, we hypothesized that Sestrin2 may act as a leucine sensor for the mTORC1 pathway. Indeed, through showing the Sestrin2 directly binds leucine at affinities consistent with those that are sensed by the pathway and that the leucine-binding capacity of Sestrin2 is necessary for leucine modulation of the mTORC1 pathway, we characterized Sestrin2 (and 1) as the elusive leucine sensors for the mTORC1 pathway.

### **3. Are there other regulators of the nutrient sensing pathway that have not yet been identified?**

The discovery of Sestrin2 as a leucine sensor for the mTORC1 pathway represented a major advance in understanding how amino acids are sensed. How Sestrin2 inhibits the pathway, however, is unknown, as the function of GATOR2 remains elusive. GATOR2 acts as a positive regulator of the pathway either upstream or parallel to GATOR1, but if other components regulate either of these complexes remains unclear. To address this issue, we undertook IP/MS from cells in which a component of GATOR1 was endogenously tagged. Through this, we identified KICSTOR (for KPTN, ITFG2, C12orf66, and SZT2-containing regulator of mTORC1), a four-membered protein complex that acts as a negative regulator of the nutrient sensing pathway. Further, we found that KICSTOR is necessary for targeting GATOR1, but not GATOR2, to the lysosomal surface, and is necessary for the interaction of GATOR1 with its substrate, the Rag GTPases, and with GATOR2. Moreover, disruption of SZT2 *in vivo* leads to hyperactive mTORC1 signaling in a number of tissues, and three of the components of KICSTOR are mutated in human epilepsy or brain malformation

disorders, arguing that KICSTOR, like many components of the mTORC1 signaling pathway, plays an important role in human disease.

## References

Abraham, R.T., and Wiederrecht, G.J. (1996). Immunopharmacology of rapamycin. *Annu Rev Immunol* 14, 483-510.

Alfaiz, A.A., Micale, L., Mandriani, B., Augello, B., Pellico, M.T., Chrast, J., Xenarios, I., Zelante, L., Merla, G., and Reymond, A. (2014). TBC1D7 mutations are associated with intellectual disability, macrocrania, patellar dislocation, and celiac disease. *Hum Mutat* 35, 447-451.

Bar-Peled, L., Chantranupong, L., Cherniack, A.D., Chen, W.W., Ottina, K.A., Grabiner, B.C., Spear, E.D., Carter, S.L., Meyerson, M., and Sabatini, D.M. (2013). A Tumor suppressor complex with GAP activity for the Rag GTPases that signal amino acid sufficiency to mTORC1. *Science* 340, 1100-1106.

Bar-Peled, L., Schweitzer, L.D., Zoncu, R., and Sabatini, D.M. (2012). Ragulator Is a GEF for the Rag GTPases that Signal Amino Acid Levels to mTORC1. *Cell* 150, 1196-1208.

Barbet, N.C., Schneider, U., Helliwell, S.B., Stansfield, I., Tuite, M.F., and Hall, M.N. (1996). TOR controls translation initiation and early G1 progression in yeast. *Molecular Biology of the Cell* 7, 25-42.

Bateup, H.S., Johnson, C.A., Denefrio, C.L., Saulnier, J.L., Kornacker, K., and Sabatini, B.L. (2013). Excitatory/inhibitory synaptic imbalance leads to hippocampal hyperexcitability in mouse models of tuberous sclerosis. *Neuron* 78, 510-522.

Baulac, S. (2016). mTOR signaling pathway genes in focal epilepsies. *Prog Brain Res* 226, 61-79.

Blommaart, E.F., Luiken, J.J., Blommaart, P.J., van Woerkom, G.M., and Meijer, A.J. (1995). Phosphorylation of ribosomal protein S6 is inhibitory for autophagy in isolated rat hepatocytes. *The Journal of biological chemistry* 270, 2320-2326.

Brown, E.J., Albers, M.W., Shin, T.B., Ichikawa, K., Keith, C.T., Lane, W.S., and Schreiber, S.L. (1994). A mammalian protein targeted by G1-arresting rapamycin-receptor complex. *Nature* 369, 756-758.

Capo-Chichi, J.-M., Tcherkezian, J., Hamdan, F.F., Décarie, J.C., Dobrzeniecka, S., Patry, L., Nadon, M.-A., Mucha, B.E., Major, P., Shevell, M., *et al.* (2013). Disruption of TBC1D7, a subunit of the TSC1-TSC2 protein complex, in intellectual disability and megalencephaly. *J Med Genet* 50, 740-744.

Chiarini, F., Evangelisti, C., McCubrey, J.A., and Martelli, A.M. (2015). Current treatment strategies for inhibiting mTOR in cancer. *Trends Pharmacol Sci* 36, 124-135.



Conti, V., Pantaleo, M., Barba, C., Baroni, G., Mei, D., Buccoliero, A.M., Giglio, S., Giordano, F., Baek, S.T., Gleeson, J.G., *et al.* (2015). Focal dysplasia of the cerebral cortex and infantile spasms associated with somatic 1q21.1-q44 duplication including the AKT3 gene. *Clin Genet* 88, 241-247.

D'Gama, A.M., Geng, Y., Couto, J.A., Martin, B., Boyle, E.A., LaCoursiere, C.M., Hossain, A., Hatem, N.E., Barry, B.J., Kwiatkowski, D.J., *et al.* (2015). Mammalian target of rapamycin pathway mutations cause hemimegalencephaly and focal cortical dysplasia. *Ann Neurol* 77, 720-725.

Dann, S.G., and Thomas, G. (2006). The amino acid sensitive TOR pathway from yeast to mammals. *FEBS Letters* 580, 2821-2829.

Dibble, C.C., Elis, W., Menon, S., Qin, W., Klekota, J., Asara, J.M., Finan, P.M., Kwiatkowski, D.J., Murphy, L.O., and Manning, B.D. (2012). TBC1D7 is a third subunit of the TSC1-TSC2 complex upstream of mTORC1. *Molecular Cell* 47, 535-546.

Efeyan, A., Schweitzer, L.D., Bilate, A.M., Chang, S., Kirak, O., Lamming, D.W., and Sabatini, D.M. (2014). RagA, but not RagB, is essential for embryonic development and adult mice. *Dev Cell* 29, 321-329.

Efeyan, A., Zoncu, R., Chang, S., Gumper, I., Snitkin, H., Wolfson, R.L., Kirak, O., Sabatini, D.D., and Sabatini, D.M. (2013). Regulation of mTORC1 by the Rag GTPases is necessary for neonatal autophagy and survival. *Nature* 493, 679-683.

Eng, C.P., Sehgal, S.N., and Vézina, C. (1984). Activity of rapamycin (AY-22,989) against transplanted tumors. *J Antibiot* 37, 1231-1237.

Fox, H.L., Pham, P.T., Kimball, S.R., Jefferson, L.S., and Lynch, C.J. (1998). Amino acid effects on translational repressor 4E-BP1 are mediated primarily by L-leucine in isolated adipocytes. *American Journal of Physiology -- Legacy Content* 275, C1232-1238.

Gangloff, Y.-G., Mueller, M., Dann, S.G., Svoboda, P., Sticker, M., Spetz, J.-F., Um, S.H., Brown, E.J., Cereghini, S., Thomas, G., *et al.* (2004). Disruption of the mouse mTOR gene leads to early postimplantation lethality and prohibits embryonic stem cell development. *Molecular and Cellular Biology* 24, 9508-9516.

Ganley, I.G., Lam, D.H., Wang, J., Ding, X., Chen, S., and Jiang, X. (2009). ULK1.ATG13.FIP200 complex mediates mTOR signaling and is essential for autophagy. *J Biol Chem* 284, 12297-12305.

García-Martínez, J.M., and Alessi, D.R. (2008). mTOR complex 2 (mTORC2) controls hydrophobic motif phosphorylation and activation of serum- and glucocorticoid-induced protein kinase 1 (SGK1). In *Biochem J* (Portland Press Limited), pp. 375-385.

Goorden, S.M.I., Hoogeveen-Westerveld, M., Cheng, C., van Woerden, G.M., Mozaffari, M., Post, L., Duckers, H.J., Nellist, M., and Elgersma, Y. (2011). Rheb is essential for murine development. *Molecular and Cellular Biology* 31, 1672-1678.

Grabiner, B.C., Nardi, V., Birsoy, K., Possemato, R., Shen, K., Sinha, S., Jordan, A., Beck, A.H., and Sabatini, D.M. (2014). A diverse array of cancer-associated MTOR mutations are hyperactivating and can predict rapamycin sensitivity. *Cancer Discov* 4, 554-563.

Granados, A., Eng, C., and Diaz, A. (2013). Brothers with germline PTEN mutations and persistent hypoglycemia, macrocephaly, developmental delay, short stature, and coagulopathy. *J Pediatr Endocrinol Metab* 26, 137-141.

Greiwe, J.S., Kwon, G., McDaniel, M.L., and Semenkovich, C.F. (2001). Leucine and insulin activate p70 S6 kinase through different pathways in human skeletal muscle. *American journal of physiology Endocrinology and metabolism* 281, E466-471.

Guertin, D.A., Stevens, D.M., Thoreen, C.C., Burds, A.A., Kalaany, N.Y., Moffat, J., Brown, M., Fitzgerald, K.J., and Sabatini, D.M. (2006). Ablation in mice of the mTORC components raptor, rictor, or mLST8 reveals that mTORC2 is required for signaling to Akt-FOXO and PKCalpha, but not S6K1. *Dev Cell* 11, 859-871.

Hara, K., Yonezawa, K., Weng, Q.P., Kozlowski, M.T., Belham, C., and Avruch, J. (1998). Amino acid sufficiency and mTOR regulate p70 S6 kinase and eIF-4E BP1 through a common effector mechanism. *The Journal of biological chemistry* 273, 14484-14494.

Heitman, J., Movva, N.R., and Hall, M.N. (1991). Targets for cell cycle arrest by the immunosuppressant rapamycin in yeast. *Science* 253, 905-909.

Hosokawa, N., Hara, T., Kaizuka, T., Kishi, C., Takamura, A., Miura, Y., Iemura, S.-i., Natsume, T., Takehana, K., Yamada, N., *et al.* (2009). Nutrient-dependent mTORC1 association with the ULK1-Atg13-FIP200 complex required for autophagy. *Molecular Biology of the Cell* 20, 1981-1991.

Howell, J.J., and Manning, B.D. (2011). mTOR couples cellular nutrient sensing to organismal metabolic homeostasis. *Trends Endocrinol Metab* 22, 94-102.

Inoki, K., Li, Y., Zhu, T., Wu, J., and Guan, K.-L. (2002). TSC2 is phosphorylated and inhibited by Akt and suppresses mTOR signalling. *Nat Cell Biol* 4, 648-657.

Jacinto, E., Loewith, R., Schmidt, A., Lin, S., Rüegg, M.A., Hall, A., and Hall, M.N. (2004). Mammalian TOR complex 2 controls the actin cytoskeleton and is rapamycin insensitive. *Nat Cell Biol* 6, 1122-1128.

Jeong, A., and Wong, M. (2016). mTOR Inhibitors in Children: Current Indications and Future Directions in Neurology. *Curr Neurol Neurosci Rep* 16, 102.

Jung, C.H., Jun, C.B., Ro, S.-H., Kim, Y.-M., Otto, N.M., Cao, J., Kundu, M., and Kim, D.-H. (2009). ULK-Atg13-FIP200 complexes mediate mTOR signaling to the autophagy machinery. *Molecular Biology of the Cell* 20, 1992-2003.

Kang, S.A., Pacold, M.E., Cervantes, C.L., Lim, D., Lou, H.J., Ottina, K., Gray, N.S., Turk, B.E., Yaffe, M.B., and Sabatini, D.M. (2013). mTORC1 phosphorylation sites encode their sensitivity to starvation and rapamycin. *Science* 341, 1236566.

Keppler-Noreuil, K.M., Parker, V.E.R., Darling, T.N., and Martinez-Agosto, J.A. (2016). Somatic overgrowth disorders of the PI3K/AKT/mTOR pathway & therapeutic strategies. *Am J Med Genet C Semin Med Genet* 172, 402-421.

Kobayashi, T., Minowa, O., Sugitani, Y., Takai, S., Mitani, H., Kobayashi, E., Noda, T., and Hino, O. (2001). A germ-line Tsc1 mutation causes tumor development and embryonic lethality that are similar, but not identical to, those caused by Tsc2 mutation in mice. *Proc Natl Acad Sci USA* 98, 8762-8767.

Koltin, Y., Faucette, L., Bergsma, D.J., Levy, M.A., Cafferkey, R., Koser, P.L., Johnson, R.K., and Livi, G.P. (1991). Rapamycin sensitivity in *Saccharomyces cerevisiae* is mediated by a peptidyl-prolyl cis-trans isomerase related to human FK506-binding protein. *Molecular and Cellular Biology* 11, 1718-1723.

Komatsu, M. (2005). Impairment of starvation-induced and constitutive autophagy in Atg7-deficient mice. *The Journal of Cell Biology* 169, 425-434.

Kuma, A., Hatano, M., Matsui, M., Yamamoto, A., Nakaya, H., Yoshimori, T., Ohsumi, Y., Tokuhiya, T., and Mizushima, N. (2004). The role of autophagy during the early neonatal starvation period. *Nature* 432, 1032-1036.

Lamming, D.W., Ye, L., Katajisto, P., Goncalves, M.D., Saitoh, M., Stevens, D.M., Davis, J.G., Salmon, A.B., Richardson, A., Ahima, R.S., *et al.* (2012). Rapamycin-Induced Insulin Resistance Is Mediated by mTORC2 Loss and Uncoupled from Longevity. *Science* 335, 1638-1643.

Laplante, M., and Sabatini, D.M. (2009). An emerging role of mTOR in lipid biosynthesis. *Curr Biol* 19, R1046-1052.

Laplante, M., and Sabatini, D.M. (2012). mTOR Signaling in Growth Control and Disease. *Cell* 149, 274-293.

Layman, D.K., and Walker, D.A. (2006). Potential Importance of Leucine in Treatment of Obesity and the Metabolic Syndrome.

Lee, J.H., Huynh, M., Silhavy, J.L., Kim, S., Dixon-Salazar, T., Heiberg, A., Scott, E., Bafna, V., Hill, K.J., Collazo, A., *et al.* (2012). De novo somatic mutations in components of the PI3K-AKT3-mTOR pathway cause hemimegalencephaly. *Nat Genet* 44, 941-945.

Liu, P., Gan, W., Chin, Y.R., Ogura, K., Guo, J., Zhang, J., Wang, B., Blenis, J., Cantley, L.C., Tokar, A., Su, B., and Wei, W. (2015). PtdIns(3,4,5)P<sub>3</sub>-dependent Activation of the mTORC2 Kinase Complex. *Cancer Discov* 5, 1194–1209.

Loewith, R., Jacinto, E., Wullschleger, S., Lorberg, A., Crespo, J.L., Bonenfant, D., Oppliger, W., Jenoe, P., and Hall, M.N. (2002). Two TOR complexes, only one of which is rapamycin sensitive, have distinct roles in cell growth control. *Molecular Cell* 10, 457-468.

Lynch, C.J., Fox, H.L., Vary, T.C., Jefferson, L.S., and Kimball, S.R. (2000). Regulation of amino acid-sensitive TOR signaling by leucine analogues in adipocytes. *Journal of cellular biochemistry* 77, 234-251.

Manning, B.D., Tee, A.R., Logsdon, M.N., Blenis, J., and Cantley, L.C. (2002). Identification of the tuberous sclerosis complex-2 tumor suppressor gene product tuberin as a target of the phosphoinositide 3-kinase/akt pathway. *Molecular Cell* 10, 151-162.

Menon, S., Dibble, C.C., Talbott, G., Hoxhaj, G., Valvezan, A.J., Takahashi, H., Cantley, L.C., and Manning, B.D. (2014). Spatial Control of the TSC Complex Integrates Insulin and Nutrient Regulation of mTORC1 at the Lysosome. *Cell* 156, 771-785.

Mirzaa, G.M., Campbell, C.D., Solovieff, N., Goold, C.P., Jansen, L.A., Menon, S., Timms, A.E., Conti, V., Biag, J.D., Olds, C., *et al.* (2016). Association of MTOR Mutations With Developmental Brain Disorders, Including Megalencephaly, Focal Cortical Dysplasia, and Pigmentary Mosaicism. *JAMA Neurol* 73, 836-845.

Murakami, M., Ichisaka, T., Maeda, M., Oshiro, N., Hara, K., Edenhofer, F., Kiyama, H., Yonezawa, K., and Yamanaka, S. (2004). mTOR is essential for growth and proliferation in early mouse embryos and embryonic stem cells. *Molecular and Cellular Biology* 24, 6710-6718.

Nair, K.S., Schwartz, R.G., and Welle, S. (1992). Leucine as a regulator of whole body and skeletal muscle protein metabolism in humans. *American Journal of Physiology -- Legacy Content* 263, E928-934.

Panten, U., Christians, J., von Kriegstein, E., Poser, W., and Hasselblatt, A. (1974). Studies on the mechanism of L-leucine-and alpha-ketoisocaproic acid-induced insulin release from perfused isolated pancreatic islets. *Diabetologia* 10, 149-154.

Potier, M., Darcel, N., and Tomé, D. (2009). Protein, amino acids and the control of food intake. *Current Opinion in Clinical Nutrition and Metabolic Care* 12, 54-58.

Potter, C.J., Pedraza, L.G., and Xu, T. (2002). Akt regulates growth by directly phosphorylating Tsc2. *Nat Cell Biol* 4, 658-665.

Rennebeck, G., Kleymenova, E.V., Anderson, R., Yeung, R.S., Artzt, K., and Walker, C.L. (1998). Loss of function of the tuberous sclerosis 2 tumor suppressor gene results in embryonic lethality characterized by disrupted neuroepithelial growth and development. *Proc Natl Acad Sci USA* 95, 15629-15634.

Sabatini, D.M., Erdjument-Bromage, H., Lui, M., Tempst, P., and Snyder, S.H. (1994). RAFT1: a mammalian protein that binds to FKBP12 in a rapamycin-dependent fashion and is homologous to yeast TORs. *Cell* 78, 35-43.

Sabers, C.J., Martin, M.M., Brunn, G.J., Williams, J.M., Dumont, F.J., Wiederrecht, G., and Abraham, R.T. (1995). Isolation of a protein target of the FKBP12-rapamycin complex in mammalian cells. *J Biol Chem* 270, 815-822.

Sancak, Y., Bar-Peled, L., Zoncu, R., Markhard, A.L., Nada, S., and Sabatini, D.M. (2010). Ragulator-Rag Complex Targets mTORC1 to the Lysosomal Surface and Is Necessary for Its Activation by Amino Acids. *Cell* 141, 290-303.

Sancak, Y., Peterson, T.R., Shaul, Y.D., Lindquist, R.A., Thoreen, C.C., Bar-Peled, L., and Sabatini, D.M. (2008). The Rag GTPases Bind Raptor and Mediate Amino Acid Signaling to mTORC1. *Science* 320, 1496-1501.

Sarbassov, D.D., Ali, S.M., Kim, D.-H., Guertin, D.A., Latek, R.R., Erdjument-Bromage, H., Tempst, P., and Sabatini, D.M. (2004). Rictor, a novel binding partner of mTOR, defines a rapamycin-insensitive and raptor-independent pathway that regulates the cytoskeleton. *Curr Biol* 14, 1296-1302.

Sarbassov, D.D., Guertin, D.A., Ali, S.M., and Sabatini, D.M. (2005). Phosphorylation and regulation of Akt/PKB by the rictor-mTOR complex. *Science* 307, 1098-1101.

Saxena, A., and Sampson, J.R. (2015). Epilepsy in Tuberous Sclerosis: Phenotypes, Mechanisms, and Treatments. *Semin Neurol* 35, 269-276.

Sengupta, S., Peterson, T.R., and Sabatini, D.M. (2010). Regulation of the mTOR complex 1 pathway by nutrients, growth factors, and stress. *Molecular Cell* 40, 310-322.

Settembre, C., Zoncu, R., Medina, D.L., Vetrini, F., Erdin, S., Erdin, S., Huynh, T., Ferron, M., Karsenty, G., Vellard, M.C., *et al.* (2012). A lysosome-to-nucleus signalling mechanism senses and regulates the lysosome via mTOR and TFEB. *The EMBO Journal* 31, 1095-1108.

Shaw, R.J., and Cantley, L.C. (2006). Ras, PI(3)K and mTOR signalling controls tumour cell growth. *Nature* 441, 424-430.

Tamburini, J., Green, A.S., Bardet, V., Chapuis, N., Park, S., Willems, L., Uzunov, M., Ifrah, N., Dreyfus, F., Lacombe, C., *et al.* (2009). Protein synthesis is resistant to rapamycin and constitutes a promising therapeutic target in acute myeloid leukemia. *Blood* 114, 1618-1627.

Thoreen, C.C., Kang, S.A., Chang, J.W., Liu, Q., Zhang, J., Gao, Y., Reichling, L.J., Sim, T., Sabatini, D.M., and Gray, N.S. (2009). An ATP-competitive mammalian target of rapamycin inhibitor reveals rapamycin-resistant functions of mTORC1. *J Biol Chem* 284, 8023-8032.

Tsun, Z.-Y., Bar-Peled, L., Chantranupong, L., Zoncu, R., Wang, T., Kim, C., Spooner, E., and Sabatini, D.M. (2013). The folliculin tumor suppressor is a GAP for the RagC/D GTPases that signal amino acid levels to mTORC1. *Molecular Cell* 52, 495-505.

Wagle, N., Grabiner, B.C., Van Allen, E.M., Amin-Mansour, A., Taylor-Weiner, A., Rosenberg, M., Gray, N., Barletta, J.A., Guo, Y., Swanson, S.J., *et al.* (2014a). Response and acquired resistance to everolimus in anaplastic thyroid cancer. *N Engl J Med* 371, 1426-1433.

Wagle, N., Grabiner, B.C., Van Allen, E.M., Hodis, E., Jacobus, S., Supko, J.G., Stewart, M., Choueiri, T.K., Gandhi, L., Cleary, J.M., *et al.* (2014b). Activating mTOR mutations in a patient with an extraordinary response on a phase I trial of everolimus and pazopanib. *Cancer Discov* 4, 546-553.

Wang, S., Tsun, Z.-Y., Wolfson, R.L., Shen, K., Wyant, G.A., Plovanich, M.E., Yuan, E.D., Jones, T.D., Chantranupong, L., Comb, W., *et al.* (2015). Metabolism. Lysosomal amino acid transporter SLC38A9 signals arginine sufficiency to mTORC1. *Science* 347, 188-194.

Xu, K., Liu, P., and Wei, W. (2014). mTOR signaling in tumorigenesis. *Biochim Biophys Acta* 1846, 638-654.

Zoncu, R., Bar-Peled, L., Efeyan, A., Wang, S., Sancak, Y., and Sabatini, D.M. (2011). mTORC1 Senses Lysosomal Amino Acids Through an Inside-Out Mechanism That Requires the Vacuolar H<sup>+</sup>-ATPase. *Science* 334, 678-683.

**CHAPTER 1 Appendix:**

**Reprinted from Cell:**

**Nutrient Sensing Mechanisms Across Evolution**

**Lynne Chantranupong\*, Rachel L. Wolfson\*, and David M. Sabatini**

Whitehead Institute for Biomedical Research and Massachusetts Institute of  
Technology, Department of Biology, 9 Cambridge Center, Cambridge, MA 02142, USA

Howard Hughes Medical Institute, Department of Biology, Massachusetts Institute of  
Technology, Cambridge, MA 02139, USA

Koch Institute for Integrative Cancer Research, 77 Massachusetts Avenue, Cambridge,  
MA

\*These authors contributed equally to this work

Correspondence should be addressed to D.M.S.

Tel: 617-258-6407; Fax: 617-452-3566; Email: [sabatini@wi.mit.edu](mailto:sabatini@wi.mit.edu)

## **ABSTRACT**







For organisms to coordinate their growth and development with nutrient availability they must be able to sense nutrient levels in their environment. Here, we review select nutrient sensing mechanisms in a few diverse organisms. We discuss how these mechanisms reflect the nutrient requirements of specific species and how they have adapted to the emergence of multicellularity in eukaryotes.



## INTRODUCTION

All organisms have the capacity to sense the presence and absence of the nutrients required to generate energy and the building blocks of cells. In this review we survey a variety of nutrient sensing strategies and discuss how these mechanisms have evolved to suit the particular needs and environments of diverse organisms.

We first illustrate how varied sensing mechanisms can be using examples from unicellular organisms, including the sensing of amino acids by *E. coli* and of ammonium and glucose by *S. cerevisiae*. We then shift our focus to sensing pathways conserved in most eukaryotes, including those anchored by the AMPK, GCN2, and TOR kinases (**Figure 1**). We emphasize how in multicellular organisms the architectures of these core pathways has been adapted to respond to hormones in addition to nutrients and to control feeding. Furthermore, we highlight how the emergence of subcellular compartments in eukaryotes allows for new ways to store and sense nutrients.

| Nutrient-sensing pathway | Nutrient(s) sensed                         | Bacteria                                                                          | Fungi                                                                             | Plants                                                                            | Nematodes                                                                          | Drosophila                                                                          | Humans                                                                              |
|--------------------------|--------------------------------------------|-----------------------------------------------------------------------------------|-----------------------------------------------------------------------------------|-----------------------------------------------------------------------------------|------------------------------------------------------------------------------------|-------------------------------------------------------------------------------------|-------------------------------------------------------------------------------------|
|                          |                                            |  |  |  |  |  |  |
| PII<br>Chemo-receptors   | Nitrogen                                   | ■                                                                                 |                                                                                   | ■                                                                                 |                                                                                    |                                                                                     |                                                                                     |
|                          | Amino acids, ribose, galactose, dipeptides | ■                                                                                 |                                                                                   |                                                                                   |                                                                                    |                                                                                     |                                                                                     |
|                          | SPS                                        |                                                                                   | ■                                                                                 |                                                                                   |                                                                                    |                                                                                     |                                                                                     |
| Snf3/Rgt2                | Glucose                                    |                                                                                   | ■                                                                                 |                                                                                   |                                                                                    |                                                                                     |                                                                                     |
| MEP2                     | Ammonium                                   |                                                                                   | ■                                                                                 |                                                                                   |                                                                                    |                                                                                     |                                                                                     |
|                          |                                            |                                                                                   |                                                                                   |                                                                                   |                                                                                    |                                                                                     |                                                                                     |
| AMPK                     | Energy                                     |                                                                                   | ■                                                                                 |                                                                                   |                                                                                    |                                                                                     |                                                                                     |
| GCN2                     | Amino acids                                |                                                                                   | ■                                                                                 |                                                                                   |                                                                                    |                                                                                     |                                                                                     |
| TOR                      | Amino acids, glucose, energy               |                                                                                   | ■                                                                                 |                                                                                   |                                                                                    |                                                                                     |                                                                                     |

**Figure 1: Nutrient sensing pathways throughout evolution.** An overview of the nutrient sensing pathways described in this review. Pathways specific to unicellular organisms are denoted, followed by the sensing pathways that are conserved from yeast to man. Black bars indicate the presence of the pathway within the denoted species or organism.

## PROKARYOTES

Bacteria have evolved many interesting mechanisms for sensing diverse nutrients, undoubtedly an adaptation to living in environments where the concentrations and types of nutrients can vary unpredictably. We have chosen to discuss mechanisms that serve as examples of important concepts, such as the use of enzymes or receptors to detect molecules of interest, or the indirect sensing of a nutrient through the levels of metabolites generated from it. The variety of post-translational modifications that bacterial sensing pathways use, from phosphorylation to adenylylation and methylation, is remarkable as is the concentration range over which some nutrients can be detected.

### **Chemoreceptors: Coupling extracellular nutrient concentrations to cell motility**

Bacteria can face large fluctuations in the levels of nutrients in their environment and so motile species couple nutrient sensing to taxis to bias their movements towards higher nutrient concentrations. While we focus on nutrient-regulated chemotaxis in *E. coli*, the process is conserved in many prokaryotes (Szurmant and Ordal, 2004).

*E. coli* swim by rotating their flagella, bundles of filaments localized at the pole and powered by a rotary motor (Berg, 2008; Eisenbach, 1996). The motor is bidirectional: counterclockwise rotation produces smooth swimming whereas clockwise rotation leads to random tumbling due to dispersal of the flagellar filaments (Larsen et al., 1974; Turner et al., 2000). The default rotation of the motor is counterclockwise, and nutrients signal through transmembrane chemoreceptors to maintain this state to promote directed movement along a nutrient gradient. The absence of nutrients triggers a pathway that permits flagella to alternate between clockwise and counterclockwise rotations so that cells forage their environment in a random walk (Berg and Brown, 1972; Sourjik and Wingreen, 2012).

*E. coli* express five dimeric, single pass transmembrane chemoreceptors, Tar, Tsr, Tap, Trg, and Aer, which function as distinct nutrient sensors. In aggregate, they

allow *E. coli* to detect and respond to a broad spectrum of extracellular molecules, with aspartate, maltose,  $\text{Co}^{2+}$  and  $\text{Ni}^{2+}$  binding to Tar (Reader et al., 1979; Wang and D E Koshland, 1980); ribose and galactose to Trg (Kondoh et al., 1979); flavin adenine dinucleotide to Aer (Szurmant and Ordal, 2004); serine to Tsr; and dipeptides to Tap (Hedblom and Adler, 1980; Manson et al., 1986). Of the five receptors, Tar and Tsr are the most abundant (Sourjik and Berg, 2004). Remarkably, the chemoreceptors sense ligand concentrations as low as 3 nM and function over a concentration range of five orders of magnitude (Mesibov et al., 1973). This high sensitivity stems from the clustering at the cell pole of the receptors into higher order arrays, enabling one ligand binding event to affect multiple neighboring receptors and effectors (Bray et al., 1998; Briegel et al., 2009; Kentner et al., 2006; Levit et al., 2002; Maddock and Shapiro, 1993; Sourjik and Berg, 2004; Zhang et al., 2007), which presumably allows cells to detect even highly dilute nutrient environments.

The chemoreceptors signal through CheA, a homodimeric histidine kinase that constitutively associates with the chemoreceptors and its adaptor protein, CheW (**Figure 2A**). In the absence of a ligand, CheA phosphorylates the associated response regulator, CheY (Borkovich et al., 1989; Hess et al., 1988; Hess et al., 1987; Stock et al., 1988), which then diffuses to the flagellar motor to promote clockwise rotation (Dyer et al., 2009; Sarkar et al., 2010; Scharf et al., 1998; Welch et al., 1993). Nutrients diffuse into the periplasm through channels in the outer membrane and directly or indirectly contact chemoreceptors to trigger a conformational change that inhibits CheA and CheY (Ottemann et al., 1999), causing bacteria to swim in a positive direction for longer periods of time.

A crucial aspect of chemotaxis is adaptation - the ability to restore prestimulus behavior. Chemoreceptor methylation by the methyltransferase CheR and demethylation by the methylesterase CheB facilitates adaptation (Anand and Stock, 2002; Bren and Eisenbach, 2000; Kondoh et al., 1979). In addition to phosphorylating CheY, the CheA kinase phosphorylates and activates CheB, which demethylates the chemoreceptor and reduces its capacity to activate CheA despite persistently low ligand

concentrations. Conversely, sustained increases in nutrient concentrations lead to an accumulation of receptor methylation over time as CheB is inactive and CheR constitutively active. This enhances the ability of the chemoreceptor to stimulate CheA despite constant high concentrations of attractant. Thus, CheB promotes adaptation to decreasing levels of attractants while CheR promotes adaptation to increasing levels of attractants. Methylation therefore resets the signaling state of the receptors so that *E. coli* can adapt to the present environment and be poised to respond to subsequent changes (Wadhams and Armitage, 2004; Weis and D E Koshland, 1988).

The capacity to couple motility to nutrient concentrations allows bacteria to forage for limited resources. However, all bacteria, motile or not, must possess mechanisms that relay nutrient levels to the metabolic systems that counteract nutrient deficits so as to maintain the metabolites needed for viability and growth. One such mechanism is the PII protein pathway, which uses a cascade of posttranslational modifications to control nitrogen assimilation.

### **PII proteins: Controllers of nitrogen assimilation**

Under nitrogen-limiting conditions, many prokaryotes increase nitrogen assimilation by synthesizing nitrogen-containing organic molecules, such as amino acids, from inorganic nitrogen compounds in the environment. Assimilation occurs via a dedicated glutamine synthase (GS)/glutamate synthase (GOGAT) cascade that generates glutamate from 2-oxoglutarate (2-OG; also known as  $\alpha$ -ketoglutarate), ammonium, and ATP. The first step of the process, catalyzed by GS, produces glutamine, and thus its presence represents nitrogen sufficiency, while 2-OG, its precursor, signals nitrogen deficiency (Forchhammer, 2007; Leigh and Dodsworth, 2007). The PII proteins play a key role in sensing nitrogen deficiency and although they vary greatly in structure and function they are found in most prokaryotes and plants (Heinrich et al., 2004)(**Figure 1**).

Within the PII superfamily of proteins the related GlnB and GlnK proteins in *E. coli* have been particularly well studied (Leigh and Dodsworth, 2007). These proteins have significant homology only to other PII proteins and form homotrimeric complexes. Their main function is to control the adenylation of GS, which inhibits it and thus reduces nitrogen assimilation (**Figure 2B**) (Leigh and Dodsworth, 2007). The PII proteins exist in two forms: unmodified and uridylylated. Only when unmodified do they bind to and activate the adenylyltransferase (ATase) enzyme (encoded by *glnE*) to adenylylate GS (Brown et al., 1971; Stadtman, 2001). The uridylylated form, on the other hand, stimulates the deadenylylation activity of ATase (Jaggi et al, 1997).

How nitrogen is sensed is complex and involves two sensors, the PII proteins themselves as well as the uridylyltransferase (UTase) enzyme (encoded by *glnD*) that uridylylates the PII proteins. Under conditions of nitrogen excess, UTase directly binds to and is inhibited by glutamine, which is at high levels when nitrogen is abundant (Jiang et al, 1998a). The glutamine-bound UTase is unable to uridylylate GlnB, which accumulates in its unmodified form and therefore allosterically activates the adenylylation activity of ATase (Adler et al., 1975; Mangum et al., 1973). This leads to the accumulation of adenylylated, and therefore inactive, GS. During nitrogen deprivation, however, 2-OG levels increase and the binding of 2-OG to unmodified GlnB allosterically inhibits its ability to activate adenylylation by ATase (Jiang et al, 1998c). The GlnB homotrimer has three 2-OG binding sites, the first of which binds 2-OG with micromolar affinity, well below its physiological concentration of 0.1-0.9 mM. Because the binding of 2-OG to GlnB exhibits high negative cooperativity, the second and third sites are occupied only at the high 2-OG concentrations that occur upon nitrogen deprivation. Only upon binding multiple molecules of 2-OG does unmodified GlnB adopt a conformation in which it is unable to activate the adenylylation activity of ATase, leaving GS unmodified and thus active (Jiang et al., 1998a; Jiang et al., 1998b, c) (Adler et al., 1975; Mangum et al., 1973). While high levels of 2-OG inhibit the activity of unmodified GlnB, uridylylated GlnB is unaffected by high levels of this metabolite. GlnK, a PII protein that is highly similar to GlnB, also regulates AmtB, an ammonia transporter,

in response to nitrogen availability, by binding to and inhibiting the transporter under high glutamine levels (Coutts, 2002; Hoving et al., 1996).

While we have focused on the implications of 2-OG binding to the PII proteins, they are also well appreciated to bind ATP, which acts synergistically with 2-OG at low concentrations and is necessary for both GlnB and uridylylated GlnB to be able to stimulate the adenylation and deadenylation reactions, respectively, of ATase (Jiang et al, 1998c). While GlnB binds ATP with micromolar affinity and free ATP concentrations in the cell can be as high as 1 mM (Jiang and Ninfa, 2007; Jiang et al., 1998a), ATP binding, like that of 2-OG, displays negative cooperativity (Jiang and Ninfa, 2007). The first crystal structure of GlnK in complex with AmtB showed that ADP could bind in place of ATP (Conroy et al., 2007), leading to the hypothesis that PII proteins may also act as energy sensors by responding to the ratio of ADP to ATP. However, more recent data suggest that additional work is needed to validate this hypothesis (Bennett et al., 2009; Chapman et al., 1971; Huergo et al., 2013; Radchenko et al., 2013; Zhang et al., 2009). In addition to roles in sensing nitrogen and perhaps energy, some PII proteins may also be carbon sensors (Feria Bourrellier et al., 2010; Huergo et al., 2013).

For several reasons the sensing system anchored by the PII proteins is fascinating. First, two separate sensors detect two distinct metabolites, one that represents nitrogen depletion (2-OG) and the other abundance (glutamine). Second, because 2-OG binding exhibits negative cooperativity, the PII proteins are sensitive to differential flux through the nitrogen assimilation pathway rather than acting as binary switches. Lastly, the PII protein pathway is a good example of a particular sensing strategy: instead of directly sensing, like chemoreceptors, the nutrient of interest, it senses metabolites involved in nitrogen assimilation, thus providing specificity to this process over other ammonium-using reactions.



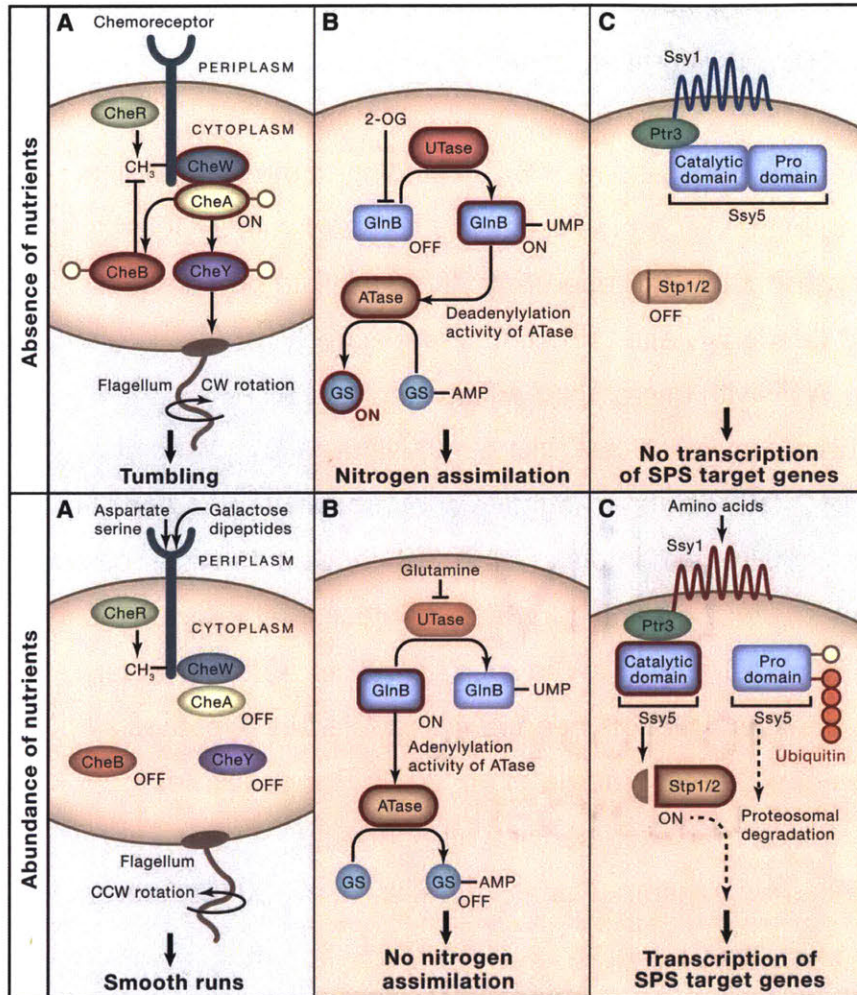


**Figure 2: Select sensing pathways in unicellular organisms.**

A. Chemotaxis in *E. coli*: In the absence of nutrients, the chemoreceptor activates the CheA kinase associated with CheW. CheA in turn phosphorylates and activates two critical effectors: CheY, which promotes clockwise rotation in the flagellar motor and random tumbling motions, and CheB, a demethylase involved in the adaptation process which counteracts CheR, the constitutive methylase. Conversely, the presence of nutrients suppresses this pathway and the default counterclockwise rotation of the rotor ensues to yield smooth runs.

B. PII proteins in alpha-proteobacteria: This tightly regulated protein family serves to control the adenylation state and activity of glutamine synthase (GS). When nitrogen is absent, the precursor of nitrogen assimilation reactions, 2-OG, accumulates, binds to,



and inhibits the unmodified PII protein GlnB, which is unable to stimulate the adenylation reaction of ATase. The unmodified and active form of GS accumulates. When nitrogen is abundant, glutamine levels are high, and this molecule binds and inhibits UTase, which permits the unmodified form of GlnB to accumulate and promote GS inhibition, by activating the adenylation of GS by ATase.

C. SPS pathway in *S. cerevisiae*: Extracellular amino acids bind directly to Ssy1, a transceptor with homology to amino acid permeases but lacking transport activity, to activate the SPS (Ssy1-Ptr3-Ssy5) pathway. Amino acids bind to Ssy1 to stimulate a conformational change in Ssy5, resulting in the phosphorylation and subsequent ubiquitin-mediated degradation of its inhibitory pro-domain. Ptr3 acts as an adapter to mediate this process. Release of the catalytic domain of Ssy5 permits it to cleave the latent transcription factors Stp1 and Stp2, which translocate to the nucleus to activate transcription of genes involved in amino acid transport and metabolism. (Figure adapted from Conrad et al, 2014).

## **EUKARYOTES**

### **Nutrient sensing systems unique to yeast**

In this section we discuss several pathways that sense extracellular nutrients and are specific to yeast, including those controlled by Ssy1, MEP2, Snf3, and Rgt2. Like bacterial chemoreceptors, these transmembrane proteins sense a diverse set of nutrients including amino acids, ammonium, and glucose. They connect the status of the external world to varied intracellular processes - from the expression of transporters to the formation of pseudohyphae. Unlike bacterial chemoreceptors, Ssy1, MEP2, Snf3, and Rgt2 are homologous to nutrient transporters and are an important class of sensors sometimes termed transceptors. Many of these transceptors play key roles in allowing yeast to decide which nutrient to uptake and utilize when many are available and thus ensure an optimal growth rate.

### **MEP2: A putative extracellular ammonium sensor**

Yeast evaluate and respond to a diverse set of nitrogen-containing compounds, and have a hierarchical preference for nitrogen sources. In a process termed nitrogen catabolite repression, the presence of desired sources such as ammonium and glutamine represses the transcription of genes involved in scavenging and metabolizing poor sources such as proline (Zaman et al., 2008). Yeast can utilize ammonium as their sole source of nitrogen and assimilate it via biochemical reactions akin to those described in prokaryotes: glutamate dehydrogenase transaminates  $\alpha$ -ketoglutarate to produce glutamate, which glutamine synthase uses with ammonium to make glutamine (Marini et al., 1994).

*S. cerevisiae* trigger a dimorphic transition under limiting ammonium conditions. Diploid cells form pseudohyphae that extend from the colony into the surrounding medium (Gimeno et al., 1992), permitting normally sessile yeast colonies to forage for nutrients at a distance from their colonization point (Gimeno et al., 1992). For this

metamorphosis to take place, the lack of ammonium outside the cell must be sensed and transduced to downstream signaling pathways that control filamentous growth. MEP2 is proposed to mediate the sensing role in this pathway (Lorenz and Heitman, 1998).

The MEP (methylamine permease) proteins are members of a family of ammonium channels conserved from bacteria to animals (Marini et al., 1997a; Siewe et al., 1996), although their role in physiology has diverged in metazoans, as discussed below. In yeast, there are three MEP proteins, the most divergent being MEP2 (Marini et al., 1997b; Marini et al., 1994), and all three can uptake extracellular ammonium ions into cells. Of the three, MEP2 has the highest affinity with a  $K_m$  of 1-2  $\mu$ M which contrasts with that of MEP3, which is 1-2 mM (Marini et al., 1997b). Given the dual role of MEP2 in detecting low ammonium concentrations in the environment and scavenging it for use as a nitrogen source, it makes sense that the highest affinity transporter of the three evolved to be the sensor. Under low or absent ammonium, MEP2 is essential for pseudohyphal growth and expressed on the plasma membrane (Dubois and Grenson, 1979; Rutherford et al., 2008) (**Figure 2C**). When ammonium is plentiful, MEP2 is internalized and targeted for degradation (Marini et al., 1997b; Zurita-Martinez et al., 2007).

Substantial evidence supports the notion that MEP2 is an ammonium sensor that controls pseudohyphal growth upon ammonium deprivation (Lorenz and Heitman, 1998). First, MEP2, but not MEP1 or MEP3, is required for pseudohyphal formation under these conditions, and its first intracellular loop is critical for this action (Lorenz and Heitman, 1998). Later mutagenesis studies revealed that a transport deficient MEP2 prevents pseudohyphal growth despite proper localization and expression (Marini et al., 2006). However, transport is necessary but not sufficient for ammonium sensing as there are transport proficient but signaling defective MEP2 mutants (Rutherford et al., 2008). The identity of the proteins that MEP2 engages to induce signaling remains unknown. Current evidence points to the involvement of GPA2, a G protein alpha subunit, and RAS2, in increasing cAMP levels to activate protein kinase A (PKA) in

response to the absence of ammonium (Gimeno et al., 1992; Kübler et al., 1997; Lorenz and Heitman, 1997; Lorenz and Heitman, 1998; Van Nuland et al., 2006).

As a transceptor, passage of ammonium through MEP2 is likely to induce a conformational change that enables it to interact with downstream effectors that signal pseudohyphal growth. Conformational changes have been observed in the bacterial homologue of MEP2, AmtB, but these remain to be linked to ammonium sensing (Andrade et al., 2005; Khademi et al., 2004; Zheng et al., 2004).

While ammonium is a valuable nitrogen source for bacteria, fungi, and plants, at high levels it is cytotoxic to animals (Biver et al., 2008). Therefore, in animals ammonium transport is essential for its excretion, and MEP-like proteins have persisted throughout evolution (Marini et al., 1997a). Reflecting their functional conservation, human orthologs of MEP2, the erythroid specific Rh(rhesus)-type proteins, can transport ammonium in yeast (Marini et al., 2000; Marini et al., 1997a). Proteins of the Rh family are expressed in various organs and play critical roles in physiology. For instance, renal cortex cells excrete ammonium into urine via an Rh transporter (Biver et al., 2008; Garvin et al., 1988; Knepper et al., 1989). A role for these proteins as ammonium sensors has not been ascertained.

### **Extracellular amino acid sensing: The SPS pathway**

Yeast coordinate signals from several major pathways to detect amino acids and alter gene expression and developmental decisions. While the GCN2 and TOR pathways discussed later respond to intracellular amino acids, the Ssy1-Ptr3-Ssy5 (SPS) pathway senses extracellular amino acids (Klasson et al., 1999). The SPS pathway is conserved in other yeast, such as *Candida albicans*, but not in higher eukaryotes (Davis et al., 2011), which have evolved distinct pathways for sensing extracellular amino acids (Conigrave et al., 2000; Cummings and Overduin, 2007) (**Figure 1**).

Ssy1 is a transporter-like protein in the plasma membrane of *S. cerevisiae* that functions, like MEP2, as a transceptor. Although it has sequence homology to amino acid permeases (AAP), it lacks transport activity, and, unlike other AAPs, possesses a long N-terminal extension that is important for transmitting the availability of nutrients to downstream signaling elements (Bernard and Andre, 2001; Iraqui et al., 1999; Forsberg and Ljungdahl, 2001). Ssy1 forms a complex with Ptr3 and Ssy5 that, when amino acids are present, activates a signaling pathway that enhances the transcription of amino acid transport and metabolism genes (Iraqui et al., 1999).

Ssy5 is an endoprotease composed of an inhibitory pro-domain and a catalytic domain (Abdel-Sater et al., 2004; Andreasson, 2006). Amino acid binding to Ssy1 on the extracellular side of the plasma membrane induces a conformational change in Ssy5 that leads to the phosphorylation and ubiquitin-mediated degradation of its pro-domain (Abdel-Sater et al., 2011; Pfirrmann et al., 2010; Forsberg and Ljungdahl, 2001). This relieves the inhibition of the catalytic domain of Ssy5, which can cleave and activate Stp1 and Stp2, transcription factors that translocate into the nucleus to activate relevant genes. Ptr3, the third subunit of SPS, is essential for Ssy5 activation, and is an adaptor that helps transduce conformational changes from Ssy1 to Ssy5 upon amino acid binding, and to bring the prodomain of Ssy5 into proximity with its kinase to facilitate its phosphorylation (Omnus and Ljungdahl, 2013; Forsberg and Ljungdahl, 2001). Evidence that SPS acts as a direct sensor of amino acids came from mutagenesis experiments demonstrating that certain Ssy1 mutants can alter the sensitivity of the SPS complex to extracellular amino acids (Poulsen et al., 2008). Interestingly, *S. cerevisiae* which harbor mutations in either Ptr3 or Ssy1 have increased vacuolar pools of basic amino acids (Klasson et al., 1999). This observation suggests that in the absence of a signal relaying the presence of extracellular amino acids, yeast attempt to increase their vacuolar stores of amino acids, perhaps allowing them to be more independent of extracellular amino acid availability. Ssy1 is an interesting variant of the transceptor class of sensors because, unlike MEP2, it does not retain transport activity.

## **Snf3 and Rgt2: Extracellular glucose sensors**

In addition to sensing extracellular amino acids, *S. cerevisiae* also detect extracellular glucose. Fermentation of this hexose yields the energy and carbon precursors needed to fuel growth, and glucose rapidly stimulates restructuring of the transcriptome to permit yeast to take full advantage of its presence (Zaman et al., 2008). In a process termed carbon catabolite repression, glucose and fructose repress processes involved in the metabolism of less preferred carbon sources, with this repression occurring primarily at the transcriptional level (Gancedo, 1998; Santangelo, 2006). Here, we discuss the glucose-sensing pathway that regulates Rgt1, a transcription factor, and is necessary for glucose utilization. In the absence of glucose the Snf1 (AMPK) pathway discussed later is essential for the use of less preferred carbon sources (Zaman et al., 2008)

Under glucose limitation, Rgt1, in complex with the Ssn6-Tup1 repressor and the Mth1 and Std1 co-repressors, binds to the promoters of hexose transporter genes (*HXT*) and inhibits their transcription (Kim et al., 2003; Lakshmanan et al., 2003; Ozcan and Johnston, 1995; Polish, 2005; Theodoris et al., 1994; Tomas-Cobos and Sanz, 2002). Glucose binds to two transporter-like glucose sensors, Snf3 and Rgt2, which are needed to activate *HXT* expression. Snf3 senses low glucose concentrations and elevates the transcription of high affinity hexose transporter genes while Rgt2 senses high glucose levels and promotes low-affinity hexose transporter expression (Bisson et al., 1987; Ozcan et al., 1996). Glucose binding to Snf3 and Rgt2 recruits Mth1 and Std1, through an unknown mechanism, to the plasma membrane, where they are subsequently phosphorylated, ubiquitylated, and degraded (Flick, 2003; Kim et al., 2006; Moriya and Johnston, 2004; Schmidt et al., 1999). Without its co-repressors, Ssn6-Tup1 also dissociates from Rgt1 (Roy et al., 2013), leaving it free to be phosphorylated by the cAMP-dependent protein kinase (PKA) and to become a transcriptional activator of the *HXT* genes (Jouandot et al., 2011).

The Snf3/Rgt2 pathway represents yet another example of a nutrient sensing pathway controlled by transceptors. In addition, analogous to the regulation of the PII proteins by 2-OG, the Snf3/Rgt2 pathway senses varied glucose levels rather than behaving like an on-off switch. Unlike the PII proteins, which use negative cooperativity between 2-OG binding sites to allow for graded responses, the Snf3/Rgt2 pathway utilizes two separate sensors, with different affinities for the nutrient of interest.

### **Nutrient sensing pathways conserved from yeast to mammals**

In this section we highlight the AMPK, GCN2, and TOR pathways, which are conserved, at least in part, from yeast to man. In multicellular organisms, evolution has adapted the architectures of these pathways so they can sense hormonal cues in addition to the nutrients that the pathways detect in yeast. Given their roles in sensing essential nutrients, like amino acids and glucose, it is perhaps not surprising that the three pathways regulate feeding behavior.

Lastly, we briefly discuss how the emergence of the vacuole/lysosome in eukaryotes and its use as a storage depot for nutrients in fungi (Klionsky et al., 1990; Li and Kane, 2009), and likely mammals, has led to a need to sense its contents, which is a recently appreciated obligation of the TOR pathway.

### **AMPK: A eukaryotic fuel gauge**

A key event in the emergence of eukaryotes and their diversification and increase in complexity was the engulfment of oxidative bacteria, the predecessors of mitochondria. It has been argued that prokaryotes lack the energetic resources to maintain large amounts of regulatory DNA, but that the acquisition of mitochondria nearly 4 billion years ago alleviated the pressure to remove excess DNA and permitted eukaryotes to explore hundreds of thousands-fold more genes (Lane and Martin, 2010).

Eukaryotes must sense their cellular energy balance and relay it to mitochondria and other parts of the cell that help maintain energy homeostasis (Hardie et al., 2012). A key energy sensor is the serine/threonine-directed AMP-activated protein kinase (AMPK), which regulates many catabolic and anabolic processes in response to energy levels (Gowans and Hardie, 2014).

AMPK was initially discovered in mammals as a kinase that phosphorylates and inactivates acetyl-CoA carboxylase (ACC) and HMG-CoA reductase, rate-limiting enzymes in fatty acid and cholesterol synthesis, respectively (Carling et al., 1989; Carling and Hardie, 1986). The *S. cerevisiae* homolog of AMPK, Snf1 (sucrose nonfermenting), had been found earlier in a screen for yeast that failed to grow on nonfermentable carbon sources, but it was not recognized as a homolog of AMPK until later (Carlson et al., 1981; Mitchelhill et al., 1994; Woods et al., 1994). AMPK orthologs have also been identified in plants and are referred to as SNF-1 related kinases (SnRK1). SnRK1 from rye endosperm can complement yeast *snf1* mutants, highlighting the conserved function of AMPK (Alderson et al., 1991).

In response to decreasing energy levels, AMPK and Snf1 phosphorylate substrates that activate processes that generate ATP and inhibit those that consume it. The conservation of the pathway throughout evolution is apparent in the high degree of similarity between the key effectors of AMPK and Snf1. For instance, both AMPK and Snf1 control glucose-linked processes. Snf1 inactivates the Mig1 transcriptional repressor, relieving glucose-repressed genes (Chronakis et al., 2004). Analogously, AMPK stimulates glucose uptake and glycolysis and inhibits glycogen synthesis (Yuan et al., 2013). Additional key effectors include the TORC1 and mTORC1 complexes, which function as master regulators of growth in yeast and mammals, respectively, and are discussed below. By regulating mTORC1 and TORC1, AMPK and Snf1 govern the switch between anabolism and catabolism to maintain metabolic homeostasis. In mammals, AMPK inhibits mTORC1 via two mechanisms. First, it phosphorylates and activates the TSC2 GTPase activating protein, a major inhibitor of the pathway (Inoki et al., 2003b). Second, it phosphorylates raptor, a subunit of mTORC1, resulting in 14-3-3



binding and inhibition of mTORC1 kinase activity (Gwinn et al., 2008). Likewise, Snf1 has also been proposed to phosphorylate critical subunits of TORC1 (Braun et al., 2014). Aside from these well-characterized targets, AMPK and Snf1 likely have hundreds of additional substrates that control a wide range of processes (Hardie et al., 2012; Mihaylova and Shaw, 2011).

How do energy levels regulate AMPK? AMPK binds adenine nucleotides to sense the ratio of ADP or AMP to ATP, a critical barometer of the energy state of the cell. In times of nutrient abundance, this ratio is low. Upon energetic stress, the ratio rises as ATP levels drop with a concomitant rise in ADP, which is converted to AMP due to high cytosolic adenylate kinase activity (Hardie and Hawley, 2001). As opposed to ATP levels, AMP and ADP levels are more sensitive indicators of energy status; a 2-fold drop in ATP levels reflects a 50-fold drop in AMP (Hardie and Mackintosh, 1992). Furthermore, despite the millimolar concentrations of cellular ATP, a significant proportion of it is in complex with  $Mg^{2+}$  and does not bind well to AMPK (Xiao et al., 2011).

The mechanism of adenine nucleotide regulation of AMPK has been extensively characterized. AMPK is a trimeric complex composed of  $\alpha$  kinase,  $\beta$  carbohydrate binding, and  $\gamma$  regulatory subunits (Kemp, 2004; Scott et al., 2004). There are theoretically four nucleotides binding sites in the  $\gamma$  subunit, although one remains empty and another constitutively binds AMP (Xiao et al., 2007). A tripartite mechanism controls AMPK in mammalian cells. First, AMPK binds AMP and undergoes a conformational change that enhances the ability of the kinases LKB1 and CaMKKKB to phosphorylate and activate it. Second, AMP binding to AMPK protects it against dephosphorylation by currently unidentified phosphatases. Third, AMP further allosterically activates the kinase up to 13 fold (Carling et al., 1989; Gowans and Hardie, 2014). ATP binding antagonizes all of these effects (Corton et al., 1995). As a result of the two nucleotide binding sites, both of which can bind AMP, ADP, or ATP, AMPK regulation is graded in response to energy status, just like PII protein function is in response to 2-OG. As AMP

levels rise under extreme energetic stress, AMP binds both sites to maximally activate AMPK.

Recent studies have uncovered conservation between the regulatory mechanisms of fungal and plant AMPK homologues and those of the mammalian kinase. In yeast, Snf1 is also heterotrimeric, binds nucleotides and is regulated by opposing kinases and phosphatases (Hong et al., 2003; Hong et al., 2005; Jin et al., 2007; Sutherland et al., 2003; Townley and Shapiro, 2007). However, unlike AMPK, it appears that ADP, not AMP, promotes phosphorylation of Snf1 by inhibiting its dephosphorylation, and AMP does not allosterically activate Snf1 (Mayer et al., 2011; Mitchelhill et al., 1994; Woods et al., 1994). Hence, in yeast there is a bipartite mechanism of activation, with ADP playing a prominent role.

With the onset of multicellularity, physiological processes evolved in metazoans that maintain homeostasis for the organism as a whole, and AMPK acquired new modes of regulation. Specifically, hormones and cytokines enable the nutrient-sensing organs of multicellular organisms to communicate the nutritional state to other organs to elicit tissue-specific responses. The coordinated actions of leptin, insulin, and ghrelin, amongst others, regulate the organismal response to nutrients, or lack thereof, and are well appreciated to regulate AMPK. Upon food consumption, blood glucose levels rise and pancreatic beta cells release insulin, which promotes anabolic and inhibits catabolic processes in many tissues. These effects are mediated in part through Akt, a kinase that inhibits AMPK by phosphorylating it at Ser<sup>485/491</sup>, and antagonizing LKB1-mediated Thr<sup>172</sup> phosphorylation, which normally activates AMPK (Horman et al., 2006).

Many nutrient-regulated hormones signal to the brain to control feeding behavior. Under fasting or starvation conditions, enteroendocrine cells of the stomach release ghrelin, which signals hunger. Conversely, during feeding, adipocytes release leptin, which signals satiety. These hormones alter the activity of neuronal circuits in the hypothalamic arcuate nucleus, the appetite control center of the brain (Dietrich and Horvath, 2011; Hardie et al., 2012; Pinto et al., 2004). Several studies point to a role for

AMPK in the control of feeding. Ghrelin activates AMPK in the hypothalamus and leads to a subsequent increase in food intake. Overexpression of a dominant negative form of AMPK in the hypothalamus restrains feeding while direct injection of pharmacological AMPK activators results in hyperphagia (Andersson et al., 2004; Minokoshi et al., 2004). These effects are likely mediated through modulation of AMPK in presynaptic neurons that impinge on neurons critical for feeding control (Gowans and Hardie, 2014; Yang et al., 2011). Ghrelin likely binds GHSR1, a G protein coupled receptor in the presynaptic neuron, triggering the release of  $Ca^{2+}$  that stimulates CaMKKK to activate AMPK (Yang et al., 2011). Meanwhile, leptin may function in a manner similar to insulin by activating the PI3K-Akt axis and controlling the phosphorylation state of AMPK (Dagon et al., 2012). Therefore, as complex feeding behaviors arose in multicellular organisms, AMPK was coopted to function in neuronal circuits to control intake of food.

### **GCN2: A sensor of amino acid deprivation**

Alongside the SPS pathway, which senses extracellular amino acids in yeast, eukaryotes evolved a parallel pathway to detect intracellular amino acid levels: the general amino acid control non-derepressible 2 (GCN2) pathway. GCN2 senses the uncharged tRNAs that accumulate upon amino acid deprivation. GCN2 attenuates translation, which not only consumes amino acids but is also one of the most energy demanding processes in the cell (Lane and Martin, 2010).

While GCN2 is found only in eukaryotes, the use of uncharged tRNAs to signal amino acid deprivation is conserved to bacteria. Upon amino acid starvation in *E. coli*, uncharged tRNAs bind directly to ribosomes, leading to the production of the odd nucleotides guanosine tetraphosphate and guanosine pentaphosphate (Cashel and Gallant, 1969). These nucleotides repress the synthesis of stable RNAs (rRNA and tRNA) and activate amino acid biosynthetic genes to promote survival in a process referred to as the stringent response (Srivatsan and Wang, 2008).

In yeast GCN2 is dedicated to sensing uncharged tRNAs (Hinnebusch, 1984). Under conditions of amino acid limitation or a defect in an amino acyl tRNA synthetase, *S. cerevisiae* upregulate the transcription of genes involved in amino acid biosynthesis, a process termed general amino acid control (Hinnebusch, 1988; Hinnebusch, 2005; Wek et al., 1995). When present, uncharged tRNAs bind to the histidyl tRNA synthetase-like domain of GCN2, which lacks residues critical for synthetase activity and histidine specific binding, thus enabling GCN2 to respond to a variety of uncharged tRNAs (Wek et al., 1989; Wek et al., 1995). The binding triggers GCN2 homodimerization (Narasimhan et al., 2004) and autophosphorylation (Diallinas and Thireos, 1994), allowing it to phosphorylate and inhibit its only known substrate, eukaryotic initiation factor 2a (eIF2a) (Dever et al., 1992). This phosphorylation prevents efficient translation initiation of most mRNAs by limiting the pool of ternary complex, which consists of eIF2, GTP, and methionyl initiator tRNA and is required for translation initiation (Abastado et al., 1991; Dever et al., 1992; Hinnebusch, 1993).

While most mRNAs are translationally repressed upon amino acid deprivation, the mRNA encoding the GCN4 transcription factor is derepressed so that GCN4 can accumulate and activate the expression of genes that promote amino acid biosynthesis (Abastado et al., 1991; Dever et al., 1992; Hinnebusch, 1993). A cluster of four upstream open reading frames (uORFs) in the 5' untranslated region of the GCN2 mRNA permits this unique regulation (Hinnebusch, 2005). Under nutrient replete conditions, a ternary complex forms at the first uORF. It then dissociates and another forms at the subsequent uORFs, thus preventing translation of the main ORF. However, upon starvation, ternary complex formation is delayed, and rebinding at latter uORFs reduced. Larger proportions of preinitiation complexes bypass the uORFs and form ternary complexes before reaching and translating the main ORF (Abastado et al., 1991; Hinnebusch, 1984; Mueller and Hinnebusch, 1986).

In mammals, GCN2 pathway architecture is reminiscent of that in yeast (Berlenga et al., 1999; Sood et al., 2000) as it is activated by a limitation in an essential amino acid or inhibition in the synthesis of a nonessential amino acid. uORFs also

regulate the translation of the mammalian GCN4 orthologue, ATF4, a basic leucine zipper transcription factor (Vattem and Wek, 2004). ATF4 induces a cascade of transcriptional regulators that contribute to a gene expression program that modulates apoptosis, autophagy, and amino acid metabolism, including upregulation of select amino acyl tRNA synthetases and amino acid transporters (B'chir et al., 2013; Bunpo et al., 2009; Harding et al., 2000; Harding et al., 2003; Krokowski et al., 2013). Deletion of GCN2 in mice decreases their viability during prenatal and postnatal development under conditions of nutritional stress, most notably leucine deprivation (Zhang et al., 2002). When challenged with a leucine-free diet for several days, GCN2-null mice lose more body weight than wild type counterparts and a significant proportion perish (Anthony et al., 2004).

Like AMPK, GCN2 has acquired a critical role in controlling feeding behavior in animals. When rodents encounter a food source that lacks a single essential amino acid, they recognize this deficiency and reduce the intake of the imbalanced food (Koehnle et al., 2003). GCN2 activity in the anterior piriform cortex (APC) mediates this behavior. Injection of amino acid alcohol derivatives such as threoninol into the APC increases the levels of uncharged tRNAs and promotes the rejection of diets low in the corresponding amino acid (Hao et al., 2005). Furthermore, mice with full body or brain specific GCN2 deletions fail to reject food depleted of leucine or threonine, unlike wild type counterparts (Hao et al., 2005; Maurin et al., 2005). At the signaling level, ingestion of a meal imbalanced in amino acid composition rapidly elevates phosphorylated eIF2 $\alpha$  in APC neurons of wild type, but not GCN2-null mice (Hao et al., 2005; Maurin et al., 2005)(Gietzen et al., 2004). The need to adapt feeding behavior to changes in nutrient levels is by no means restricted to animals. *Drosophila* also sense changes in dietary amino acids and reduce their intake of foods deficient in essential amino acids (Bjordan et al., 2014; Ribeiro and Dickson, 2010; Toshima and Tanimura, 2012; Vargas et al., 2010). As in animals, GCN2 plays a critical role within neuronal circuits to mediate this rejection by repressing GABA signaling within dopaminergic neurons of the brain (Bjordan et al., 2014). Together, these findings point to a role for the detection of uncharged tRNAs by GCN2 in controlling circuits in flies and animals that protect

against the consumption of imbalanced food sources.

A separate pathway discussed below, TORC1/mTORC1, evolved in parallel to the GCN2 pathway to sense the availability of intracellular amino acids. The mechanisms for crosstalk between the TORC1/mTORC1 and GCN2 pathways were acquired at least twice during evolution, albeit in opposing directions. While in yeast GCN2 lies downstream of TORC1, it functions upstream of mTORC1 in mammals (Anthony et al., 2004; Cherkasova and Hinnebusch, 2003; Kubota et al., 2003; Staschke et al., 2010).

### **TOR/mTOR: Master regulators of growth**

Nutrient availability strongly influences the growth of all organisms and starvation conditions can alter developmental programs in both unicellular and multicellular organisms (Oldham, 2000). When faced with nutritional limitation, *S. cerevisiae* exit the mitotic cycle and enter a stationary phase (Zaman et al., 2008), *C. elegans* persist for several months in a state of stasis known as dauer larvae (Klass and Hirsh, 1976) and *Drosophila* postpone their development (Edgar, 2006). Despite the diversity of these organisms, one common pathway, anchored by the target of rapamycin (TOR) kinase, regulates entry into these alternative states in response to environmental cues. Unlike the GCN2 and AMPK pathways, the TOR pathway is unique in that it integrates not a few but many diverse inputs, particularly in mammals. In fact, GCN2 and AMPK both feed into TOR to convey amino acid or energy deprivation, respectively. While we focus on the two major inputs that control mTOR activity - nutrients and growth factors – numerous additional cues converge on it (Laplante and Sabatini, 2012).

The study of TOR began several decades ago with the isolation of a potent antifungal compound from the soils of Rapa Nui, more commonly known as Easter Island. This macrolide, named rapamycin in deference to its site of discovery, garnered clinical and research interest because of its powerful immunosuppressive and anti-proliferative qualities (Morris, 1992; Segall et al., 1986). Genetic studies in yeast led to the identification of TOR1 and TOR2 as key genes mediating rapamycin sensitivity

(Cafferkey et al., 1993; Kunz et al., 1993), and biochemical work in mammals revealed the mTOR (mechanistic target of rapamycin) protein as the direct target of rapamycin (Brown et al., 1994; Sabatini et al., 1994; Sabers et al., 1995). mTOR is a serine/threonine protein kinase that responds to a variety of environmental cues, including nutrient, energy, and growth factor levels, as well as diverse forms of stress, to regulate many anabolic and catabolic processes (Howell et al., 2013; Kim et al., 2013; Laplante and Sabatini, 2012).

Unlike most eukaryotes, *S. cerevisiae*, encode two different TOR proteins, Tor1 and Tor2, which nucleate distinct multi-protein complexes (Helliwell et al., 1994; Loewith et al., 2002). TOR complex 1 (TORC1) consists of Tor1 bound to Kog1, Lst8, and Tco89 and promotes ribosome biogenesis and nutrient uptake under favorable growth conditions. Inhibition of TORC1 by nutrient starvation or rapamycin treatment leads to the activation of macroautophagy and nutrient and stress-responsive transcription factors like GLN3, which is required for the use of secondary nitrogen sources (Jacinto et al., 2004; Wullschleger et al., 2006). TORC2 contains Tor2 bound to Avo1-3, Bit61, and Lst8, is largely rapamycin insensitive, and is thought to regulate spatial aspects of growth, such as cytoskeletal organization (Loewith et al., 2002; Reinke et al., 2004; Wedaman et al., 2003).

Mammals also have two mTOR-containing complexes but only one gene encoding mTOR. mTOR complex 1 (mTORC1) consists of raptor, mLST8, PRAS40, and Deptor (Laplante and Sabatini, 2012) and modulates mass accumulation through the control of many anabolic and catabolic processes, including protein, lipid, and nucleotide synthesis; ribosome and lysosome biogenesis; and autophagy. mTORC2 controls cell proliferation and survival and is further reviewed elsewhere (Jacinto et al., 2004; Oh and Jacinto, 2011; Sarbassov et al., 2004).

The connection between TORC1 and the response to the nutritional state emerged from observations in *S. cerevisiae*, *D. melanogaster*, and mammalian cells where TOR inhibition leads to phenotypes akin to those observed under starvation

(Barbet et al., 1996; Oldham, 2000; Peng et al., 2002; Zhang et al., 2000).

Environmental amino acid levels were found to activate the mTORC1 pathway as measured by the phosphorylation of S6K1 and 4EBP1, two well-known mTORC1 substrates (Hara, 1998; Wang et al., 1998), and to signal independently of the growth factor input to mTORC1 (Hara, 1998; Nobukuni et al., 2005; Rocco et al., 2005; Smith et al., 2005; Svanberg and Moller-Loswick, 1996; Wang et al., 1998)

More recent work showing that the Rag GTPases are necessary and sufficient for mTORC1 to sense amino acids (Kim et al., 2008; Sancak et al., 2008) is beginning to reveal the logic of how the pathway integrates inputs from nutrients and growth factors. What has emerged is a bipartite mechanism of mTORC1 activation involving two distinct small GTPases: first, the control of mTORC1 subcellular localization by nutrients through the Rag GTPases, and, second, the control of mTORC1 kinase activity by growth factors and energy levels through the Rheb GTPases (Zoncu et al., 2011). Both inputs are needed for full activation of mTORC1 as in the absence of either the pathway is off.

The Rag GTPases exist as heterodimers of the related and functionally redundant RagA or RagB bound to RagC or RagD, which are also very similar (Hirose et al., 1998; Schürmann et al., 1995; Sekiguchi et al., 2001). Under nutrient replete conditions the Rag GTPases bind mTORC1 and promote its recruitment to the lysosomal surface where its activator Rheb also resides (Buerger et al., 2006; Saito et al., 2005; Sancak et al., 2008) (**Figure 3**). The function of each Rag within the heterodimer is poorly understood and their regulation is undoubtedly complex as many distinct factors play key roles. A lysosome-associated molecular machine consisting of the Ragulator and vacuolar ATPase (v-ATPase) complexes regulates the Rag GTPases and is necessary for the sensing of amino acids by mTORC1 (Sancak et al., 2010; Zoncu et al., 2011). Ragulator binds the Rag GTPases to the lysosome and also has nucleotide exchange activity for RagA/B (Bar-Peled et al., 2012; Sancak et al., 2010), but the function of the v-ATPase in the pathway is unknown. Two GTPase activating protein (GAP) complexes, which are both tumor suppressors, promote GTP hydrolysis



by the Rag GTPases, with GATOR1 acting on RagA/B (Bar-Peled et al., 2013) and Folliculin-FNIP2 on RagC/D (Tsun et al., 2013). Lastly, a distinct complex called GATOR2 negatively regulates GATOR1 through an unknown mechanism (Bar-Peled et al., 2013). The Sestrins were recently identified as GATOR2-interacting proteins that negatively regulate mTORC1 (Chantranupong et al., 2014; Parmigiani et al., 2014).

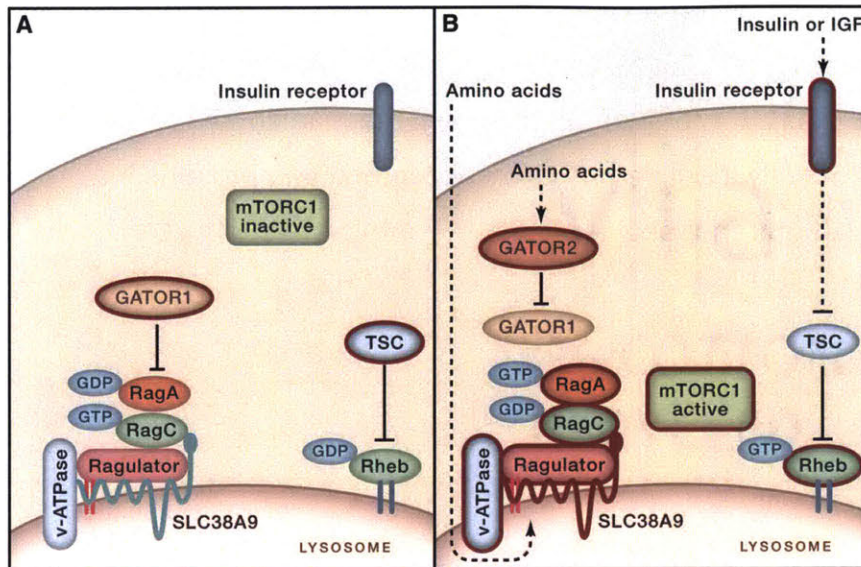


**Figure 3: Nutrient sensing by the TOR pathway.**

A. In the absence of amino acids and growth factors, mTORC1 is inactive. This is controlled by two separate signaling pathways. First, in the absence of amino acids GATOR1 is an active GAP towards RagA, causing it to become GDP bound. In this state, mTORC1 does not localize to the lysosomal surface. Secondly, in the absence of insulin or growth factors, TSC is an active GAP towards Rheb and stimulates it to be GDP bound.

B. In the presence of amino acids and growth factors, mTORC1 is active. Amino acids within the lysosome signal through SLC38A9 to activate the amino acid sensing branch. Ragulator is active, causing RagA to be GTP bound. This binding state is reinforced by the fact that GATOR1 is inactive in the presence of amino acids, as GATOR2 inhibits it. The Rag heterodimer in this nucleotide conformation state recruits mTORC1 to the lysosomal surface. In addition, the presence of insulin or growth factors activates a pathway that inhibits TSC, leaving Rheb GTP bound. In this state, Rheb activates mTORC1 when it translocates to the lysosomal surface.

Growth factors and energy levels regulate the Rheb input to mTORC1 (Inoki et al., 2003a; Long et al., 2005) through a heterotrimeric complex comprised of the tuberous sclerosis complex (TSC) proteins, TSC1, TSC2, and TBC1D7, which together act as a GAP for Rheb (Brugarolas et al., 2004; Dibble et al., 2012; Garami et al., 2003; Inoki et al., 2003a; Long et al., 2005; Sancak et al., 2008; Saucedo et al., 2003; Stocker et al., 2003; Tee et al., 2002). Not all unicellular organisms encode all components of the TSC axis. For instance, *S. cerevisiae* only have a gene for Rheb, and it is not required for growth or viability, unlike TOR itself, suggesting that it likely plays a diminished, if any, role in the TOR pathway in budding yeast (Urano et al., 2000). In contrast, *S. pombe*, which diverged from *S. cerevisiae* more than 400 million years ago, encode TSC1, TSC2, and Rheb (Rhb1), whose functions mirror their mammalian equivalents. Rhb1 is essential for growth and it is negatively regulated by TSC1 and TSC2, whose loss results in defects in amino acid uptake and the nitrogen starvation response (Ma et al., 2013; Mach et al., 2000; Matsumoto et al., 2002; Nakashima et al., 2010; Urano et al., 2007; Uritani et al., 2006; van Slegtenhorst et al., 2004)

While in mammals, growth is intimately linked to amino acid availability, yeast are more concerned with the quality and abundance of nitrogen and can uptake and metabolize a host of nitrogen sources, including amino acids which are deaminated to yield ammonia which will rapidly become ammonium in the cell. In yeast, the aforementioned SPS and GCN2 pathways directly or indirectly, respectively, sense amino acid levels but the actual intracellular signal for TORC1 remains less clear (Broach, 2012). Early studies showed that TORC1 is a major regulator of the nitrogen catabolite repression program (Hardwick et al., 1999; Shamji et al., 2000), although later work emphasizes that TORC1 is likely not the sole player regulating this pathway (Broach, 2012). Further studies are needed to ascertain whether TOR is involved in the sensing of an as yet unidentified nitrogen source in yeast.

More recent evidence indicates that TORC1 is involved in amino acid signaling in yeast (Binda et al., 2009; De Virgilio and Loewith, 2006). TORC1 resides on the vacuole, the equivalent of the metazoan lysosome, although it does not shuttle on and

off its surface in response to nutrient levels as it does in mammals (Binda et al., 2009). Homologs of the Rag GTPases, Gtr1 and Gtr2, exist in yeast and they associate with a vacuolar docking complex consisting of Ego1 and Ego3, which has some structural similarity to Ragulator (Bun-Ya et al., 1992; Dubouloz et al., 2005; Gao and Kaiser, 2006; Kogan et al., 2010). Yeast also have GATOR1 and GATOR2 equivalents, called SEACIT and SEACAT (Panchaud et al., 2013a, b). SEACIT has been proposed to inhibit TORC1 in response to deprivation of sulfur-containing amino acids, such as methionine and cysteine, and controls glutamine synthesis and consumption (Laxman et al., 2014; Laxman et al., 2013; Sutter et al., 2013). Although TORC1 has been posited to respond to amino acids, constitutively active Gtr1 does not make the TORC1 pathway completely resistant to leucine deprivation, unlike constitutively active RagA/B, which in mammals makes mTORC1 signaling resistant to total amino acid deprivation (Binda et al., 2009; Sancak et al., 2008; Efeyan et al., 2012). Furthermore, the Gtr GTPases are dispensable for growth on glutamine or ammonium (Stracka et al., 2014) and constitutively active Gtr1 fails to rescue the TORC1 signaling defect under ammonium deprivation (Binda et al., 2009). If amino acids signal to TORC1, the mechanisms of its activation are likely to be distinct from those through which amino acids activate mTORC1. For instance, orthologs of Sestrins do not exist in yeast, suggesting divergence in the regulation of the upstream components of the nutrient-sensing pathway.

While many components of the pathway upstream of mTORC1 have been identified, the identity of the amino acid sensor(s) remains elusive. Amino acid sensing could initiate from the extracellular, cytosolic, or lysosomal compartments (**Figure 4**). The presence of many mTORC1 pathway components on the lysosome suggests that this organelle is more than simply a scaffold surface for mTORC1 activation. Rather, there is the intriguing possibility that lysosomes act as storage sites for amino acids, and that amino acid availability within this compartment is sensed by mTORC1. The storage of nutrients in vacuoles, which is established in yeast, may also occur in mammalian cells as some studies suggest that certain amino acids, like arginine, are highly enriched in lysosomes relative to the cytosol (Harms et al., 1981). A cell free

assay revealed that the lysosome itself contains the minimal machinery needed for the amino acid-mediated recruitment of mTORC1 to the lysosomal surface (Zoncu et al., 2011).

In an “inside-out” model of sensing, a lysosome-based transmembrane protein would be an alluring candidate amino acid sensor. One such protein is SLC38A9, a newly identified Ragulator-interacting amino acid transporter that resides in the lysosomal membrane and is required for arginine sensing by mTORC1 (Rebsamen et al., 2015; Wang et al., 2015). Like Ssy1 of the SPS pathway, SLC38A9 contains an N-terminal extension that appears necessary for the downstream signaling event (Bernard et al, 2001; Wang et al., 2015). In cells lacking SLC38A9 the mTORC1 pathway has a selective defect in sensing arginine, suggesting that SLC38A9 is an attractive candidate to be an arginine sensor (Wang et al., 2015). While the mechanism through which SLC38A9 regulates the mTORC1 pathway remains unknown, this transporter is the best candidate so far identified for reporting the contents of lysosomes to mTORC1 in the cytosol. It is very likely that in addition to sensing lysosomal amino acids, mTORC1 will be found to also sense cytosolic amino acids and integrate information from both amino acid pools.



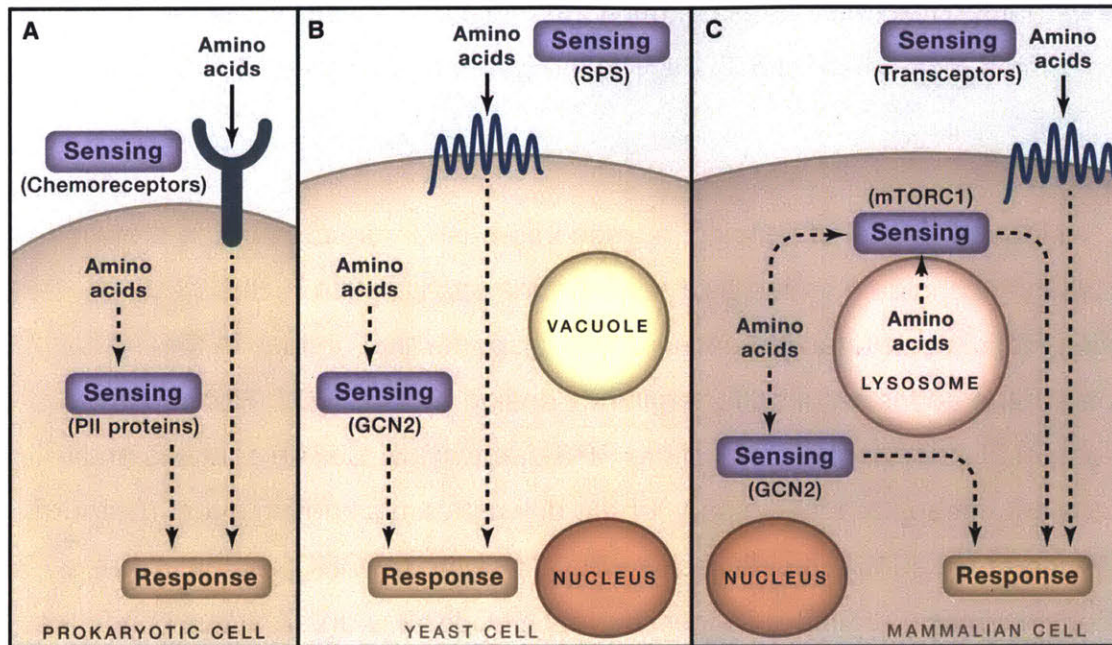


**Figure 4: Evolution of nutrient sensing with the emergence of multicellularity and compartmentalization.**

A. Prokaryotes have two compartments that may contain amino acids: the extracellular space and the cytosol. Amino acid transporters such as the chemoreceptors Tsr and Tar can sense extracellular amino acids. A variety of sensors, including the PII proteins, can detect intracellular amino acids.

B. Similar to prokaryotes, yeast sense extracellular amino acids via plasma membrane transporters, such as Ssy1. In addition, they sense cytosolic amino acid availability with sensors like GCN2. Unlike prokaryotes, however, eukaryotes have organelles such as the vacuole, an additional compartment which may contain amino acids. While it has not yet been established if yeast directly sense amino acid levels within the vacuole, they do contain organelles which can act as alternate storage depots for nutrients and are therefore another potential compartment in which sensing may occur.

C. In mammalian cells, there are three distinct compartments in which sensing may occur, similar to yeast. First, extracellular nutrients are sensed via transporters, not discussed in detail in this review. In addition, cytosolic amino acids are sensed by the

GCN2 pathway. Finally, amino acids stored within the lysosome are sensed by the mTORC1 pathway.

## Perspectives

Nutrient sensors are of diverse structure and function, from membrane spanning transceptors like MEP2 and Ssy1 to the cytosolic kinases AMPK and GCN2. They can directly sense nutrients of interest, such as ammonium by MEP2, or indirectly via a metabolite, such 2-OG by the PII proteins. While direct nutrient sensing will give a good reflection of its overall levels, indirect sensing strategies may allow the sensor to detect each nutrient under specific contexts, such as when flux through the GS/GOGAT pathway is low in the case of the PII proteins.

In eukaryotic cells, the vacuole/lysosome emerged as a nutrient storage compartment and there is increasing evidence that a function of mTORC1 is to sense lysosomal contents and/or function. Although it is unclear if this is true in yeast, the presence of TORC1 on the vacuolar surface suggests it will also be the case in this organism although it is unclear if a homologue of SLC38A9 exists. Many intriguing questions remain concerning nutrient sensing by mTORC1/TORC1. Does the pathway sense all amino acids, or are there particular single amino acids or combinations that are especially important? It is already known that leucine or arginine withdrawal inhibits mTORC1 signaling almost as well as total amino acid deprivation in a few cell lines in culture (Hara, 1998) but how true is this *in vivo* or in diverse cell types? Furthermore, could other Rag-independent mechanisms be involved in relaying amino acid signals to mTORC1? A recent work revealed that in mammalian cells, glutamine, unlike leucine, signals to mTORC1 in a v-ATPase dependent but Rag GTPase independent manner (Jewell et al., 2015). Are different amino acids differentially important in the cytosol versus lysosome? The lysosome is enriched for basic amino acids, hinting that these amino acids may matter more than others in sensing that initiates from this organelle (Harms et al., 1981), which is consistent with the specific defect of cells lacking SLC38A9 in sensing arginine (Wang et al., 2015). Finally, how well conserved the sensors are between organisms will hint at how different or similar the amino acid and nutrient inputs are that drive mTORC1/TORC1 signaling in diverse organisms.



## **ACKNOWLEDGEMENTS**

We thank Zhi-Yang Tsun for insightful input and Tom DiCesare for assistance with figures. This work was supported by grants from the NIH (R01 CA103866 and AI47389) and Department of Defense (W81XWH- 07-0448) to D.M.S. and fellowship support from the NIH to L.C. (F31 CA180271), and to R.L.W. (T32 GM007753). D.M.S. is an investigator of the Howard Hughes Medical Institute.

## REFERENCES

- Abastado, J.P., Miller, P.F., Jackson, B.M., and Hinnebusch, A.G. (1991). Suppression of ribosomal reinitiation at upstream open reading frames in amino acid-starved cells forms the basis for GCN4 translational control. *Molecular and cellular biology* *11*, 486-496.
- Abdel-Sater, F., El Bakkoury, M., Urrestarazu, A., Vissers, S., and Andre, B. (2004). Amino Acid Signaling in Yeast: Casein Kinase I and the Ssy5 Endoprotease Are Key Determinants of Endoproteolytic Activation of the Membrane-Bound Stp1 Transcription Factor. *24*, 9771-9785.
- Abdel-Sater, F., Jean, C., Merhi, A., Vissers, S., and Andre, B. (2011). Amino Acid Signaling in Yeast: Activation of Ssy5 Protease Is Associated with Its Phosphorylation-induced Ubiquitylation. *286*, 12006-12015.
- Adler, S.P., Purich, D., and Stadtman, E.R. (1975). Cascade control of Escherichia coli glutamine synthetase. Properties of the PII regulatory protein and the uridylyltransferase-uridylyl-removing enzyme.
- Alderson, A., Sabelli, P.A., Dickinson, J.R., Cole, D., Richardson, M., Kreis, M., Shewry, P.R., and Halford, N.G. (1991). Complementation of *snf1*, a mutation affecting global regulation of carbon metabolism in yeast, by a plant protein kinase cDNA. *Proceedings of the National Academy of Sciences of the United States of America* *88*, 8602-8605.
- Anand, G.S., and Stock, A.M. (2002). Kinetic basis for the stimulatory effect of phosphorylation on the methylesterase activity of CheB. *Biochemistry* *41*, 6752-6760.
- Andersson, U., Filipsson, K., Abbott, C.R., Woods, A., Smith, K., Bloom, S.R., Carling, D., and Small, C.J. (2004). AMP-activated protein kinase plays a role in the control of food intake. *Journal of Biological Chemistry* *279*, 12005-12008.
- Andrade, S.L.A., Dickmanns, A., Ficner, R., and Einsle, O. (2005). Expression, purification and crystallization of the ammonium transporter Amt-1 from *Archaeoglobus fulgidus*. *Acta Crystallographica Section F: Structural Biology and Crystallization Communications* *61*, 861-863.
- Andreasson, C. (2006). Regulation of transcription factor latency by receptor-activated proteolysis. *20*, 1563-1568.
- Anthony, T.G., McDaniel, B.J., Byerley, R.L., McGrath, B.C., Cavener, D.R., McNurlan, M.A., and Wek, R.C. (2004). Preservation of liver protein synthesis during dietary leucine deprivation occurs at the expense of skeletal muscle mass in mice deleted for eIF2 kinase GCN2. *Journal of Biological Chemistry* *279*, 36553-36561.

B'chir, W., Maurin, A.-C., Carraro, V., Averous, J., Jousse, C., Muranishi, Y., Parry, L., Stepien, G., Fafournoux, P., and Bruhat, A. (2013). The eIF2 $\alpha$ /ATF4 pathway is essential for stress-induced autophagy gene expression. *Nucleic Acids Research*, gkt563.

Bar-Peled, L., Chantranupong, L., Cherniack, A.D., Chen, W.W., Ottina, K.A., Grabiner, B.C., Spear, E.D., Carter, S.L., Meyerson, M., and Sabatini, D.M. (2013). A Tumor Suppressor Complex with GAP Activity for the Rag GTPases That Signal Amino Acid Sufficiency to mTORC1. *Science* 340, 1100-1106.

Bar-Peled, L., Schweitzer, L.D., Zoncu, R., and Sabatini, D.M. (2012). Ragulator Is a GEF for the Rag GTPases that Signal Amino Acid Levels to mTORC1. *Cell* 150, 1196-1208.

Barbet, N.C., Schneider, U., and Helliwell, S.B. (1996). TOR controls translation initiation and early G1 progression in yeast. *Molecular biology of ...*

Bennett, B., Kimball, E., Gao, M., and Osterhout, R. (2009). Absolute metabolite concentrations and implied enzyme active site occupancy in : *Escherichia coli* : Abstract : *Nature Chemical Biology*.

Berg, H.C. (2008). Bacterial flagellar motor. *Current Biology*.

Berg, H.C., and Brown, D.A. (1972). Chemotaxis in *Escherichia coli* analysed by Three-dimensional Tracking. *Nature* 239, 500-504.

Berlanga, J.J., Santoyo, J., and de Haro, C. (1999). Characterization of a mammalian homolog of the GCN2 eukaryotic initiation factor 2 $\alpha$  kinase. *European Journal of Biochemistry* 265, 754-762.

Bernard, F., and Andre, B. (2001). Genetic analysis of the signalling pathway activated by external amino acids in *Saccharomyces cerevisiae* - Bernard - 2001 - *Molecular Microbiology* - Wiley Online Library.

Binda, M., Urban, J., Sturgill, T.W., Loewith, R., and De Virgilio, C. (2009). The Vam6 GEF Controls TORC1 by Activating the EGO Complex. *Molecular cell*.

Bisson, L.F., Neigeborn, L., Carlson, M., and Fraenkel, D.G. (1987). The SNF3 gene is required for high-affinity glucose transport in *Saccharomyces cerevisiae*.

Biver, S., Belge, H., Bourgeois, S., Van Vooren, P., Nowik, M., Scohy, S., Houillier, P., Szpirer, J., Szpirer, C., Wagner, C.A., *et al.* (2008). A role for Rhesus factor Rhcg in renal ammonium excretion and male fertility. *Nature* 456, 339-343.

Bjordal, M., Arquier, N., Kniazeff, J., Pin, J.P., and Léopold, P. (2014). Sensing of amino acids in a dopaminergic circuitry promotes rejection of an incomplete diet in *Drosophila*. *Cell* 156, 510-521.

Borkovich, K.A., Kaplan, N., Hess, J.F., and Simon, M.I. (1989). Transmembrane signal transduction in bacterial chemotaxis involves ligand-dependent activation of phosphate group transfer. *Proceedings of the National Academy of Sciences of the United States of America* 86, 1208-1212.

Borkovich, K.A., and Simon, M.I. (1990). The dynamics of protein phosphorylation in bacterial chemotaxis. *Cell* 63, 1339-1348.

Braun, K.A., Vaga, S., Dombek, K.M., Fang, F., Palmisano, S., Aebersold, R., and Young, E.T. (2014). Phosphoproteomic analysis identifies proteins involved in transcription-coupled mRNA decay as targets of Snf1 signaling. *Science Signaling* 7, ra64-ra64.

Bray, D., Levin, M.D., and Morton-Firth, C.J. (1998). Receptor clustering as a cellular mechanism to control sensitivity. *Nature* 393, 85-88.

Bren, A., and Eisenbach, M. (2000). How signals are heard during bacterial chemotaxis: protein-protein interactions in sensory signal propagation. *Journal of bacteriology* 182, 6865-6873.

Briegel, A., Ortega, D.R., Tocheva, E.I., Wuichet, K., Li, Z., Chen, S., Müller, A., Iancu, C.V., Murphy, G.E., Dobro, M.J., *et al.* (2009). Universal architecture of bacterial chemoreceptor arrays. *Proceedings of the National Academy of Sciences of the United States of America* 106, 17181-17186.

Broach, J.R. (2012). Nutritional control of growth and development in yeast. *Genetics* 192, 73-105.

Brown, E.J., Albers, M.W., Shin, T.B., Ichikawa, K., Keith, C.T., Lane, W.S., and Schreiber, S.L. (1994). A mammalian protein targeted by G1-arresting rapamycin-receptor complex. *Nature* 369, 756-758.

Brown, M.S., Segal, A., and Stadtman, E.R. (1971). Modulation of Glutamine Synthetase Adenylylation and Deadenylylation Is Mediated by Metabolic Transformation of the PII-Regulatory Protein.

Brugarolas, J., Lei, K., Hurley, R.L., Manning, B.D., Reiling, J.H., Hafen, E., Witters, L.A., Ellisen, L.W., and Kaelin, W.G. (2004). Regulation of mTOR function in response to hypoxia by REDD1 and the TSC1/TSC2 tumor suppressor complex. *Genes & Development* 18, 2893-2904.

- Buerger, C., DeVries, B., and Stambolic, V. (2006). Localization of Rheb to the endomembrane is critical for its signaling function. *Biochemical and Biophysical Research Communications* 344, 869-880.
- Bun-Ya, M., Harashima, S., and Oshima, Y. (1992). Putative GTP-binding protein, Gtr1, associated with the function of the Pho84 inorganic phosphate transporter in *Saccharomyces cerevisiae*. *Molecular and cellular biology* 12, 2958-2966.
- Bunpo, P., Dudley, A., Cundiff, J.K., Cavener, D.R., Wek, R.C., and Anthony, T.G. (2009). GCN2 Protein Kinase Is Required to Activate Amino Acid Deprivation Responses in Mice Treated with the Anti-cancer Agent L-Asparaginase. *Journal of Biological Chemistry* 284, 32742-32749.
- Cafferkey, R., Young, P.R., McLaughlin, M.M., Bergsma, D.J., Koltin, Y., Sathe, G.M., Faucette, L., Eng, W.K., Johnson, R.K., and Livi, G.P. (1993). Dominant missense mutations in a novel yeast protein related to mammalian phosphatidylinositol 3-kinase and VPS34 abrogate rapamycin cytotoxicity. *Molecular and cellular biology* 13, 6012-6023.
- Carling, D., Clarke, P.R., Zammit, V.A., and Hardie, D.G. (1989). Purification and characterization of the AMP-activated protein kinase. Copurification of acetyl-CoA carboxylase kinase and 3-hydroxy-3-methylglutaryl-CoA reductase kinase activities. *European Journal of Biochemistry* 186, 129-136.
- Carling, D., and Hardie, D.G. (1986). Isolation of a cyclic AMP-independent protein kinase from rat liver and its effects on the enzymic activity of acetyl-CoA carboxylase. *Biochemical Society transactions*.
- Carlson, M., Osmond, B.C., and Botstein, D. (1981). Mutants of yeast defective in sucrose utilization. *Genetics* 98, 25-40.
- Cashel, M., and Gallant, J. (1969). Two compounds implicated in the function of the RC gene of *Escherichia coli*. *Nature* 221, 838-841.
- Chantranupong, L., Wolfson, R.L., Orozco, J.M., Saxton, R.A., Scaria, S.M., Bar-Peled, L., Spooner, E., Isasa, M., Gygi, S.P., and Sabatini, D.M. (2014). The Sestrins Interact with GATOR2 to Negatively Regulate the Amino-Acid-Sensing Pathway Upstream of mTORC1. *Cell Reports* 9, 1-8.
- Chapman, A.G., Fall, L., and Atkinson, D.E. (1971). Adenylate Energy Charge in *Escherichia coli* During Growth and Starvation.
- Cherkasova, V.A., and Hinnebusch, A.G. (2003). Translational control by TOR and TAP42 through dephosphorylation of eIF2 $\alpha$  kinase GCN2. *Genes Dev* 17, 859-872.

Chronakis, M.P., Gligoris, T., and Tzamarias, D. (2004). The Snf1 kinase controls glucose repression in yeast by modulating interactions between the Mig1 repressor and the Cyc8-Tup1 co-repressor. *EMBO reports* 5, 368-372.

Conigrave, A.D., Quinn, S.J., and Brown, E.M. (2000). I-Amino acid sensing by the extracellular Ca<sup>2+</sup>-sensing receptor.

Conroy, M.J., Durand, A., Lupo, D., Li, X.D., Bullough, P.A., Winkler, F.K., and Merrick, M. (2007). The crystal structure of the Escherichia coli AmtB-GlnK complex reveals how GlnK regulates the ammonia channel. *104*, 1213-1218.

Corton, J.M., Gillespie, J.G., Hawley, S.A., and Hardie, D.G. (1995). 5-Aminoimidazole-4-Carboxamide Ribonucleoside. *European Journal of Biochemistry* 229, 558-565.

Coutts, G. (2002). Membrane sequestration of the signal transduction protein GlnK by the ammonium transporter AmtB. *21*, 536-545.

Cummings, D.E., and Overduin, J. (2007). Gastrointestinal regulation of food intake. *117*, 13-23.

Dagon, Y., Hur, E., Zheng, B., Wellenstein, K., Cantley, L.C., and Kahn, B.B. (2012). p70S6 kinase phosphorylates AMPK on serine 491 to mediate leptin's effect on food intake. *Cell metabolism* 16, 104-112.

Davis, M.M., Alvarez, F.J., Ryman, K., Holm, Å.A., Ljungdahl, P.O., and Engström, Y. (2011). Wild-Type Drosophila melanogaster as a Model Host to Analyze Nitrogen Source Dependent Virulence of Candida albicans. *6*, e27434.

De Virgilio, C., and Loewith, R. (2006). The TOR signalling network from yeast to man. *The International Journal of Biochemistry & Cell Biology* 38, 1476-1481.

Dever, T.E., Feng, L., Wek, R.C., Cigan, A.M., Donahue, T.F., and Hinnebusch, A.G. (1992). Phosphorylation of initiation factor 2 $\alpha$  by protein kinase GCN2 mediates gene-specific translational control of GCN4 in yeast. *Cell* 68, 585-596.

Diallinas, G., and Thireos, G. (1994). Genetic and biochemical evidence for yeast GCN2 protein kinase polymerization. *Gene* 143, 21-27.

Dibble, C.C., Elis, W., Menon, S., Qin, W., Klekota, J., Asara, J.M., Finan, P.M., Kwiatkowski, D.J., Murphy, L.O., and Manning, B.D. (2012). TBC1D7 is a third subunit of the TSC1-TSC2 complex upstream of mTORC1. *Molecular cell* 47, 535-546.

Didion, T., Regenberg, B., Jørgensen, M.U., Kielland-Brandt, M.C., and Andersen, H.A. (1998). The permease homologue Ssy1p controls the expression of amino acid and peptide transporter genes in Saccharomyces cerevisiae. *27*, 643-650.

- Dietrich, M.O., and Horvath, T.L. (2011). Synaptic Plasticity of Feeding Circuits: Hormones and Hysteresis. *Cell* 146, 863-865.
- Dubois, E., and Grenson, M. (1979). Methylamine/ammonia uptake systems in *Saccharomyces cerevisiae*: multiplicity and regulation. *Molecular and General Genetics* MGG 175, 67-76.
- Dubouloz, F., Deloche, O., Wanke, V., Cameroni, E., and De Virgilio, C. (2005). The TOR and EGO Protein Complexes Orchestrate Microautophagy in Yeast. *Molecular cell* 19, 15-26.
- Durand, A., and Merrick, M. (2006). In Vitro Analysis of the *Escherichia coli* AmtB-GlnK Complex Reveals a Stoichiometric Interaction and Sensitivity to ATP and 2-Oxoglutarate. 281, 29558-29567.
- Dyer, C.M., Vartanian, A.S., Zhou, H., and Dahlquist, F.W. (2009). A Molecular Mechanism of Bacterial Flagellar Motor Switching. *Journal of Molecular Biology* 388, 71-84.
- Edgar, B.A. (2006). How flies get their size: genetics meets physiology. *Nature Reviews Genetics* 7, 907-916.
- Efeyan, A., Zoncu, R., Chang, S., Gumper, I., Snitkin, H., Wolfson, R.L., Kirak, O., Sabatini, D.D., and Sabatini, D.M. (2012). Regulation of mTORC1 by the Rag GTPases is necessary for neonatal autophagy and survival. *Nature* 493, 679-683.
- Eisenbach, M. (1996). Control of bacterial chemotaxis. *Molecular microbiology* 20, 903-910.
- Feria Bourrellier, A.B., Valot, B., Guillot, A., Ambard-Bretteville, F., Vidal, J., and Hodges, M. (2010). Chloroplast acetyl-CoA carboxylase activity is 2-oxoglutarate-regulated by interaction of PII with the biotin carboxyl carrier subunit. 107, 502-507.
- Flick, K.M. (2003). Grr1-dependent Inactivation of Mth1 Mediates Glucose-induced Dissociation of Rgt1 from HXT Gene Promoters. 14, 3230-3241.
- Forchhammer, K. (2007). Glutamine signalling in bacteria. 12, 358-370.
- Gancedo, J.M. (1998). Yeast Carbon Catabolite Repression. *Microbiology and molecular biology reviews* : MMBR 62, 334-361.
- Gao, M., and Kaiser, C.A. (2006). A conserved GTPase-containing complex is required for intracellular sorting of the general amino-acid permease in yeast. *Nature cell biology* 8, 657-667.

Garami, A., Zwartkruis, F., Nobukuni, T., and Joaquin, M. (2003). ScienceDirect.com - Molecular Cell - Insulin Activation of Rheb, a Mediator of mTOR/S6K/4E-BP Signaling, Is Inhibited by TSC1 and 2. *Molecular cell*.

Garvin, J.L., Burg, M.B., and Knepper, M.A. (1988). Active NH<sub>4</sub> absorption by the thick ascending limb. *Am J Physiol*.

Gietzen, D.W., Ross, C.M., Hao, S., and Sharp, J.W. (2004). Phosphorylation of eIF2 $\alpha$  Is Involved in the Signaling of Indispensable Amino Acid Deficiency in the Anterior Piriform Cortex of the Brain in Rats. *The Journal of nutrition* 134, 717-723.

Gimeno, C.J., Ljungdahl, P.O., Styles, C.A., and Fink, G.R. (1992). Unipolar cell divisions in the yeast *S. cerevisiae* lead to filamentous growth: regulation by starvation and RAS. *Cell* 68, 1077-1090.

Gowans, G.J., and Hardie, D.G. (2014). AMPK: a cellular energy sensor primarily regulated by AMP. *Biochemical Society transactions* 42, 71-75.

Gwinn, D.M., Shackelford, D.B., Egan, D.F., Mihaylova, M.M., Mery, A., Vasquez, D.S., Turk, B.E., and Shaw, R.J. (2008). AMPK phosphorylation of raptor mediates a metabolic checkpoint. *Molecular cell* 30, 214-226.

Hao, S., Sharp, J.W., Ross-Inta, C.M., McDaniel, B.J., Anthony, T.G., Wek, R.C., Cavener, D.R., McGrath, B.C., Rudell, J.B., Koehnle, T.J., *et al.* (2005). Uncharged tRNA and Sensing of Amino Acid Deficiency in Mammalian Piriform Cortex. *Science (New York, NY)* 307, 1776-1778.

Hara, K. (1998). Amino Acid Sufficiency and mTOR Regulate p70 S6 Kinase and eIF-4E BP1 through a Common Effector Mechanism. *Journal of Biological Chemistry* 273, 14484-14494.

Hardie, D.G., and Hawley, S.A. (2001). AMP-activated protein kinase: the energy charge hypothesis revisited. *BioEssays* 23, 1112-1119.

Hardie, D.G., and Mackintosh, R.W. (1992). AMP-activated protein kinase - An archetypal protein kinase cascade? *BioEssays* 14, 699-704.

Hardie, D.G., Ross, F.A., and Hawley, S.A. (2012). AMPK: a nutrient and energy sensor that maintains energy homeostasis. *Nature reviews Molecular cell biology* 13, 251-262.

Harding, H.P., Novoa, I., Zhang, Y., Zeng, H., Wek, R., Schapira, M., and Ron, D. (2000). Regulated Translation Initiation Controls Stress-Induced Gene Expression in Mammalian Cells. *Molecular cell* 6, 1099-1108.



Harding, H.P., Zhang, Y., Zeng, H., Novoa, I., Lu, P.D., Calfon, M., Sadri, N., Yun, C., Popko, B., Paules, R., *et al.* (2003). An Integrated Stress Response Regulates Amino Acid Metabolism and Resistance to Oxidative Stress. *Molecular cell* 11, 619-633.

Hardwick, J.S., Kuruvilla, F.G., Tong, J.K., Shamji, A.F., and Schreiber, S.L. (1999). Rapamycin-modulated transcription defines the subset of nutrient-sensitive signaling pathways directly controlled by the Tor proteins. *Proceedings of the National Academy of Sciences of the United States of America* 96, 14866-14870.

Harms, E., Gochman, N., and Schneider, J.A. (1981). ScienceDirect.com - Biochemical and Biophysical Research Communications - Lysosomal pool of free-amino acids. *Biochemical and Biophysical* ....

Hedblom, M.L., and Adler, J. (1980). Genetic and biochemical properties of *Escherichia coli* mutants with defects in serine chemotaxis. *Journal of bacteriology* 144, 1048-1060.

Heinrich, A., Maheswaran, M., and Ruppert, U. (2004). The *Synechococcus elongatus* PII signal transduction protein controls arginine synthesis by complex formation with N-acetyl-l-glutamate kinase - Heinrich - 2004 - *Molecular Microbiology* - Wiley Online Library.

Helliwell, S.B., Wagner, P., Kunz, J., Deuter-Reinhard, M., Henriquez, R., and Hall, M.N. (1994). TOR1 and TOR2 are structurally and functionally similar but not identical phosphatidylinositol kinase homologues in yeast. *Molecular biology of the cell* 5, 105-118.

Hess, J.F., Oosawa, K., Kaplan, N., and Simon, M.I. (1988). Phosphorylation of three proteins in the signaling pathway of bacterial chemotaxis. *Cell* 53, 79-87.

Hess, J.F., Oosawa, K., Matsumura, P., and Simon, M.I. (1987). Protein phosphorylation is involved in bacterial chemotaxis. *Proceedings of the National Academy of Sciences of the United States of America* 84, 7609-7613.

Hinnebusch, A.G. (1984). Evidence for translational regulation of the activator of general amino acid control in yeast. *Proceedings of the National Academy of Sciences of the United States of America* 81, 6442-6446.

Hinnebusch, A.G. (1988). Mechanisms of gene regulation in the general control of amino acid biosynthesis in *Saccharomyces cerevisiae*. *Microbiological reviews* 52, 248-273.

Hinnebusch, A.G. (1993). Gene-specific translational control of the yeast GCN4 gene by phosphorylation of eukaryotic initiation factor 2. *Molecular microbiology* 10, 215-223.

Hinnebusch, A.G. (2005). Translational regulation of GCN4 and the general amino acid control of yeast. *Annual review of microbiology* 59, 407-450.

Hirose, E., Nakashima, N., Sekiguchi, T., and Nishimoto, T. (1998). RagA is a functional homologue of *S. cerevisiae* Gtr1p involved in the Ran/Gsp1-GTPase pathway. *Journal of cell science* 111 ( Pt 1), 11-21.

Hong, S.-P., Leiper, F.C., Woods, A., Carling, D., and Carlson, M. (2003). Activation of yeast Snf1 and mammalian AMP-activated protein kinase by upstream kinases. *Proceedings of the National Academy of Sciences of the United States of America* 100, 8839-8843.

Hong, S.-P., Momcilovic, M., and Carlson, M. (2005). Function of Mammalian LKB1 and Ca<sup>2+</sup>/Calmodulin-dependent Protein Kinase Kinase  $\alpha$  as Snf1-activating Kinases in Yeast. *Journal of Biological Chemistry* 280, 21804-21809.

Horman, S., Vertommen, D., Heath, R., Neumann, D., Mouton, V., Woods, A., Schlattner, U., Wallimann, T., Carling, D., Hue, L., *et al.* (2006). Insulin antagonizes ischemia-induced Thr172 phosphorylation of AMP-activated protein kinase alpha-subunits in heart via hierarchical phosphorylation of Ser485/491. *Journal of Biological Chemistry* 281, 5335-5340.

Hoving, S., Molenaar, D., and Stegeman, B. (1996). An alternative PII protein in the regulation of glutamine synthetase in *Escherichia coli* - Van Heeswijk - 2003 - *Molecular Microbiology* - Wiley Online Library.

Howell, J.J., Ricoult, S.J.H., Ben Sahra, I., and Manning, B.D. (2013). A growing role for mTOR in promoting anabolic metabolism. *Biochemical Society transactions* 41, 906-912.

Huergo, L.F., Chandra, G., and Merrick, M. (2013). P(II) signal transduction proteins: nitrogen regulation and beyond. 37, 251-283.

Inoki, K., Li, Y., Xu, T., and Guan, K.-L. (2003a). Rheb GTPase is a direct target of TSC2 GAP activity and regulates mTOR signaling. *Genes & Development* 17, 1829-1834.

Inoki, K., Zhu, T., and Guan, K.-L. (2003b). TSC2 mediates cellular energy response to control cell growth and survival. *Cell* 115, 577-590.

Iraqui, I., Vissers, S., Bernard, F., de Craene, J.-O., Boles, E., Urrestarazu, A., and André, B. (1999). Amino Acid Signaling in *Saccharomyces cerevisiae*: a Permease-Like Sensor of External Amino Acids and F-Box Protein Grr1p Are Required for Transcriptional Induction of the AGP1 Gene, Which Encodes a Broad-Specificity Amino Acid Permease.

- Jacinto, E., Loewith, R., Schmidt, A., Lin, S., Rüegg, M.A., Hall, A., and Hall, M.N. (2004). Mammalian TOR complex 2 controls the actin cytoskeleton and is rapamycin insensitive. *Nature cell biology* 6, 1122-1128.
- Javelle, A., Severi, E., Thornton, J., and Merrick, M. (2004). Ammonium Sensing in *Escherichia coli*: ROLE OF THE AMMONIUM TRANSPORTER AmtB AND AmtB-GlnK COMPLEX FORMATION. 279, 8530-8538.
- Jewell, J.L., Kim, Y.C., Russell, R.C., Yu, F.-X., Park, H.W., Plouffe, S.W., Tagliabracci, V.S., and Guan, K.-L. (2015). Metabolism. Differential regulation of mTORC1 by leucine and glutamine. *Science* 347, 194-198.
- Jiang, P., and Ninfa, A.J. (2007). *Escherichia coli* PII Signal Transduction Protein Controlling Nitrogen Assimilation Acts As a Sensor of Adenylate Energy Charge in *Vitro* †. 46, 12979-12996.
- Jiang, P., Peliska, J., and Ninfa, A. (1998a). Enzymological Characterization of the Signal-Transducing Uridyltransferase/Uridyl-Removing Enzyme (EC 2.7.7.59) of *Escherichia coli* and Its Interaction with the PII Protein † - *Biochemistry (ACS Publications)*.
- Jiang, P., Peliska, J.A., and Ninfa, A.J. (1998b). Reconstitution of the Signal-Transduction Bicyclic Cascade Responsible for the Regulation of *Ntr* Gene Transcription in *Escherichia coli* †. 37, 12795-12801.
- Jiang, P., Peliska, J.A., and Ninfa, A.J. (1998c). The Regulation of *Escherichia coli* Glutamine Synthetase Revisited: Role of 2-Ketoglutarate in the Regulation of Glutamine Synthetase Adenylation State †. 37, 12802-12810.
- Jin, X., Townley, R., and Shapiro, L. (2007). Structural Insight into AMPK Regulation: ADP Comes into Play. *Structure* 15, 1285-1295.
- Jouandot, D., Roy, A., and Kim, J. (2011). Functional dissection of the glucose signaling pathways that regulate the yeast glucose transporter gene (*HXT*) repressor *Rgt1* - Jouandot - 2011 - *Journal of Cellular Biochemistry* - Wiley Online Library.
- Kemp, B.E. (2004). Bateman domains and adenosine derivatives form a binding contract. *The Journal of Clinical Investigation* 113, 182-184.
- Kentner, D., Thiem, S., Hildenbeutel, M., and Sourjik, V. (2006). Determinants of chemoreceptor cluster formation in *Escherichia coli*. *Molecular microbiology* 61, 407-417.
- Khademi, S., O'Connell III, J., Remis, J., Robles-Colmenares, Y., Miercke, L.J.W., and Stroud, R.M. (2004). Mechanism of Ammonia Transport by Amt/MEP/Rh: Structure of AmtB at 1.35 Å. *Science (New York, NY)* 305, 1587-1594.

- Kim, E., Goraksha-Hicks, P., Li, L., Neufeld, T.P., and Guan, K.-L. (2008). Regulation of TORC1 by Rag GTPases in nutrient response. *Nature cell biology* 10, 935-945.
- Kim, J.H., Brachet, V., Moriya, H., and Johnston, M. (2006). Integration of Transcriptional and Posttranslational Regulation in a Glucose Signal Transduction Pathway in *Saccharomyces cerevisiae*. 5, 167-173.
- Kim, J.H., Polish, J., and Johnston, M. (2003). Specificity and Regulation of DNA Binding by the Yeast Glucose Transporter Gene Repressor Rgt1. 23, 5208-5216.
- Kim, S.G., Buel, G.R., and Blenis, J. (2013). Nutrient regulation of the mTOR Complex 1 signaling pathway. *Molecules and cells* 35, 463-473.
- Klass, M., and Hirsh, D. (1976). Non-ageing developmental variant of *Caenorhabditis elegans*. , Published online: 08 April 1976; | doi:10.1038/260523a0 260, 523-525.
- Klasson, H., Fink, G.R., and Ljungdahl, P.O. (1999). Ssy1p and Ptr3p are plasma membrane components of a yeast system that senses extracellular amino acids. 19, 5405-5416.
- Klionsky, D.J., Herman, P.K., and Emr, S.D. (1990). The fungal vacuole: composition, function, and biogenesis. *Microbiological reviews* 54, 266.
- Knepper, M.A., Packer, R., and Good, D.W. (1989). Ammonium transport in the kidney. *Physiological reviews*.
- Koehnle, T.J., Russell, M.C., and Gietzen, D.W. (2003). Rats Rapidly Reject Diets Deficient in Essential Amino Acids. *The Journal of nutrition* 133, 2331-2335.
- Kogan, K., Spear, E.D., Kaiser, C.A., and Fass, D. (2010). Structural Conservation of Components in the Amino Acid Sensing Branch of the TOR Pathway in Yeast and Mammals. *Journal of Molecular Biology* 402, 388-398.
- Kondoh, H., Ball, C.B., and Adler, J. (1979). Identification of a methyl-accepting chemotaxis protein for the ribose and galactose chemoreceptors of *Escherichia coli*. *Proceedings of the National Academy of Sciences of the United States of America* 76, 260-264.
- Krokowski, D., Han, J., Saikia, M., Majumder, M., Yuan, C.L., Guan, B.-J., Bevilacqua, E., Bussolati, O., Bröer, S., Arvan, P., *et al.* (2013). A self-defeating anabolic program leads to  $\beta$ -cell apoptosis in endoplasmic reticulum stress-induced diabetes via regulation of amino acid flux. *The Journal of biological chemistry* 288, 17202-17213.

Kübler, E., Mösch, H.U., Rupp, S., and Lisanti, M.P. (1997). Gpa2p, a G-protein alpha-subunit, regulates growth and pseudohyphal development in *Saccharomyces cerevisiae* via a cAMP-dependent mechanism. *Journal of Biological Chemistry* 272, 20321-20323.

Kubota, H., Obata, T., Ota, K., Sasaki, T., and Ito, T. (2003). Rapamycin-induced Translational Derepression of GCN4 mRNA Involves a Novel Mechanism for Activation of the eIF2 $\alpha$  Kinase GCN2. *Journal of Biological Chemistry* 278, 20457-20460.

Kunz, J., Henriquez, R., Schneider, U., Deuter-Reinhard, M., Movva, N.R., and Hall, M.N. (1993). Target of rapamycin in yeast, TOR2, is an essential phosphatidylinositol kinase homolog required for G1 progression. *Cell* 73, 585-596.

Lakshmanan, J., Mosley, A.L., and zcan, S. (2003). Repression of transcription by Rgt1 in the absence of glucose requires Std1 and Mth1. *44*, 19-25.

Lane, N., and Martin, W. (2010). The energetics of genome complexity. *Nature* 467, 929-934.

Laplante, M., and Sabatini, D.M. (2012). mTOR Signaling in Growth Control and Disease. *Cell* 149, 274-293.

Larsen, S.H., Reader, R.W., Kort, E.N., Tso, W.-W., and Adler, J. (1974). Change in direction of flagellar rotation is the basis of the chemotactic response in *Escherichia coli*. , Published online: 03 May 1974; | doi:10.1038/249074a0 249, 74-77.

Laxman, S., Sutter, B.M., Shi, L., and Tu, B.P. (2014). Npr2 inhibits TORC1 to prevent inappropriate utilization of glutamine for biosynthesis of nitrogen-containing metabolites. *Science Signaling* 7, ra120.

Laxman, S., Sutter, B.M., Wu, X., Kumar, S., Guo, X., Trudgian, D.C., Mirzaei, H., and Tu, B.P. (2013). Sulfur amino acids regulate translational capacity and metabolic homeostasis through modulation of tRNA thiolation. *Cell* 154, 416-429.

Leigh, J.A., and Dodsworth, J.A. (2007). Nitrogen Regulation in Bacteria and Archaea. *61*, 349-377.

Levit, M.N., Grebe, T.W., and Stock, J.B. (2002). Organization of the Receptor-Kinase Signaling Array That Regulates *Escherichia coli* Chemotaxis. *Journal of Biological Chemistry* 277, 36748-36754.

Li, S.C., and Kane, P.M. (2009). The yeast lysosome-like vacuole: endpoint and crossroads. *Biochimica et biophysica acta* 1793, 650-663.

Loewith, R., Jacinto, E., Wullschleger, S., and Lorberg, A. (2002). Two TOR complexes, only one of which is rapamycin sensitive, have distinct roles in cell growth control. *Molecular ....*

Long, X., Lin, Y., Ortiz-Vega, S., Yonezawa, K., and Avruch, J. (2005). Rheb Binds and Regulates the mTOR Kinase. *Current Biology* 15, 702-713.

Lorenz, M.C., and Heitman, J. (1997). Yeast pseudohyphal growth is regulated by GPA2, a G protein alpha homolog. *The EMBO Journal* 16, 7008-7018.

Lorenz, M.C., and Heitman, J. (1998). The MEP2 ammonium permease regulates pseudohyphal differentiation in *Saccharomyces cerevisiae*. *The EMBO Journal* 17, 1236-1247.

Ma, N., Liu, Q., Zhang, L., Henske, E.P., and Ma, Y. (2013). TORC1 Signaling Is Governed by Two Negative Regulators in Fission Yeast. *Genetics* 195, 457-468.

Mach, K.E., Furge, K.A., and Albright, C.F. (2000). Loss of Rhb1, a Rheb-Related GTPase in Fission Yeast, Causes Growth Arrest With a Terminal Phenotype Similar to That Caused by Nitrogen Starvation. *Genetics* 155, 611-622.

Maddock, J., and Shapiro, L. (1993). Polar location of the chemoreceptor complex in the *Escherichia coli* cell. *Science (New York, NY)* 259, 1717-1723.

Mangum, J., Magni, G., and Stadtman, E. (1973). Regulation of glutamine synthetase adenylation and deadenylation by the enzymatic uridylylation and deuridylylation of the PII regulatory protein.

Manson, M.D., Blank, V., Brade, G., and Higgins, C.F. (1986). Peptide chemotaxis in *E. coli* involves the Tap signal transducer and the dipeptide permease. *Nature* 321, 253-256.

Marini, A.-M., Matassi, G., Raynal, V., André, B., Cartron, J.-P., and Chérif-Zahar, B. (2000). The human Rhesus-associated RhAG protein and a kidney homologue promote ammonium transport in yeast. *Nature Genetics* 26, 341-344.

Marini, A.-M., Urrestarazu, A., Beauwens, R., and André, B. (1997a). The Rh (Rhesus) blood group polypeptides are related to NH<sub>4</sub><sup>+</sup> transporters. *Trends in biochemical sciences* 22, 460-461.

Marini, A.M., Boeckstaens, M., Benjelloun, F., Chérif-Zahar, B., and André, B. (2006). Structural involvement in substrate recognition of an essential aspartate residue conserved in Mep/Amt and Rh-type ammonium transporters. *Current genetics* 49, 364-374.

Marini, A.M., Soussi-Boudekou, S., Vissers, S., and André, B. (1997b). A family of ammonium transporters in *Saccharomyces cerevisiae*. *Molecular and cellular biology* 17, 4282-4293.

Marini, A.M., Vissers, S., Urrestarazu, A., and André, B. (1994). Cloning and expression of the MEP1 gene encoding an ammonium transporter in *Saccharomyces cerevisiae*. *The EMBO Journal* 13, 3456.

Matsumoto, S., Bandyopadhyay, A., Kwiatkowski, D.J., Maitra, U., and Matsumoto, T. (2002). Role of the Tsc1-Tsc2 Complex in Signaling and Transport Across the Cell Membrane in the Fission Yeast *Schizosaccharomyces pombe*. *Genetics* 161, 1053-1063.

Maurin, A.-C., Jousse, C., Averous, J., Parry, L., Bruhat, A., Cherasse, Y., Zeng, H., Zhang, Y., Harding, H.P., Ron, D., *et al.* (2005). The GCN2 kinase biases feeding behavior to maintain amino acid homeostasis in omnivores. *Cell metabolism* 1, 273-277.

Mayer, F.V., Heath, R., Underwood, E., Sanders, M.J., Carmena, D., McCartney, R.R., Leiper, F.C., Xiao, B., Jing, C., Walker, P.A., *et al.* (2011). ADP Regulates SNF1, the *Saccharomyces cerevisiae* Homolog of AMP-Activated Protein Kinase. *Cell metabolism* 14, 707-714.

Mesibov, R., Ordal, G.W., and Adler, J. (1973). The range of attractant concentrations for bacterial chemotaxis and the threshold and size of response over this range. Weber law and related phenomena. *The Journal of general physiology* 62, 203-223.

Mihaylova, M.M., and Shaw, R.J. (2011). The AMPK signalling pathway coordinates cell growth, autophagy and metabolism. *Nature cell biology* 13, 1016-1023.

Minokoshi, Y., Alquier, T., Furukawa, N., Kim, Y.-B., Lee, A., Xue, B., Mu, J., Fofelle, F., Ferré, P., Birnbaum, M.J., *et al.* (2004). AMP-kinase regulates food intake by responding to hormonal and nutrient signals in the hypothalamus. *Nature* 428, 569-574.

Mitchell, K.I., Stapleton, D., Gao, G., House, C., Michell, B., Katsis, F., Witters, L.A., and Kemp, B.E. (1994). Mammalian AMP-activated protein kinase shares structural and functional homology with the catalytic domain of yeast Snf1 protein kinase. *Journal of Biological Chemistry* 269, 2361-2364.

Moriya, H., and Johnston, M. (2004). Glucose sensing and signaling in *Saccharomyces cerevisiae* through the Rgt2 glucose sensor and casein kinase I.

Morris, R.E. (1992). Rapamycins: Antifungal, antitumor, antiproliferative, and immunosuppressive macrolides. *Transplantation Reviews* 6, 39-87.

Mueller, P.P., and Hinnebusch, A.G. (1986). Multiple upstream AUG codons mediate translational control of GCN4. *Cell* 45, 201-207.

Nakashima, A., Sato, T., and Tamanoi, F. (2010). Fission yeast TORC1 regulates phosphorylation of ribosomal S6 proteins in response to nutrients and its activity is inhibited by rapamycin. *Journal of cell science* 123, 777-786.

Narasimhan, J., Staschke, K.A., and Wek, R.C. (2004). Dimerization is required for activation of eIF2 kinase Gcn2 in response to diverse environmental stress conditions. *Journal of Biological Chemistry* 279, 22820-22832.

Nobukuni, T., Joaquin, M., Rocco, M., Dann, S.G., Kim, S.Y., Gulati, P., Byfield, M.P., Backer, J.M., Natt, F., Bos, J.L., *et al.* (2005). Amino acids mediate mTOR/raptor signaling through activation of class 3 phosphatidylinositol 3OH-kinase. *Proceedings of the National Academy of Sciences of the United States of America* 102, 14238-14243.

Oh, W.J., and Jacinto, E. (2011). mTOR complex 2 signaling and functions. [dxdoi.org](http://dx.doi.org).  
Oldham, S. (2000). Genetic and biochemical characterization of dTOR, the *Drosophila* homolog of the target of rapamycin. *Genes & Development* 14, 2689-2694.

Omnus, D.J., and Ljungdahl, P.O. (2013). Rts1-protein phosphatase 2A antagonizes Ptr3-mediated activation of the signaling protease Ssy5 by casein kinase I. *PLoS One* 8, 1480-1492.

Ottemann, K.M., Xiao, W., Shin, Y.-K., and Koshland Jr, D.E. (1999). A Piston Model for Transmembrane Signaling of the Aspartate Receptor. *Science (New York, NY)* 285, 1751-1754.

Ozcan, S., Dover, J., Rosenwald, A.G., Wölfel, S., and Johnston, M. (1996). Two glucose transporters in *Saccharomyces cerevisiae* are glucose sensors that generate a signal for induction of gene expression.

Ozcan, S., and Johnston, M. (1995). Three different regulatory mechanisms enable yeast hexose transporter (HXT) genes to be induced by different levels of glucose.  
Panchaud, N., Peli-Gulli, M.-P., and De Virgilio, C. (2013a). Amino Acid Deprivation Inhibits TORC1 Through a GTPase-Activating Protein Complex for the Rag Family GTPase Gtr1. *Science Signaling* 6, ra42.

Panchaud, N., Peli-Gulli, M.-P., and De Virgilio, C. (2013b). SEACing the GAP that nEGOCiates TORC1 activation: Evolutionary conservation of Rag GTPase regulation. *Cell Cycle* 12, 2948-2952.

Parmigiani, A., Nourbakhsh, A., Ding, B., Wang, W., Kim, Y.C., Akopiants, K., Guan, K.-L., Karin, M., and Budanov, A.V. (2014). Sestrins Inhibit mTORC1 Kinase Activation through the GATOR Complex. *Cell Reports* 9, 1281-1291.

Peng, T., Golub, T.R., and Sabatini, D.M. (2002). The Immunosuppressant Rapamycin Mimics a Starvation-Like Signal Distinct from Amino Acid and Glucose Deprivation. *Molecular and cellular biology* 22, 5575-5584.



Pfirrmann, T., Heessen, S., Omnus, D.J., Andreasson, C., and Ljungdahl, P.O. (2010). The Prodomain of Ssy5 Protease Controls Receptor-Activated Proteolysis of Transcription Factor Stp1. *30*, 3299-3309.

Pinto, S., Roseberry, A.G., Liu, H., Diano, S., Shanabrough, M., Cai, X., Friedman, J.M., and Horvath, T.L. (2004). Rapid Rewiring of Arcuate Nucleus Feeding Circuits by Leptin. *Science (New York, NY)* *304*, 110-115.

Polish, J.A. (2005). How the Rgt1 Transcription Factor of *Saccharomyces cerevisiae* Is Regulated by Glucose. *169*, 583-594.

Poulsen, P., Gaber, R.F., and Kielland-Brandt, M.C. (2008). Hyper- and hyporesponsive mutant forms of the *Saccharomyces cerevisiae* Ssy1 amino acid sensor. *25*, 164-176.  
Radchenko, M.V., Thornton, J., and Merrick, M. (2013). PII signal transduction proteins are ATPases whose activity is regulated by 2-oxoglutarate.

Reader, R.W., Tso, W.-W., Springer, M.S., Goy, M.F., and Adler, J. (1979). Pleiotropic Aspartate Taxis and Serine Taxis Mutants of *Escherichia coli*. *Microbiology* *111*, 363-374.

Rebsamen, M., Pochini, L., Stasyk, T., de Araújo, M.E.G., Galluccio, M., Kandasamy, R.K., Snijder, B., Fauster, A., Rudashevskaya, E.L., Bruckner, M., *et al.* (2015). SLC38A9 is a component of the lysosomal amino acid sensing machinery that controls mTORC1. *Nature*.

Reinke, A., Anderson, S., McCaffery, J.M., Yates III, J., Aronova, S., Chu, S., Fairclough, S., Iverson, C., Wedaman, K.P., and Powers, T. (2004). TOR Complex 1 Includes a Novel Component, Tco89p (YPL180w), and Cooperates with Ssd1p to Maintain Cellular Integrity in *Saccharomyces cerevisiae*. *Journal of Biological Chemistry* *279*, 14752-14762.

Ribeiro, C., and Dickson, B.J. (2010). Sex peptide receptor and neuronal TOR/S6K signaling modulate nutrient balancing in *Drosophila*. *Current biology : CB* *20*, 1000-1005.

Roccio, M., Bos, J.L., and Zwartkuis, F.J.T. (2005). Regulation of the small GTPase Rheb by amino acids. *Oncogene* *25*, 657-664.

Roy, A., Shin, Y.J., Cho, K.H., and Kim, J.-H. (2013). Mth1 regulates the interaction between the Rgt1 repressor and the Ssn6-Tup1 corepressor complex by modulating PKA-dependent phosphorylation of Rgt1.

Rutherford, J.C., Chua, G., Hughes, T., Cardenas, M.E., and Heitman, J. (2008). A Mep2-dependent Transcriptional Profile Links Permease Function to Gene Expression during Pseudohyphal Growth in *Saccharomyces cerevisiae*. *Molecular biology of the cell* *19*, 3028-3039.

Sabatini, D.M., Erdjument-Bromage, H., Lui, M., Tempst, P., and Snyder, S.H. (1994). RAFT1: A mammalian protein that binds to FKBP12 in a rapamycin-dependent fashion and is homologous to yeast TORs. *Cell* 78, 35-43.

Sabers, C.J., Martin, M.M., Brunn, G.J., Williams, J.M., Dumont, F.J., Wiederrecht, G., and Abraham, R.T. (1995). Isolation of a Protein Target of the FKBP12-Rapamycin Complex in Mammalian Cells. *Journal of Biological Chemistry* 270, 815-822.

Saito, K., Araki, Y., Kontani, K., Nishina, H., and Katada, T. (2005). Novel role of the small GTPase Rheb: its implication in endocytic pathway independent of the activation of mammalian target of rapamycin. *Journal of Biochemistry* 137, 423-430.

Sancak, Y., Bar-Peled, L., Zoncu, R., Markhard, A.L., Nada, S., and Sabatini, D.M. (2010). Ragulator-Rag complex targets mTORC1 to the lysosomal surface and is necessary for its activation by amino acids. *Cell* 141, 290-303.

Sancak, Y., Peterson, T.R., Shaul, Y.D., Lindquist, R.A., Thoreen, C.C., Bar-Peled, L., and Sabatini, D.M. (2008). The Rag GTPases bind raptor and mediate amino acid signaling to mTORC1. *Science (New York, NY)* 320, 1496-1501.

Santangelo, G.M. (2006). Glucose Signaling in *Saccharomyces cerevisiae*. *Microbiology and molecular biology reviews* : MMBR 70, 253-282.

Sarbassov, D.D., Ali, S.M., Kim, D.-H., Guertin, D.A., Latek, R.R., Erdjument-Bromage, H., Tempst, P., and Sabatini, D.M. (2004). Rictor, a Novel Binding Partner of mTOR, Defines a Rapamycin-Insensitive and Raptor-Independent Pathway that Regulates the Cytoskeleton. *Current Biology* 14, 1296-1302.

Sarkar, M.K., Paul, K., and Blair, D. (2010). Chemotaxis signaling protein CheY binds to the rotor protein FliN to control the direction of flagellar rotation in *Escherichia coli*. *Proceedings of the National Academy of Sciences of the United States of America* 107, 9370-9375.

Saucedo, L.J., Gao, X., Chiarelli, D.A., Li, L., Pan, D., and Edgar, B.A. (2003). Rheb promotes cell growth as a component of the insulin/TOR signalling network. *Nature cell biology* 5, 566-571.

Scharf, B.E., Fahrner, K.A., Turner, L., and Berg, H.C. (1998). Control of direction of flagellar rotation in bacterial chemotaxis. *Proceedings of the National Academy of Sciences of the United States of America* 95, 201-206.

Schmidt, M.C., McCartney, R.R., Zhang, X., Tillman, T.S., Solimeo, H., Wölfl, S., Almonte, C., and Watkins, S.C. (1999). Std1 and Mth1 Proteins Interact with the Glucose Sensors To Control Glucose-Regulated Gene Expression in *Saccharomyces cerevisiae*.

Schürmann, A., Brauers, A., Maßmann, S., Becker, W., and Joost, H.-G. (1995). Cloning of a Novel Family of Mammalian GTP-binding Proteins (RagA, RagBs, RagB1) with Remote Similarity to the Ras-related GTPases. *The Journal of biological chemistry* *270*, 28982-28988.

Scott, J.W., Hawley, S.A., Green, K.A., Anis, M., Stewart, G., Scullion, G.A., Norman, D.G., and Hardie, D.G. (2004). CBS domains form energy-sensing modules whose binding of adenosine ligands is disrupted by disease mutations. *The Journal of Clinical Investigation* *113*, 274-284.

Segall, J.E., Block, S.M., and Berg, H.C. (1986). Temporal comparisons in bacterial chemotaxis. *Proceedings of the National Academy of Sciences of the United States of America* *83*, 8987-8991.

Sekiguchi, T., Hirose, E., Nakashima, N., Ii, M., and Nishimoto, T. (2001). Novel G proteins, Rag C and Rag D, interact with GTP-binding proteins, Rag A and Rag B. *The Journal of biological chemistry* *276*, 7246-7257.

Shamji, A.F., Kuruvilla, F.G., and Schreiber, S.L. (2000). Partitioning the transcriptional program induced by rapamycin among the effectors of the Tor proteins. *Current Biology* *10*, 1574-1581.

Siewe, R.M., Weil, B., Burkovski, A., Eikmanns, B.J., Eikmanns, M., and Krämer, R. (1996). Functional and Genetic Characterization of the (Methyl)ammonium Uptake Carrier of *Corynebacterium glutamicum*. *Journal of Biological Chemistry* *271*, 5398-5403.

Smith, E.M., Finn, S.G., Tee, A.R., Browne, G.J., and Proud, C.G. (2005). The tuberous sclerosis protein TSC2 is not required for the regulation of the mammalian target of rapamycin by amino acids and certain cellular stresses. *The Journal of biological chemistry* *280*, 18717-18727.

Sood, R., Porter, A.C., Olsen, D., Cavener, D.R., and Wek, R.C. (2000). A Mammalian Homologue of GCN2 Protein Kinase Important for Translational Control by Phosphorylation of Eukaryotic Initiation Factor-2 $\alpha$ . *Genetics* *154*, 787-801.

Sourjik, V., and Berg, H.C. (2004). Functional interactions between receptors in bacterial chemotaxis. *Nature* *428*, 437-441.

Sourjik, V., and Wingreen, N.S. (2012). Responding to chemical gradients: bacterial chemotaxis. *Current opinion in cell biology* *24*, 262-268.

Srivatsan, A., and Wang, J.D. (2008). Control of bacterial transcription, translation and replication by (p)ppGpp. *Current Opinion in Microbiology* *11*, 100-105.

Stadtman, E.R. (2001). The Story of Glutamine Synthetase Regulation. 276, 44357-44364.

Staschke, K.A., Dey, S., Zaborske, J.M., Palam, L.R., McClintick, J.N., Pan, T., Edenberg, H.J., and Wek, R.C. (2010). Integration of General Amino Acid Control and Target of Rapamycin (TOR) Regulatory Pathways in Nitrogen Assimilation in Yeast. *Journal of Biological Chemistry* 285, 16893-16911.

Stock, A., Chen, T., Welsh, D., and Stock, J. (1988). CheA protein, a central regulator of bacterial chemotaxis, belongs to a family of proteins that control gene expression in response to changing environmental conditions. *Proceedings of the National Academy of Sciences of the United States of America* 85, 1403-1407.

Stocker, H., Radimerski, T., Schindelholz, B., Wittwer, F., Belawat, P., Daram, P., Breuer, S., Thomas, G., and Hafen, E. (2003). Rheb is an essential regulator of S6K in controlling cell growth in *Drosophila*. *Nature cell biology* 5, 559-565.

Stracka, D., Jozefczuk, S., Rudroff, F., Sauer, U., and Hall, M.N. (2014). Nitrogen Source Activates TOR (Target of Rapamycin) Complex 1 via Glutamine and Independently of Gtr/Rag Proteins. *Journal of Biological Chemistry* 289, 25010-25020.

Sutherland, C.M., Hawley, S.A., McCartney, R.R., Leech, A., Stark, M.J.R., Schmidt, M.C., and Hardie, D.G. (2003). Elm1p Is One of Three Upstream Kinases for the *Saccharomyces cerevisiae* SNF1 Complex. *Current Biology* 13, 1299-1305.

Sutter, B.M., Wu, X., Laxman, S., and Tu, B.P. (2013). Methionine inhibits autophagy and promotes growth by inducing the SAM-responsive methylation of PP2A. *Cell* 154, 403-415.

Svanberg, E., and Moller-Loswick, A.C. (1996). Effects of amino acids on synthesis and degradation of skeletal muscle proteins in humans. *American Journal of ...*

Szurmant, H., and Ordal, G.W. (2004). Diversity in chemotaxis mechanisms among the bacteria and archaea. *Microbiology and molecular biology reviews : MMBR* 68, 301-319.

Tee, A.R., Fingar, D.C., Manning, B.D., Kwiatkowski, D.J., Cantley, L.C., and Blenis, J. (2002). Tuberous sclerosis complex-1 and -2 gene products function together to inhibit mammalian target of rapamycin (mTOR)-mediated downstream signaling. *Proceedings of the National Academy of Sciences of the United States of America* 99, 13571-13576.

Thelander, M., Olsson, T., and Ronne, H. (2004). Snf1-related protein kinase 1 is needed for growth in a normal day-night light cycle. *The EMBO Journal* 23, 1900-1910.

- Theodoris, G., Fong, N.M., Coons, D.M., and Bisson, L.F. (1994). High-copy suppression of glucose transport defects by HXT4 and regulatory elements in the promoters of the HXT genes in *Saccharomyces cerevisiae*.
- Tomas-Cobos, L., and Sanz, P. (2002). Active Snf1 protein kinase inhibits expression of the *Saccharomyces cerevisiae* HXT1 glucose transporter gene. *368*, 657.
- Toshima, N., and Tanimura, T. (2012). Taste preference for amino acids is dependent on internal nutritional state in *Drosophila melanogaster*. *The Journal of experimental biology* *215*, 2827-2832.
- Townley, R., and Shapiro, L. (2007). Crystal Structures of the Adenylate Sensor from Fission Yeast AMP-Activated Protein Kinase. *Science (New York, NY)* *315*, 1726-1729.
- Tsun, Z.-Y., Bar-Peled, L., Chantranupong, L., Zoncu, R., Wang, T., Kim, C., Spooner, E., and Sabatini, D.M. (2013). The Folliculin Tumor Suppressor Is a GAP for the RagC/D GTPases That Signal Amino Acid Levels to mTORC1. *Molecular cell* *52*, 495-505.
- Turner, L., Ryu, W.S., and Berg, H.C. (2000). Real-Time Imaging of Fluorescent Flagellar Filaments. *Journal of bacteriology* *182*, 2793-2801.
- Urano, J., Sato, T., Matsuo, T., Otsubo, Y., Yamamoto, M., and Tamanoi, F. (2007). Point mutations in TOR confer Rheb-independent growth in fission yeast and nutrient-independent mammalian TOR signaling in mammalian cells. *Proceedings of the National Academy of Sciences of the United States of America* *104*, 3514-3519.
- Urano, J., Tabancay, A.P., Yang, W., and Tamanoi, F. (2000). The *Saccharomyces cerevisiae* Rheb G-protein is involved in regulating canavanine resistance and arginine uptake. *Journal of Biological Chemistry* *275*, 11198-11206.
- Uritani, M., Hidaka, H., Hotta, Y., Ueno, M., Ushimaru, T., and Toda, T. (2006). Fission yeast Tor2 links nitrogen signals to cell proliferation and acts downstream of the Rheb GTPase. *Genes to Cells* *11*, 1367-1379.
- Van Nuland, A., Vandormael, P., Donaton, M., Alenquer, M., Lourenço, A., Quintino, E., Versele, M., and Thevelein, J.M. (2006). Ammonium permease-based sensing mechanism for rapid ammonium activation of the protein kinase A pathway in yeast. *Molecular microbiology* *59*, 1485-1505.
- van Slegtenhorst, M., Carr, E., Stoyanova, R., Kruger, W.D., and Henske, E.P. (2004). *Tsc1+* and *tsc2+* Regulate Arginine Uptake and Metabolism in *Schizosaccharomyces pombe*. *Journal of Biological Chemistry* *279*, 12706-12713.

Vargas, M.A., Luo, N., Yamaguchi, A., and Kapahi, P. (2010). A role for S6 kinase and serotonin in postmating dietary switch and balance of nutrients in *D. melanogaster*. *Current biology* : CB 20, 1006-1011.

Vattem, K.M., and Wek, R.C. (2004). Reinitiation involving upstream ORFs regulates ATF4 mRNA translation in mammalian cells. *Proceedings of the National Academy of Sciences of the United States of America* 101, 11269-11274.

Wadhams, G.H., and Armitage, J.P. (2004). Making sense of it all: bacterial chemotaxis. *Nature reviews Molecular cell biology* 5, 1024-1037.

Wang, E.A., and D E Koshland, J. (1980). Receptor structure in the bacterial sensing system. *Proceedings of the National Academy of Sciences of the United States of America* 77, 7157-7161.

Wang, S., Tsun, Z.-Y., Wolfson, R.L., Shen, K., Wyant, G.A., Plovanich, M.E., Yuan, E.D., Jones, T.D., Chantranupong, L., Comb, W., *et al.* (2015). Metabolism. Lysosomal amino acid transporter SLC38A9 signals arginine sufficiency to mTORC1. *Science* 347, 188-194.

Wang, X., Campbell, L.E., Miller, C.M., and Proud, C.G. (1998). Amino acid availability regulates p70 S6 kinase and multiple translation factors. *The Biochemical journal* 334 ( Pt 1), 261-267.

Wedaman, K.P., Reinke, A., Anderson, S., Yates III, J., McCaffery, J.M., and Powers, T. (2003). Tor Kinases Are in Distinct Membrane-associated Protein Complexes in *Saccharomyces cerevisiae*. *Molecular biology of the cell* 14, 1204-1220.

Weis, R.M., and D E Koshland, J. (1988). Reversible receptor methylation is essential for normal chemotaxis of *Escherichia coli* in gradients of aspartic acid. *Proceedings of the National Academy of Sciences of the United States of America* 85, 83-87.

Wek, R.C., Jackson, B.M., and Hinnebusch, A.G. (1989). Juxtaposition of domains homologous to protein kinases and histidyl-tRNA synthetases in GCN2 protein suggests a mechanism for coupling GCN4 expression to amino acid availability. *Proceedings of the National Academy of Sciences of the United States of America* 86, 4579-4583.

Wek, S.A., Zhu, S., and Wek, R.C. (1995). The histidyl-tRNA synthetase-related sequence in the eIF-2 alpha protein kinase GCN2 interacts with tRNA and is required for activation in response to starvation for different amino acids. *Molecular and cellular biology* 15, 4497-4506.

Welch, M., Oosawa, K., Aizawa, S., and Eisenbach, M. (1993). Phosphorylation-dependent binding of a signal molecule to the flagellar switch of bacteria. *Proceedings of the National Academy of Sciences of the United States of America* 90, 8787-8791.

- Woods, A., Munday, M.R., Scott, J., Yang, X., Carlson, M., and Carling, D. (1994). Yeast SNF1 is functionally related to mammalian AMP-activated protein kinase and regulates acetyl-CoA carboxylase in vivo. *Journal of Biological Chemistry* 269, 19509-19515.
- Wullschleger, S., Loewith, R., and Hall, M.N. (2006). TOR Signaling in Growth and Metabolism. *Cell* 124, 471-484.
- Xiao, B., Heath, R., Saiu, P., Leiper, F.C., Leone, P., Jing, C., Walker, P.A., Haire, L., Eccleston, J.F., Davis, C.T., *et al.* (2007). Structural basis for AMP binding to mammalian AMP-activated protein kinase. *Nature* 449, 496-500.
- Xiao, B., Sanders, M.J., Underwood, E., Heath, R., Mayer, F.V., Carmena, D., Jing, C., Walker, P.A., Eccleston, J.F., Haire, L.F., *et al.* (2011). Structure of mammalian AMPK and its regulation by ADP. *Nature* 472, 230-233.
- Yang, Y., Atasoy, D., Su, H.H., and Sternson, S.M. (2011). Hunger States Switch a Flip-Flop Memory Circuit via a Synaptic AMPK-Dependent Positive Feedback Loop. *Cell* 146, 992-1003.
- Yuan, H.-X., Xiong, Y., and Guan, K.-L. (2013). Nutrient Sensing, Metabolism, and Cell Growth Control. *Molecular cell* 49, 379-387.
- Zaman, S., Lippman, S.I., Zhao, X., and Broach, J.R. (2008). How *Saccharomyces* Responds to Nutrients. [dxdoi.org](http://dxdoi.org).
- Zhang, H., Stallock, J.P., Ng, J.C., Reinhard, C., and Neufeld, T.P. (2000). Regulation of cellular growth by the *Drosophila* target of rapamycin dTOR. *Genes Dev* 14, 2712-2724.
- Zhang, P., Khursigara, C.M., Hartnell, L.M., and Subramaniam, S. (2007). Direct visualization of *Escherichia coli* chemotaxis receptor arrays using cryo-electron microscopy. *Proceedings of the National Academy of Sciences of the United States of America* 104, 3777-3781.
- Zhang, P., McGrath, B.C., Reinert, J., Olsen, D.S., Lei, L., Gill, S., Wek, S.A., Vattem, K.M., Wek, R.C., Kimball, S.R., *et al.* (2002). The GCN2 eIF2 $\alpha$  Kinase Is Required for Adaptation to Amino Acid Deprivation in Mice. *Molecular and cellular biology* 22, 6681-6688.
- Zhang, Y., Pohlmann, E.L., and Roberts, G.P. (2009). Effect of Perturbation of ATP Level on the Activity and Regulation of Nitrogenase in *Rhodospirillum rubrum*. 191, 5526-5537.
- Zheng, L., Kostrewa, D., Bernèche, S., Winkler, F.K., and Li, X.-D. (2004). The mechanism of ammonia transport based on the crystal structure of AmtB of *Escherichia*

coli. *Proceedings of the National Academy of Sciences of the United States of America* 101, 17090-17095.

Zoncu, R., Bar-Peled, L., Efeyan, A., Wang, S., Sancak, Y., and Sabatini, D.M. (2011). mTORC1 Senses Lysosomal Amino Acids Through an Inside-Out Mechanism That Requires the Vacuolar H<sup>+</sup>-ATPase. *Science Signaling* 334, 678-683.

Zurita-Martinez, S.A., Puria, R., Pan, X., Boeke, J.D., and Cardenas, M.E. (2007). Efficient Tor Signaling Requires a Functional Class C Vps Protein Complex in *Saccharomyces cerevisiae*. *Genetics* 176, 2139-2150.



## CHAPTER 2

Reprinted from *Nature Genetics*:

### Recurrent mTORC1-activating *RRAGC* mutations in follicular lymphoma

Jessica Okosun<sup>1,17</sup>, Rachel L Wolfson<sup>2,3,17</sup>, Jun Wang<sup>4</sup>, Shamzah Araf<sup>1</sup>, Lucy Wilkins<sup>1</sup>, Brian M. Castellano<sup>5</sup>, Leire Escudero-Ibarz<sup>6</sup>, Ahad Fahad Al Seraihi<sup>1</sup>, Julia Richter<sup>7</sup>, Stephan H. Bernhart<sup>8,9,10</sup>, Alejo Efeyan<sup>2,3</sup>, Sameena Iqbal<sup>1</sup>, Janet Matthews<sup>1</sup>, Andrew Clear<sup>1</sup>, José Afonso Guerra-Assunção<sup>4</sup>, Csaba Bödör<sup>11</sup>, Hilmar Quentmeier<sup>12</sup>, Christopher Mansbridge<sup>13</sup>, Peter Johnson<sup>13</sup>, Andrew Davies<sup>13</sup>, Jonathan C. Strefford<sup>13</sup>, Graham Packham<sup>13</sup>, Sharon Barrans<sup>14</sup>, Andrew Jack<sup>14</sup>, Ming-Qing Du<sup>6</sup>, Maria Calaminici<sup>1</sup>, T. Andrew Lister<sup>1</sup>, Rebecca Auer<sup>1</sup>, Silvia Montoto<sup>1</sup>, John G. Gribben<sup>1</sup>, Reiner Siebert<sup>7</sup>, Claude Chelala<sup>4</sup>, Roberto Zoncu<sup>5</sup>, David M. Sabatini<sup>2,3,15,16,18</sup>, Jude Fitzgibbon<sup>1,18</sup>

<sup>1</sup>Centre for Haemato-Oncology, Barts Cancer Institute, Queen Mary University of London, London, United Kingdom.

<sup>2</sup>Whitehead Institute for Biomedical Research and Massachusetts Institute of Technology, Department of Biology, Cambridge, United States

<sup>3</sup>Howard Hughes Medical Institute, Department of Biology, Cambridge, United States

<sup>4</sup>Centre for Molecular Oncology, Barts Cancer Institute, Queen Mary University of London, London, United Kingdom.

<sup>5</sup>Department of Molecular and Cell Biology, University of California Berkeley, California, United States

<sup>6</sup>Division of Molecular Histopathology, Department of Pathology, University of Cambridge, Cambridge, United Kingdom

<sup>7</sup>Institute of Human Genetics, University Hospital Schleswig-Holstein Campus Kiel/Christian-Albrechts University Kiel, Kiel, Germany

<sup>8</sup>Transcriptome Bioinformatics, LIFE Research Center for Civilization Diseases, Leipzig, Germany;

<sup>9</sup>Interdisciplinary Center for Bioinformatics, University of Leipzig, Leipzig, Germany;

<sup>10</sup>Bioinformatics Group, Department of Computer, University of Leipzig, Leipzig, Germany

<sup>11</sup>MTA-SE Lendulet Molecular Oncohematology Research Group, 1st Department of Pathology and Experimental Cancer Research, Semmelweis University, Budapest, Hungary.

<sup>12</sup>Leibniz-Institute DSMZ, German Collection of Microorganisms and Cell Cultures, Braunschweig, Germany

<sup>13</sup>Cancer Sciences Unit, Faculty of Medicine, University of Southampton, Southampton, United Kingdom

<sup>14</sup>Haematological Malignancy Diagnostic Service, St. James's Institute of Oncology, Leeds, United Kingdom

<sup>15</sup>Koch Institute for Integrative Cancer Research, Cambridge, United States

<sup>16</sup>Broad Institute of Harvard and Massachusetts Institute of Technology, Cambridge, United States

<sup>17</sup>These authors contributed equally to this work.

<sup>18</sup>These authors jointly supervised this work.

Correspondence should be addressed to J.O. ([j.e.okosun@qmul.ac.uk](mailto:j.e.okosun@qmul.ac.uk)) or D.M.S. ([sabatini@wi.mit.edu](mailto:sabatini@wi.mit.edu))

**Experiments in Fig. 1, 2, S1-6 were performed by J.O. with help from all other authors.**

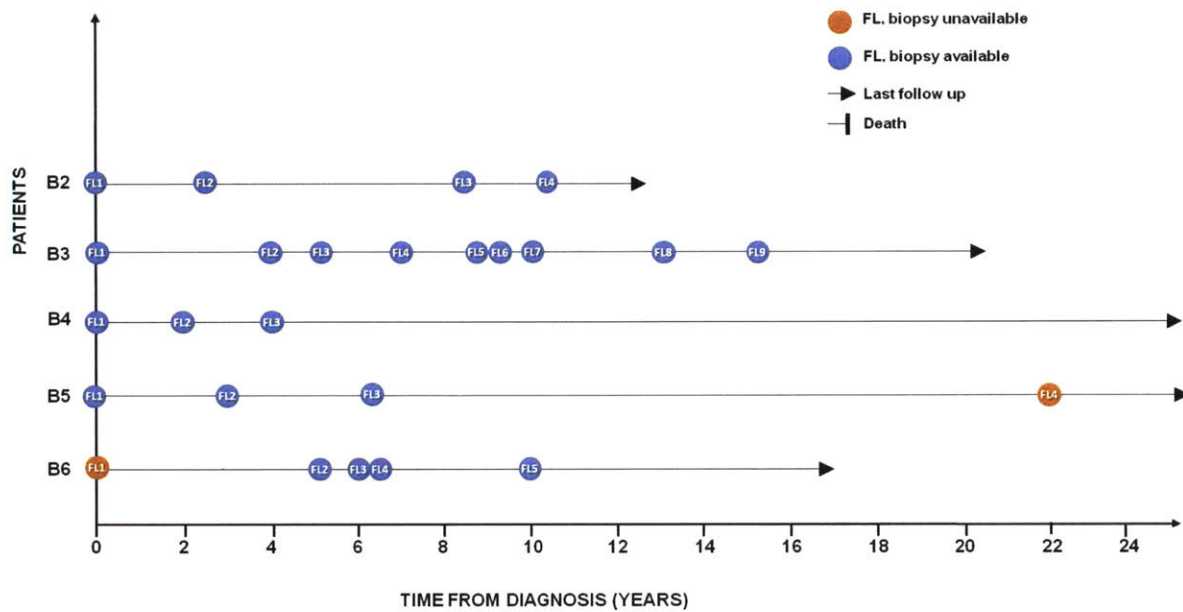
**Experiments in Fig. 3, 4, and S7 were performed by R.L.W.**

## Abstract

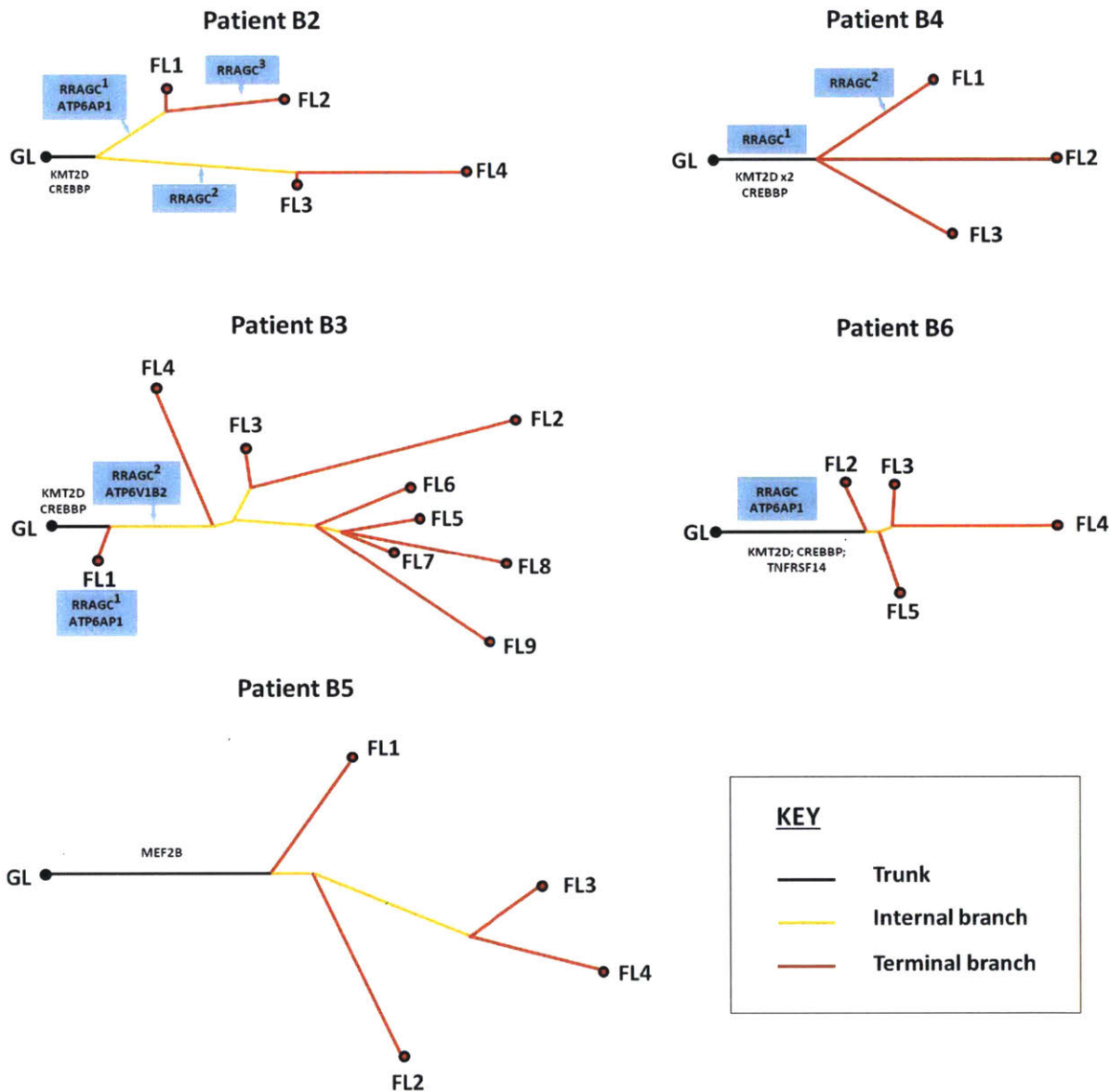
Follicular lymphoma is an incurable B-cell malignancy<sup>1</sup> characterized by the t(14;18) and mutations in one or more components of the epigenome<sup>2,3</sup>. Whilst frequent gene mutations in signaling pathways, including JAK-STAT, NOTCH and NF- $\kappa$ B, have also been defined<sup>2-7</sup>, the spectrum of these mutations typically overlap with the closely-related diffuse large B cell lymphoma (DLBCL)<sup>6-13</sup>. A combination of discovery exome and extended targeted sequencing revealed recurrent somatic mutations in *RRAGC* uniquely enriched in FL patients (17%). More than half of the mutations preferentially co-occurred with *ATP6V1B2* and *ATP6AP1* mutations, components of the vacuolar H<sup>+</sup>-adenosine triphosphate ATPase (v-ATPase) known to be necessary for amino acid-induced mTORC1 activation. The RagC mutants increased raptor binding whilst rendering mTORC1 signaling resistant to amino acid deprivation. Collectively, the activating nature of the *RRAGC* mutations, their existence within the dominant clone and stability during disease progression supports their potential as an excellent candidate to be therapeutically exploited.

Follicular lymphoma (FL) is one of the commonest non-Hodgkin's lymphomas (NHLs). Whilst the majority of affected individuals exhibit a characteristic protracted disease course with multiple relapses, others develop aggressive disease and histological transformation with shortened overall survival. Genome-wide profiling studies have primarily focused on single time-point analyses or the subset of patients that have undergone histological transformation in order to determine the genetic mediators of progression<sup>2,3</sup>. To gain further insight into the genetic diversity of FL, we undertook temporal analyses on individuals diagnosed with FL that underwent several relapse episodes without transformation. These data uncovered recurrent mutations in components of the mTORC1 signaling pathway, specific to FL.

Exome sequencing was performed on 24 tumors (from 5 patients) and matched constitutional DNA, with an average sequencing depth of 140x and 97.5% of the targeted bases covered by >10-fold (Online Methods and **Supplementary Table 1**). The clinical course from diagnoses to last follow-up ranged from 12.5 to 25 years (**Supplementary Table 2** and **Supplementary Fig. 1**). A median of 94 non-synonymous mutations per tumor were identified and validated mutations of interest by a combination of Sanger and tagged-amplicon sequencing (**Supplementary Tables 3 and 4**). Consistent with our earlier longitudinal study of paired FL and transformed FL<sup>2</sup>, tumors from the same individual confirmed a branched evolutionary pattern and demonstrated that all tumors evolve from a dominant ancestral clone (**Supplementary Fig. 2**). Moreover, mutations in *KMT2D*, *CREBBP* and *MEF2B* were present on the trunks of the phylogenetic trees in all five individuals, consistent with the role of epigenetic deregulation as critical early events in the majority of FLs<sup>2,3,14,15</sup>.



**Supplementary Figure 1. Clinical timeline for the discovery WES cases.** This illustrates the timelines of the disease events during the clinical course of each patient's disease further indicating the available samples that were sequenced in this study.



**Supplementary Figure 2. Phylogenetic reconstruction demonstrating the clonal evolution history of each of the 5 WES cases.** In each case, a phylogenetic tree was constructed using the somatic non-synonymous variants detected in the WES analyses. All trees are rooted at the germline (GL) sequence with the trunk of the tree representing variants shared by all the tumor biopsies and depicts a common ancestral origin. Internal branches indicate variants that are shared by more than one subsequent progressed or relapse tumor and the terminal branches illustrate variants that are unique or phase-specific to that biopsy alone. Early initiating genes are shown on the trunk of the tree. Novel genes identified in this study, *RRAGC*, *ATP6V1B2* and *ATP6AP1* are also

illustrated. For *RRAGC* mutations, the superscript numbers in case B2, B3 and B4 indicate the different *RRAGC* mutations identified in those individual biopsies.

**Supplementary Table 1. Sequencing metrics for the 5 WES cases**

|                                                | Germline (GL) | Tumor |
|------------------------------------------------|---------------|-------|
| Mean number of reads per sample (M)            | 103.7         | 119.9 |
| Mean sequenced nucleotides (Gb)                | 6.4           | 7.2   |
| Mean coverage (X)                              | 127.0         | 142.7 |
| % of target bases covered by at least 10 reads | 98.2%         | 97.3% |

**Supplementary Table 2. Clinical features and treatment details for the five discovery cases analysed by whole exome sequencing**

| Patient ID | Age at Diagnosis (Years) | Sex | Stage at Diagnosis | t(14;18) | FL Grade at Diagnosis | Disease event | Treatment                                    |
|------------|--------------------------|-----|--------------------|----------|-----------------------|---------------|----------------------------------------------|
| <b>B2</b>  | 55                       | F   | 4                  | Y        | 1                     | Diagnosis     | FL1 (Apr 02): Expectant management           |
|            |                          |     |                    |          |                       | Progression   | FL2 (Dec 04): Chl                            |
|            |                          |     |                    |          |                       | Relapse       | FL3 (Dec 10): R-CHOP + R maintenance         |
|            |                          |     |                    |          |                       | Relapse       | FL4 (Feb 12): Bendamustine + GA101           |
| <b>B3</b>  | 36                       | F   | 4                  | Y        | 1                     | Diagnosis     | FL1 (Dec 93): Expectant management           |
|            |                          |     |                    |          |                       | Progression   | FL2 (Dec 97): Chl + Bexxar                   |
|            |                          |     |                    |          |                       | Relapse       | FL3 (Dec 98): FMD then CHOP                  |
|            |                          |     |                    |          |                       | Progression   | FL4 (Aug 00): Expectant management           |
|            |                          |     |                    |          |                       | Relapse       | FL5 (Apr 02): Velcade                        |
|            |                          |     |                    |          |                       | Relapse       | FL6 (Oct 02): Expectant management           |
|            |                          |     |                    |          |                       | Progression   | FL7 (Aug 03): Post-radiotherapy              |
|            |                          |     |                    |          |                       | Relapse       | FL8 (Oct 06): Chl + Rituximab                |
|            |                          |     |                    |          |                       | Relapse       | FL9 (Sept 08): IFRT                          |
| <b>B4</b>  | 37                       | M   | Unk                | Y        | 1                     | Diagnosis     | FL1 (Mar 89): Chl                            |
|            |                          |     |                    |          |                       | Relapse       | FL2 (May 91): Chl                            |
|            |                          |     |                    |          |                       | Relapse       | FL3 (Jan 93): Surgical excision, followed by |



|           |                                                        |   |   |   |   |             | autologous SCT                                                               |  |
|-----------|--------------------------------------------------------|---|---|---|---|-------------|------------------------------------------------------------------------------|--|
| <b>B5</b> | 46                                                     | M | 4 | Y | 2 | Diagnosis   | FL1 (May 88): Expectant management                                           |  |
|           |                                                        |   |   |   |   | Progression | FL2 (Jan 91): Chl, then cyclophosphamide                                     |  |
|           |                                                        |   |   |   |   | Progression | FL3 (Sept 97): Expectant management                                          |  |
|           |                                                        |   |   |   |   | Progression | FL4 (Dec 03): Rituximab + anti-CD22                                          |  |
| <b>B6</b> | 50                                                     | F | 3 | Y | 1 | Diagnosis   | FL1 (Feb 97): Expectant management                                           |  |
|           |                                                        |   |   |   |   | Progression | No biopsy (Aug 01): Chl                                                      |  |
|           |                                                        |   |   |   |   | Relapse     | FL2 (May 02): CHOP                                                           |  |
|           |                                                        |   |   |   |   | Relapse     | FL3 (May 03): BEAM-R, then fludarabine                                       |  |
|           |                                                        |   |   |   |   | Relapse     | FL4 (Oct 03): Etoposide, cytarabine followed by vincristine and methotrexate |  |
| Relapse   | FL5 (Feb 07): Velcade + Rituximab, followed by RIC-SCT |   |   |   |   |             |                                                                              |  |

Chl: chlorambucil; CHOP: cyclophosphamide, doxorubicin, vincristine, prednisolone; R: rituximab; GA101: obinutuzumab; FMD: fludarabine, mitoxantrone, dexamethasone; IFRT: involved field radiotherapy; Unk: unknown; BEAM: carmustine, etoposide, cytarabine, melphalan; RIC-SCT: reduced intensity conditioning stem cell transplantation

Remarkably, our data disclosed a novel finding of somatic non-silent mutations in the gene *RRAGC*, which encodes a Ras-related GTP-binding protein (RagC), occurring in four of the five cases. Notably, in cases B4 and B6, the *RRAGC* mutations (p.Pro118Leu and p.Lys74Arg) were conserved during disease progression whereas in cases B2 and B3, a convergent pattern of clonal selection was seen with different mutations occurring at different time points in the disease evolution (**Fig. 1a**). Copy number variation were rarely observed at the *RRAGC* locus, 1p34.3, in both our current data and previous single-nucleotide polymorphism (SNP) array datasets<sup>2</sup> (**Supplementary Fig. 3**). These together with the *RRAGC* variant allele frequencies (VAF) were consistent with heterozygous mutations (VAF range: 0.17-0.5), whilst clonality plots verified that the VAFs were comparable to those of early driver mutations

demonstrating that the *RRAGC* mutations reside within the dominant clone of the tumor biopsies (**Fig. 1b**).

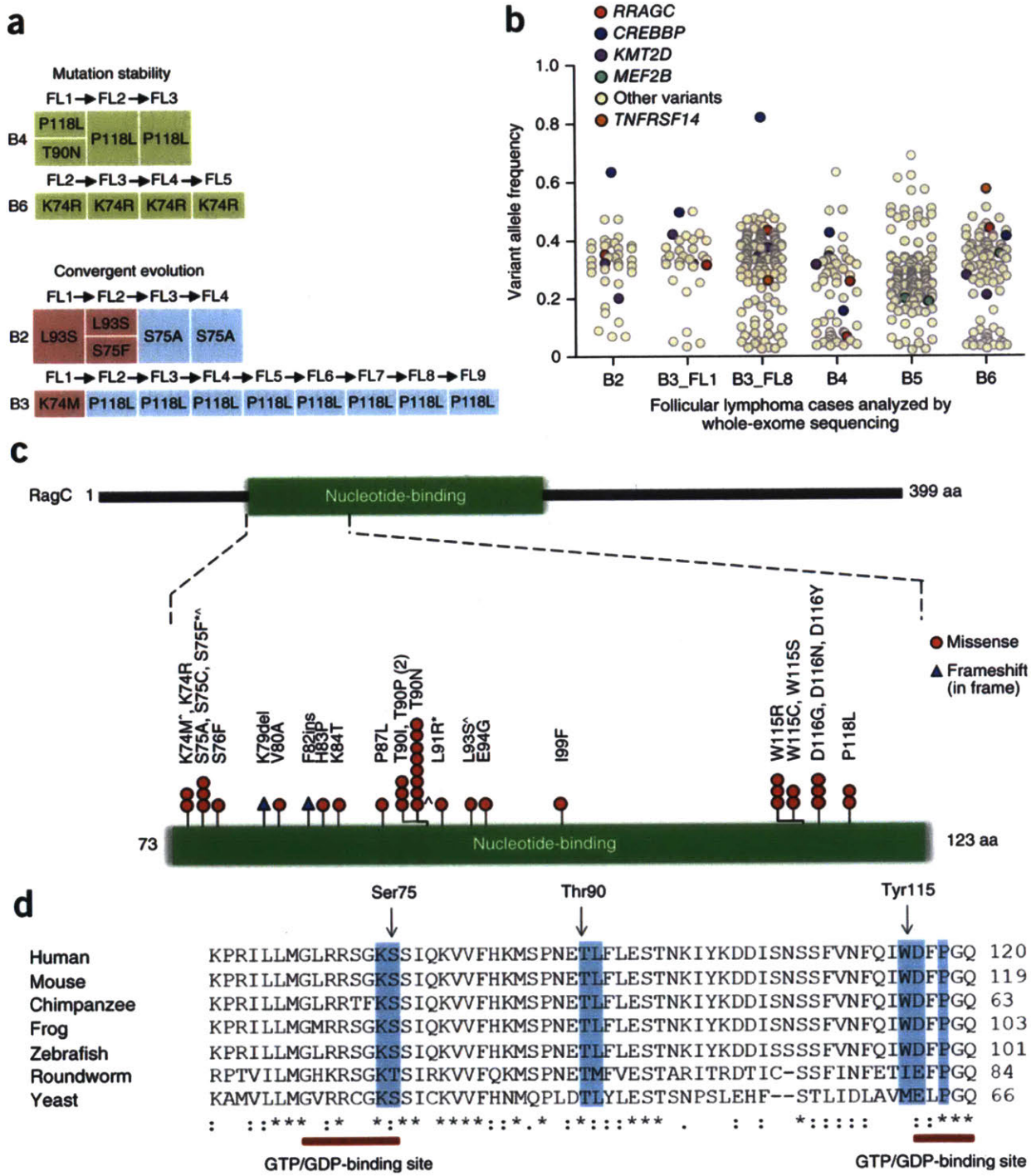
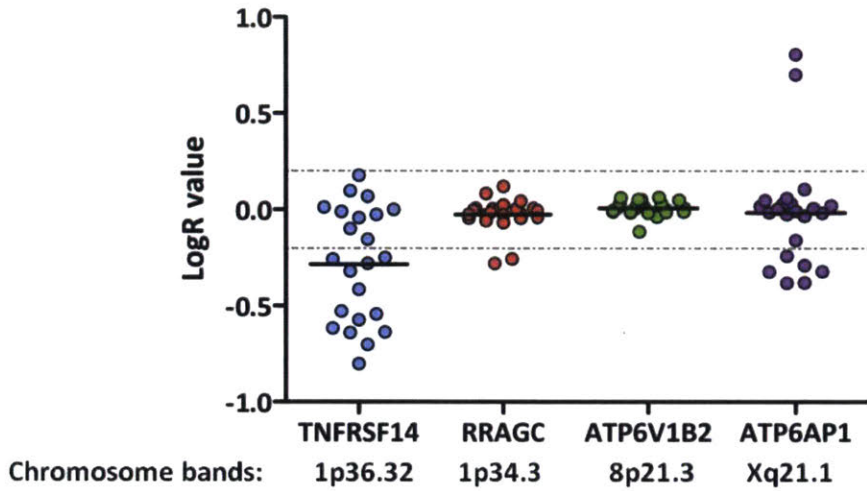


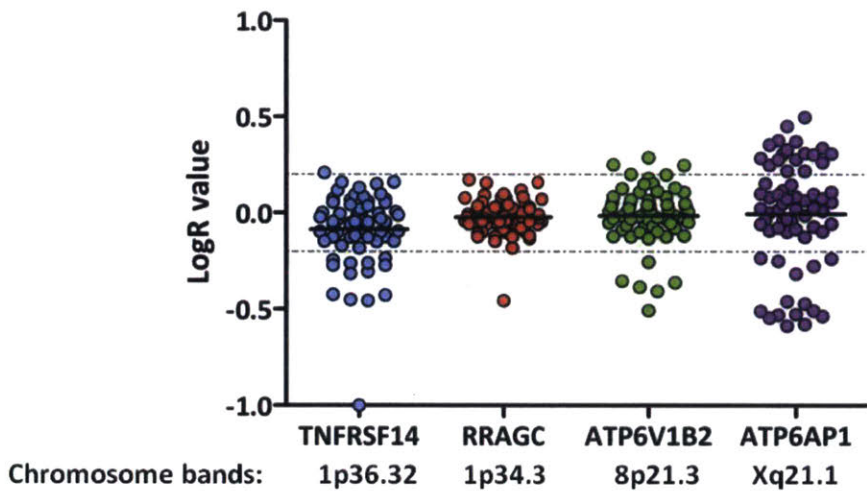
**Figure 1: Identification of frequent *RRAGC* mutations in follicular lymphoma.**  
 (a) Two different patterns of conservation of *RRAGC* mutations in successive tumor biopsies during follicular lymphoma progression in the discovery whole-exome sequencing cases: mutation stability and convergent evolution. (b) VAF distribution and

density for all the nonsynonymous mutations identified in the five cases analyzed by whole-exome sequencing. In each case, the first available biopsy is depicted, with the exception of B3, where two time points are illustrated (B3\_FL1 and B3\_FL8). (c) Schema of the RRAGC protein domain and the locations of the 37 mutations identified in this study affecting 32 cases (NCBI, NP\_071440.1). A caret indicates a second *RRAGC* mutation occurring in a different disease event from the same patient, and an asterisk indicates a second *RRAGC* mutation in the same biopsy of a particular patient. Multiple circles for the same amino acid represent multiple cases with mutations affecting the same residue. (d) Sequence alignment of a section of the RRAGC nucleotide-binding domain. Conserved residues across all the listed species are indicated by an asterisk. The locations of the GTP/GDP-binding sites are indicated by red horizontal bars (at positions 68–75 and 116–120), and the recurrent hotspot residues are highlighted in light blue.

### Discovery WES cases



### Extension SNP6.0 dataset



### Supplementary Figure 3. Copy number of *RRAGC* compared to other gene loci.

The top panel shows the LogR values for each of the gene locus indicated from all 24 samples from the 5 WES cases, whilst the bottom panel shows the LogR values from our previously published SNP6.0 dataset comprising of 29 different FL samples and its paired transformed FL. The gene locus for *TNFRSF14*, 1p36.32, was chosen as a reference loci as it is commonly subject to frequent copy number deletions in FL. The



horizontal dashed line indicates the LogR value of -0.2 with values below this measure indicative of deletions and those above 0.2 indicative of gains.

To determine the prevalence of *RRAGC* mutations, targeted sequencing was performed in an extension cohort of 141 FL samples (including the original 5 cases) and 32 cases with paired transformed FL. *RRAGC* mutations were present in 17% of cases (**Table 1**). The mutations were predominantly missense, with exception of two in-frame frameshift mutations, restricted to exons 1 and 2 (**Fig. 1c** and **Supplementary Table 5**). The clustering of mutations corresponded to the nucleotide-binding domain with hotspots centering on amino acids p.Ser75, p.Thr90, p.Try115, p.Asp116 and p.Pro118, residues highly conserved between species (**Fig. 1c** and **Fig. 1d**). In 10 patients with constitutional DNA, the somatic nature of the mutations was confirmed. To investigate the full complement of *RRAGC* mutations in other malignancies, we performed Sanger sequencing, restricting our analyses to exon 1 and 2, in a further 329 related mature B-cell NHLs and 51 B-cell lymphoma cell lines alongside an analysis of publically available sequencing datasets. *RRAGC* mutations were absent in other hematological malignancies, including myeloid and other mature B-cell NHL entities (**Table 1**) with the exception of infrequent mutations in the closely-related DLBCL. We found that *RRAGC* was rarely mutated in non-hematological neoplasms (0.3% of nearly 10,000 samples) included in the Cancer Genomics database (cBioportal)<sup>21</sup>, with the majority of mutations arising in residues beyond p.Pro118 (**Supplementary Table 6**). *RRAGC* mutations are therefore highly enriched in FL with their nature and frequency suggesting that the changes are likely to be functionally relevant in this lymphoma.

**Table 1 Frequency of *RRAGC* mutations in lymphoma and other hematological malignancies**

| <b>Tumor type</b>                       | <b>Occurrence<br/>No./total No.</b> | <b>Frequency</b> |
|-----------------------------------------|-------------------------------------|------------------|
| <b>FL</b>                               | 25/141                              | 17.7%            |
| Diagnostic                              | 13/94                               | 13.8%            |
| Relapse                                 | 12/47                               | 25.5%            |
| <b>FL and tFL pairs</b>                 | 6/32 <sup>#</sup>                   | 18.8%            |
| <b>DLBCL<sup>^</sup></b>                | 3/174                               | 1.7%             |
| GCB                                     | 1/67                                | 1.5%             |
| ABC                                     | 1/43                                | 2.3%             |
| PMBL                                    | 1/29                                | 3.4%             |
| U                                       | 0/35                                | 0%               |
| <b>DLBCL<sup>*</sup></b>                | 1/185                               | 0.5%             |
| <b>B cell lymphomas</b>                 |                                     |                  |
| Burkitt lymphoma <sup>*</sup>           | 0/42                                | 0%               |
| CLL/SLL <sup>^</sup>                    | 0/96                                | 0%               |
| CLL <sup>*</sup>                        | 0/258                               | 0%               |
| MCL <sup>*</sup>                        | 0/29                                | 0%               |
| SMZL <sup>^</sup>                       | 0/48                                | 0%               |
| Other B-cell lymphomas                  | 0/48                                | 0%               |
| <b>Cell lines (B-NHL)</b>               | 2/51                                | 3.9%             |
| <b>Other hematological malignancies</b> |                                     |                  |
| AML <sup>*</sup>                        | 0/200                               | 0%               |
| CML <sup>*</sup>                        | 0/129                               | 0%               |
| MM <sup>*</sup>                         | 0/203                               | 0%               |
| <b>Benign reactive lymph nodes</b>      | 0/10                                | 0%               |

tFL, transformed follicular lymphoma; DLBCL, diffuse large B cell lymphoma; GCB, germinal center B-cell subtype DLBCL defined by gene-expression profiling (GEP); ABC, activated B-cell subtype of DLBCL defined by GEP; PMBL, primary mediastinal B-cell lymphoma defined by GEP; U, unclassifiable by GEP; CLL, chronic lymphocytic leukemia; MCL, mantle cell lymphoma; SMZL, splenic marginal zone lymphoma; AML, acute myeloid leukemia; CML, chronic myeloid leukemia; MM, multiple myeloma.

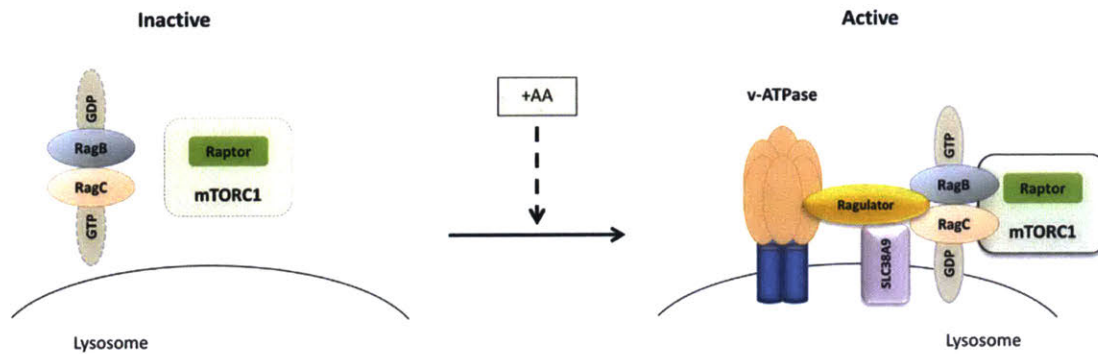
<sup>#</sup>comprising 5 cases with mutations in both FL and tFL and 1 case with only the tFL sample

<sup>^</sup> Sanger sequencing restricted to *RRAGC* exon 1 and 2

<sup>\*</sup>Mined from publicly available cancer genome datasets (see **URL**)<sup>10,12,13,16-20,</sup>

RagC is one of four members of the Rag GTPase family in mammals, which form obligate heterodimers between RagA/B and RagC/D<sup>22,23</sup>. The Rag GTPases form a supercomplex on the lysosomal surface with Ragulator, the v-ATPase and SLC38A9 (**Supplementary Fig. 4**), essential for inducing mechanistic target of rapamycin complex 1 (mTORC1) activation in response to amino acid sufficiency<sup>24-31</sup>. Other members of the Rag GTPase family and mTORC1 components (*RRAGA*, *RRAGB*, *RRAGD*, *MTOR*, *RPTOR* and *MLST8*) were infrequently mutated (**Supplementary Table 5**). To expand this search, we examined our FL datasets to ascertain if other regulatory complexes upstream and downstream of Rag GTPases were subject to genetic aberrations. This approach uncovered mutations in two subunits of the v-ATPase complex, *ATP6V1B2* and *ATP6AP1*. The v-ATPase complex resides within intracellular compartments such as the lysosome and is composed of two domains, a cytosolic V1 domain responsible for ATP hydrolysis and a transmembrane V0 that enables proton translocation<sup>32</sup>. *ATP6V1B2* is a non-catalytic subunit within the V1 domain, and *ATP6AP1* is thought to be an accessory subunit that regulates the function of the v-ATPase complex<sup>33</sup>. To assess the relationship between these v-ATPase subunit mutations, *RRAGC* and FL-associated genes, we resequenced our extension cohort of 141 FL cases identifying 11.3% and 9.9% of cases with *ATP6V1B2* and *ATP6AP1* mutations, respectively (**Fig. 2a** and **Supplementary Table 7, 8**). Interestingly, mutations in *RRAGC*, *ATP6V1B2* and *ATP6AP1* showed strong correlations with more than half of the *RRAGC* mutations co-occurring with either *ATP6V1B2* or *ATP6AP1* (Fisher's exact test,  $P < 0.0001$ ), whereas *ATP6V1B2* and *ATP6AP1* mutations were mutually exclusive. Mutations in *ATP6V1B2* were all missense, with a hotspot at c.1199G>A; p.Arg400Gln representing 80% of all mutations detected (**Fig. 2b**). In comparison, mutations in *ATP6AP1* included both missense and frameshift mutations most localizing to the C-terminal end of the ATP-synthase domain (**Fig. 2c**). Deep targeted sequencing (mean coverage 4655x) of 15 co-mutated cases demonstrated no definitive hierarchy in mutation order of *RRAGC* and *ATP6V1B2* or *ATP6AP1* suggesting that both alterations are acquired concomitantly during similar clonal selective sweeps (**Fig. 2d**). Together, over a quarter of patients (27.4%; 39 of 141 cases) had mutations in one or more of the three genes.





**Supplementary Figure 4. Model of components of the amino acid–induced mTORC1 pathway.** At low amino acid levels (left), the Rag heterodimer (RagB-RagC) is in a nucleotide-bound configuration incompatible for the recruitment and activation of mTORC1. In the presence of sufficient amino acids (right), a supercomplex comprising the v-ATPase, Ragulator, SLC38A9 and the Rag GTPase heterodimer translocates to the lysosomal surface. This changes the Rag heterodimer into its active form with RagB being GTP bound and RagC being GDP bound, resulting in the recruitment and activation of mTORC1.

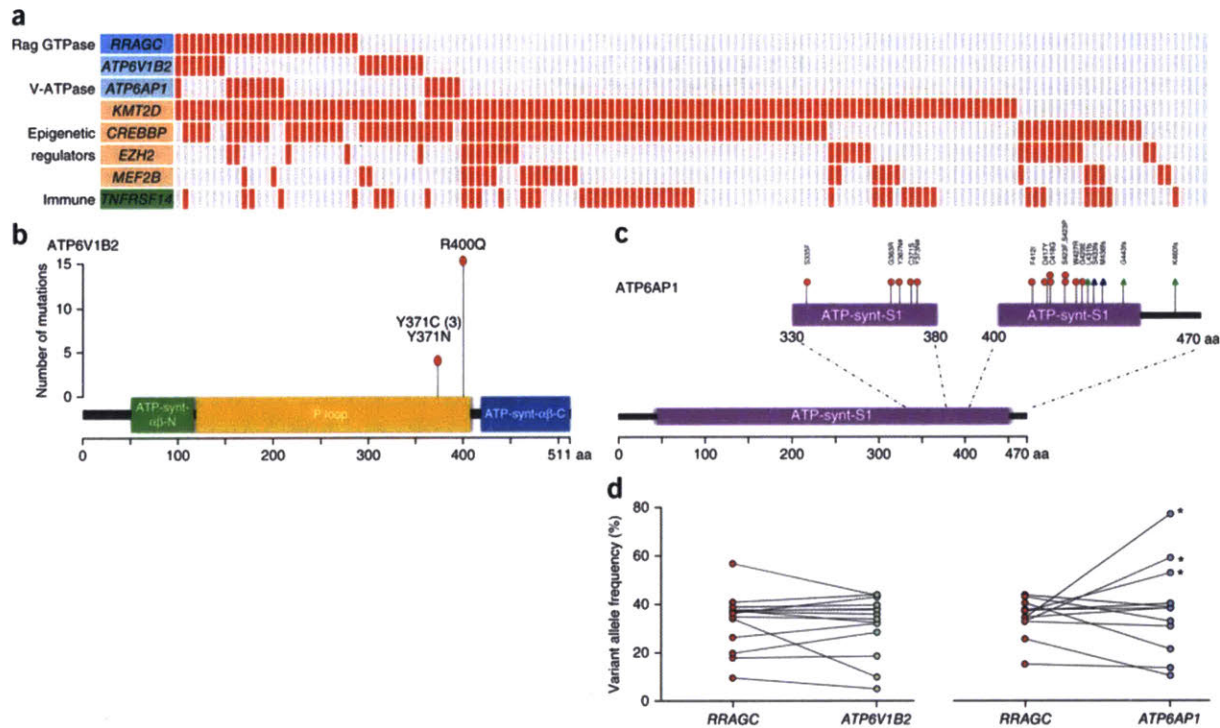
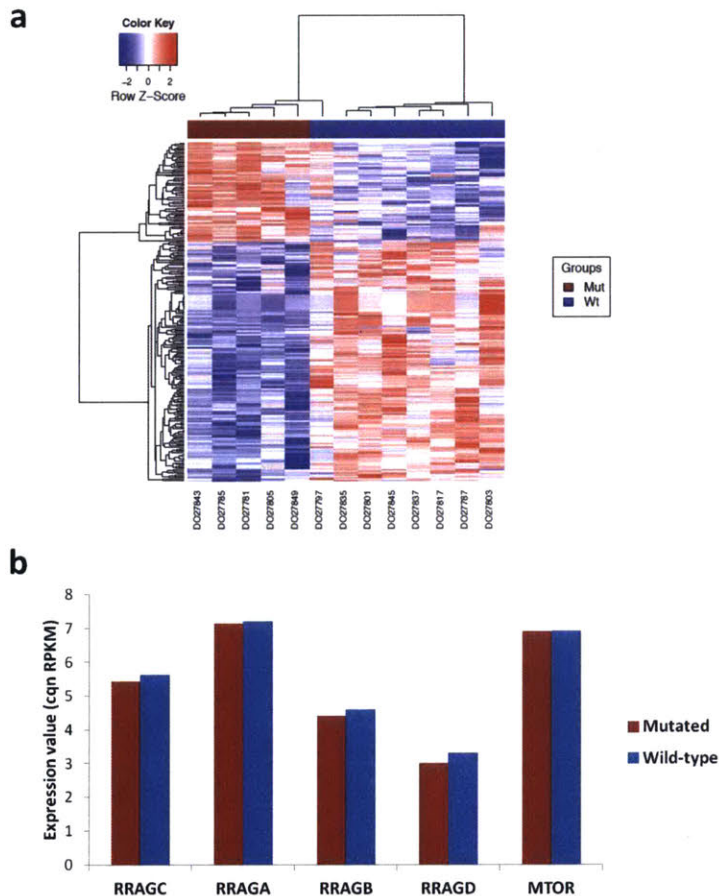


**Figure 2: Frequent and co-occurring mutations in *ATP6V1B2* and *ATP6AP1*.** (a) Distribution of mutations in *RRAGC*, *ATP6V1B2*, *ATP6AP1* and other known follicular lymphoma-associated genes in 141 follicular lymphoma cases. Each column represents an individual case, and each row denotes a specific gene. Red indicates the presence of mutations, and light gray indicates the absence thereof. (b) Schema of the protein domains of *ATP6V1B2* and the locations of the identified mutations (NCBI, NP\_001684.2). (c) Schema of the protein domains of *ATP6AP1* and the locations of the identified mutations (NCBI, NP\_001174.2). Red circles represent missense mutations resulting in substitutions, blue triangles represent in-frame insertion-deletions and green triangles represent out-of-frame insertion-deletions. A number sign indicates substitutions occurring in the same case. ATP-synt- $\alpha\beta$ -N, ATP synthase  $\alpha/\beta$  family  $\beta$ -barrel domain; P loop, phosphate-binding loop; ATP-synt- $\alpha\beta$ -C, ATP synthase  $\alpha/\beta$  chain C-terminal domain; ATP-synt-S1, ATP synthase subunit S1. (d) Comparison of the allele frequencies in 26 co-mutated (*RRAGC* versus *ATP6V1B2* and *RRAGC* versus *ATP6AP1*) samples (comprising 15 cases, some with multiple biopsies). Male cases are marked with an asterisk and

demonstrate expected increases in allelic frequencies of *ATP6AP1* mutations, as the gene locus resides on the X chromosome.

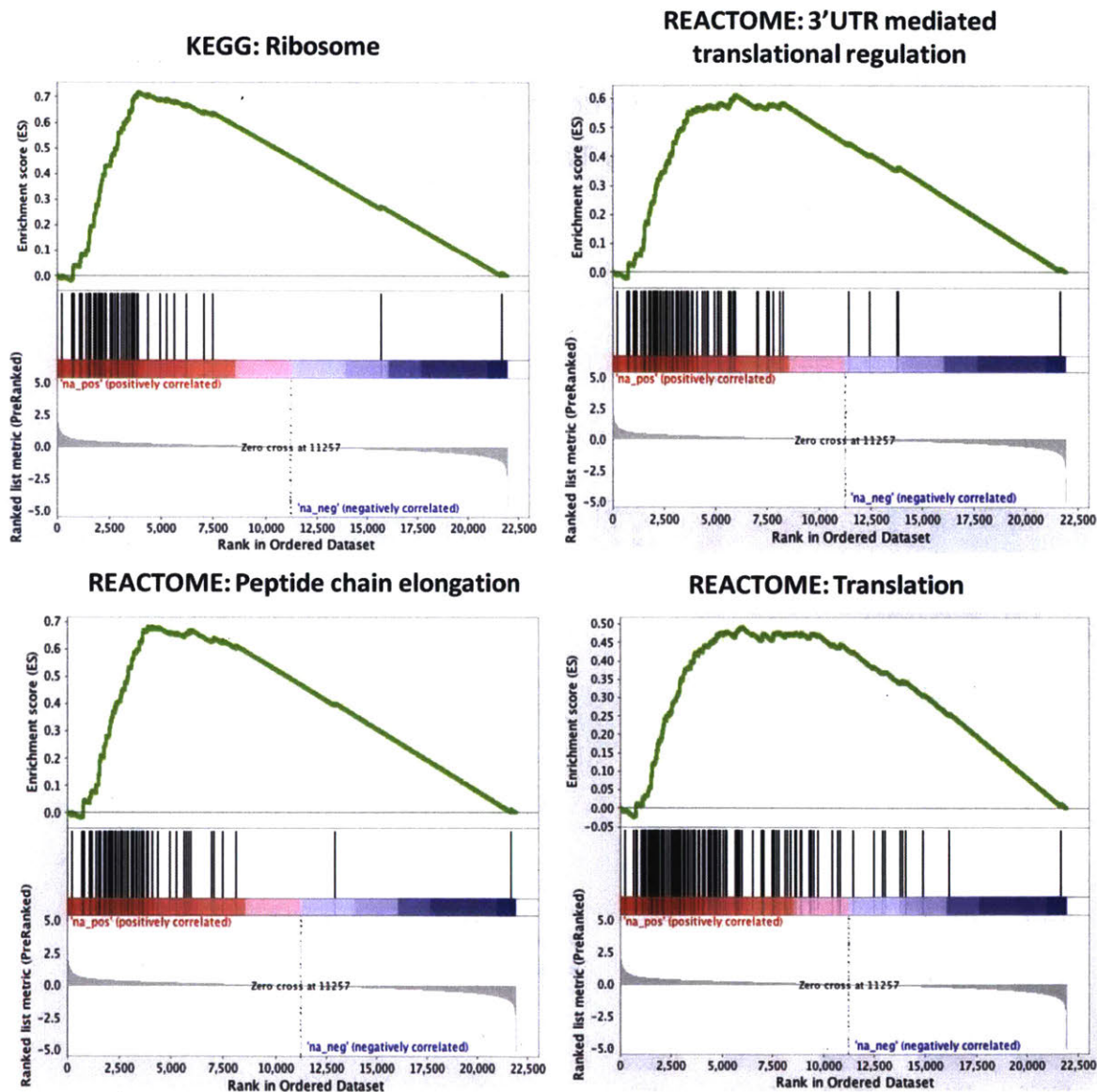
To begin understanding the pathogenic role of *RRAGC* mutations, we examined RNA-seq data in 13 FL cases (**Supplementary Table 9**) and identified 257 differentially expressed genes between mutated and wild-type cases (**Supplementary Fig. 5a**). There was no difference in *RRAGC* expression between mutated and wild-type cases (**Supplementary Fig. 5b**). Gene set enrichment analyses (GSEA) showed that *RRAGC*-mutated cases were characterized by up-regulated expression for gene sets involved in translation regulation, well-known downstream mTOR targets<sup>34,35</sup> (**Supplementary Fig. 6 and Supplementary Table 10**), implicating altered signaling as a consequence of these mutations.



**Supplementary Figure 5. Differential gene expression between *RRAGC* mutated vs wild-type FL cases.** (a) Heat map from the unsupervised hierarchical clustering of genes that are differentially expressed between *RRAGC* mutated (red bar, N = 5)



compared to wild-type tumors (blue bar, N = 8). This consisted of 75 up-regulated and 182 down-regulated genes based on a raw  $P$  value of  $<0.01$ , false discovery rate (FDR) of  $<0.25$  and fold change of  $>2$ . (b) Gene expression values for RRAGC, MTOR and the other Rag GTPases. No difference in expression was noted between mutated compared to wild-type tumors. Cqn, conditional quantile normalization; RPKM, reads per kilobase per million



**Supplementary Figure 6. Representative GSEA plots.** GSEA of gene expression data derived from RNA-seq of 5 *RRAGC* mutated vs 8 wild-type cases. This showed significant enrichment for gene sets in several processes involved in translation and cell cycle regulation, which were up-regulated in the *RRAGC* mutated tumors compared to

wild-type tumors. Hits displayed below the graph show where the members of the gene set appear in the ranked list of genes. FDR q-values and further gene sets are fully listed in **Supplementary Table 9**.

The direct binding of Rag GTPase heterodimers to mTORC1 is a key event in the activation of mTORC1 by amino acids<sup>23-29</sup>. Under these conditions, the active Rag heterodimer, composed of GTP-loaded RagA/B bound to GDP-loaded RagC/D, directly interacts with raptor (**Supplementary Fig. 4**), a component of mTORC1<sup>25</sup>. We first assessed the effects of 8 RagC mutants detected in our FL series (p.Lys74Arg, p.Ser75Asn, p.Ser75Phe, p.Thr90Asn, p.Ile99Phe, p.Tyr115Arg, p.Asp116Gly and p.Pro118Leu) on their raptor binding capacity by co-expressing each RagC mutant (RagC<sup>mut</sup>) together with wild-type RagB in HEK-293T cells. These RagB-RagC<sup>mut</sup> heterodimers co-immunoprecipitated substantially more endogenous raptor than a fully wild-type RagB-RagC heterodimer (**Fig. 3a**). Importantly, the increased raptor binding was specific to the identified FL *RRAGC* mutations, as RagC mutations in other cancer types did not demonstrate the same capacity (**Supplementary Fig. 7a**). Interestingly, the increased raptor binding observed with the RagC<sup>mut</sup> was similar to that seen with RagC p.Ser75Asn, a previously characterized mutant with decreased affinity for GTP that therefore functions like a 'GDP-bound' mutant, mimicking the RagC conformation that is necessary for mTORC1 activation by amino acids<sup>25, 36-39</sup> (**Fig. 3a**). The similar increase in raptor binding caused by the RagC mutants and RagC p.Ser75Asn provided the first indication that the *RRAGC* mutations observed in FL are likely activating. To examine the impact of these mutations in B-cell lymphomas, we stably expressed three recurring FL mutants (p.Ser75Phe, p.Thr90Asn and p.Trp115Arg) and the 'GDP-binding' mutant, RagC p.Ser75Asn, in four germinal center NHL cell lines (Karpas-422, Raji, OCI-Ly7 and OCI-Ly8) and these reaffirmed our findings of increased raptor binding over wild-type RagC (**Fig. 3b and Supplementary Fig. 7b-d**). To test the effects of the RagC mutants on mTORC1 signaling, we stably expressed these four mutants in HEK-293T cells. Overexpression of all four mutants increased mTORC1 activity, even under complete amino acid deprivation as detected by the phosphorylation of S6 kinase 1 (S6K1), an established mTORC1 substrate (**Supplementary Fig. 7e**). Furthermore, all

RagC<sup>mut</sup>s tested rendered mTORC1 signaling partially or fully insensitive to leucine or arginine deprivation, amino acids of particular importance for mTORC1 pathway activation<sup>24, 40, 41</sup> (Figs. 3c, 3d and Supplementary Fig. 7f, 7g). Similarly, in Karpas-422 cells, overexpression of two mutants, p.Thr90Asn and p.Trp115Arg, but not wild-type RagC, led to increased mTORC1 signaling in the absence of leucine, validating the mTORC1 activating properties of the RagC mutants (Fig. 3e and Supplementary Fig. 7h).

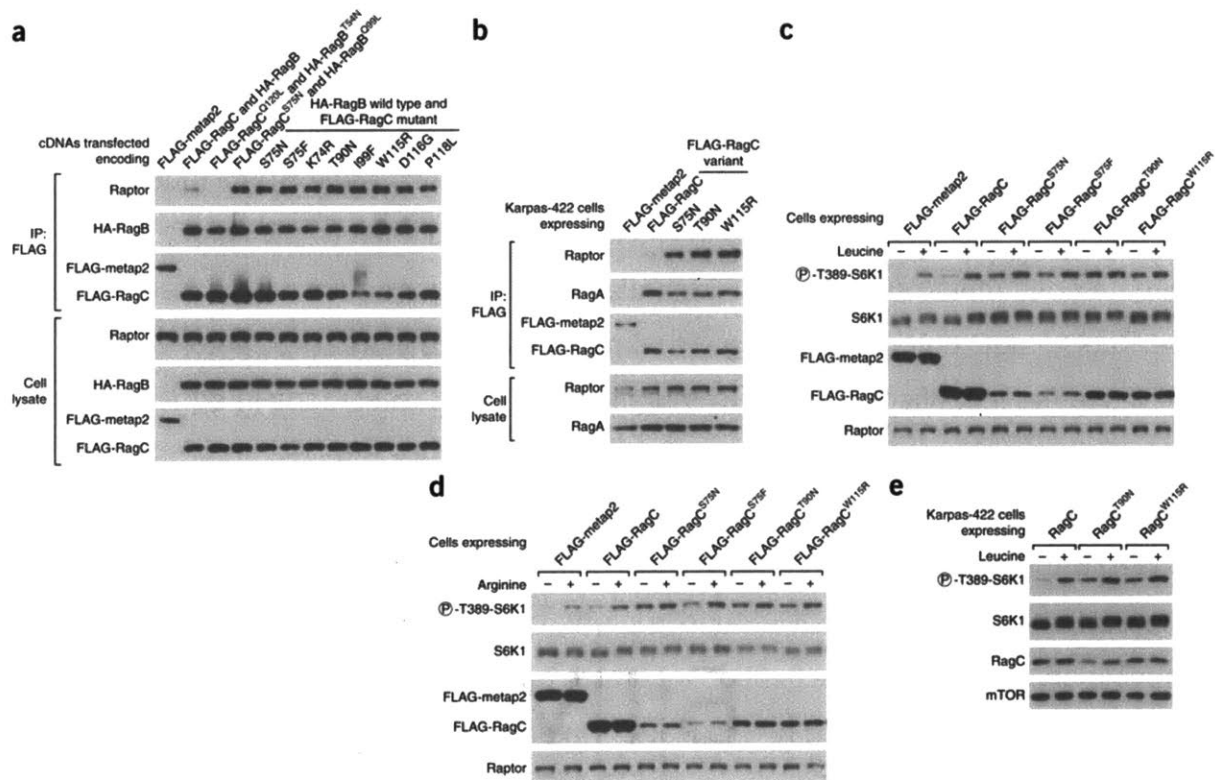
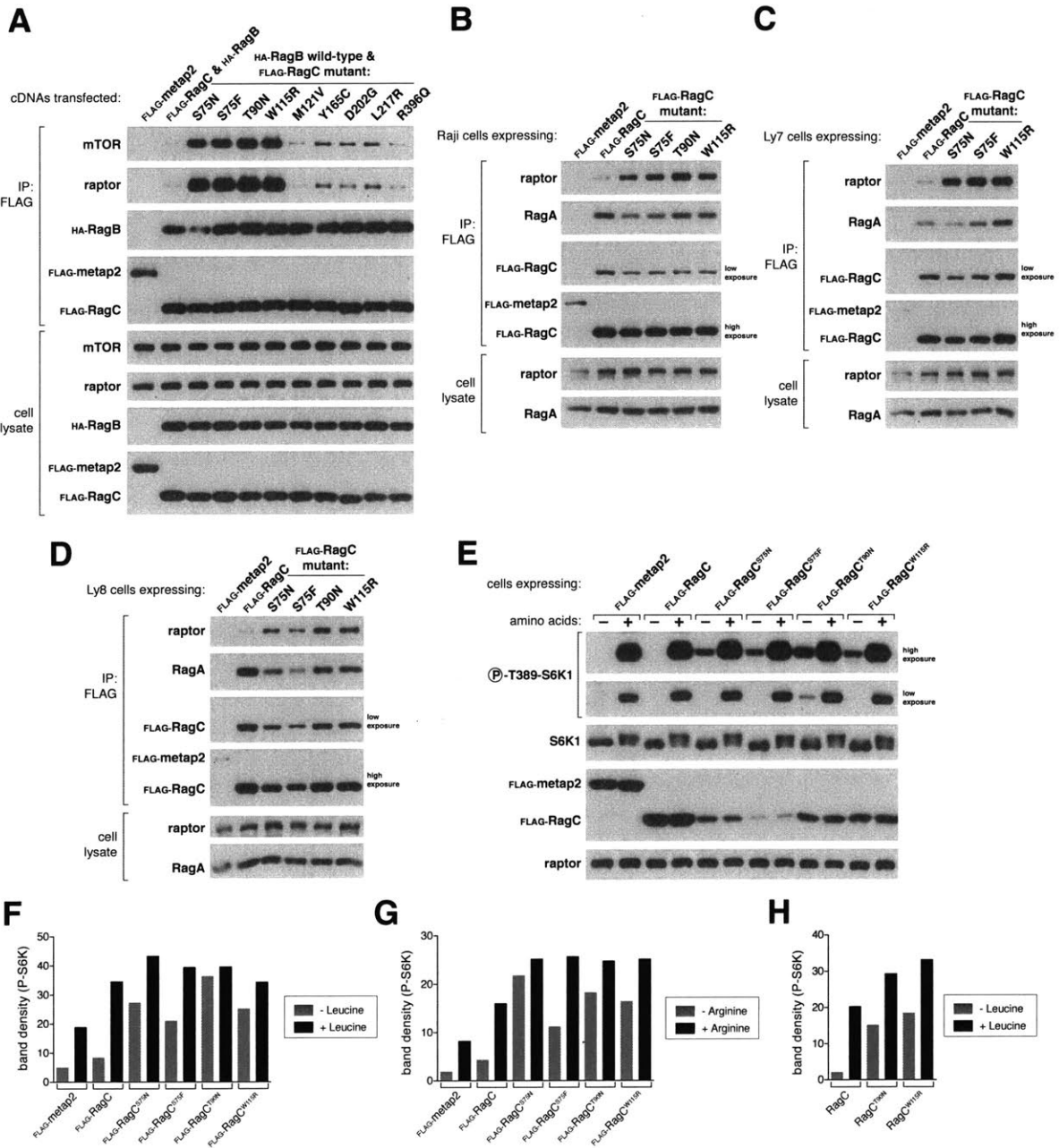


**Figure 3: Effects of RagC variants on mTORC1 signaling. (a)**

Coimmunoprecipitation of Rag heterodimers containing the RagC variants and raptor, an mTORC1 component. Anti-FLAG immunoprecipitates were collected from HEK293T cells transiently expressing the indicated constructs, and cell lysates and immunoprecipitates were analyzed by immunoblotting. RagB Gln99Leu and RagC Gln120Leu are 'GTP-locked' mutants<sup>36, 47</sup>, and RagC Ser75Asn and RagB Thr54Asn function as 'GDP-bound' mutants<sup>25, 36, 37, 38, 39</sup>. IP, immunoprecipitation; HA, hemagglutinin. (b) Coimmunoprecipitation showing that two recurrent variants from follicular lymphoma, Thr90Asn and Trp115Arg RagC, and the previously characterized Ser75Asn RagC mutant coimmunoprecipitate more endogenous raptor than wild-type

RagC in Karpas-422 cells, a germinal center B cell lymphoma line. Anti-FLAG immunoprecipitates from Karpas-422 cells stably expressing the indicated proteins were collected and analyzed as in **a**. **(c)** Immunoblot analysis of cell lysates for the indicated proteins, showing that stable overexpression of Ser75Asn, Ser75Phe, Thr90Asn and Trp115Arg RagC renders cells partially or fully insensitive to leucine deprivation. HEK293T cells stably expressing the indicated proteins were starved of leucine for 50 min and restimulated with leucine for 10 min. P-T389-S6K1, S6K1 phosphorylated at Thr389. **(d)** Immunoassay showing that stable overexpression of the indicated RagC mutants leads to an increase in mTORC1 signaling in the absence of arginine. HEK293T cells stably expressing the indicated proteins were starved of arginine for 50 min, restimulated with arginine for 10 min and analyzed as in **c**. **(e)** Immunoassay showing that stable overexpression of the indicated RagC mutants but not wild-type RagC leads to increased mTORC1 signaling in the absence of leucine in Karpas-422 cells. Karpas-422 cells stably expressing the indicated proteins were treated and analyzed as in **b**.

Supp. Figure 7



**Supplementary Figure 7. Recurrent follicular lymphoma RagC mutants activate the mTORC1 pathway.** (a) Follicular lymphoma RagC mutants (RagC<sup>S75F</sup>, RagC<sup>S75N</sup>, RagC<sup>T90N</sup> and RagC<sup>W115R</sup>) dramatically increase mTORC1 binding (mTOR and raptor), whereas *RRAGC* mutations identified in solid cancers (p.M121V,



p.Y165C, p.D202G, p.L217R and p.R396Q) did not coimmunoprecipitate mTORC1 as strongly. Anti-FLAG immunoprecipitates were collected and analyzed as in **Figure 3a**. **(b)** All four RagC mutants coimmunoprecipitate more raptor than wild-type RagC in Raji cells. Anti-FLAG immunoprecipitates from Raji cells stably expressing the indicated proteins were collected and analyzed as in **Figure 3a**. **(c)** Three RagC mutants (RagC S75N, RagC S75F and RagC W115R) coimmunoprecipitate more raptor than wild-type RagC when overexpressed in OCI-Ly7 cells. Anti-FLAG immunoprecipitates from OCI-Ly7 cells stably expressing the indicated proteins were collected and analyzed as in **Figure 3a**. **(d)** Four RagC mutants increase raptor binding over wild-type RagC in OCI-Ly8 cells. Anti-FLAG immunoprecipitates from Ly8 cells stably expressing the indicated proteins were collected and analyzed as in **Figure 3a**. **(e)** Stable overexpression of RagC S75N, RagC S75F, RagC T90N and RagC W115R renders the cells partially insensitive to full amino acid deprivation. HEK293T cells that stably expressed the indicated proteins were starved of amino acids for 50 min and restimulated with amino acids for 10 min. The cell lysates were analyzed as in **Figure 3b**. **(f)** Quantification of the amount of phosphorylated S6K1 in **Figure 3c**, under leucine starvation or starvation followed by restimulation in HEK293T cells stably expressing the indicated proteins. **(g)** Quantification of the amount of phosphorylated S6K1 in **Figure 3d**, under arginine starvation or starvation followed by restimulation in HEK293T cells stably expressing the indicated proteins. **(h)** Quantification of the amount of phosphorylated S6K1 in **Figure 3e**, under leucine starvation or starvation followed by restimulation in Karpas-422 cells stably expressing the indicated proteins.

To determine if RagC mutations affect their capacity to bind guanine nucleotides, we employed a specific *in vitro* assay in which nucleotide binding to purified Rag heterodimers could be assessed by purifying wild-type and mutant RagC in complex with a RagB mutant (p.Asp163Asn) that preferentially binds to xanthosine nucleotides. Employing this RagB mutant allowed us to measure guanine nucleotide binding to the RagC mutant only, even in the presence of RagB<sup>42,43</sup>. Two classes of RagC mutants emerged from this analysis. One class, including RagC Ser75Asn and Ser75Phe, had

significantly decreased affinity for GTP in comparison to wild-type RagC, and a preference for binding GDP over GTP (**Figs. 4a-b**). These mutants are analogous to the Ras Ser17Asn mutant, which disrupts coordination of the magnesium cofactor leading to decreased affinity for all nucleotides<sup>37,38</sup>. Interestingly, this Ras mutant suppresses signaling, not through decreased GTP binding, but rather through its high affinity for ras guanine nucleotide exchange factors (GEFs), thus preventing guanine nucleotide exchange on wild-type Ras<sup>38, 44, 45</sup>. Further studies will be needed to uncover if the same mechanism is true for the RagC mutants, as a GEF for RagC has yet to be identified. The second class of mutants, Thr90Asn and Trp115Arg, display a slight preference for GDP binding over GTP, without an overall decrease in GTP binding in comparison to wild-type RagC (**Fig. 4a, b**). While the relative nucleotide affinity of these mutants is biased towards GDP, this may not account for their signaling effects in cells, as intracellular GTP concentrations are 10-20 times higher than those of GDP<sup>46</sup>. Importantly, the levels of RagC were consistent in our assays indicating that the variation in nucleotide binding cannot be accounted for by differences in protein levels (**Fig. 4c**). While this second class of mutants may activate the mTORC1 pathway through mechanisms not involving changes in nucleotide loading, further work is needed to uncover the exact mechanism through which they lead to increased raptor binding.

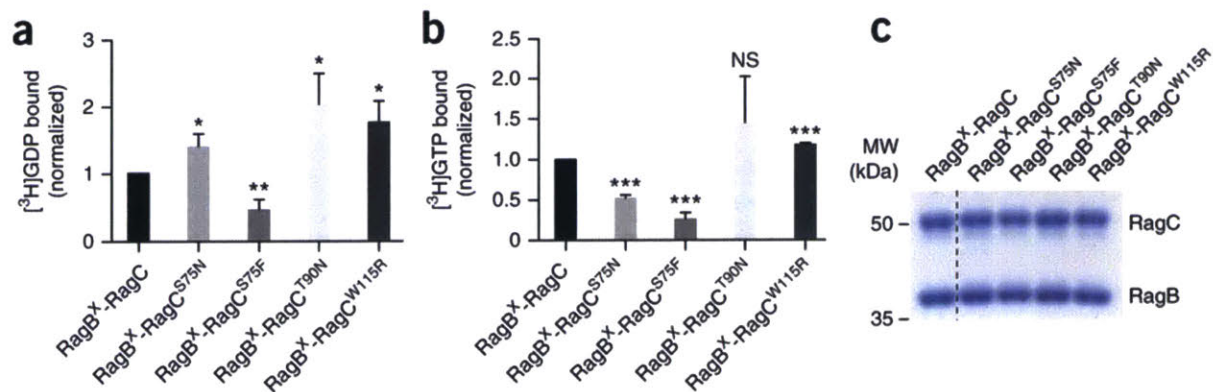


**Figure 4: RagC mutants have altered nucleotide binding affinity.** (a,b) Nucleotide binding assayed by filter binding, with the indicated RagC heterodimer incubated with [<sup>3</sup>H]GDP (a) or [<sup>3</sup>H]GTP (b). RagB<sup>x</sup> is the specific Asp163Asn RagB mutant. Each value represents the normalized mean ± s.d. for *n* = 3 experiments. Statistical differences were assessed comparing each sample to the binding observed with the RagB-RagC

wild-type heterodimer. Student's *t* test, \**P* < 0.05, \*\**P* < 0.01, \*\*\**P* < 0.005; NS, not significant. (c) SDS-PAGE analysis of aliquots of the purified Rag heterodimers used in the nucleotide-binding assays; the gel was stained with Coomassie.

As the v-ATPase complex is functionally linked with the Rag GTPases and Ragulator in sensing amino acids and activating mTORC1 signaling<sup>29</sup>, the co-existence of *RRAGC* with either *ATP6V1B2* or *ATP6AP1* mutations raises the question of a functional epistasis. ATP-hydrolysis and the v-ATPase rotator conformation are crucial for relaying the amino acid signal from the lysosomal lumen to the Rag GTPases<sup>29</sup> and therefore, our working hypothesis is that mutations in these v-ATPase subunits help convey a 'false' amino acid sufficiency signal or alter interactions between v-ATPase, Ragulator and the Rag GTPases, which requires experimental clarification.

In conclusion, our study identifies frequent mutations in components of the lysosome-centric mTORC1 signaling cascade in FL. We demonstrate that *RRAGC* mutants confer a gain-of-function mechanism by bypassing the amino acid deprivation state to activate mTORC1 signaling. Together, the emergence of frequent activating *RRAGC* mutations that are clonally represented and maintained during progression is particularly valuable and might be exploited as a therapeutic target, however, its utility as a predictive biomarker of mTOR inhibitor sensitivity warrants further investigation.

**URLs.** cBioportal for Cancer Genomics, <http://www.cbioportal.org/>; ICGC data portal, <https://dcc.icgc.org/>

**Accession codes.** Exome sequencing data have been deposited at the European Genome-phenome Archive (EGA) under accession number EGAS00001001190.

## **ACKNOWLEDGMENTS**

We are indebted to the patients for donating tumor specimens as part of this study. We would like to thank G.Clark at the Francis Crick Institute for automated DNA sequencing and the Genome Centre for Illumina Miseq sequencing. We acknowledge the support of Barts, Cambridge, Leeds and Southampton's Experimental Cancer Medicine and Cancer Research UK Centers. This work was supported by grants from Kay Kendall Leukaemia Fund and Cancer Research UK (awarded to J.F.) J.O. is a recipient of the Kay Kendall Leukaemia Fund (KKLF) Junior Clinical Research Fellowship (KKL 557).

## **AUTHOR CONTRIBUTIONS**

J.O. and J.F. conceived the study. J.O., D.M.S. and J.F. directed the study. C.M., G.P., P.J., A.D., J.C.S., M.D., S.B., A.J., T.A.L., R.A., S.M. and J.G.G. provided patient samples and clinical data. M.C., A.J. and M.D. conducted pathological review of specimens. J.M. collated clinical information. S.I. prepared and processed samples. H.Q. provided cell lines DNA. J.O., R.L.W., S.A., L.W., B.M.C., L.E-I., A.F.A-S., A.C., C.B. and R.Z. performed experiments. J.W., J.A.G-A., S.H.B. and C.C. performed the bioinformatic analysis. J.R. and R.S. coordinated and verified the ICGC dataset. J.O., R.L.W., J.W., D.M.S and J.F. analyzed and interpreted the data. J.O., R.L.W. and J.F. wrote the manuscript. All authors read and approved the final manuscript.

## **COMPETING FINANCIAL INTERESTS**

We declare no competing financial interests.

## References:

1. Swenson, W.T. *et al.* Improved survival of follicular lymphoma patients in the United States. *J Clin Oncol* **23**, 5019-26 (2005).
2. Okosun, J. *et al.* Integrated genomic analysis identifies recurrent mutations and evolution patterns driving the initiation and progression of follicular lymphoma. *Nat Genet* **46**, 176-81 (2014).
3. Pasqualucci, L. *et al.* Genetics of follicular lymphoma transformation. *Cell Rep* **6**, 130-40 (2014).
4. Karube, K. *et al.* Recurrent mutations of NOTCH genes in follicular lymphoma identify a distinctive subset of tumours. *J Pathol* **234**, 423-30 (2014).
5. Yildiz, M. *et al.* Activating STAT6 mutations in follicular lymphoma. *Blood* (2014).
6. Morin, R.D. *et al.* Somatic mutations altering EZH2 (Tyr641) in follicular and diffuse large B-cell lymphomas of germinal-center origin. *Nat Genet* **42**, 181-5 (2010).
7. Pasqualucci, L. *et al.* Inactivating mutations of acetyltransferase genes in B-cell lymphoma. *Nature* **471**, 189-95 (2011).
8. Compagno, M. *et al.* Mutations of multiple genes cause deregulation of NF-kappaB in diffuse large B-cell lymphoma. *Nature* **459**, 717-21 (2009).
9. Lenz, G. *et al.* Oncogenic CARD11 mutations in human diffuse large B cell lymphoma. *Science* **319**, 1676-9 (2008).
10. Lohr, J.G. *et al.* Discovery and prioritization of somatic mutations in diffuse large B-cell lymphoma (DLBCL) by whole-exome sequencing. *Proc Natl Acad Sci U S A* **109**, 3879-84 (2012).
11. Ngo, V.N. *et al.* Oncogenically active MYD88 mutations in human lymphoma. *Nature* **470**, 115-9 (2011).
12. Morin, R.D. *et al.* Frequent mutation of histone-modifying genes in non-Hodgkin lymphoma. *Nature* **476**, 298-303 (2011).
13. Pasqualucci, L. *et al.* Analysis of the coding genome of diffuse large B-cell lymphoma. *Nat Genet* **43**, 830-7 (2011).
14. Bödör, C. *et al.* EZH2 mutations are frequent and represent an early event in follicular lymphoma. *Blood* **122**, 3165-8 (2013).
15. Green, M.R. *et al.* Hierarchy in somatic mutations arising during genomic evolution and progression of follicular lymphoma. *Blood* **121**, 1604-11 (2013).
16. Beà, S. *et al.* Landscape of somatic mutations and clonal evolution in mantle cell lymphoma. *Proc Natl Acad Sci U S A* **110**, 18250-5 (2013).
17. Landau, D.A. *et al.* Evolution and impact of subclonal mutations in chronic lymphocytic leukemia. *Cell* **152**, 714-26 (2013).
18. Lohr, J.G. *et al.* Widespread genetic heterogeneity in multiple myeloma: implications for targeted therapy. *Cancer Cell* **25**, 91-101 (2014).
19. Morin, R.D. *et al.* Mutational and structural analysis of diffuse large B-cell lymphoma using whole-genome sequencing. *Blood* **122**, 1256-65 (2013).
20. Schmitz, R. *et al.* Burkitt lymphoma pathogenesis and therapeutic targets from structural and functional genomics. *Nature* **490**, 116-20 (2012).
21. Gao, J. *et al.* Integrative analysis of complex cancer genomics and clinical profiles using the cBioPortal. *Sci Signal* **6**, p11 (2013).
22. Nakashima, N., Noguchi, E. & Nishimoto, T. Saccharomyces cerevisiae putative G protein, Gtr1p, which forms complexes with itself and a novel protein designated as

- Gtr2p, negatively regulates the Ran/Gsp1p G protein cycle through Gtr2p. *Genetics* **152**, 853-67 (1999).
23. Sekiguchi, T., Hirose, E., Nakashima, N., Li, M. & Nishimoto, T. Novel G proteins, Rag C and Rag D, interact with GTP-binding proteins, Rag A and Rag B. *J Biol Chem* **276**, 7246-57 (2001).
  24. Kim, E., Goraksha-Hicks, P., Li, L., Neufeld, T.P. & Guan, K.L. Regulation of TORC1 by Rag GTPases in nutrient response. *Nat Cell Biol* **10**, 935-45 (2008).
  25. Sancak, Y. *et al.* The Rag GTPases bind raptor and mediate amino acid signaling to mTORC1. *Science* **320**, 1496-501 (2008).
  26. Bar-Peled, L. *et al.* A Tumor suppressor complex with GAP activity for the Rag GTPases that signal amino acid sufficiency to mTORC1. *Science* **340**, 1100-6 (2013).
  27. Bar-Peled, L., Schweitzer, L.D., Zoncu, R. & Sabatini, D.M. Ragulator is a GEF for the rag GTPases that signal amino acid levels to mTORC1. *Cell* **150**, 1196-208 (2012).
  28. Sancak, Y. *et al.* Ragulator-Rag complex targets mTORC1 to the lysosomal surface and is necessary for its activation by amino acids. *Cell* **141**, 290-303 (2010).
  29. Zoncu, R. *et al.* mTORC1 senses lysosomal amino acids through an inside-out mechanism that requires the vacuolar H(+)-ATPase. *Science* **334**, 678-83 (2011).
  30. Rebsamen, M. *et al.* SLC38A9 is a component of the lysosomal amino acid sensing machinery that controls mTORC1. *Nature* (2015).
  31. Wang, S. *et al.* Metabolism. Lysosomal amino acid transporter SLC38A9 signals arginine sufficiency to mTORC1. *Science* **347**, 188-94 (2015).
  32. Forgac, M. Vacuolar ATPases: rotary proton pumps in physiology and pathophysiology. *Nat Rev Mol Cell Biol* **8**, 917-29 (2007).
  33. Jansen, E.J. & Martens, G.J. Novel insights into V-ATPase functioning: distinct roles for its accessory subunits ATP6AP1/Ac45 and ATP6AP2/(pro) renin receptor. *Curr Protein Pept Sci* **13**, 124-33 (2012).
  34. Iadevaia, V., Huo, Y., Zhang, Z., Foster, L.J. & Proud, C.G. Roles of the mammalian target of rapamycin, mTOR, in controlling ribosome biogenesis and protein synthesis. *Biochem Soc Trans* **40**, 168-72 (2012).
  35. Ben-Sahra, I., Howell, J.J., Asara, J.M. & Manning, B.D. Stimulation of de novo pyrimidine synthesis by growth signaling through mTOR and S6K1. *Science* **339**, 1323-8 (2013).
  36. Tsun, Z.Y. *et al.* The folliculin tumor suppressor is a GAP for the RagC/D GTPases that signal amino acid levels to mTORC1. *Mol Cell* **52**, 495-505 (2013).
  37. Feig, L.A. & Cooper, G.M. Relationship among guanine nucleotide exchange, GTP hydrolysis, and transforming potential of mutated ras proteins. *Mol Cell Biol* **8**, 2472-8 (1988).
  38. Feig, L.A. Tools of the trade: use of dominant-inhibitory mutants of Ras-family GTPases. *Nat Cell Biol* **1**, E25-7 (1999).
  39. John, J. *et al.* Kinetic and structural analysis of the Mg(2+)-binding site of the guanine nucleotide-binding protein p21H-ras. *J Biol Chem* **268**, 923-9 (1993).
  40. Hara, K. *et al.* Amino acid sufficiency and mTOR regulate p70 S6 kinase and eIF-4E BP1 through a common effector mechanism. *J Biol Chem* **273**, 14484-94 (1998).

41. Nicklin, P. *et al.* Bidirectional transport of amino acids regulates mTOR and autophagy. *Cell* **136**, 521-34 (2009).
42. Hoffenberg, S. *et al.* Functional and structural interactions of the Rab5 D136N mutant with xanthine nucleotides. *Biochem Biophys Res Commun* **215**, 241-9 (1995).
43. Schmidt, G. *et al.* Biochemical and biological consequences of changing the specificity of p21ras from guanosine to xanthosine nucleotides. *Oncogene* **12**, 87-96 (1996).
44. Farnsworth, C.L. & Feig, L.A. Dominant inhibitory mutations in the Mg(2+)-binding site of RasH prevent its activation by GTP. *Mol Cell Biol* **11**, 4822-9 (1991).
45. Lai, C.C., Boguski, M., Broek, D. & Powers, S. Influence of guanine nucleotides on complex formation between Ras and CDC25 proteins. *Mol Cell Biol* **13**, 1345-52 (1993).
46. Proud, C.S. Guanine nucleotides, protein phosphorylation and the control of translation. *Trends Biochem Sci.* **11**, 73-77 (1986).
47. Krengel, U. *et al.* Three-dimensional structures of H-ras p21 mutants: molecular basis for their inability to function as signal switch molecules. *Cell* **62**, 539-48 (1990)

## ONLINE METHODS:

**Patients and samples.** Samples were obtained from individuals with FL and non-FL tumors following approval from the Institutional Review Board and local ethics committee of all participating centers. Informed written consent was obtained from all individuals. The discovery cohort (**Supplementary Table 2** and **Supplementary Fig.1**) comprised five patients who had not undergone histologic transformation and selected on the basis of available fresh frozen tumor lymph node biopsies, matched constitutional DNA and samples from multiple disease episodes. The clonality between tumor biopsies obtained from multiple disease episodes from an individual patient were confirmed by *BCL2-IGH* breakpoint analysis as previously described<sup>2</sup>. The FL validation cohort (**Supplementary Table 11**) comprised either diagnostic or relapse FL (n = 141 cases) or paired FL-tFL tumor biopsies (n=32 cases) obtained from two centers (Barts Cancer Institute and University of Southampton). The clinical characteristics of the cohort are shown in **Supplementary Table 12**. Non-FL tumors for validation included DNA from 174 DLBCL, 96 CLL and 48 SMZL tumors. Histology of all tumors was confirmed by pathological review.

**Whole exome sequencing and analysis.** Whole exome capture libraries were constructed from 2-3ug of tumor or constitutional DNA after shearing, end repair, phosphorylation and ligation to barcoded sequencing adaptor, using the Human All Exon V5 SureSelect XT (Agilent Technologies). Enriched exome libraries were multiplexed and sequenced on the HiSeq 2500 (Illumina) to generate 100bp paired-end reads. Sequencing metrics are provided in **Supplementary Table 1**. The processing and analysis of whole exome sequencing data were performed using our previous pipeline<sup>2</sup>. Briefly, sequencing reads were aligned to the reference genome hg19, using Burrows-Wheeler Aligner (BWA)<sup>48</sup>. Local alignments and base quality scores were adjusted using the Genome Analysis Toolkit (GATK)<sup>49</sup> version 2.5.2.

**Variant detection and mutation annotation.** Somatic SNVs and indels were identified using the Strelka pipeline as previously described<sup>2</sup>. For each sample, the number of reads supporting the reference and variant alleles at each position was extracted. VAFs were calculated by dividing the number of supporting variant reads to the total reads obtained. To improve the variant calls across all the tumors from the same patient,



identified variants were further genotyped and verified across all tumors and matched normal using VarScan2's multi-sample calling method 'mpileup2cns'<sup>50</sup>, based on reads with mapping quality > 30 and minimum base quality of 20 at the targeted site.

Annotation of variants was attained using the SNPnexus tool<sup>51</sup>.

**Sanger sequencing of genomic DNA.** Direct bidirectional Sanger sequencing of *RRAGC* exon 1 and 2, *ATP6V1B2* (all exons), *ATP6AP1* (all exons) and *ATP6AP2* (all exons) from genomic DNA from tumors and matched normal samples was performed following direct PCR amplification, using specific primers, and enzymatic clean up using Exo-Sap (USB Corporation).

**Phylogenetic analyses.** Evolutionary trees were reconstructed for each individual based on the distance matrix between GL, FL and relapse FL samples derived from the numbers of somatic non-synonymous variants from each biopsy, using the Neighbor-Joining algorithm<sup>52</sup> implemented in the PHYLIP package as previously reported<sup>2</sup>. Once the consensus phylogenetic tree was determined, it was redrawn starting from GL leading to the putative CPC, then to FL and subsequent relapse FL samples, with the branch length proportional to the number of somatic changes i.e. genetic distance between the samples.

**Copy number variation of the *RRAGC* locus.** Copy number variation and copy neutral loss of heterozygosity for *ATP6AP1*, *ATP6V1B2*, *RRAGC* and *TNFRSF14* gene loci were extracted from our previous SNP array analyses using the methodology previously described<sup>2</sup>. To detect copy number imbalances from our discovery WES data, VarScan2 "copynumber" module was first employed, using the minimum read coverage as 20, and both mapping and base qualities as  $\geq 20$  for usable reads, to generate raw copy number calls. Raw calls were adjusted for GC content and re-centered to 0 based on the modal LogR value determined by kernel density estimates, using VarScan2 "copyCaller" module. Outliers were identified and modified using the data winsorizing procedure. The DNACopy R Bioconductor package (Seshan VE and Olshen A. DNACopy: DNA copy number data analysis. R package version 1.40.0) was employed to identify joint segments of LogR values using the circular binary segmentation (CBS) algorithm. To identify regions of LOH, variants (including SNPs and short indels) against the reference genome were first identified for paired normal and

tumour samples using VarScan2. Next, B-allele frequency (BAF) files were created, allowing the minimum read depth of 10 for both tumour and normal. The ASCAT R package<sup>53</sup> was then used to assess CNAs and LOH regions, using the logR and BAF files derived from VarScan variant calls, with the depth information normalized by dividing the depth of each variant by the median depth across all variants.

**Targeted sequencing of Rag GTPases and mTORC1-associated genes.** Target-specific primers for FL-associated genes<sup>2</sup> and 7 mTORC1-associated genes (*RRAGA*, *RRAGB*, *RRAGC*, *RRAGD*, *MTOR*, *RPTOR* and *MLST8*) were custom designed using Fluidigm's D3 Assay design service. Targeted enrichment was performed by Access Array (Fluidigm) in a multiplex format using genomic DNA (50ng) according to the manufacturer's Multiplex Amplicon Tagging Protocol. The multiplexed library pools were sequenced on the Illumina Miseq platform. All samples were screened in duplicate with the inclusion of normal tonsil DNA controls in each run. Variants were called and annotated as previously described<sup>2</sup>. In brief, reads were aligned to hg19 using BOWTIE2<sup>54</sup>. SAMtools<sup>55</sup> were used to generate sorted BAM files and the VarScan2 tool was used to examine the pileup file to call variants.

**Deep tagged-amplicon sequencing for *RRAGC*, *ATP6V1B2* and *ATP6AP1* genes.** Universal adapter sequences were tagged to the 5' and 3' end of target-specific primers of approximately 200±20bp in length. Based on our initial experiments that showed clustering of variants within specific exons of the 3 genes, subsequent analyses were restricted to *RRAGC* (exons 1 and 2), *ATP6V1B2* (exons 11 and 12) and *ATP6AP1* (exons 9 and 10). Primer sequences are shown in **Supplementary Table 13**. 100ng of genomic DNA were amplified in 2 to 4-plex PCR reactions using non-overlapping tagged-primers with the HotStar Taq Plus kit (Qiagen) under limited cycling conditions. Amplified PCR fragments were subsequently pooled in equimolar ratios by sample and prepared for sequencing with the attachment sample specific indexes and Illumina adaptor sequences. Indexed libraries were pooled and sequenced on a single lane of an Illumina MiSeq instrument using the V2 300-cycles Miseq reagent kit (Illumina) generating 150-bp paired end reads. Each sample was screened in duplicate. Variant calling and annotation are as described above.

**RNA-sequencing analysis.** RNA-seq data for all 13 FL samples (5 mutants and 8 wild-type) were downloaded from the International Cancer Genome Consortium (ICGC) data repository (see URLs). Details of the samples are summarized in **Supplementary Table 9**. Raw read counts for all annotated ENSEMBL genes across the 13 samples were extracted from the “exp\_seq.MALY-DE.tsv” file in the ICGC data repository. Only genes that achieved at least one read count per million reads (CPM) in at least five samples were selected, with these criteria producing 22,126 filtered genes in total. After applying scale normalization, read counts were converted to  $\log_2$ -cpm using the voom function<sup>56</sup> with associated weights ready for linear modeling. Differential gene expression (DGE) analyses between mutant and wild-type groups were further performed using the limma R package, which powers DGE analyses for RNA-seq and microarray data<sup>57</sup>. A double threshold of raw  $p$  value  $<0.01$  and an absolute fold change  $> 2$  were used to define significantly differentially expressed (DE) genes (**Supplementary Figure 5a**). Based on the t-statistic of filtered genes from the limma test, GSEA was performed against the predefined curated gene sets (c2) acquired from the MSigDB collection<sup>58</sup>, including KEGG and Reactome gene sets. Top significantly enriched gene sets were selected based on FDR  $q$ -value  $<0.05$  (**Supplementary Table 10**).

**Materials.** Reagents were obtained from the following sources: HRP-labeled anti-mouse and anti-rabbit secondary antibody from Santa Cruz Biotechnology; antibodies to phospho-T389 S6K1, S6K1, mTOR, and FLAG epitope from Cell Signaling Technology; antibody to the HA epitope from Bethyl laboratories; antibody to raptor from Millipore. RPMI, FLAG M2 affinity gel, GTP, GDP, and amino acids from Sigma Aldrich; XDP and XTP from Jena Biosciences; [<sup>3</sup>H]-labeled GTP and GDP from Perkin Elmer; DMEM from SAFC Biosciences; Complete Protease Cocktail from Roche; Inactivated Fetal Calf Serum (IFS) and simply blue stain from Invitrogen; amino acid-free RPMI from US Biologicals.

**Cell lines and tissue culture.** HEK-293T cells were cultured in DMEM 10% IFS supplemented with 2 mM glutamine, penicillin (100 IU/mL), and streptomycin (100  $\mu$ g/mL). Karpas-422, Raji, OCI-Ly7, and OCI-Ly8 cells were cultured in RPMI 10% IFS

supplemented with 2 mM glutamine, penicillin (100 IU/mL), and streptomycin (100 µg/mL). All cell lines were maintained at 37°C and 5% CO<sub>2</sub>.

**Virus production and viral transduction.** The production of lentiviruses was achieved by transfection of viral HEK-293T cells with pLJM60-FLAG-metap2 or pLJM60-FLAG-RagC (wild-type or mutant) constructs, with the VSV-G envelope and CMV ΔVPR packaging plasmids. Similarly, the production of retroviruses for infection of the Karpas-422 cells was achieved by transfection of viral HEK-293T cells with pMXs-RagC (wild-type or mutant) constructs, with the VSV-G envelope and gag/pol packaging plasmids. Twenty-four hours after transfection, the media was changed to DME with 30% IFS. After another 24 hours, the virus-containing supernatant was collected from the cells and passed through a 0.45 µm filter. Target cells were plated in 6-well plates with virus containing media and 8 µg/mL polybrene. Spin infections were performed by centrifugation at 2,200 rpm for 1 hour. Twenty-four hours later, the media was changed to fresh media containing either puromycin (when infected with the lentivirus) or blasticidin (when infected with the retrovirus) for selection.

**Cell lysis and immunoprecipitation.** Cells were rinsed once with ice-cold PBS and immediately lysed with Triton lysis buffer (1% Triton, 10 mM β-glycerol phosphate, 10 mM pyrophosphate, 40 mM Hepes pH 7.4, 2.5 mM MgCl<sub>2</sub> and 1 tablet of EDTA-free protease inhibitor [Roche] (per 25 ml buffer). The cell lysates were centrifuged at 13,000 rpm in a microcentrifuge at 4°C for 10 minutes. For anti-FLAG-immunoprecipitations, the FLAG-M2 affinity gel was washed three times with lysis buffer. 30 µl of a 50% slurry of the affinity gel in lysis buffer was then added to cleared cell lysates and rotated for 2 hours at 4°C. The beads were washed once with lysis buffer and 3 times with lysis buffer containing 500 mM NaCl after the incubation. Immunoprecipitated proteins were denatured by the addition of 50 µl of sample buffer and boiled for 5 minutes as described<sup>24</sup>, resolved by 8%–16% SDS-PAGE, and analyzed by immunoblotting.

For co-transfection experiments in HEK-293T cells, 2 million cells were plated in 10 cm culture dishes. Twenty-four hours later, cells were transfected via the polyethylenimine method<sup>59</sup> with the pRK5-based cDNA expression plasmids indicated in the figures in the following amounts: 800 ng Flag-Metap2 or 400 ng Flag-RagC (wild-type and mutants);

400 ng of RagB (wild-type and mutants). The total amount of plasmid DNA in each transfection was normalized to 5 µg with empty pRK5. Thirty-six hours after transfection, cells were lysed as described above.

For experiments that required amino acid, leucine, or arginine starvation or restimulation, cells were treated as previously described<sup>35</sup>. Briefly, cells were incubated in amino acid, leucine, or arginine free RPMI for 50 minutes and then stimulated with amino acids, leucine, or arginine for 10 minutes.

**Nucleotide binding assays.** 40 pmols of FLAG-RagC (wild-type or mutant)-HA-RagB<sup>D163N</sup> were loaded with either 8 µCi of [<sup>3</sup>H]GDP or 8 µCi of [<sup>3</sup>H]GTP (5-20 Ci/mmol) and co-loaded with either 62.5 nM XDP or 62.5 nM XTP in a total volume of 80ul of CHAPS buffer, supplemented with 2.5 mM DTT, 10 µg BSA, and 6.25 mM EDTA. The CHAPS buffer contained 0.3% CHAPS, 40 mM HEPES [pH 7.4], and 30 mM NaCl. The complexes were rotated for 10 minutes at room temperature and then stabilized with 25 mM MgCl<sub>2</sub>, rotated for another 10 minutes at room temperature, and then incubated on ice for 1 hour to allow the binding reaction to occur. 10 µl samples were taken, in triplicate, and spotted on nitrocellulose filters, which were washed three times with 1 ml of wash buffer (1.5% CHAPS, 40 mM HEPES [pH 7.4], 150 mM NaCl, and 5 mM MgCl<sub>2</sub>). Filter-associated radioactivity was quantified using a TriCarb scintillation counter (PerkinElmer).

**Statistical analysis.** Fisher's exact tests were used for comparison between two groups. For analysis of the nucleotide binding assay groups, two-tailed t tests were used. P values of less than 0.05 were considered to indicate statistical significance.

## References:

48. Li, H & Durbin, R. Fast and accurate short read alignment with Burrows-Wheeler etc. *Bioinformatics* (2009)
49. DePristo, M.A. et al. A framework for variation discovery and genotyping using next-generation DNA sequencing data. *Nat Genet* **43**, 491-8 (2011).
50. Koboldt, D.C et al. VarScan2: Somatic mutation and copy number alteration discovery in cancer by exome sequencing. *Genome Res* **22**, 568-76 (2012).
51. Dayem Ullah, A.Z., Lemoine, N.R. & Chelala, C. SNPnexus: a web server for functional annotation of novel and publicly known genetic variants (2012 update). *Nucleic Acids Res* **40**, W65-70 (2012).
52. Saitou, N. & Nei, M. The neighbor-joining method: a new method for reconstructing phylogenetic trees. *Mol Biol Evol* **4**, 406-25 (1987).
53. Van Loo, P. et al. Allele-specific copy number analysis of tumors. *Proc Natl Acad Sci U S A* **107**, 16910-5 (2010).
54. Langmead, B. & Salzberg, S.L. Fast gapped-read alignment with Bowtie 2. *Nat Methods* **9**, 357-9 (2012).
55. Li, H. et al. The Sequence Alignment/Map format and SAMtools. *Bioinformatics* **25**, 2078-9 (2009).
56. Law, C.W., Chen, Y., Shi, W. & Smyth, G.K. voom: Precision weights unlock linear model analysis tools for RNA-seq read counts. *Genome Biol* **15**, R29 (2014).
57. Ritchie, M.E. et al. limma powers differential expression analyses for RNA-sequencing and microarray studies. *Nucleic Acids Res* (2015).
58. Subramanian, A. et al. Gene set enrichment analysis: a knowledge-based approach for interpreting genome-wide expression profiles. *Proc Natl Acad Sci U S A* **102**, 15545-50 (2005).
59. Boussif, O. et al. A versatile vector for gene and oligonucleotide transfer into cells in culture and in vivo: polyethylenimine. *Proc Natl Acad Sci U S A* **92**, 7297-301 (1995).

## CHAPTER 3

Reprinted from Cell Reports:

### **The Sestrins interact with GATOR2 to negatively regulate the amino acid sensing pathway upstream of mTORC1**

**Lynne Chantranupong<sup>1,2,3,4,6</sup>, Rachel L. Wolfson<sup>1,2,3,4,6</sup>, Jose M. Orozco<sup>1,2,3,4</sup>, Robert A. Saxton<sup>1,2,3,4</sup>, Sonia M. Scaria<sup>1,2</sup>, Liron Bar-Peled<sup>1,2,3,4†</sup>, Eric Spooner<sup>1</sup>, Marta Isasa<sup>5</sup>, Steven P. Gygi<sup>5</sup>, and David M. Sabatini<sup>1,2,3,4</sup>**

<sup>1</sup>Whitehead Institute for Biomedical Research and Massachusetts Institute of Technology, Department of Biology, 9 Cambridge Center, Cambridge, MA 02142, USA

<sup>2</sup>Howard Hughes Medical Institute, Department of Biology, Massachusetts Institute of Technology, Cambridge, MA 02139, USA

<sup>3</sup>Koch Institute for Integrative Cancer Research, 77 Massachusetts Avenue, Cambridge, MA 02139, USA

<sup>4</sup>Broad Institute of Harvard and Massachusetts Institute of Technology, 7 Cambridge Center, Cambridge MA 02142, USA

<sup>5</sup>Department of Cell Biology, Harvard Medical School, 240 Longwood Avenue, Boston, MA 02115, USA

<sup>6</sup>Co-first author

†Present address: Department of Chemical Physiology, The Scripps Research Institute, La Jolla, CA 92037, USA

Correspondence should be addressed to D.M.S.

Tel: 617-258-6407; Fax: 617-452-3566; Email: [sabatini@wi.mit.edu](mailto:sabatini@wi.mit.edu)

**Experiments in Fig. 1A were performed by L.C. and L.B.P. and analyzed by L.C. and R.L.W.**

**Experiments in Fig. 1B were performed by L.C. and S.M.S.**

**Experiments in Fig. 1C-E were performed by R.L.W.**

**Experiments in Fig. 1F were performed by L.C.**

**Experiments in Fig. S1A were performed by R.L.W.**

**Experiments in Fig. S1B-D were performed by L.C.**

**Experiments in Fig. S1E were performed by R.A.S.**

**Experiments in Fig. 2 were performed by L.C. with help J.M.O. with Fig. 2C.**

**Experiments in Fig. S2A-C were performed by R.L.W.**

**Experiments in Fig. S2D-F were performed by L.C.**

**Experiments in Fig. 3A were performed by J.M.O.**

**Experiments in Fig. 3B were performed by L.C. and R.L.W.**

**Experiments in Fig. S3A were performed by L.C.**

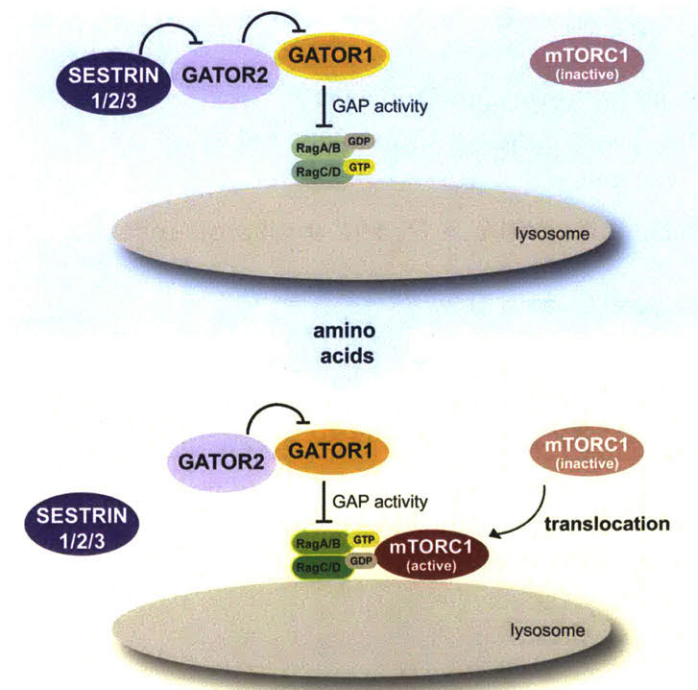
**Experiments in Fig. S3B were performed by R.L.W.**

**Experiments in Fig. 4 and S4 were performed by R.L.W.**

## Abstract

The mTORC1 kinase is a major regulator of cell growth that responds to numerous environmental cues. A key input is amino acids, which act through the heterodimeric Rag GTPases (RagA/B bound to RagC/D) to promote the translocation of mTORC1 to the lysosomal surface, its site of activation. GATOR2 is a complex of unknown function that positively regulates mTORC1 signaling by acting upstream of or in parallel to GATOR1, which is a GTPase activating protein (GAP) for RagA/B and an inhibitor of the amino acid sensing pathway. Here, we find that the Sestrins, a family of poorly understood growth regulators (Sestrin1-3), interact with GATOR2 in an amino acid-sensitive fashion. Sestrin2-mediated inhibition of mTORC1 signaling requires GATOR1 and the Rag GTPases, and the Sestrins regulate the localization of mTORC1 in response to amino acids. Thus, we identify the Sestrins as GATOR2-interacting proteins that regulate the amino acid sensing branch of the mTORC1 pathway.

## Graphical Abstract





## Introduction

The mechanistic target of rapamycin complex 1 (mTORC1) protein kinase is a master growth regulator that senses diverse environmental cues, such as growth factors, cellular stresses, and nutrient and energy levels. When activated, mTORC1 phosphorylates substrates that potentiate anabolic processes, such as mRNA translation and lipid synthesis, and that limit catabolic ones, such as autophagy. mTORC1 deregulation occurs in a broad spectrum of diseases, including diabetes, epilepsy, and cancer (Howell et al., 2013; Kim et al., 2013; Laplante and Sabatini, 2012).

Many upstream inputs, including growth factors and energy levels, signal to mTORC1 through the TSC complex, which regulates Rheb, a small GTPase that is an essential activator of mTORC1 (Brugarolas et al., 2004; Garami et al., 2003; Inoki et al., 2003; Long et al., 2005; Sancak et al., 2008; Saucedo et al., 2003; Stocker et al., 2003; Tee et al., 2002). Amino acids do not appear to signal to mTORC1 through the TSC-Rheb axis and instead act through the heterodimeric Rag GTPases, which consist of RagA or RagB bound to RagC or RagD (Hirose et al., 1998; Kim et al., 2008; Nobukuni et al., 2005; Roccio et al., 2005; Sancak et al., 2008; Schürmann et al., 1995; Sekiguchi et al., 2001; Smith et al., 2005). The Rags control the subcellular localization of mTORC1 and amino acids promote its recruitment to the lysosomal surface, where Rheb also resides (Buerger et al., 2006; Dibble et al., 2012; Menon et al., 2014; Saito et al., 2005; Sancak et al., 2008). Several positive components of the pathway upstream of the Rag GTPases have been identified. The Ragulator complex localizes the Rags to the lysosomal surface and, along with the vacuolar-ATPase, promotes the exchange of GDP for GTP on RagA/B (Bar-Peled et al., 2012; Sancak et al., 2010; Zoncu et al., 2011). The distinct FLCN-FNIP complex acts on RagC/D and stimulates its hydrolysis of GTP into GDP (Tsun et al., 2013). When RagA/B is loaded with GTP and RagC/D with GDP, the heterodimers bind and recruit mTORC1 to the lysosomal surface, where it can come in contact with its activator Rheb.

Recent work has identified the GATOR1 complex as a major negative regulator of the amino acid sensing pathway and its loss causes mTORC1 signaling to be

completely insensitive to amino acid starvation (Bar-Peled et al., 2013; Panchaud et al., 2013). GATOR1 consists of DEPDC5, Nprl2, and Nprl3, and is a GTPase activating protein (GAP) for RagA/B. The GATOR2 complex, which has five known subunits (WDR24, WDR59, Mios, Sec13, and Seh1L), is a positive component of the pathway and upstream of or parallel to GATOR1, but its molecular function is unknown (Bar-Peled et al., 2013).

Here, we identify the Sestrins as interacting partners of GATOR2. The Sestrins are three related proteins (Sestrin1-3) of poorly characterized molecular functions (Buckbinder et al., 1994; Budanov et al., 2002; Peeters et al., 2003). Sestrin2 inhibits mTORC1 signaling and has been proposed to activate AMPK upstream of TSC as well as to interact with TSC (Budanov and Karin, 2008). We find that the Sestrins interact with GATOR2 in an amino acid sensitive fashion, regulate the subcellular localization of mTORC1, and require GATOR1 and the Rag GTPases to inhibit mTORC1 signaling. Thus, we conclude that the Sestrins are components of the amino acid sensing pathway upstream of mTORC1.

### **The Sestrins Interact with GATOR2 in an Amino Acid-Sensitive Fashion**

To begin to probe how the GATOR complexes might be regulated, we sought to identify GATOR2-interacting proteins. In mass spectrometric analyses of anti-FLAG immunoprecipitates prepared from HEK-293T cells stably expressing FLAG-tagged GATOR2 components (WDR24, Mios, or WDR59), we consistently detected peptides derived from Sestrin2, at levels comparable to those from the bona fide GATOR2 component Sec13 (**Figure 1A**). Sestrin1 and Sestrin3 were also present, albeit at lower amounts than Sestrin2 (**Figure 1A**).

Consistent with the Sestrins being GATOR2-interacting proteins, recombinant FLAG-tagged Sestrin1, Sestrin2, or Sestrin3 when transiently co-expressed in HEK-293T cells co-immunoprecipitated GATOR2, but not GATOR1 or the metap2 control protein (**Figure 1B**). When stably expressed in HEK-293T cells, FLAG-Sestrin2 co-immunoprecipitated endogenous GATOR2 as detected through its Mios component (**Figure 1C**). The reciprocal was also true because stably expressed FLAG-WDR24 co-immunoprecipitated abundant amounts of endogenous Sestrin2 alongside the

established components of GATOR2 (**Figure S1A**). In contrast, FLAG-DEPDC5, a GATOR1 component, did not co-immunoprecipitate endogenous Sestrin2, suggesting that GATOR1 and Sestrin2 do not make a readily detectable interaction (**Figure S1A**). Given that GATOR1 is known to interact with GATOR2 (Bar-Peled et al., 2013), we tested the effect of expressing increasing amounts of FLAG-Sestrin2 on this interaction and found that Sestrin2 did not perturb the ability of GATOR1 to co-immunoprecipitate GATOR2 (**Figure S1B**).

Amino acids regulate the interaction between multiple critical components of the amino acid pathway (Bar-Peled et al., 2012; Sancak et al., 2010; Sancak et al., 2008; Tsun et al., 2013; Zoncu et al., 2011). Likewise, amino acid deprivation strongly increased the GATOR2-Sestrin2 interaction, whether monitored by immunoprecipitating GATOR2 or Sestrin2 and probing for endogenous Sestrin2 or GATOR2, respectively (**Figure 1D, 1E**). Pretreatment of cells with rapamycin, an allosteric mTORC1 inhibitor, or Torin1, an ATP-competitive mTOR inhibitor, did not prevent the amino acid-induced decrease in the GATOR2-Sestrin2 interaction, indicating that mTORC1 activity does not control the interaction (**Figure S1C**). Consistent with the notion that the pathways upstream of mTORC1 that sense amino acids and growth factors are largely independent, insulin treatment of cells did not regulate the Sestrin2-GATOR2 interaction (**Figure 1E**). Interestingly, however, glucose deprivation led to a modest increase in the amount of Sestrin2 bound to GATOR2, albeit to a much lesser extent than that caused by amino acid starvation (**Figure 1E**). Glucose levels have been previously described as an upstream input to the Ragulator-v-ATPase input to Rag GTPases (Efeyan et al., 2012a), and these results are consistent with glucose also affecting the GATOR2 input to the Rags.

Given the robust interaction between Sestrin2 and GATOR2, we reasoned that within cells the levels of GATOR2 might affect those of Sestrin2, in an analogous fashion to the components of other complexes, like Ragulator or GATOR1 (Bar-Peled et al., 2013; Sancak et al., 2008). Indeed, endogenous Sestrin2 expression was severely depressed in cells in which strongly suppressed either the Mios or WDR24 components of GATOR2 via CRISPR/Cas9-mediated genome editing (**Figure S1D**).

Together, these results identify the Sestrins as GATOR2 interacting proteins and establish that Sestrin2 and GATOR2 interact in an amino-acid sensitive fashion, suggesting a regulatory role for the Sestrins in signaling amino acid sufficiency to mTORC1.

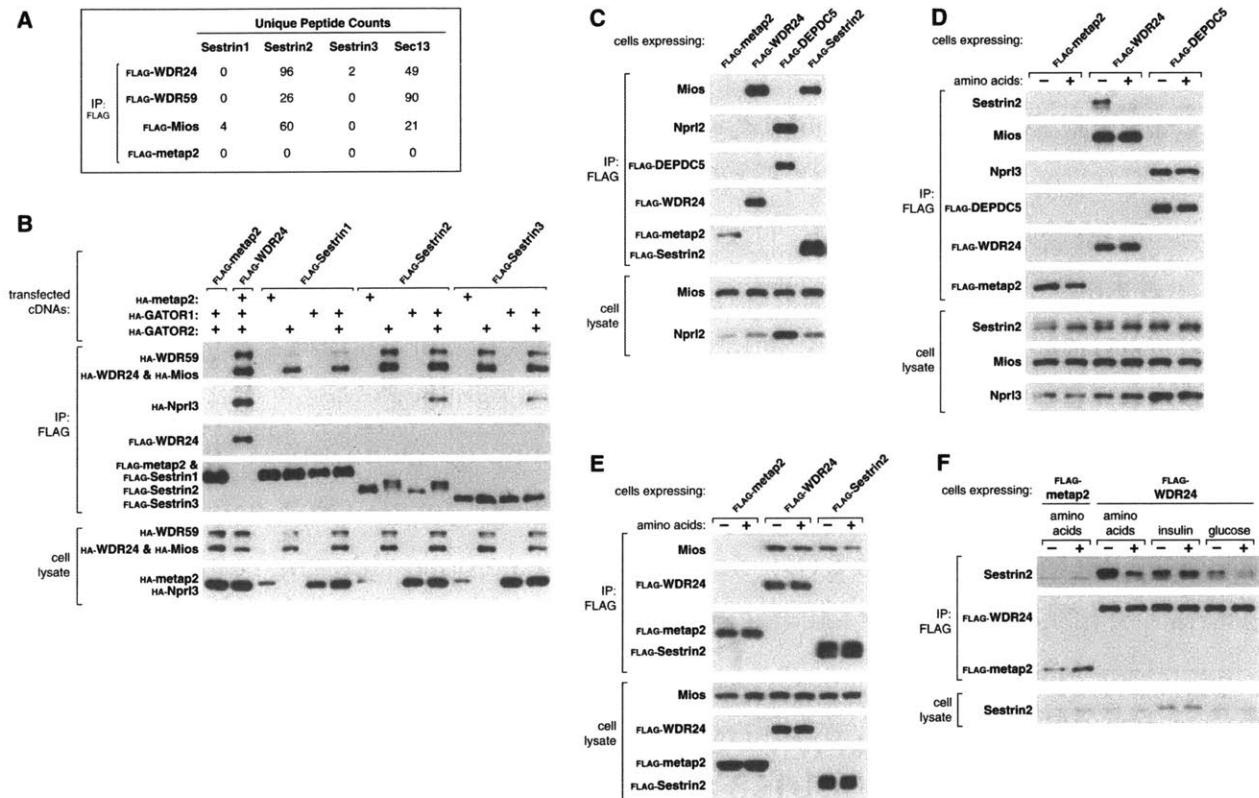


### Figure 1: The Sestrins interact with GATOR2, but not GATOR1, in an amino acid-sensitive fashion

(A) GATOR2 interacts with the Sestrins. Mass spectrometric analyses identify Sestrin-derived peptides in immunoprecipitates from HEK-293T cells stably expressing FLAG-tagged GATOR2 components.

(B) Recombinant Sestrin 1, 2, and 3 interact with recombinant GATOR2 but not GATOR1. Anti-FLAG immunoprecipitates were collected from HEK-293T cells expressing the indicated cDNAs in expression vectors and were analyzed, along with cell lysates, by immunoblotting for the relevant epitope tags.

(C) Stably expressed Sestrin2 co-immunoprecipitates endogenous GATOR2 components. Immunoprecipitates were prepared from HEK-293T cells stably expressing

the indicated FLAG-tagged proteins, and were analyzed along with cell lysates by immunoblotting for the indicated proteins.

(D) Stably expressed GATOR2 and endogenous Sestrin2 interact in an amino acid dependent fashion. HEK-293T cells stably expressing the indicated FLAG-tagged proteins were starved of amino acids for 50 minutes, or starved and then stimulated with amino acids for 10 minutes. Anti-FLAG immunoprecipitates were analyzed as in (C).

(E) Stably expressed Sestrin2 interacts with endogenous GATOR2 in an amino acid-sensitive fashion. HEK-293T cells expressing the indicated epitope tagged proteins were amino acid starved or starved and restimulated with amino acids as in (D), and anti-FLAG immunoprecipitates were analyzed as in (C).

(F) The GATOR2-Sestrin2 interaction is sensitive to both amino acid and glucose availability, but is not affected by growth factors. HEK-293T cells stably expressing the indicated FLAG-tagged proteins were starved of either amino acids, glucose, or growth factors for 50 minutes, or starved and restimulated with amino acids, glucose, or insulin, respectively, for 10 minutes. Anti-FLAG immunoprecipitates were analyzed as in (C).

**Figure S1**

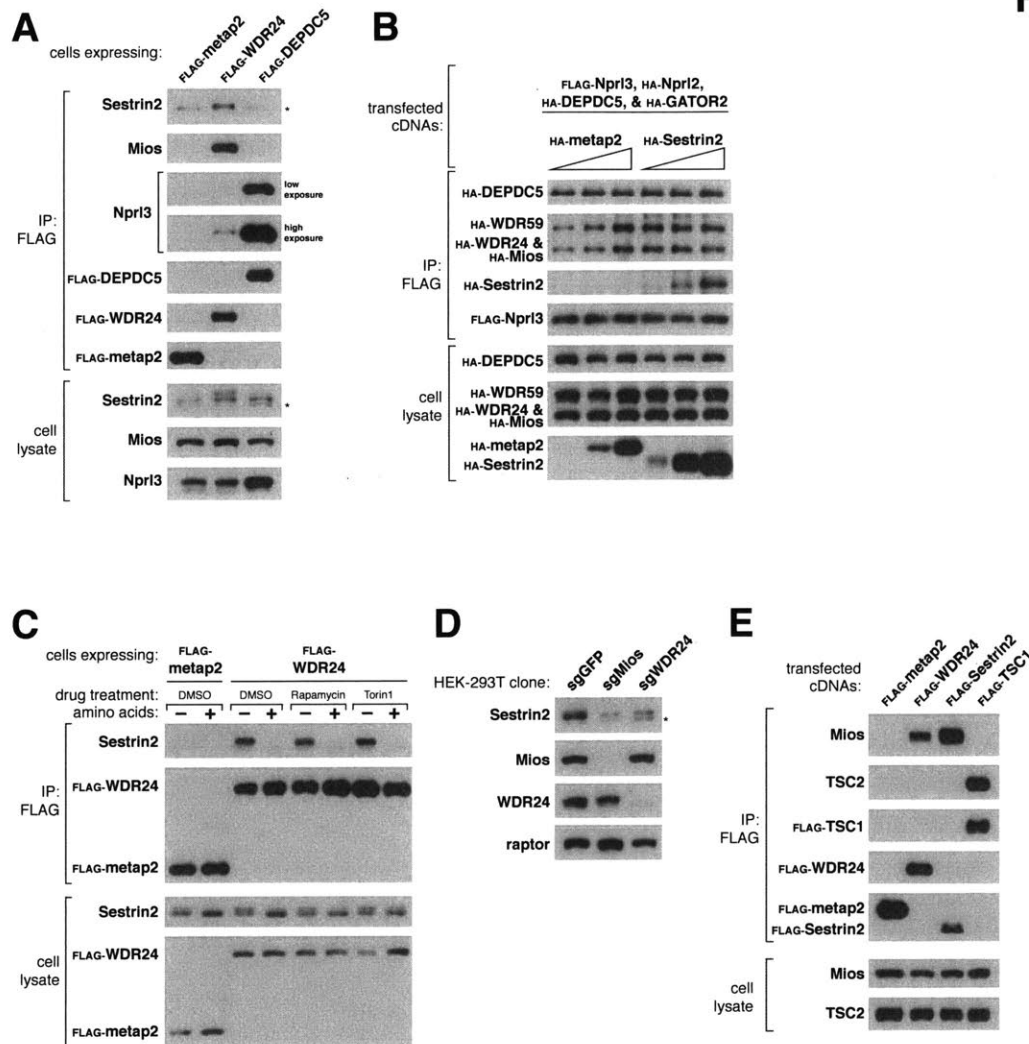


**Figure S1, related to Figure 1: Regulation of the GATOR2-Sestrin2 interaction by nutrients and not insulin and GATOR2 is important for Sestrin2 stability.**

(A) Stably expressed components of GATOR2, but not GATOR1, interact with endogenous Sestrin2. Anti-FLAG immunoprecipitates were analyzed as in Figure 1C. The asterisk indicates a nonspecific band that appears in all lanes at a molecular weight just below that of endogenous Sestrin2.

(B) Sestrin2 does not disrupt the interaction between GATOR1 and GATOR2. Anti-FLAG immunoprecipitates were collected and analyzed as in Figure 1B from HEK-293T cells transiently overexpressing the indicated cDNAs.

(C) The amino acid-sensitive interaction between GATOR2 and Sestrin2 is not

dependent on mTOR activity. HEK-293T cells stably expressing the indicated FLAG-tagged proteins were starved or starved and restimulated with amino acids as in Figure 1D, and concurrently treated with either DMSO, 250 nM rapamycin, or 250 nM Torin1 for 60 minutes.

(D) Sestrin2 levels are decreased in cells with reduced expression of GATOR2. Cell lysates from HEK-293T cells genetically modified with the indicated guide RNAs using the CRISPR-Cas9 system were immunoblotted for levels of the indicated endogenous proteins.

(E) Recombinant TSC1 does not co-immunoprecipitate endogenous Sestrin2. Anti-FLAG immunoprecipitates were collected from HEK-293T cells expressing the indicated cDNAs and were analyzed by immunoblotting for endogenous proteins.

## The Sestrins inhibit the amino acid sensing pathway upstream of mTORC1

The Sestrins have previously been reported to be negative regulators of mTORC1 signaling and to function by activating AMPK, which in turn stimulates TSC to inhibit Rheb, and by binding TSC (Budanov and Karin, 2008). In our experimental system, under conditions where GATOR2 and Sestrin2 interact, we were unable to detect an interaction between recombinant TSC1 and endogenous Sestrin2 (**Figure S1E**). Given the strong interaction of Sestrin2 with GATOR2, we reasoned that Sestrin2 might regulate the capacity of the mTORC1 pathway to sense amino acids. Indeed, stable over-expression of Sestrin2 dose-dependently inhibited mTORC1 activation by amino acids, as determined by the phosphorylation of S6K1, confirming its role as a negative regulator (**Figure 2A and S2A**). In addition, consistent with previous reports (Budanov and Karin, 2008), stable over-expression of FLAG-Sestrin2 caused a dramatic reduction in cell size (**Figure 2B**), a well-known consequence of mTORC1 inhibition (Fingar et al., 2002).

In HEK-293T cells, inhibition of just Sestrin1 or Sestrin2, caused by either short-hairpin RNA (shRNA)-mediated knockdown or CRISPR/Cas9-mediated knockout, caused only a slight defect in mTORC1 inhibition upon amino acid withdrawal (**Figures 2C and S2B-E**). The double knockdown of Sestrin1 and Sestrin3 had a similarly weak effect (**Figure 2C**) while that of Sestrin1 and Sestrin2 more robustly rescued mTORC1 signaling in the absence of amino acids (**Figure 2E**). Finally, when we inhibited all three Sestrins by expressing shRNAs targeting Sestrin1 and Sestrin3 in Sestrin2-null cells created with the CRISPR/Cas9 system, we obtained a strong but still partial rescue of mTORC1 signaling upon amino acid deprivation (**Figure 2C**). In addition, triple knockdown of all three Sestrins using shRNAs in HEK-293E cells rendered the cells insensitive to glucose deprivation (**Figure S2F**). These data indicate that the Sestrins play redundant roles within the mTORC1 pathway and collectively are necessary for the full inhibition of mTORC1 signaling that occurs in the absence of amino acids or glucose.



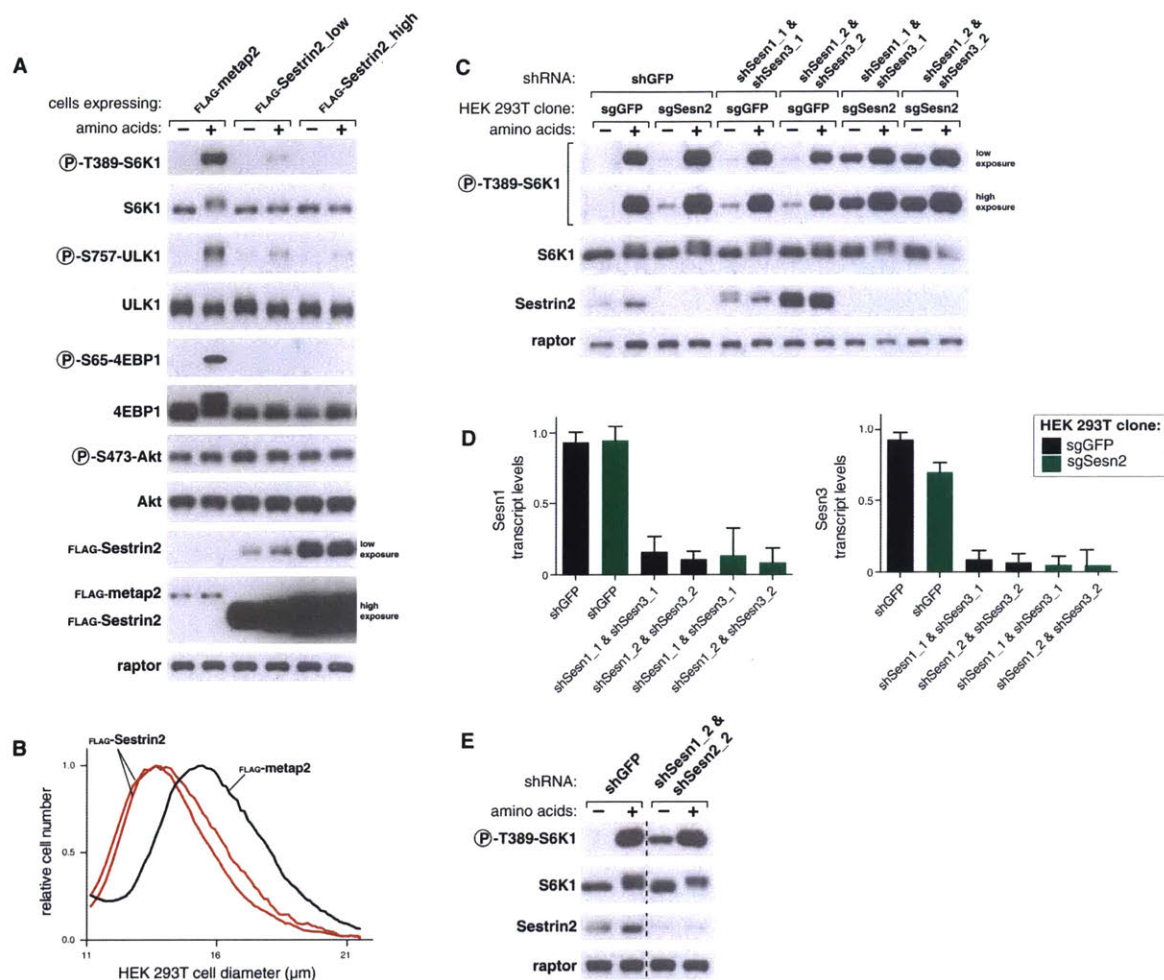


**Figure 2: The Sestrins are negative regulators of the amino acid sensing pathway upstream of mTORC1.**

(A) Stable overexpression of Sestrin2 inhibits mTORC1 signaling, but does not affect the phosphorylation of Akt. HEK-293T cells stably expressing the indicated proteins were starved of amino acids for 50 minutes, or starved and restimulated with amino acids for 10 minutes. Immunoblotting of cell lysates allowed for the analysis of levels and the phosphorylation states of the indicated proteins.

(B) Stable overexpression of Sestrin2 severely decreased cell size. HEK-293T cells stably expressing the indicated proteins and wild-type HEK-293T cells were analyzed for cell size.

(C) A decrease in the levels of the Sestrins leads to an inability to fully inhibit mTORC1 signaling under amino acid deprivation. HEK-293T cells which were genetically

modified with the indicated guide RNAs using the CRISPR/Cas9 system were subsequently treated with the indicated shRNAs, then starved of amino acids for 50 minutes, or starved and restimulated with amino acids for 10 minutes, and analyzed as in (A).

(D) The indicated shRNAs reduced the mRNA levels of Sestrin1 and 3. Quantitative polymerase chain reaction (qPCR) was performed on the samples described in (C) to assess the efficacy of shRNA-mediated knockdown of Sestrin1 and 3. Errors depicted are standard error of the mean calculated based on samples from a single qPCR run.

(E) Double-knockdown of Sestrin1 and 2 exaggerates the observed phenotype. Cells were treated and cell lysates were analyzed as in (A).

**Figure S2**

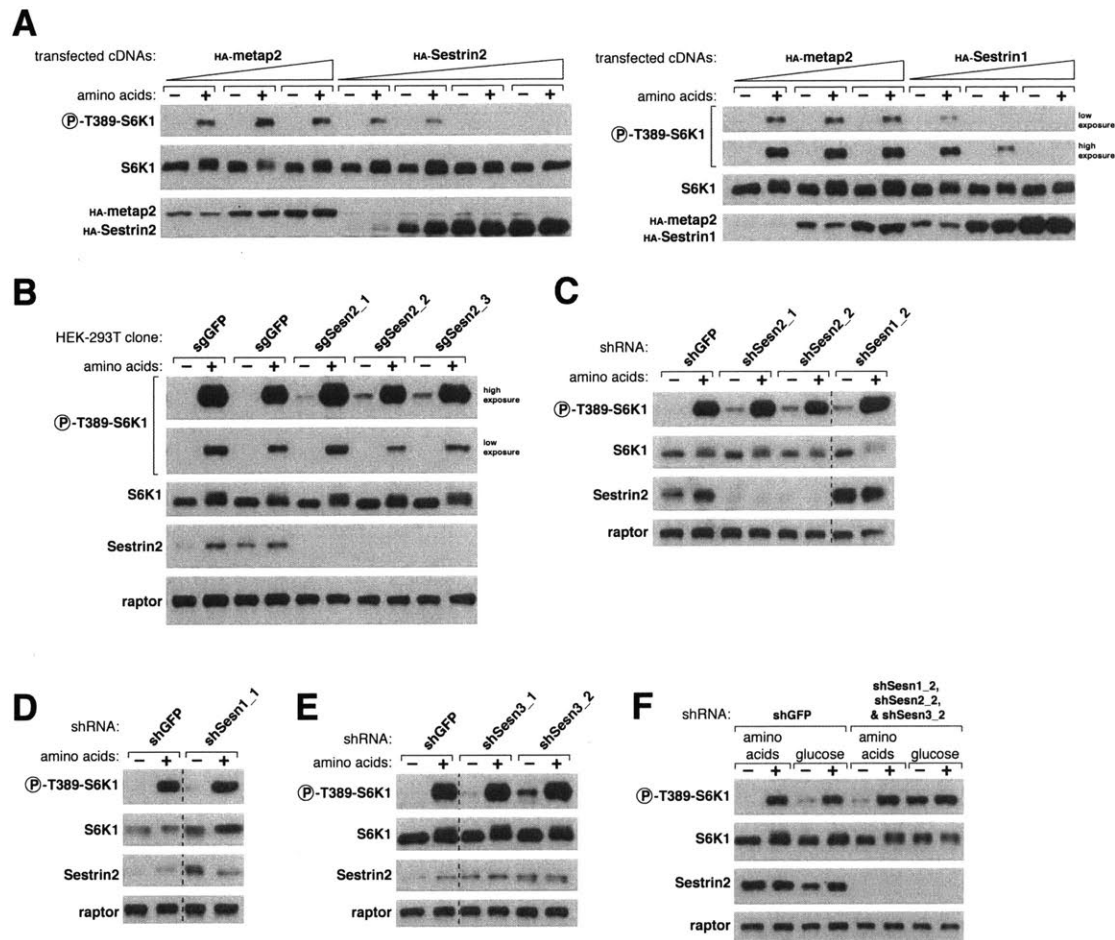


**Figure S2, related to Figure 2: The Sestrins are necessary for full inhibition of mTORC1 signaling in the absence of amino acids.**

(A) Sestrin1 and 2 dose-dependently inhibit mTORC1 signaling. Recombinant Sestrin1 or 2 were transiently overexpressed in HEK-293T cells, which were amino acid starved or starved and restimulated with amino acids as in Figure 1D. Cell lysates were immunoblotted for levels and phosphorylation states of the indicated proteins.

(B) Sestrin2-null cells have a slight defect in their ability to inhibit mTORC1 signaling in the absence of amino acids. Sestrin2-null HEK-293T cells, or HEK-293T cells which were treated with a guide RNA targeting GFP, were amino acid starved or starved and restimulated as in Figure 1D and levels and phosphorylation states of the indicated proteins were analyzed by immunoblotting. Three distinct guide RNAs targeting Sestrin2 were used to produce three different Sestrin2-null clones.

(C) shRNA-mediated knockdown of Sestrin1 or Sestrin2 leads to a slight increase in mTORC1 signaling under amino acid deprivation conditions. HEK-293T cells were treated with the indicated shRNAs, amino acid starved or starved and restimulated as described in Figure 1D, and cell lysates were analyzed by immunoblotting.

(D) Knockdown of Sestrin1 leads to a slight defect in the ability to inhibit mTORC1 signaling in the absence of amino acids. Cells were treated and cell lysates were analyzed as in (C).

(E) shRNA-mediated depletion of Sestrin3 leads to a phenotype that is consistent with that of knockdown of Sestrin 1 or 2. Cells were treated and cell lysates were analyzed as in (C).

(F) shRNA-mediated knockdown of all three Sestrins in HEK-293E cells renders the cells completely insensitive to glucose deprivation. Cells were starved of glucose for 50 minutes and restimulated with 500mM glucose for 10 minutes. Cell lysates were analyzed as in (C).

## The Sestrins function upstream of GATOR1 and the Rag GTPases

To further understand how the Sestrins play a regulatory role in the amino acid sensing pathway, we investigated whether they require other components of the pathway to inhibit mTORC1 signaling. The nucleotide loading state of the Rag GTPase heterodimer is critical for the proper sensing of amino acids by mTORC1 (Sancak et al., 2008). Amino acids promote GTP loading of RagA/B and GDP loading of RagC/D, enabling them to recruit mTORC1 to the lysosomal surface (Sancak et al., 2008). The GAP activity of GATOR1 leads to GTP hydrolysis of RagA/B and inhibition of the pathway (Bar-Peled et al., 2013).

Several lines of evidence support the notion that the Sestrins lie upstream of the Rags and depend on GATOR1 to function as negative regulators of mTORC1. First, concomitant overexpression of recombinant Sestrin2 and the dominant active RagB<sup>Q99L</sup>-RagC<sup>S75N</sup> pair prevented Sestrin2-mediated inhibition of the pathway, thus placing the Sestrins upstream of the Rag GTPases (**Figure 3A**). Second, while Sestrin2 overexpression strongly abrogated signaling in cells expressing GATOR1, in Npr13-null HEK-293E cells produced via the CRISPR/Cas9-system, Sestrin2 failed to inhibit the constitutive mTORC1 signaling observed in the absence of GATOR1. Thus, GATOR1 is epistatic to Sestrin2 (**Figure 3B**).

Given that Sestrin2 functions upstream of GATOR1, we tested the possibility that it might inhibit the pathway by enhancing the GAP activity of GATOR1, however, GATOR1 GAP activity is unaltered when isolated from cells overexpressing Sestrin2 (**Figure S3A**).

Previous work has shown that lysosome-associated machinery, which includes the v-ATPase, is necessary for the amino acid-induced activation of mTORC1 (Zoncu et al., 2011). Interestingly, inhibition of the v-ATPase with concanamycin A (ConA), which decreased mTORC1 signaling, also reduced the interaction between Sestrin2 and GATOR2 in the absence of amino acids (**Figure S3B**).

Taken together, these results demonstrate that Sestrin2 requires GATOR1 and the Rags in order to inhibit mTORC1 signaling and are consistent with it having a modulatory role in the amino acid sensing pathway upstream of mTORC1.



**Figure S3**

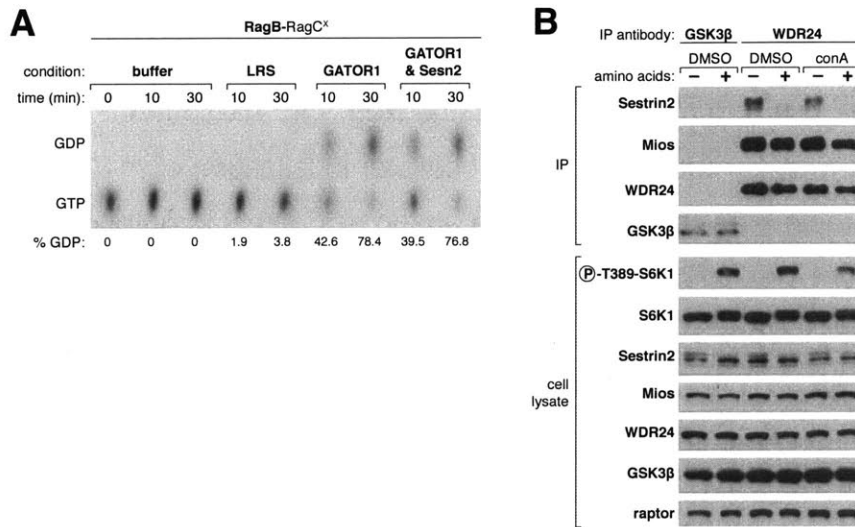


**Figure S3, related to Figure 3: The Sestrins do not affect the GAP activity of GATOR1 and inhibition of the v-ATPase affects the Sestrin2-GATOR2 interaction.**

(A) GATOR1 purified from HEK-293T cells overexpressing Sestrin2 is equally active towards RagB as GATOR1 purified from cells without Sestrin2 overexpression. Five picomoles of Flag RagB HA RagC 181N were loaded with [ $\alpha^{32}$ P]GTP and incubated with the indicated proteins. LRS is leucyl tRNA synthetase. GTP hydrolysis was determined by thin layer chromatography.

(B) Inhibition of the v-ATPase with concanmycin A (ConA) reduces the interaction between GATOR2 and Sestrin2. HEK-293T cells were treated with either 11.5  $\mu$ M ConA or DMSO for 1 hour, during which time the cells were starved of amino acids for 1 hour or starved for 50 minutes and restimulated with amino acids for 10 minutes. Immunoprecipitates were collected using either an antibody targeting WDR24 or a control protein, GSK3 $\beta$ , and were analyzed, along with cell lysates, by immunoblotting for the indicated proteins.

## The Sestrins are necessary for the amino acid-regulated subcellular localization of mTORC1

Given that Sestrin2 is upstream of GATOR1 and the Rags, we reasoned that the Sestrins might inhibit the pathway by controlling the subcellular localization of mTORC1, analogous to previously characterized regulators of the amino acid sensing pathway (Bar-Peled et al., 2013; Petit et al., 2013; Sancak et al., 2010; Sancak et al., 2008; Tsun et al., 2013; Zoncu et al., 2011). Consistent with this notion, in HEK-293T cells stably overexpressing FLAG-Sestrin2, mTORC1 failed to translocate to LAMP2-positive lysosomes despite the presence of amino acids (**Figure 4A** and **S4A**). Conversely, shRNA-mediated knockdown of Sestrin1 and Sestrin2 led to increased levels of lysosome-associated mTORC1 even in the absence of amino acids (**Figure 4B**). The shRNA-mediated knockdown of Sestrin1 and Sestrin3 in Sestrin2-null cells further increased the localization of mTORC1 to lysosomes under amino acid deprivation conditions (**Figure S4B**). In combination, these results indicate that the Sestrins are negative regulators of mTORC1 signaling and are necessary for the amino acid-dependent localization of mTORC1 to the lysosomal surface (**Figure 4C**)



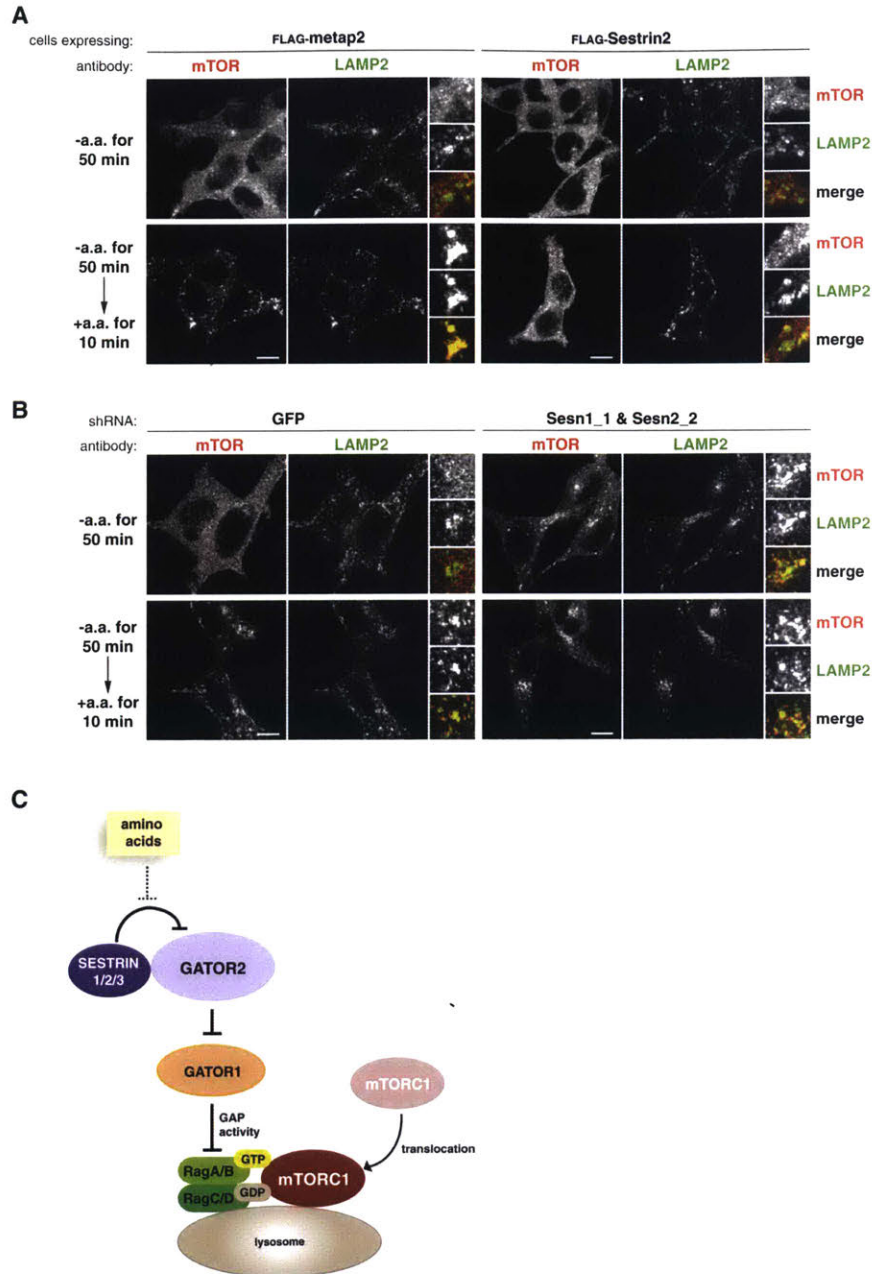


**Figure 4: The Sestrins control mTORC1 localization in response to amino acids**

(A) Sestrin2 overexpression prevents proper mTORC1 recruitment to lysosomes. HEK-293T cells stably expressing the indicated recombinant proteins were starved or starved and restimulated with amino acids for the indicated times prior to processing for immunofluorescence. Insets depict selected fields that were magnified 3.24 times and their overlays.

(B) Sestrin1 and Sestrin2 loss results in constitutive mTORC1 localization to the

lysosome. HEK-293T cells stably expressing the indicated shRNA constructs were processed as described above in (A).

Figure S4

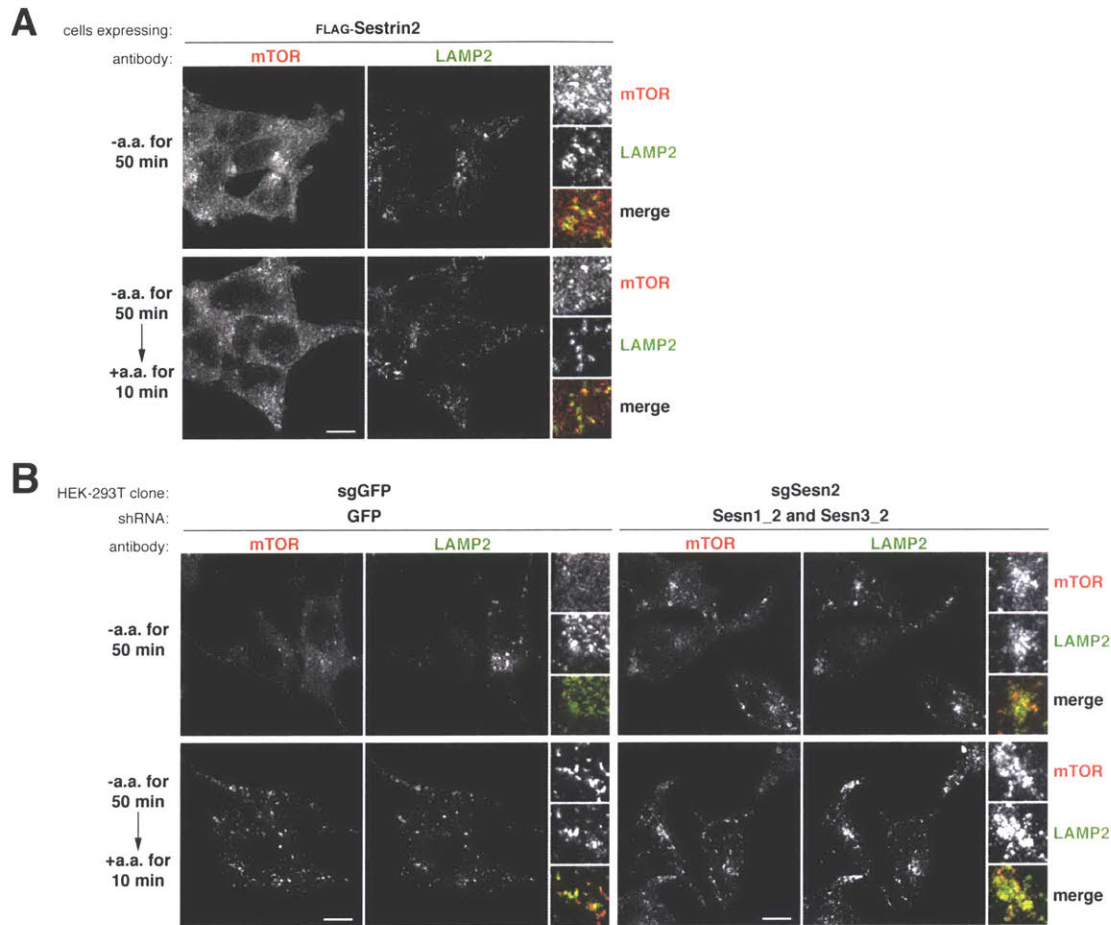


**Figure S4, related to Figure 4: The Sestrins control amino acid-dependent mTORC1 localization to the lysosome.**

(A) Overexpression of FLAG-Sestrin2 impairs proper mTOR localization to the lysosome in response to amino acids. HEK-293T cells stably overexpressing the indicated recombinant proteins were processed for immunofluorescence as indicated in Figure 4A.

(B) Knockdown of Sestrin1 and Sestrin3 leads to an increase in mTOR localization to the lysosomes under amino acid deprivation. shRNA-mediated knockdown of the indicated genes was performed in Sestrin2-null cells generated by the CRISPR/Cas9 system and processed for immunofluorescence as indicated in Figure 4A. All scale bars represent 10  $\mu$ m.

## Discussion

Amino acids must be present in the cellular environment for mTORC1 to be active and are sensed through a signaling pathway that culminates with the nucleotide loading of the Rag GTPases (reviewed in (Bar-Peled and Sabatini, 2014; Efeyan et al., 2012b; Kim et al., 2013; Yuan et al., 2013)). Many regulators impact the nucleotide loading state of the Rags in response to amino acid availability, most notably Ragulator and GATOR1, which are a GEF and GAP, respectively, for RagA/B. GATOR2 is a poorly studied complex that acts upstream of or in parallel with GATOR1 and is a positive component of the mTORC1 pathway. Here, we identify the Sestrins as GATOR2-interacting proteins that require GATOR1 and the Rags to function as negative regulators of the amino acid pathway upstream of mTORC1. In addition, we show that amino acids levels regulate the strength of the interaction between Sestrin2 and GATOR2, and that the Sestrins are necessary for mTORC1 recruitment to the lysosomal surface in response to amino acids.

Interestingly, inhibition of the v-ATPase, a known regulator of mTORC1 activity which engages in amino acid-regulated interactions with Ragulator on the lysosomal surface, disrupts the Sestrin2-GATOR2 interaction in the absence of amino acids (**Figure S3B**). As of yet, the relationship between the branch involving the GATOR complexes and the branch involving the Ragulator/v-ATPase complexes upstream of mTORC1 has not been thoroughly investigated, and these data imply that there may be some crosstalk between the two branches. However, further work must be performed to determine if the effect of concanamycin A on the Sestrin2-GATOR2 interaction is a direct or an indirect effect of inhibiting the v-ATPase.

Our work raises several interesting questions. First, the mechanism through which the Sestrins act as negative regulators of mTORC1 signaling remains unknown. Although initially our most appealing hypotheses, the Sestrins do not appear to inhibit the pathway by disrupting the interaction between GATOR1 and GATOR2 (**Figure S1B**), nor do they affect the GAP activity of GATOR1 towards RagA/B (**Figure S3A**). Another possibility is that the Sestrins inhibit GATOR2 function, which is in turn necessary to signal amino acid sufficiency to the Rags. The function of GATOR2 is

unknown, and therefore, while this is a tempting mechanism through which the Sestrins may affect the mTORC1 pathway, it is currently impossible to test.

Although the Sestrins have weak homology to a family of alkyl hydroxyperoxidase enzymes in *Mycobacterium tuberculosis*, they do not appear to possess any reductase activity (Budanov et al., 2004; Woo et al., 2009). An intriguing possibility is that the Sestrins possess an enzymatic function that is linked to their role as negative regulators of the amino acid sensing branch of mTORC1, but further studies are needed to understand if the Sestrins retain any enzymatic activity.

Another question is what role, if any, the Sestrins play in tumorigenesis. Here, we demonstrate that loss of the Sestrins renders cells unable to fully inhibit mTORC1 in the absence of amino acids. Similarly, GATOR1-null cells retain constitutive mTORC1 signaling in the absence of amino acids. DEPDC5, Npr12, and Npr13, which together encode GATOR1, are thought to act as tumor suppressor genes (Bar-Peled et al., 2013). It has previously been posited that the Sestrins may act as tumor suppressor genes (Budanov et al., 2010), and mutations in all three Sestrin genes have been detected by cancer genome sequencing efforts (Bamford et al., 2004). However, we show here that the three Sestrins have a large degree of redundancy, and thus a cancer cell may need to lose two or all Sestrins to significantly affect mTORC1 signaling, which may be unlikely.

Finally, the Sestrins have previously been reported to be negative regulators of mTORC1 signaling through AMPK and TSC, which act in the growth factor sensing branch upstream of mTORC1, distinct from the amino acid sensing branch (Budanov and Karin, 2008). Although it is clear from our work that the Sestrins affect the amino acid sensing pathway, it remains to be clarified whether they modulate both of these branches upstream of mTORC1, and what the relative importance of each of these potential effects is. While we were unable to detect any interaction between recombinant Sestrin2 and endogenous TSC (**Figure S1E**), further work is needed to fully understand the effect of the Sestrins on these two separate signaling pathways.

## Experimental Procedures

### Materials

Reagents were obtained from the following sources: LAMP2 H4B4 and HRP-labeled anti-mouse and anti-rabbit secondary antibodies from Santa Cruz Biotechnology; antibodies to phospho-T389 S6K1, S6K1, Sestrin2, mTOR, Mios and FLAG epitope from Cell Signaling Technology; antibodies to the HA epitope from Bethyl laboratories. RPMI, FLAG M2 affinity gel, ATP, GDP, and amino acids from Sigma Aldrich; DMEM from SAFC Biosciences; XtremeGene9 and Complete Protease Cocktail from Roche; Alexa 488 and 568-conjugated secondary antibodies; Inactivated Fetal Calf Serum (IFS) from Invitrogen; amino acid-free RPMI from US Biologicals. The WDR24 and WDR59 antibodies were generously provided by Jianxin Xie (Cell Signaling Technology).

### Cell lysis and immunoprecipitation

Cells were rinsed once with ice-cold PBS and lysed immediately with Triton lysis buffer (1% Triton, 10 mM  $\beta$ -glycerol phosphate, 10 mM pyrophosphate, 40 mM Hepes pH 7.4, 2.5 mM  $MgCl_2$  and 1 tablet of EDTA-free protease inhibitor [Roche] (per 25 ml buffer). The cell lysates were clarified by centrifugation at 13,000 rpm at 4°C in a microcentrifuge for 10 minutes. For anti-FLAG-immunoprecipitations, the FLAG-M2 affinity gel was washed with lysis buffer 3 times. 30  $\mu$ l of a 50% slurry of the affinity gel was then added to cleared cell lysates and incubated with rotation for 2 hours at 4°C. The beads were washed 3 times with lysis buffer containing 500 mM NaCl. In the case of transient cotransfection assays to explore the interaction of the Sestrins with GATOR2, beads were incubated in the final salt wash for 30 minutes to reduce non-specific binding. Immunoprecipitated proteins were denatured by the addition of 50  $\mu$ l of sample buffer and boiling for 5 minutes as described (Kim et al., 2002), resolved by 8%–16% SDS-PAGE, and analyzed by immunoblotting.

For co-transfection experiments in HEK-293T cells, 2 million cells were plated in 10 cm culture dishes. Twenty-four hours later, cells were transfected via the polyethylenimine method (Boussif et al., 1995) with the pRK5-based cDNA expression

plasmids indicated in the figures in the following amounts: 300 ng Flag-Metap2, 100 ng Flag-WDR24, 50 ng Flag-Sestrin1, 25 ng Flag-Sestrin2, or 200 ng Flag-Sestrin3; 2 ng of Flag-S6K1, or 200 ng each of HA-Mios, HA-WDR59, HA-WDR24, HA-Sec13, HA-Seh1L, HA-Depdc5, HA-Nprl3, or HA-Nprl2. The total amount of plasmid DNA in each transfection was normalized to 5 µg with empty pRK5. Thirty-six hours after transfection, cells were lysed as described above.

For experiments which required amino acid starvation or restimulation, cells were treated as previously described (Tsun et al., 2013). Briefly, cells were incubated in amino acid free RPMI for 50 minutes and then stimulated with amino acids for 10 minutes. For glucose starvation, cells were incubated in RPMI media lacking glucose but containing amino acids and dialyzed serum for 50 minutes, followed by a 10 minute restimulation with 5 mM D-Glucose. For insulin deprivation, cells were incubated in RPMI without serum for 50 minutes and restimulated with 1ug/ml insulin for 10 minutes. Finally, when Torin1 or Rapamycin was used, cells were incubated with 250 nM of each throughout the starvation and restimulation period.

### **Generation of CRISPR/Cas9 genetically modified cells**

To generate HEK-293T cells with loss of GATOR2 components or Sesn2, the following sense (S) and antisense (AS) oligonucleotides encoding the guide RNAs were cloned into the pX330 vector (Petit et al., 2013).

sgMios\_1S: caccgATCACATCAGTAAACATGAG

sgMios\_1AS: aaacCTCATGTTTACTGATGTGATc

sgWDR24\_1S: caccgACCCAGGGCTGTGGTCACAC

sgWDR24\_1AS: aaacGTGTGACCACAGCCCTGGGTc

sgWDR59\_1S: caccgCGGGGGAGATGGCGGCGCGA

sgWDR59\_1AS: aaacTCGCGCCGCCATCTCCCCCGc

sgSesn2\_1S: caccgAGAGCCTCGAGCAGCACCTG

sgSesn2\_1AS: aaacCAGGTGCTGCTCGAGGCTCTc

sgSesn2\_2S: caccGGACTACCTGCGGTTGCCCC

sgSesn2\_2AS: aaacGGGCGAACCGCAGGTAGTCC

sgSesn2\_3S: caccGCCACAGCCAAACACGAAGG

sgSesn2\_3AS: aaacCCTTCGTGTTTGGCTGTGGC

sgGFP\_1S: caccgTGAACCGCATCGAGCTGAA

sgGFP\_1AS: aaacTTCAGCTCGATGCGGTTCAc

sgNprl3\_1S: caccGGCTTTCAGGCTCCGTTCGA

sgNprl3\_1AS: aaacTCGAACGGAGCCTGAAAGCC

On day one, 200,000 cells were seeded into 6 wells of a 6-well plate. Twenty-four hours post seeding, each well was transfected with 250 ng shGFP pLKO, 1 ug of the pX330 guide construct, 0.5 ug of empty pRK5 using XtremeGene9. The following day, cells were trypsinized, pooled in a 10 cm dish, and selected with puromycin to eliminate untransfected cells. Forty-eight hours after selection, the media was aspirated and replenished with fresh media lacking puromycin. The following day, cells were single cell sorted with a flow cytometer into the wells of a 96-well plate containing 150 ul of DMEM supplemented with 30% IFS. Cells were grown for two weeks and the resultant colonies were trypsinized and expanded. Clones were validated for loss of the relevant protein via immunoblotting.

## **Acknowledgements**

We thank all members of the Sabatini Lab for helpful insights, in particular Zhi-Yang Tsun for imaging advice and William Comb and Yoav Shaul for qPCR advice. We also thank Dr. Michael Mi for assistance with mass spectrometry analysis. This work was



supported by grants from the NIH (R01 CA103866 and AI47389) and Department of Defense (W81XWH-07-0448) to D.M.S., and fellowship support from the NIH to L.C. (F31 CA180271), R.L.W. (T32 GM007753), J.M.O. (T32 GM007753), S.M.S. (Paul Gray UROP Fund (3143900), and M.I. (GM67945). D.M.S. is an investigator of the Howard Hughes Medical Institute.

## References

- Bamford, S., Dawson, E., Forbes, S., Clements, J., Pettett, R., Dogan, A., Flanagan, A., Teague, J., Futreal, P.A., Stratton, M.R., *et al.* (2004). The COSMIC (Catalogue of Somatic Mutations in Cancer) database and website. *British Journal of Cancer*.
- Bar-Peled, L., Chantranupong, L., Cherniack, A.D., Chen, W.W., Ottina, K.A., Grabiner, B.C., Spear, E.D., Carter, S.L., Meyerson, M., and Sabatini, D.M. (2013). A Tumor Suppressor Complex with GAP Activity for the Rag GTPases That Signal Amino Acid Sufficiency to mTORC1. *Science* *340*, 1100-1106.
- Bar-Peled, L., and Sabatini, D.M. (2014). Regulation of mTORC1 by amino acids. *Trends in cell biology* *24*, 400-406.
- Bar-Peled, L., Schweitzer, L.D., Zoncu, R., and Sabatini, D.M. (2012). Ragulator Is a GEF for the Rag GTPases that Signal Amino Acid Levels to mTORC1. *Cell* *150*, 1196-1208.
- Boussif, O., Lezoualc'h, F., Zanta, M.A., Mergny, M.D., Scherman, D., Demeneix, B., and Behr, J.P. (1995). A versatile vector for gene and oligonucleotide transfer into cells in culture and in vivo: polyethylenimine. *Proceedings of the National Academy of Sciences of the United States of America* *92*, 7297-7301.
- Brugarolas, J., Lei, K., Hurley, R.L., Manning, B.D., Reiling, J.H., Hafen, E., Witters, L.A., Ellisen, L.W., and Kaelin, W.G. (2004). Regulation of mTOR function in response to hypoxia by REDD1 and the TSC1/TSC2 tumor suppressor complex. *Genes & Development* *18*, 2893-2904.
- Buckbinder, L., Talbott, R., Seizinger, B.R., and Kley, N. (1994). Gene regulation by temperature-sensitive p53 mutants: identification of p53 response genes. *Proceedings of the National Academy of Sciences of the United States of America* *91*, 10640-10644.
- Budanov, A.V., and Karin, M. (2008). p53 Target Genes Sestrin1 and Sestrin2 Connect Genotoxic Stress and mTOR Signaling. *Cell* *134*, 451-460.
- Budanov, A.V., Lee, J.H., and Karin, M. (2010). Stressin' Sestrins take an aging fight. *EMBO Molecular Medicine* *2*, 388-400.
- Budanov, A.V., Sablina, A.A., Feinstein, E., Koonin, E.V., and Chumakov, P.M. (2004). Regeneration of peroxiredoxins by p53-regulated sestrins, homologs of bacterial AhpD. *Science* *304*, 596-600.
- Budanov, A.V., Shoshani, T., Faerman, A., Zelin, E., Kamer, I., Kalinski, H., Gorodin, S., Fishman, A., Chajut, A., Einat, P., *et al.* (2002). Identification of a novel stress-responsive gene Hi95 involved in regulation of cell viability. *Oncogene* *21*, 6017-6031.

- Buerger, C., DeVries, B., and Stambolic, V. (2006). Localization of Rheb to the endomembrane is critical for its signaling function. *Biochemical and Biophysical Research Communications* 344, 869-880.
- Dibble, C.C., Elis, W., Menon, S., Qin, W., Klekota, J., Asara, J.M., Finan, P.M., Kwiatkowski, D.J., Murphy, L.O., and Manning, B.D. (2012). TBC1D7 is a third subunit of the TSC1-TSC2 complex upstream of mTORC1. *Molecular cell* 47, 535-546.
- Efeyan, A., Zoncu, R., Chang, S., Gumper, I., Snitkin, H., Wolfson, R.L., Kirak, O., Sabatini, D.D., and Sabatini, D.M. (2012a). Regulation of mTORC1 by the Rag GTPases is necessary for neonatal autophagy and survival. *Nature* 493, 679-683.
- Efeyan, A., Zoncu, R., and Sabatini, D.M. (2012b). ScienceDirect.com - Trends in Molecular Medicine - Amino acids and mTORC1: from lysosomes to disease. *Trends in Molecular Medicine*.
- Fingar, D.C., Salama, S., Tsou, C., Harlow, E., and Blenis, J. (2002). Mammalian cell size is controlled by mTOR and its downstream targets S6K1 and 4EBP1/eIF4E. *Genes Dev* 16, 1472-1487.
- Garami, A., Zwartkuis, F., Nobukuni, T., and Joaquin, M. (2003). ScienceDirect.com - Molecular Cell - Insulin Activation of Rheb, a Mediator of mTOR/S6K/4E-BP Signaling, Is Inhibited by TSC1 and 2. *Molecular cell*.
- Hirose, E., Nakashima, N., Sekiguchi, T., and Nishimoto, T. (1998). RagA is a functional homologue of *S. cerevisiae* Gtr1p involved in the Ran/Gsp1-GTPase pathway. *Journal of cell science* 111 ( Pt 1), 11-21.
- Howell, J.J., Ricoult, S.J.H., Ben Sahra, I., and Manning, B.D. (2013). A growing role for mTOR in promoting anabolic metabolism. *Biochemical Society transactions* 41, 906-912.
- Inoki, K., Li, Y., Xu, T., and Guan, K.-L. (2003). Rheb GTPase is a direct target of TSC2 GAP activity and regulates mTOR signaling. *Genes & Development* 17, 1829-1834.
- Kim, D.-H., Sarbassov, D.D., Ali, S.M., King, J.E., Latek, R.R., Erdjument-Bromage, H., Tempst, P., and Sabatini, D.M. (2002). mTOR Interacts with Raptor to Form a Nutrient-Sensitive Complex that Signals to the Cell Growth Machinery. *Cell* 110, 163-175.
- Kim, E., Goraksha-Hicks, P., Li, L., Neufeld, T.P., and Guan, K.-L. (2008). Regulation of TORC1 by Rag GTPases in nutrient response. *Nature cell biology* 10, 935-945.
- Kim, S.G., Buel, G.R., and Blenis, J. (2013). Nutrient regulation of the mTOR Complex 1 signaling pathway. *Molecules and cells* 35, 463-473.

- Laplante, M., and Sabatini, D.M. (2012). mTOR Signaling in Growth Control and Disease. *Cell* 149, 274-293.
- Long, X., Lin, Y., Ortiz-Vega, S., Yonezawa, K., and Avruch, J. (2005). Rheb Binds and Regulates the mTOR Kinase. *Current Biology* 15, 702-713.
- Menon, S., Dibble, C.C., Talbott, G., Hoxhaj, G., Valvezan, A.J., Takahashi, H., Cantley, L.C., and Manning, B.D. (2014). Spatial Control of the TSC Complex Integrates Insulin and Nutrient Regulation of mTORC1 at the Lysosome. *Cell* 156, 771-785.
- Nobukuni, T., Joaquin, M., Rocco, M., Dann, S.G., Kim, S.Y., Gulati, P., Byfield, M.P., Backer, J.M., Natt, F., Bos, J.L., *et al.* (2005). Amino acids mediate mTOR/raptor signaling through activation of class 3 phosphatidylinositol 3OH-kinase. *Proceedings of the National Academy of Sciences of the United States of America* 102, 14238-14243.
- Panchaud, N., Peli-Gulli, M.-P., and De Virgilio, C. (2013). Amino Acid Deprivation Inhibits TORC1 Through a GTPase-Activating Protein Complex for the Rag Family GTPase Gtr1. *Science Signaling* 6, ra42.
- Peeters, H., Debeer, P., Bairoch, A., Wilquet, V., Huysmans, C., Parthoens, E., Fryns, J.P., Gewillig, M., Nakamura, Y., Niiikawa, N., *et al.* (2003). PA26 is a candidate gene for heterotaxia in humans: identification of a novel PA26-related gene family in human and mouse. *Human genetics* 112, 573-580.
- Petit, C.S., Rocznik-Ferguson, A., and Ferguson, S.M. (2013). Recruitment of folliculin to lysosomes supports the amino acid-dependent activation of Rag GTPases. *The Journal of Cell Biology* 202, 1107-1122.
- Rocco, M., Bos, J.L., and Zwartkruis, F.J.T. (2005). Regulation of the small GTPase Rheb by amino acids. *Oncogene* 25, 657-664.
- Saito, K., Araki, Y., Kontani, K., Nishina, H., and Katada, T. (2005). Novel role of the small GTPase Rheb: its implication in endocytic pathway independent of the activation of mammalian target of rapamycin. *Journal of Biochemistry* 137, 423-430.
- Sancak, Y., Bar-Peled, L., Zoncu, R., Markhard, A.L., Nada, S., and Sabatini, D.M. (2010). Regulator-Rag complex targets mTORC1 to the lysosomal surface and is necessary for its activation by amino acids. *Cell* 141, 290-303.
- Sancak, Y., Peterson, T.R., Shaul, Y.D., Lindquist, R.A., Thoreen, C.C., Bar-Peled, L., and Sabatini, D.M. (2008). The Rag GTPases bind raptor and mediate amino acid signaling to mTORC1. *Science (New York, NY)* 320, 1496-1501.
- Saucedo, L.J., Gao, X., Chiarelli, D.A., Li, L., Pan, D., and Edgar, B.A. (2003). Rheb promotes cell growth as a component of the insulin/TOR signalling network. *Nature cell biology* 5, 566-571.

Schürmann, A., Brauers, A., Maßmann, S., Becker, W., and Joost, H.-G. (1995). Cloning of a Novel Family of Mammalian GTP-binding Proteins (RagA, RagBs, RagB1) with Remote Similarity to the Ras-related GTPases. *The Journal of biological chemistry* 270, 28982-28988.

Sekiguchi, T., Hirose, E., Nakashima, N., Ii, M., and Nishimoto, T. (2001). Novel G proteins, Rag C and Rag D, interact with GTP-binding proteins, Rag A and Rag B. *The Journal of biological chemistry* 276, 7246-7257.

Smith, E.M., Finn, S.G., Tee, A.R., Browne, G.J., and Proud, C.G. (2005). The tuberous sclerosis protein TSC2 is not required for the regulation of the mammalian target of rapamycin by amino acids and certain cellular stresses. *The Journal of biological chemistry* 280, 18717-18727.

Stocker, H., Radimerski, T., Schindelholz, B., Wittwer, F., Belawat, P., Daram, P., Breuer, S., Thomas, G., and Hafen, E. (2003). Rheb is an essential regulator of S6K in controlling cell growth in *Drosophila*. *Nature cell biology* 5, 559-565.

Tee, A.R., Fingar, D.C., Manning, B.D., Kwiatkowski, D.J., Cantley, L.C., and Blenis, J. (2002). Tuberous sclerosis complex-1 and -2 gene products function together to inhibit mammalian target of rapamycin (mTOR)-mediated downstream signaling. *Proceedings of the National Academy of Sciences of the United States of America* 99, 13571-13576.

Tsun, Z.-Y., Bar-Peled, L., Chantranupong, L., Zoncu, R., Wang, T., Kim, C., Spooner, E., and Sabatini, D.M. (2013). The Folliculin Tumor Suppressor Is a GAP for the RagC/D GTPases That Signal Amino Acid Levels to mTORC1. *Molecular cell* 52, 495-505.

Woo, H.A., Bae, S.H., Park, S., and Rhee, S.G. (2009). Sestrin 2 Is Not a Reductase for Cysteine Sulfinic Acid of Peroxiredoxins. *Antioxidants & Redox Signaling* 11, 739-745.

Yuan, H.-X., Xiong, Y., and Guan, K.-L. (2013). Nutrient Sensing, Metabolism, and Cell Growth Control. *Molecular cell* 49, 379-387.

Zoncu, R., Bar-Peled, L., Efeyan, A., Wang, S., Sancak, Y., and Sabatini, D.M. (2011). mTORC1 Senses Lysosomal Amino Acids Through an Inside-Out Mechanism That Requires the Vacuolar H<sup>+</sup>-ATPase. *Science Signaling* 334, 678-683.

## **Supplemental Experimental Procedures**

### **Cell lines and tissue culture**

HEK-293T and HEK-293E cells were cultured in DMEM 10% IFS supplemented with 2 mM glutamine. All cell lines were maintained at 37°C and 5% CO<sub>2</sub>.

### **Identification of Sestrin by mass spectrometry**

Immunoprecipitates from HEK-293T cells stably expressing FLAG-Metap2, FLAG-Mios, FLAG-WDR24 or FLAG-WDR59 were prepared using Triton or Chaps lysis buffer without crosslinking as described earlier. Proteins were eluted with the FLAG peptide (sequence DYKDDDDK) from the FLAG-M2 affinity gel, resolved on 4-12% NuPage gels (Invitrogen), and stained with simply blue stain (Invitrogen). Each gel lane was sliced into 10-12 pieces and the proteins in each gel slice digested overnight with trypsin. The resulting digests were analyzed by mass spectrometry as described (Sancak et al., 2008). Peptides corresponding to Sestrin family members were detected in the FLAG-Mios, FLAG-WDR24 and FLAG-WDR59 immunoprecipitates, while no peptides were detected in negative control immunoprecipitates of FLAG-Metap2.

### **Mammalian lentiviral shRNAs**

On day one, 750,000 HEK-293T cells were seeded in a 6 well plate in DMEM supplemented with 20% inactivated fetal bovine serum (IFS). Twenty-four hours later, the cells were transfected with shRNA-encoding plasmids indicated below alongside the Delta VPR envelope and CMV VSV-G packaging plasmids using XtremeGene9 transfection reagent.

Lentiviral shRNAs targeting Sestrin1, Sestrin2, and Sestrin3 were obtained from the TRC. The TRC number for each shRNA is as follows:

Human Sestrin1 shRNA\_1: TRCN0000143187

Human Sestrin1 shRNA\_2: TRCN0000435014

Human Sestrin2 shRNA\_1: TRCN0000143630

Human Sestrin2 shRNA\_2: TRCN0000122802

Human Sestrin3 shRNA\_1: TRCN0000412760

Human Sestrin3 shRNA\_2: TRCN0000088252

Twelve hours post transfection, the old media was aspirated and replaced with 2 ml fresh media. Virus-containing supernatants were collected 36 hours after replacing media and passed through a 0.45 micron filter to eliminate cells. Four million cells in the presence of 8 µg/ml polybrene (Millipore) were infected with 1 ml of virus for each construct in the case of single knockdown or with 500 ul of virus in the case of double or triple knockdown in 2 ml total volume of media and then spun at 2,200 rpm for 45 minutes at 37°C. Forty-eight hours after selection, cells were trypsinized and selected with puromycin and seeded on the 3<sup>rd</sup> day for signaling experiments, as described.

To validate knockdown of Sesn1 and Sesn3, the following primer pairs were used in an RT-PCR reaction due to the lack of antibodies to these proteins. The data were analyzed via the delta-delta Ct method (Schmittgen and Livak, 2008).

Sesn1 Forward: TGGCAATGCACAAAGATGTTG

Sesn1 Reverse: GCTACGATCCAATAGCTGGTT

Sesn3 Forward: TGCGTTTGTGATCTTGCTAATG

Sesn3 Reverse: CGCCTCTTCATCTTCCCTTTC

### **Immunofluorescence assays**

Immunofluorescence assays were performed as described in (Sancak et al., 2010). Briefly, 300,000 HEK-293T cells were plated on fibronectin-coated glass coverslips in 6-well tissue culture plates. Twenty-four hours later, the slides were rinsed with PBS once and fixed for 15 min with 4% paraformaldehyde in PBS at room temperature. The slides were rinsed three times with PBS and cells were permeabilized with 0.05% Triton X-100 in PBS for 5 min. After rinsing three times with PBS, the slides were blocked for 1 hour in Odyssey blocking buffer, and then incubated with primary antibody in Odyssey blocking buffer for 1 hr at room temperature, rinsed three times with PBS, and incubated with secondary antibodies produced in donkey (diluted 1:1000 in Odyssey blocking buffer) for 45 minutes at room temperature in the dark and washed three times with PBS. Slides were mounted on glass coverslips using Vectashield

(Vector Laboratories) and imaged on a spinning disk confocal system (Perkin Elmer).

### **Rag GTP hydrolysis assay**

GAP assays were performed essentially as previously described (Bar-Peled et al., 2013). In brief, the indicated GTPases were bound to FLAG-M2 affinity gel and loaded with XDP and [ $\alpha$ - $^{32}$ P]GTP at room temperature followed by an incubation with MgCl<sub>2</sub> to stabilize the nucleotide. The GTPases were subsequently washed to remove unbound nucleotide and eluted from the affinity gel with competing FLAG peptide. Protein concentrations were determined prior to use.

For the TLC-based GTP hydrolysis assay, 5 pmoles of the indicated Rag heterodimer was loaded with xanthine nucleotides and [ $\alpha$ - $^{32}$ P]GTP were added to 20 pmoles of purified LRS, GATOR1, or GATOR1 purified from HA-Sesn2 overexpressing cells in 45  $\mu$ l of GTPase wash buffer. The reaction was incubated at 25°C for the indicated times and eluted samples were spotted on PEI Cellulose plates and developed for 2.5 hr in 0.5 M KH<sub>2</sub>PO<sub>4</sub> pH 3.4. Plates were exposed to film and spot densities were quantified with ImageJ.



## Supplemental References

Bar-Peled, L., Chantranupong, L., Cherniack, A.D., Chen, W.W., Ottina, K.A., Grabiner, B.C., Spear, E.D., Carter, S.L., Meyerson, M., and Sabatini, D.M. (2013). A Tumor Suppressor Complex with GAP Activity for the Rag GTPases That Signal Amino Acid Sufficiency to mTORC1. *Science* 340, 1100-1106.

Sancak, Y., Bar-Peled, L., Zoncu, R., Markhard, A.L., Nada, S., and Sabatini, D.M. (2010). Ragulator-Rag complex targets mTORC1 to the lysosomal surface and is necessary for its activation by amino acids. *Cell* 141, 290-303.

Sancak, Y., Peterson, T.R., Shaul, Y.D., Lindquist, R.A., Thoreen, C.C., Bar-Peled, L., and Sabatini, D.M. (2008). The Rag GTPases bind raptor and mediate amino acid signaling to mTORC1. *Science (New York, NY)* 320, 1496-1501.

Schmittgen, T.D., and Livak, K.J. (2008). Analyzing real-time PCR data by the comparative CT method. *Nature Protocols* 3, 1101-1108.

## CHAPTER 4

Reprinted from Science Magazine:

### Sestrin2 is a leucine sensor for the mTORC1 pathway

Rachel L. Wolfson<sup>1,2,3,4,\*</sup>, Lynne Chantranupong<sup>1,2,3,4,\*</sup>, Robert A. Saxton<sup>1,2,3,4</sup>,  
Kuang Shen<sup>1,2,3,4</sup>, Sonia M. Scaria<sup>1,2</sup>, Jason R. Cantor<sup>1,2,3,4</sup>, and David M.  
Sabatini<sup>1,2,3,4</sup>

<sup>1</sup>Whitehead Institute for Biomedical Research and Massachusetts Institute of Technology, Department of Biology, 9 Cambridge Center, Cambridge, MA 02142, USA

<sup>2</sup>Howard Hughes Medical Institute, Department of Biology, Massachusetts Institute of Technology, Cambridge, MA 02139, USA

<sup>3</sup>Koch Institute for Integrative Cancer Research, 77 Massachusetts Avenue, Cambridge, MA 02139, USA

<sup>4</sup>Broad Institute of Harvard and Massachusetts Institute of Technology, 7 Cambridge Center, Cambridge MA 02142, USA

\*These authors contributed equally to this work

Correspondence should be addressed to D.M.S.

Tel: 617-258-6407; Fax: 617-452-3566; Email: [sabatini@wi.mit.edu](mailto:sabatini@wi.mit.edu)

**Experiments in Fig 1A were performed by L.C.**

**Experiments in Fig. 1B-E were performed by R.A.S.**

**Experiments in Fig. S1A-B were performed by R.L.W.**

**Experiments in Fig. 2 and S2A-B and D-F were performed by R.L.W. (with input from K.S.)**

**Experiments in Fig. S2D were performed by L.C. (with a reagent generated by S.M.S.)**

**Experiments in Fig. 3A-C, E and S3A were performed by L.C.**

**Experiments in Fig. 3D were performed by R.L.W.**

**Experiments in Fig. 4B-C were performed by L.C. (with a reagent generated by J.R.C.)**

**Experiments in Fig. 4A and Fig. S4 were performed by R.L.W.**

## **Abstract**

**Leucine is a proteogenic amino acid that also regulates many aspects of mammalian physiology, in large part by activating the mTOR complex 1 (mTORC1) protein kinase, a master growth controller. Amino acids signal to mTORC1 through the Rag guanine triphosphatases (GTPases). Several factors regulate the Rags, including GATOR1, a GTPase activating protein (GAP); GATOR2, a positive regulator of unknown function; and Sestrin2, a GATOR2-interacting protein that inhibits mTORC1 signaling. We find that leucine, but not arginine, disrupts the Sestrin2-GATOR2 interaction by binding to Sestrin2 with a  $K_d$  of 20  $\mu$ M, which is the leucine concentration that half-maximally activates mTORC1. The leucine-binding capacity of Sestrin2 is required for leucine to activate mTORC1 in cells. These results indicate that Sestrin2 is a leucine sensor for the mTORC1 pathway.**

It has long been appreciated that in addition to being a proteogenic amino acid, leucine is also a signaling molecule that directly regulates animal physiology, including satiety (1), insulin secretion (2), and skeletal muscle anabolism (3, 4). Because the liver has a low capacity to metabolize leucine, its blood concentrations fluctuate in accord with its consumption so that dietary leucine can directly impact physiology (5-7). A key mediator of the effects of leucine is the mTORC1 protein kinase (8, 9), which regulates growth by controlling processes like protein and lipid synthesis as well as autophagy.

Many environmental signals besides leucine regulate the mTORC1 pathway, including other amino acids like arginine, as well as glucose and various growth factors and forms of stress (10, 11). How mTORC1 senses and integrates these diverse inputs is not well understood, but it is clear that the Rheb and Rag guanine triphosphatases (GTPases) have necessary but distinct roles. Rheb is a monomeric GTP binding protein and the Rags function as obligate heterodimers of RagA or RagB bound to RagC or RagD (12-14). Both the Rheb and Rag GTPases localize, at least in part, to the lysosomal surface (15-18), which is an important site of mTORC1 regulation (19). In a Rag-dependent manner amino acids promote the translocation of mTORC1 to the lysosome where Rheb, if bound to GTP, stimulates its kinase activity. Growth factors trigger the GTP-loading of Rheb by driving its GTPase activating protein (GAP), the tuberous sclerosis (TSC) complex, off the lysosomal surface (18).

Regulation of the Rag GTPases by amino acids is complex, and many distinct factors have important roles (20). A lysosome-associated super-complex containing Ragulator, SLC38A9, and the vacuolar adenosine triphosphase (v-ATPase) interacts with the Rag GTPases and is necessary for the activation of mTORC1 by amino acids (21-24). Ragulator anchors the Rag heterodimers to the lysosome and has nucleotide exchange activity for RagA and RagB (21, 25). SLC38A9 is an amino acid transporter and a potential lysosomal arginine sensor (23), but the function of the v-ATPase in mTORC1 activation is unclear. Two GAP complexes stimulate GTP hydrolysis by the Rag GTPases, with GATOR1 acting on RagA and RagB (26) and Folliculin (FLCN)-Folliculin interacting protein 2 (FNIP2) on RagC and RagD (27). The separate GATOR2

complex negatively regulates GATOR1 through an unknown mechanism and is necessary for mTORC1 activation (26). Lastly, the Sestrins are GATOR2-interacting proteins that inhibit mTORC1 signaling but whose molecular function is not known (28, 29).

The amino acids sensors upstream of mTORC1 have been elusive for many years. While SLC38A9 is a strong candidate for sensing arginine at lysosomes (23), the long-sought sensor of leucine was unknown. We demonstrate that Sestrin2 is a leucine sensor for the mTORC1 pathway.

### **Leucine directly regulates the Sestrin2-GATOR2 interaction**

Activation of mTORC1 by amino acids requires the pentameric GATOR2 complex (26). Although its molecular function is unknown, epistasis-like experiments suggest that GATOR2 suppresses GATOR1, the GAP for and inhibitor of RagA and RagB (26). Within cells Sestrin2 binds to GATOR2 in an amino acid-sensitive manner (28, 29), with removal and re-addition of all amino acids from the culture media inducing and reversing the interaction, respectively (28). Although several amino acids can regulate mTORC1 signaling, arginine and leucine are the best established and deprivation of either strongly inhibits mTORC1 in various cell types (8, 30, 31). In human embryonic kidney-293T (HEK-293T) cells removal of either leucine or arginine from the cell medium inhibited mTORC1 signaling, as read out by ribosomal protein S6 kinase 1 (S6K1) phosphorylation, to similar extents. Strikingly, however, only leucine depletion caused Sestrin2 to bind to GATOR2, inducing the interaction as effectively as complete amino acid starvation (Fig. 1A). Leucine re-addition rapidly reversed the binding and amino acids did not affect the interaction between WDR24 and Mios, two core components of GATOR2 (Fig. 1A, and S1A).

Sestrin2 is homologous to two other proteins, Sestrin1 and Sestrin3 (32-34), and when overexpressed all three can interact with GATOR2 (28). As with Sestrin2, leucine starvation and stimulation strongly regulated the interaction of endogenous Sestrin1

with GATOR2 (Fig. S1B). In contrast, endogenous Sestrin3 bound to GATOR2 irrespective of leucine concentrations (Fig. S1B), suggesting that this interaction is constitutive or regulated by signals that remain to be defined.

While enzymatic events triggered by leucine might mediate the effects of leucine on the Sestrin2-GATOR2 interaction, it was tempting to consider that leucine might act directly on the complex. Consistent with this possibility, the addition of leucine, but not arginine, to ice-cold detergent lysates of cells deprived of all amino acids abrogated the interaction to the same extent as leucine-stimulation of live cells (Fig. 1B). Even more intriguingly, leucine also disrupted the interaction when added directly to immunopurified Sestrin2-GATOR2 complexes isolated from amino acid-deprived cells. Of the 18 amino acids tested at 300  $\mu$ M each, only those most similar to leucine –methionine, isoleucine, and valine– had any effect on the Sestrin2-GATOR2 interaction *in vitro* (Fig. 1C).

When added to the purified complexes, leucine dose-dependently disrupted the Sestrin2-GATOR2 complex, with the half maximal effect at about 1  $\mu$ M (Fig. 1D). Methionine and isoleucine were considerably less potent, acting at concentrations approximately 10- and 25-fold greater than leucine, respectively (Fig. 1E). These values reflect only the relative potencies of these amino acids as equilibrium conditions were not attained because the large assay volume precluded Sestrin2 from rebinding to GATOR2 once dissociated.

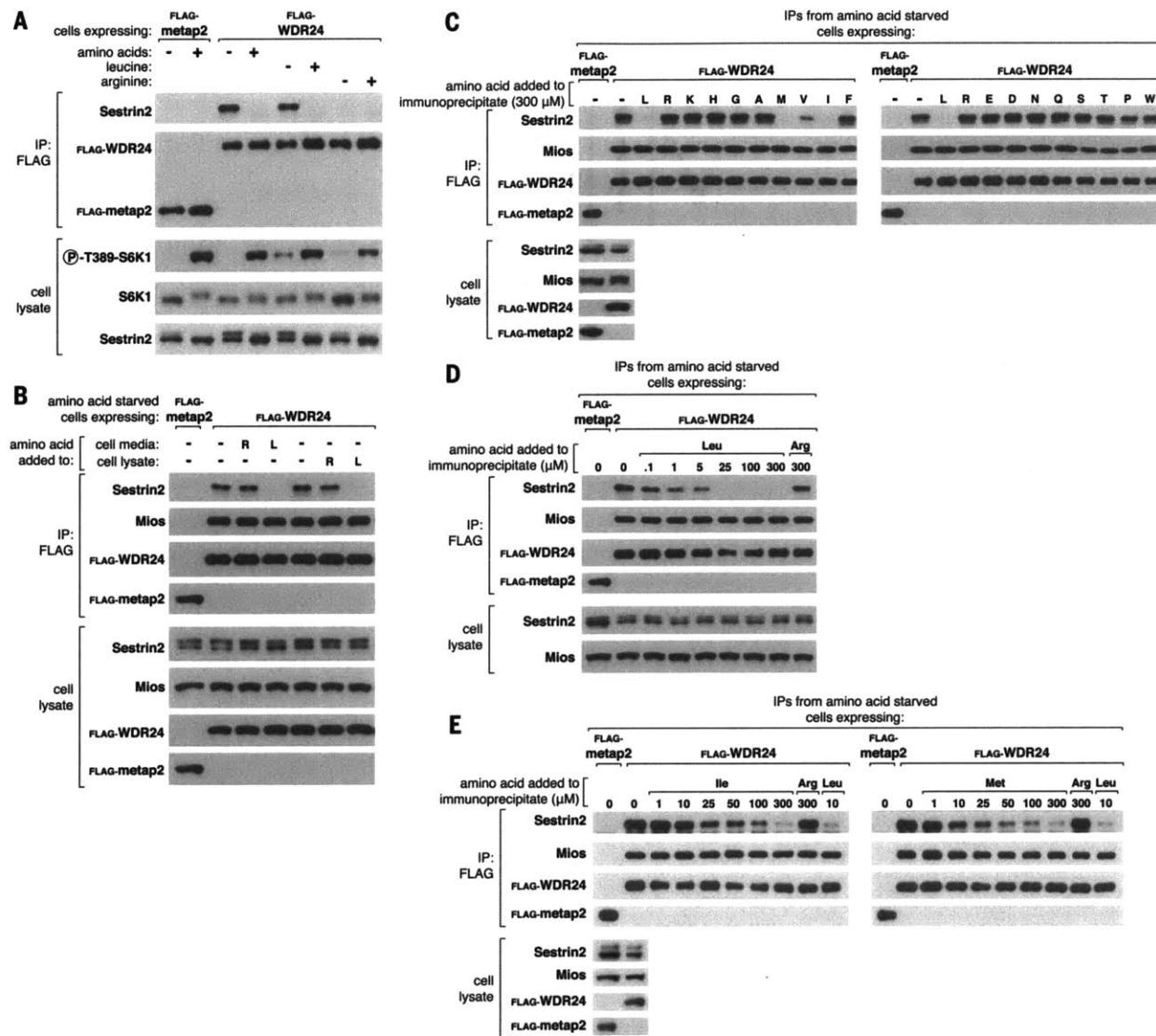


**Figure 1: Leucine, but not arginine, disrupts the Sestrin2-GATOR2 interaction in cells and *in vitro***

A) Binding of Sestrin2 to GATOR2 in HEK-293T cells stably expressing FLAG-WDR24 (a component of GATOR2). Cells were deprived of leucine, arginine, or all amino acids for 50 minutes. Where indicated, cells were re-stimulated with leucine, arginine, or all amino acids for 10 minutes and FLAG immunoprecipitates prepared from cell lysates. Immunoprecipitates and lysates were analyzed by immunoblotting for the indicated proteins. FLAG-metap2 served as a negative control.

B) Effects of leucine and arginine on the Sestrin2-GATOR2 interaction in ice-cold detergents lysates of amino acid-starved cells. HEK-293T cells stably expressing FLAG-metap2 or FLAG-WDR24 were deprived of all amino acids for 50 minutes. Leucine or

arginine was added to the culture media or cell lysates and FLAG immunoprecipitates prepared and analyzed as in (A).

C) Effects of individual amino acids on the purified Sestrin2-GATOR2 complex. FLAG immunoprecipitates were prepared from HEK-293T cells stably expressing FLAG-metap2 or FLAG-WDR24 and deprived of all amino acids for 50 minutes. Indicated amino acids (300  $\mu$ M) were added directly to the immunoprecipitates, which, after re-washing, were analyzed as in (A).

D) Disruption of the purified Sestrin2-GATOR2 complex by leucine. Experiment was performed and analyzed as in (C) except that indicated concentrations of leucine or arginine were used.

E) Disruption of the Sestrin2-GATOR2 interaction by isoleucine and methionine. Experiment was performed and analyzed as in (C) except that the indicated concentrations of isoleucine, methionine, leucine, or arginine were used.



## Supp. Figure 1

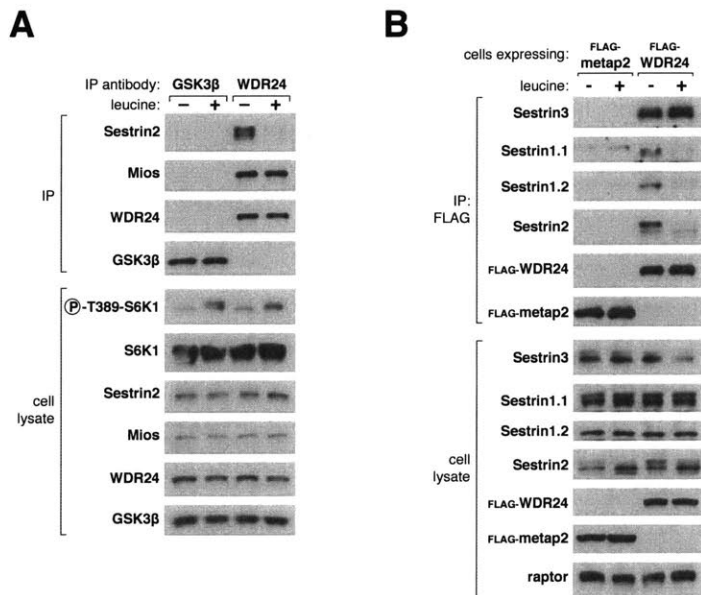


### Figure S1: Leucine disrupts the interaction between GATOR2 and Sestrin1 but not Sestrin3

A) Effect of leucine on the interaction between endogenous GATOR2 and endogenous Sestrin2. HEK-293T cells were deprived of leucine for 1 hour, or starved for 50 minutes and restimulated with leucine for 10 minutes. Immunoprecipitates were prepared using an antibody to WDR24 or a control protein (GSK3β), and, along with cell lysates, analyzed via immunoblotting for the indicated proteins.

B) Effects of leucine starvation and restimulation on the interaction between GATOR2 and endogenous Sestrin1 (two isoforms), Sestrin2, or Sestrin3. HEK-293T cells stably expressing FLAG-metap2 or FLAG-WDR24 were deprived of leucine for 50 minutes, and, where indicated, restimulated with leucine for 10 minutes. FLAG immunoprecipitates were prepared and analyzed as in Figure 1A. Asterisks denote non-specific bands.

## Sestrin2 binds leucine with a $K_d$ of 20 $\mu\text{M}$

Given that leucine disrupts the purified complex, we reasoned that leucine might directly bind to Sestrin2 or GATOR2. To test this, we developed an equilibrium binding assay in which purified proteins immobilized on agarose beads were incubated with radioactive amino acids, and the bound amino acids were quantified after washing. Radiolabeled leucine bound to Sestrin2, but not WDR24, the GATOR2 complex, or the control protein Rap2A, in a manner that was fully competed by excess non-radiolabeled leucine (Fig. 2A). In contrast, arginine did not bind to either Sestrin2 or Rap2A (Fig. S2A). Consistent with the differential sensitivities of the Sestrin1- and Sestrin3-GATOR2 complexes to leucine, Sestrin1 bound leucine to a similar extent as did Sestrin2, whereas Sestrin3 bound very weakly (Fig. 2B and S2A). *Drosophila* dSestrin (CG11299-PD) also bound leucine, albeit at lower amounts than the human protein (Fig. S2B and C).

As all of these proteins were expressed in and purified from human HEK-293T cells, it remained formally possible that an unidentified protein that co-purifies with Sestrin2 (and Sestrin1) is the actual receptor for leucine. To address this possibility, we prepared human Sestrin2 in bacteria, a heterologous system that does not encode a Sestrin homologue or even a TOR pathway. Consistent with the results obtained with Sestrin2 prepared in human cells, radiolabelled leucine bound to bacterially-produced Sestrin2, but not the RagA-RagC heterodimer, which was used as a control (Fig. 2C). Furthermore, in a thermal shift assay, leucine, but not arginine, shifted the melting temperature by up to 8.5°C of bacterially-produced Sestrin2, but not of two control proteins (Fig. 2D and S2E-F). Collectively, these data strongly argue that leucine binds directly to Sestrin2.

While the thermal shift assay is valuable for assessing the capacity of a protein to bind a ligand, this method is not suitable for obtaining an accurate  $K_d$  (35). Therefore, we used a competition binding assay with increasing amounts of unlabeled leucine to determine that leucine has a  $K_d$  for Sestrin2 of  $20 \pm 5 \mu\text{M}$  (Fig. 2E). In comparison,

methionine and isoleucine competed leucine binding with inhibitory constants ( $K_i$ ) of  $354 \pm 118 \mu\text{M}$  and  $616 \pm 273 \mu\text{M}$ , respectively (Fig. 2F and G). These values are approximately one eighteenth and one thirtieth the affinity of leucine for Sestrin2, and correlate well with the relative potencies of leucine, methionine, and isoleucine in disrupting the Sestrin2-GATOR2 interaction *in vitro* (Fig. 1D and E).

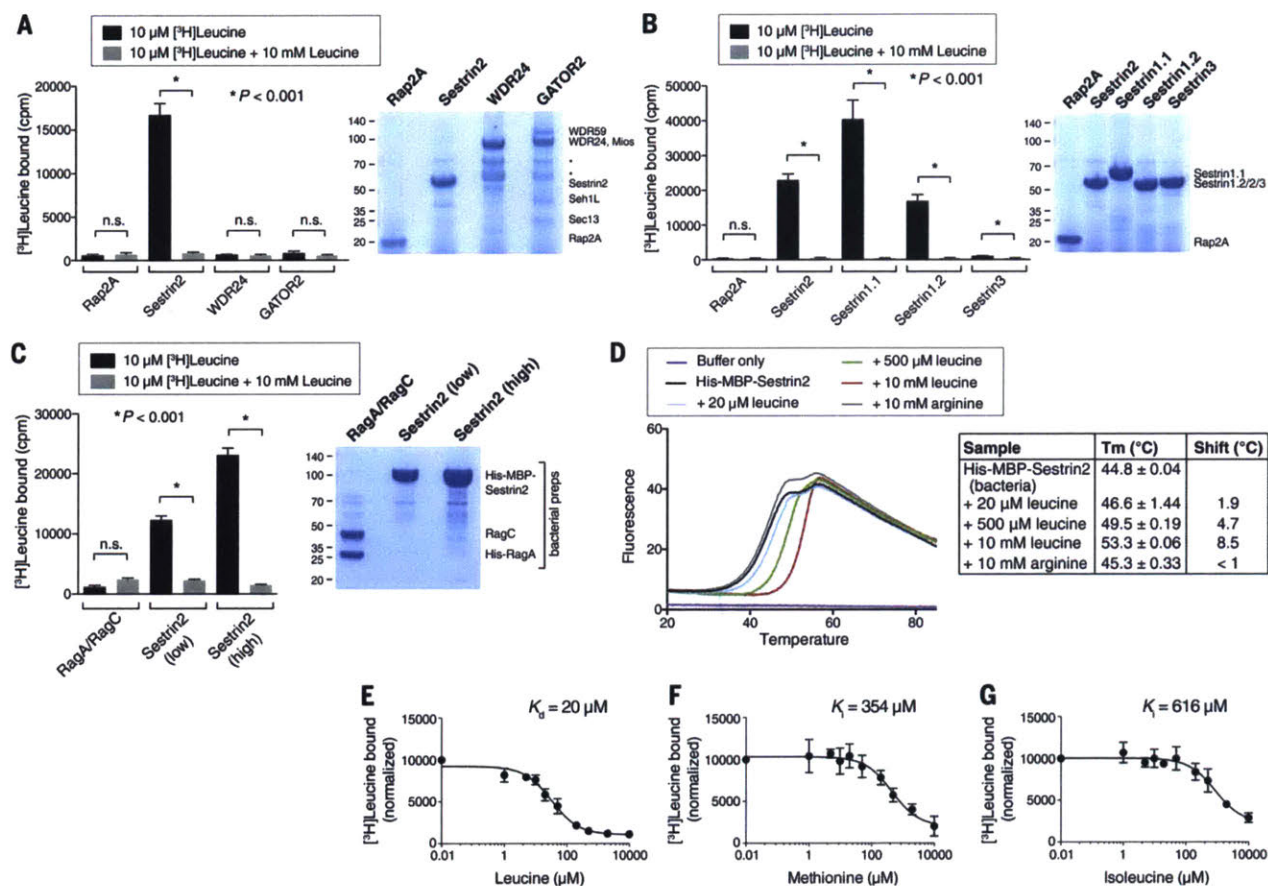


**Figure 2: Sestrin2 binds leucine with a  $K_d$  of 20  $\mu\text{M}$**

A) Binding of radiolabeled leucine to Sestrin2, but not WDR24, GATOR2, or the control protein Rap2A. FLAG immunoprecipitates prepared from HEK-293T cells transiently expressing indicated proteins or complexes were used in binding assays with [ $^3\text{H}$ ]Leucine as described in the methods. Unlabeled leucine was added where indicated. Values are Mean  $\pm$  SD for 3 technical replicates from one representative experiment. SDS-PAGE followed by Coomassie blue staining was used to analyze

immunoprecipitates prepared in parallel to those included in the binding assays.

Asterisks indicate breakdown products in the WDR24 and GATOR2 purifications.

B) Leucine-binding capacities of Sestrin1 (two isoforms), Sestrin2, and Sestrin3. FLAG immunoprecipitates were prepared and binding assays performed and analyzed as in (A).

C) Leucine binds to bacterially-produced Sestrin2, but not the RagA/RagC heterodimer. Leucine binding assays were performed as described in the methods and analyzed as in (A) with His-MBP-Sestrin2 or His-RagA/RagC bound to the Ni-NTA resin.

D) Effects of leucine and arginine on the melting temperature of bacterially-produced Sestrin2 in a thermal shift assay. His-MBP-Sestrin2 was incubated with the Sypro orange dye with or without leucine or arginine. Upon heating the sample the change in fluorescence was captured and used to calculate melting temperatures ( $T_m$ ) under the indicated conditions. Values are Mean  $\pm$  SD from 3 replicates.

E) Sestrin2 binds leucine with a  $K_d$  of 20  $\mu$ M. FLAG-Sestrin2 immunoprecipitates prepared as in (A) were used in binding assays with 10  $\mu$ M or 20  $\mu$ M [ $^3$ H]Leucine and indicated concentrations of unlabeled leucine. In the representative graph shown each point represents the normalized mean  $\pm$  SD for  $n = 3$  in an assay with 10  $\mu$ M [ $^3$ H]Leucine. The  $K_d$  was calculated from the results of six experiments (three with 10  $\mu$ M and three with 20  $\mu$ M [ $^3$ H]Leucine).

F) Methionine can compete the binding of leucine to Sestrin2. FLAG-Sestrin2 immunoprecipitates prepared as in (A) were used in binding assays with 10  $\mu$ M [ $^3$ H]Leucine and indicated concentrations of unlabeled methionine. In the graph shown each point represents the normalized mean  $\pm$  SD for  $n = 3$ . The  $K_i$  was calculated using data from the three experiments.

G) Isoleucine can compete the binding of leucine to Sestrin2. FLAG-Sestrin2 immunoprecipitates prepared as in (A) were used in binding assays with 10  $\mu$ M [ $^3$ H]Leucine and indicated concentrations of unlabeled isoleucine. In the graph shown each point represents the normalized mean  $\pm$  SD for  $n = 3$ . The  $K_i$  was calculated using data from the three experiments.

## Supp. Figure 2

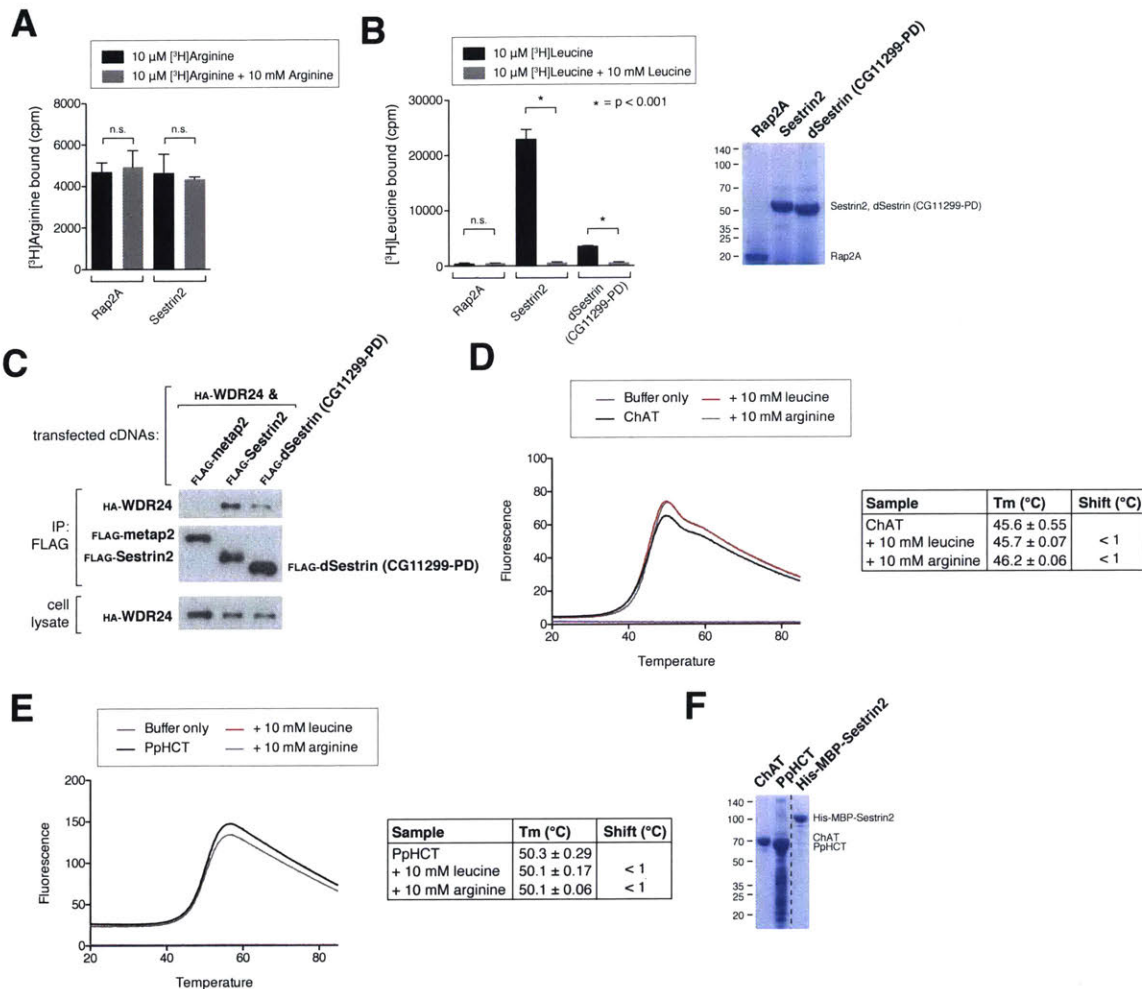


### Figure S2: Sestrin2 does not bind arginine, and the capacity of Sestrin2 to bind leucine is conserved in *Drosophila* Sestrin

A) Sestrin2 does not bind arginine. FLAG-Sestrin2 immunoprecipitates prepared as in Figure 2A were used in binding assays with [3H]Arginine with or without unlabeled arginine.

B) Effects of leucine or arginine on the melting temperature of human choline acetyltransferase (ChAT) in a thermal shift assay. ChAT prepared in bacteria was subjected to a thermal shift assay as in Figure 2C.

C) Effects of leucine or arginine on the melting temperature of another control protein, *Physconitrella patens* hydroxycinnamoyl transferase (PpHCT) in a thermal shift assay.

D) SDS-PAGE and Coomassie blue staining analyses of the bacterially prepared proteins (His-MBP-Sestrin2, ChAT, and PpHCT ) used in the thermal shift assays.

E) dSestrin (CG11299-PD) binds to leucine. Binding assays were performed and immunoprecipitates analyzed as in Figure 2A.

F) dSestrin (CG11299-PD) interacts with human WDR24, a component of GATOR2.

FLAG immunoprecipitates were prepared from HEK-293T cells expressing the indicated proteins, and immunoprecipitates and cell lysates analyzed via immunoblotting.

### **Sestrin2 regulates mTORC1 through GATOR2**

Consistent with leucine regulating mTORC1 by modulating the binding of Sestrin2 to GATOR2, 20-40  $\mu$ M leucine had half-maximal effects on both the Sestrin2-GATOR2 interaction and mTORC1 activity in HEK-293T cells (Fig. 3A and B). This concentration range encompasses the  $K_d$  of leucine for Sestrin2, indicating that the affinity of Sestrin2 for leucine is physiologically relevant.

To formally test whether Sestrin2 regulates mTORC1 by interacting with GATOR2, we identified a Sestrin2 mutant (S190W) that still binds leucine but has a severely decreased capacity to bind GATOR2 (Fig. 3C and D). In Sestrin1-3 triple null HEK-293T cells, mTORC1 signaling was active and unaffected by leucine deprivation (Fig. 3E). In these cells expression of wild-type Sestrin2 restored the leucine sensitivity of the mTORC1 pathway, but that of Sestrin2 S190W had no effect (Fig. 3E). Thus, Sestrin2 must be able to interact with GATOR2 for the mTORC1 pathway to sense the absence of leucine.



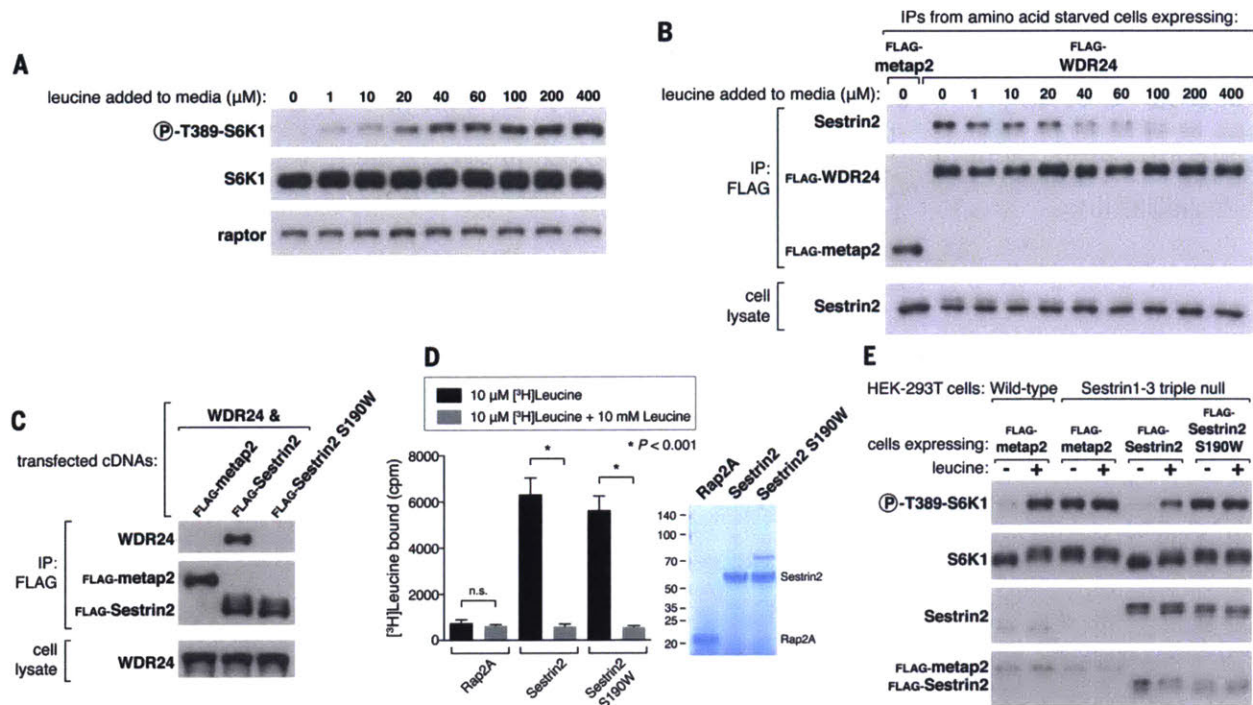


**Figure 3: Sestrin2 regulates mTORC1 through GATOR2**

A) Effects of varying leucine concentrations on mTORC1 activity, as measured by the phosphorylation of S6K1. HEK-293T cells were deprived of leucine for 50 minutes and restimulated with leucine at the indicated concentrations for 10 minutes. Cell lysates were analyzed via immunoblotting for the indicated proteins and phosphorylation states.

B) Effects of varying leucine concentrations on the Sestrin2-GATOR2 interaction. HEK-293T cells stably expressing the indicated proteins were starved and restimulated as in (A). FLAG immunoprecipitates were prepared and analyzed by immunoblotting for the indicated proteins.

C) Decreased GATOR2-binding capacity of the Sestrin2 S190W mutant. FLAG immunoprecipitates were prepared from cells transiently expressing the indicated proteins. The immunopurified complexes were treated with the indicated concentrations of leucine and then analyzed as in Figure 1C.

D) Determination of leucine-binding capacity of Sestrin2 S190W. Assays were performed and immunoprecipitates analyzed as in Figure 2A.

E) In Sestrin1-3 triple null cells expressing Sestrin2 S190W the mTORC1 pathway cannot sense the absence of leucine. Wild-type HEK-293T cells and Sestrin1-3 triple

null HEK-293T cells generated with the CRISPR/Cas9 system were used to express the indicated FLAG-tagged proteins. Cells were starved for leucine for 50 minutes and, where indicated, stimulated with leucine for 10 minutes and lysates analyzed via immunoblotting.

### Supp. Figure 3

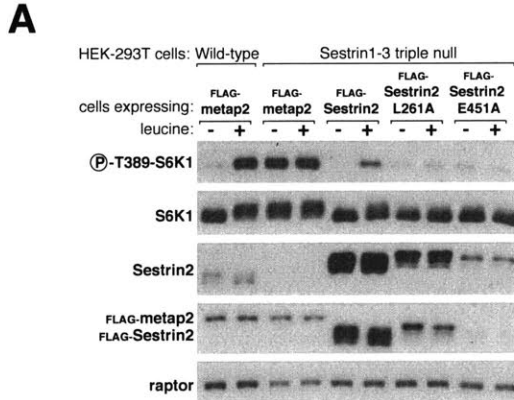


**Figure S3: Expression in Sestrin1-3 triple null cells of Sestrin2 L261A or E451A at levels much lower than wild-type Sestrin2 still renders mTORC1 signaling insensitive to leucine stimulation**

A) Expression in Sestrin1-3 triple null cells of Sestrin2 L261A or E451A does not restore the capacity of the mTORC1 pathway to sense the presence of leucine, even when mutants are expressed at levels much lower than wild-type Sestrin2. Cells were generated and analyzed as in Figure 3E. Note that wild-type recombinant Sestrin2 is overexpressed relative to endogenous levels, explaining why it partially suppresses mTORC1 signaling. The Sestrin2 E451A mutant is expressed at levels similar to the endogenous protein, and both mutants are expressed at much lower levels than wild-type Sestrin2. All forms of Sestrin2 in this experiment were expressed from the pLJC5 plasmid.



## **For leucine to activate mTORC1, Sestrin2 must be able to bind leucine**

To test whether the leucine-binding capacity of Sestrin2 is necessary for mTORC1 to sense the presence of leucine, we identified two Sestrin2 mutants, L261A and E451A, which do not bind leucine to an appreciable degree (Fig. 4A). Leucine did not significantly affect the interaction of the mutants with GATOR2 *in vitro*, consistent with Sestrin2 mediating the effects of leucine on the Sestrin2-GATOR2 complex (Fig. 4B). Expression of wild-type Sestrin2 in the Sestrin1-3 triple null cells restored the leucine sensitivity of the mTORC1 pathway in these cells, but that of either mutant inhibited signaling and rendered it insensitive to leucine (Fig. 4C and S3A). Furthermore, in Sestrin1-3 triple null cells expressing the mutants, the localization of mTOR to lysosomes in the presence of leucine was decreased, while that of RagC was not affected (Fig. S4A-D). Thus, activation of mTORC1 by leucine requires the binding of leucine to Sestrin2.

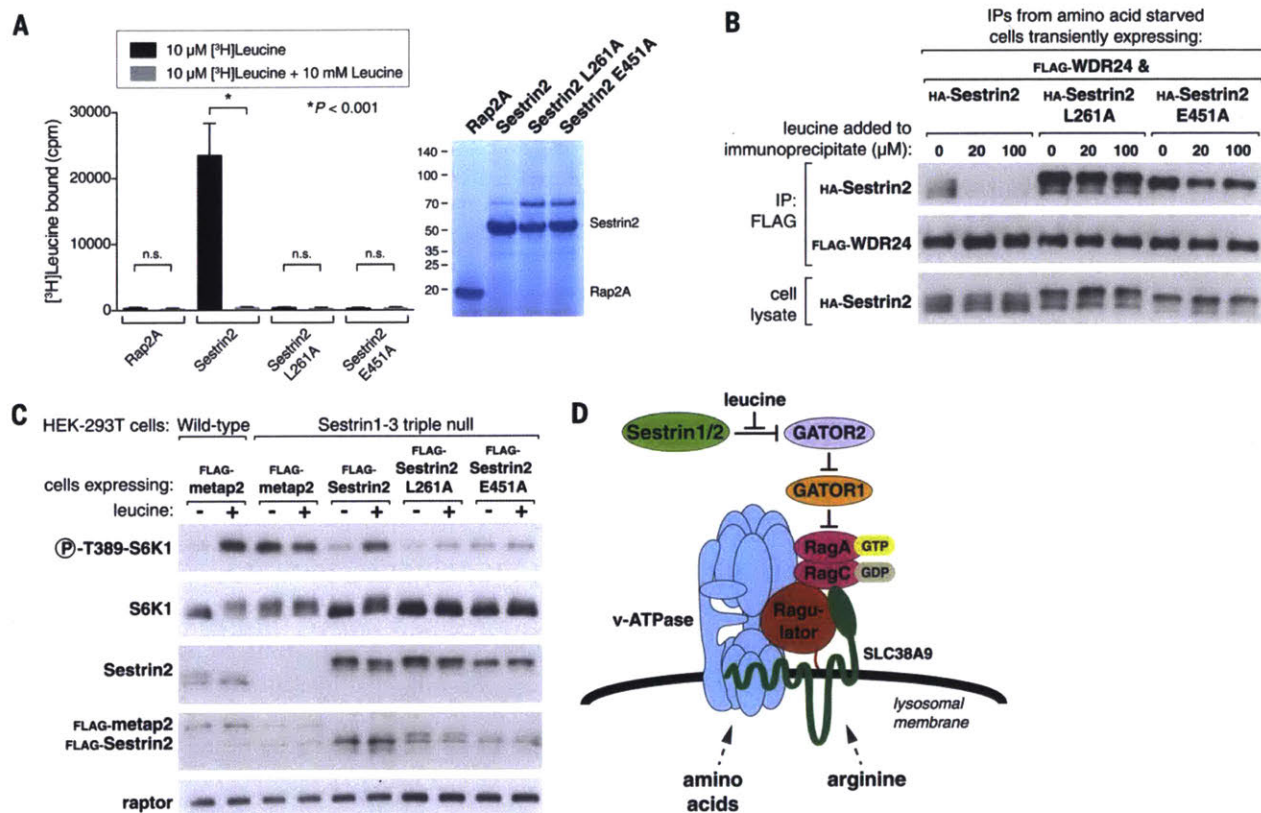


**Figure 4: The capacity of Sestrin2 to bind leucine is required for the mTORC1 pathway to sense leucine**

A) The Sestrin2 L261A and E451A mutants do not bind leucine. Binding assays were performed and immunoprecipitates analyzed as in Figure 2A.

B) Leucine-insensitivity of the interactions of Sestrin2 L261A or E451A with GATOR2. FLAG immunoprecipitates were prepared from cells transiently expressing the indicated proteins. The immunoprecipitates were treated with the indicated concentrations of leucine and analyzed as in Figure 1C.

C) In Sestrin1-3 triple null cells expressing Sestrin2 L261A or E451A the mTORC1 pathway cannot sense the presence of leucine. Cells were generated and analyzed as in Figure 3E.

D) Model showing how amino acid inputs arising from multiple sensors in distinct compartments impinge on the Rag GTPases to control mTORC1 activity.

# Supp. Figure 4

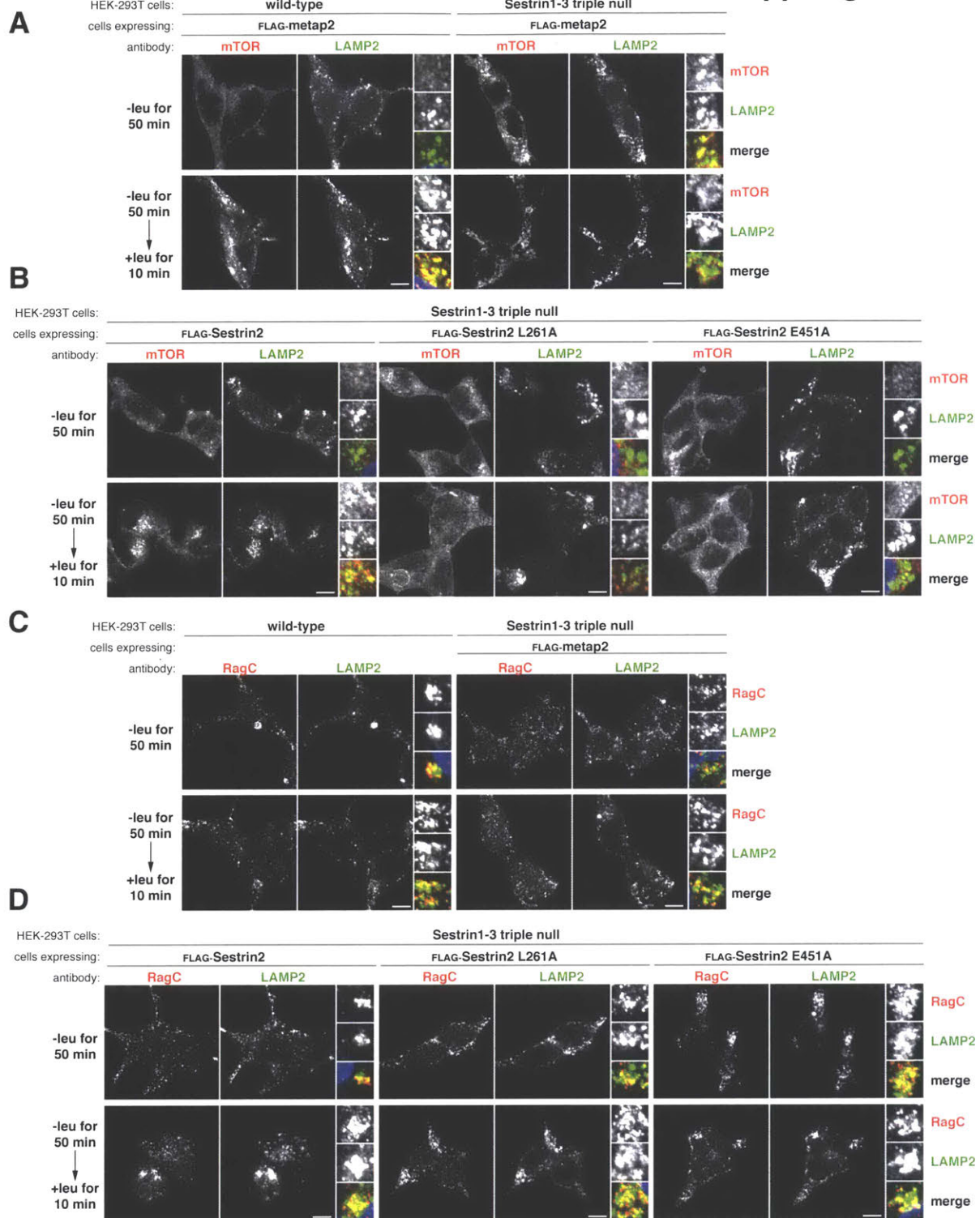


**Figure S4: Expression of Sestrin2 L261A or E451A in Sestrin1-3 triple null cells decreases the localization of mTOR to lysosomes in the presence of leucine**

A) mTOR localization upon leucine deprivation and restimulation in wild-type and Sestrin1-3 triple null cells. HEK-293T cells (wild-type or Sestrin1-3 triple null created via the CRISPR/Cas9 system) stably expressing the indicated proteins were deprived of or deprived of and restimulated with leucine for the indicated times prior to processing for immunofluorescence. Insets depict selected fields that were magnified 3.24X and their overlays. All scale bars represent 10  $\mu$ m.

B) Effects of wild-type Sestrin2, or Sestrin2 L261A or E451A, on mTOR localization. Sestrin1-3 triple null HEK-293T cells stably expressing the indicated proteins were treated and analyzed as in (A). C) RagC localizes to the lysosome in wild-type and Sestrin1-3 triple null cells. HEK-293T cells (wild-type and Sestrin1-3 triple null) were treated and processed as in (A).

D) RagC localization in Sestrin1-3 triple null cells reconstituted with wild-type Sestrin2 or either Sestrin2 mutant. Cells were processed for immunofluorescence as in (A).

## Conclusions

Sestrin2 has several properties consistent with it being a leucine sensor for the mTORC1 pathway: (1) it binds leucine at affinities consistent with the concentrations at which leucine is sensed; (2) Sestrin2 mutants that do not bind leucine cannot signal the presence of leucine to mTORC1; and (3) loss of Sestrin2 and its homologs renders the mTORC1 pathway insensitive to the absence of leucine. Although we have not investigated Sestrin1 as thoroughly, it appears to behave similarly to Sestrin2, so we propose that Sestrin1 and Sestrin2 are leucine sensors upstream of mTORC1.

Given that Sestrin2 has appreciable affinity for methionine, it would not be surprising if in contexts where leucine concentrations are low and those of methionine are high, Sestrin2 may serve as a methionine sensor for the mTORC1 pathway.

Sestrin2 binds to and likely inhibits GATOR2, but how this leads to suppression of mTORC1 awaits elucidation of the molecular function of GATOR2. In addition,

structural studies are needed to understand how the binding of leucine to Sestrin2 disrupts its interaction with GATOR2 and why leucine binds very poorly to Sestrin3.

As Sestrin1 and Sestrin2 are soluble proteins, it is likely that they sense free leucine in the cytosol. Although these concentrations are unknown, the  $K_m$  of the human leucyl-tRNA synthetase (LRS) for leucine has been reported to be 45  $\mu\text{M}$  (36), which is similar to the affinity of Sestrin2 for leucine, suggesting that cytosolic free leucine concentrations are within this range. Like Sestrin2, LRS can bind isoleucine and methionine at lower affinities than leucine (about 30 fold less in the case of LRS) (36). The similarities between the amino acid binding characteristics of Sestrin2 and LRS support the notion that the affinity and specificity of Sestrin2 for leucine are sufficient for it to serve as a leucine sensor.

Our work suggests a model in which signals emerging from distinct amino acid sensors in different cellular compartments converge on the Rag GTPases at the lysosomal surface to regulate mTORC1 activity (Fig. 4D). The putative arginine sensor SLC38A9 likely monitors lysosomal contents and Sestrin2 is almost certainly a cytosolic sensor. There must also be an amino acid sensor upstream of the GAP for RagC and RagD, the FLCN-FNIP2 complex, but its identity and cellular localization are unknown. A future challenge is to elucidate how the Rag GTPases integrate the inputs coming from the different sensors, which will likely require a much better understanding of the function of each Rag in the heterodimer. Moreover, *in vivo* characterization of the different sensors will be needed to comprehend how specific tissues adapt the amino acid sensing pathway to their particular needs.

Given that Sestrin2 (and Sestrin1) are likely to have leucine-binding pockets, these proteins may be targets for developing small molecule modulators of the mTORC1 pathway. Leucine attenuates the decrease in skeletal muscle protein synthesis that occurs in the elderly and stimulates satiety (1, 37). Thus, small molecules that potently mimic the effects of leucine on Sestrin2 could have therapeutic value. Furthermore, caloric restriction (CR) inhibits mTORC1 signaling (38, 39) and is

associated with increases in healthspan and lifespan in multiple organisms (40, 41). Thus, small molecules that antagonize the effects of leucine on Sestrin2 might have CR-mimicking properties.

## REFERENCES AND NOTES

1. M. Potier, N. Darcel, D. Tomé, Protein, amino acids and the control of food intake. *Current Opinion in Clinical Nutrition and Metabolic Care* **12**, 54-58 (2009).
2. U. Panten, J. Christians, E. von Kriegstein, W. Poser, A. Hasselblatt, Studies on the mechanism of L-leucine-and alpha-ketoisocaproic acid-induced insulin release from perfused isolated pancreatic islets. *Diabetologia* **10**, 149-154 (1974).
3. J. S. Greiwe, G. Kwon, M. L. McDaniel, C. F. Semenkovich, Leucine and insulin activate p70 S6 kinase through different pathways in human skeletal muscle. *American journal of physiology. Endocrinology and metabolism* **281**, E466-471 (2001).
4. K. S. Nair, R. G. Schwartz, S. Welle, Leucine as a regulator of whole body and skeletal muscle protein metabolism in humans. *American Journal of Physiology -- Legacy Content* **263**, E928-934 (1992).
5. D. K. Layman, D. A. Walker, Potential Importance of Leucine in Treatment of Obesity and the Metabolic Syndrome. (2006).
6. E. G. FRAME, in *Journal of Clinical Investigation*. (1958), vol. 37, pp. 1710-1723.
7. A. E. Harper, R. H. Miller, K. P. Block, in *Annual Review of Nutrition*. (1984), vol. 4, pp. 409-454.
8. H. L. Fox, P. T. Pham, S. R. Kimball, L. S. Jefferson, C. J. Lynch, Amino acid effects on translational repressor 4E-BP1 are mediated primarily by L-leucine in isolated adipocytes. *American Journal of Physiology -- Legacy Content* **275**, C1232-1238 (1998).
9. C. J. Lynch, H. L. Fox, T. C. Vary, L. S. Jefferson, S. R. Kimball, Regulation of amino acid-sensitive TOR signaling by leucine analogues in adipocytes. *Journal of cellular biochemistry* **77**, 234-251 (2000).
10. C. C. Dibble, B. D. Manning, Signal integration by mTORC1 coordinates nutrient input with biosynthetic output. *Nature Cell Biology* **15**, 555-564 (2013).
11. A. Efeyan, D. M. Sabatini, in *Biochem. Soc. Trans.* (Portland Press Ltd., 2013), vol. 41, pp. 902-905.
12. E. Hirose, N. Nakashima, T. Sekiguchi, T. Nishimoto, RagA is a functional homologue of *S. cerevisiae* Gtr1p involved in the Ran/Gsp1-GTPase pathway. *Journal of cell science* **111 ( Pt 1)**, 11-21 (1998).
13. A. Schürmann, A. Brauers, S. Maßmann, W. Becker, H.-G. Joost, Cloning of a Novel Family of Mammalian GTP-binding Proteins (RagA, RagBs, RagB1) with Remote Similarity to the Ras-related GTPases. *The Journal of biological chemistry* **270**, 28982-28988 (1995).
14. T. Sekiguchi, E. Hirose, N. Nakashima, M. Ii, T. Nishimoto, Novel G proteins, Rag C and Rag D, interact with GTP-binding proteins, Rag A and Rag B. *The Journal of biological chemistry* **276**, 7246-7257 (2001).
15. C. Buerger, B. DeVries, V. Stambolic, in *Biochemical and Biophysical Research Communications*. (2006), vol. 344, pp. 869-880.

16. K. Saito, Y. Araki, K. Kontani, H. Nishina, T. Katada, Novel role of the small GTPase Rheb: its implication in endocytic pathway independent of the activation of mammalian target of rapamycin. *Journal of biochemistry* **137**, 423-430 (2005).
17. Y. Sancak *et al.*, The Rag GTPases Bind Raptor and Mediate Amino Acid Signaling to mTORC1. *Science* **320**, 1496-1501 (2008).
18. S. Menon *et al.*, Spatial Control of the TSC Complex Integrates Insulin and Nutrient Regulation of mTORC1 at the Lysosome. *Cell* **156**, 771-785 (2014).
19. A. Efeyan, R. Zoncu, D. M. Sabatini, in *Trends Mol Med.* (2012), vol. 18, pp. 524-533.
20. L. Chantranupong, R. L. Wolfson, D. M. Sabatini, in *Cell.* (2015), vol. 161, pp. 67-83.
21. Y. Sancak *et al.*, Ragulator-Rag complex targets mTORC1 to the lysosomal surface and is necessary for its activation by amino acids. *Cell* **141**, 290-303 (2010).
22. R. Zoncu *et al.*, mTORC1 Senses Lysosomal Amino Acids Through an Inside-Out Mechanism That Requires the Vacuolar H<sup>+</sup>-ATPase. *Science Signaling* **334**, 678-683 (2011).
23. S. Wang *et al.*, Metabolism. Lysosomal amino acid transporter SLC38A9 signals arginine sufficiency to mTORC1. *Science* **347**, 188-194 (2015).
24. M. Rebsamen *et al.*, in *Nature.* (2015).
25. L. Bar-Peled, L. D. Schweitzer, R. Zoncu, D. M. Sabatini, Ragulator Is a GEF for the Rag GTPases that Signal Amino Acid Levels to mTORC1. *Cell* **150**, 1196-1208 (2012).
26. L. Bar-Peled *et al.*, A Tumor Suppressor Complex with GAP Activity for the Rag GTPases That Signal Amino Acid Sufficiency to mTORC1. *Science* **340**, 1100-1106 (2013).
27. Z.-Y. Tsun *et al.*, The Folliculin Tumor Suppressor Is a GAP for the RagC/D GTPases That Signal Amino Acid Levels to mTORC1. *Molecular cell* **52**, 495-505 (2013).
28. L. Chantranupong *et al.*, The Sestrins Interact with GATOR2 to Negatively Regulate the Amino-Acid-Sensing Pathway Upstream of mTORC1. *Cell Reports* **9**, 1-8 (2014).
29. A. Parmigiani *et al.*, Sestrins Inhibit mTORC1 Kinase Activation through the GATOR Complex. *Cell Reports* **9**, 1281-1291 (2014).
30. E. F. Blommaart, J. J. Luiken, P. J. Blommaart, G. M. van Woerkom, A. J. Meijer, Phosphorylation of ribosomal protein S6 is inhibitory for autophagy in isolated rat hepatocytes. *The Journal of biological chemistry* **270**, 2320-2326 (1995).
31. K. Hara *et al.*, Amino acid sufficiency and mTOR regulate p70 S6 kinase and eIF-4E BP1 through a common effector mechanism. *The Journal of biological chemistry* **273**, 14484-14494 (1998).
32. H. Peeters *et al.*, PA26 is a candidate gene for heterotaxia in humans: identification of a novel PA26-related gene family in human and mouse. *Human genetics* **112**, 573-580 (2003).
33. L. Buckbinder, R. Talbott, B. R. Seizinger, N. Kley, Gene regulation by temperature-sensitive p53 mutants: identification of p53 response genes.



- Proceedings of the National Academy of Sciences of the United States of America* **91**, 10640-10644 (1994).
34. A. V. Budanov *et al.*, Identification of a novel stress-responsive gene Hi95 involved in regulation of cell viability. *Oncogene* **21**, 6017-6031 (2002).
  35. T. Rogez-Florent *et al.*, in *J. Mol. Recognit.* (2014), vol. 27, pp. 46-56.
  36. X. Chen *et al.*, Modular pathways for editing non-cognate amino acids by human cytoplasmic leucyl-tRNA synthetase. *Nucleic acids research* **39**, 235-247 (2011).
  37. C. S. Katsanos, H. Kobayashi, M. Sheffield-Moore, A. Aarsland, R. R. Wolfe, A high proportion of leucine is required for optimal stimulation of the rate of muscle protein synthesis by essential amino acids in the elderly. *American journal of physiology. Endocrinology and metabolism* **291**, E381-387 (2006).
  38. M. N. Stanfel, L. S. Shamieh, M. Kaeberlein, B. K. Kennedy, The TOR pathway comes of age. *Biochimica et biophysica acta* **1790**, 1067-1074 (2009).
  39. J. Gallinetti, E. Harputlugil, J. R. Mitchell, Amino acid sensing in dietary-restriction-mediated longevity: roles of signal-transducing kinases GCN2 and TOR. *Biochemical Journal* **449**, 1-10 (2013).
  40. C. M. McCay, M. F. Crowell, L. A. Maynard, *The effect of retarded growth upon the length of life span and upon the ultimate body size. 1935.*, (1989), vol. 5, pp. 155-171; discussion 172.
  41. B. K. Kennedy, K. K. Steffen, M. Kaeberlein, Ruminations on dietary restriction and aging. *Cellular and molecular life sciences : CMLS* **64**, 1323-1328 (2007).
  42. D.-H. Kim *et al.*, mTOR Interacts with Raptor to Form a Nutrient-Sensitive Complex that Signals to the Cell Growth Machinery. *Cell* **110**, 163-175 (2002).
  43. O. Boussif *et al.*, A versatile vector for gene and oligonucleotide transfer into cells in culture and in vivo: polyethylenimine. *Proceedings of the National Academy of Sciences of the United States of America* **92**, 7297-7301 (1995).

## ACKNOWLEDGEMENTS

We thank all members of the Sabatini Lab for helpful insights, in particular Shuyu Wang for experimental advice; Olesya Levsh from the lab of Jing-Ke Weng for generously providing the control proteins used in the thermal shift assays; Navitor Pharmaceuticals for providing the His-MBP-TEV-Sestrin2 pMAL6H-C5XT plasmid; and Cell Signaling Technology (CST) for many antibodies. This work was supported by grants from the NIH (R01 CA103866 and AI47389) and Department of Defense (W81XWH-07-0448) to D.M.S., and fellowship support from the NIH to R.L.W. (T32 GM007753 and F30 CA189333) and L.C. (F31 CA180271) and from the Paul Gray UROP Fund to S.M.S. (3143900). K.S. is a Pfizer fellow of the Life Sciences Research Foundation. D.M.S. is an investigator of the Howard Hughes Medical Institute.

## **MATERIALS AND METHODS**

### **Materials**

Reagents were obtained from the following sources: HRP-labeled anti-mouse and anti-rabbit secondary antibodies from Santa Cruz Biotechnology; antibodies to phospho-T389 S6K1, S6K1, Sestrin2, Mios and the FLAG epitope from Cell Signaling Technology; antibodies to the HA epitope from Bethyl laboratories; antibody to raptor from Millipore. FLAG M2 affinity gel, ATP, and amino acids from Sigma Aldrich; RPMI without leucine, arginine, or lysine from Pierce; DMEM from SAFC Biosciences; XtremeGene9 and Complete Protease Cocktail from Roche; Inactivated Fetal Calf Serum (IFS) and SimplyBlue SafeStain from Invitrogen; amino acid-free RPMI from US Biologicals; [3H]-labelled amino acids from American Radiolabeled Chemicals. The WDR24, Mios, Sestrin1, and Sestrin3 antibodies were generously provided by Jianxin Xie of Cell Signaling Technology.

### **Cell lines and tissue culture**

HEK-293T cells were cultured in DMEM 10% IFS supplemented with 2 mM glutamine. All cell lines were maintained at 37°C and 5% CO<sub>2</sub>.

### **Cell lysis and immunoprecipitation**

Cells were rinsed one time with ice-cold PBS and immediately lysed with Triton lysis buffer (1% Triton, 10 mM  $\beta$ -glycerol phosphate, 10 mM pyrophosphate, 40 mM Hepes pH 7.4, 2.5 mM MgCl<sub>2</sub> and 1 tablet of EDTA-free protease inhibitor [Roche] (per 25 ml buffer). The cell lysates were cleared by centrifugation at 13,000 rpm at 4°C in a microcentrifuge for 10 minutes. For anti-FLAG-immunoprecipitations, the FLAG-M2 affinity gel was washed 3 times with lysis buffer. 30  $\mu$ l of a 50/50 slurry of the affinity gel was then added to clarified cell lysates and incubated with rotation for 2 hours at 4°C. Where indicated, leucine or arginine (500  $\mu$ M final) were added to lysates immediately

prior to addition of the Flag affinity gel. Following immunoprecipitation, the beads were washed one time with lysis buffer and 3 times with lysis buffer containing 500 mM NaCl. Immunoprecipitated proteins were denatured by the addition of 50  $\mu$ l of sample buffer and boiling for 5 minutes as described (42), resolved by 8%–16% SDS-PAGE, and analyzed by immunoblotting.

For co-transfection experiments in HEK-293T cells, 2 million cells were plated in 10 cm culture dishes. Twenty-four hours later, cells were transfected using the polyethylenimine method (43) with the pRK5-based cDNA expression plasmids indicated in the figures in the following amounts: 100 ng HA-WDR24 and 300 ng FLAG-Metap2, 25 ng FLAG-Sestrin2, or 50 ng FLAG-dSestrin (CG11299-PD); 100 ng FLAG-WDR24 and 15 ng each of HA-Sestrin2, HA-Sestrin2 S190W, HA-Sestrin2 L261A, or HA-Sestrin2 E451A. The total amount of plasmid DNA in each transfection was normalized to 5  $\mu$ g with empty pRK5. Thirty-six hours after transfection, cells were lysed as described above.

For experiments which required amino acid starvation or restimulation, cells were treated as previously described (27). Briefly, cells were incubated in amino acid free RPMI for 50 minutes and then restimulated with amino acids for 10 minutes. The same protocol was followed for both leucine and arginine single starvation and restimulations.

### **Purification of proteins expressed in bacteria**

Recombinant Sestrin2 was expressed in *Escherichia coli* (strain BL21 DE3 star) from the His-MBP-TEV-Sestrin2 in pMAL6H-C5XT plasmid. The bacterial cultures were grown at 30°C to an optical density of 0.4 at which point the temperature was lowered to 18°C. After 30 minutes at 18°C, the cultures were induced overnight at 18°C with 0.5 mM IPTG. The cells were subsequently resuspended in lysis buffer with TCEP (50 mM Tris pH 7.4, 200 mM NaCl, 5 mM MgCl<sub>2</sub>, 0.1% CHAPS, 1 mM TCEP, 200  $\mu$ M leucine, and protease inhibitor tablets), which was then supplemented with lysozyme and crude DNase. The cells underwent mechanical homogenization and the lysates were cleared by centrifugation and then loaded onto the Ni-NTA resin. After incubation, the resin was washed once with lysis buffer with TCEP, once with lysis buffer with TCEP + 300 mM

NaCl, and once with lysis buffer with TCEP + 25 mM imidazole. The proteins were eluted with lysis buffer with TCEP + 300 mM imidazole. The eluted proteins were concentrated and purified using size exclusion chromatography on a HiLoad 16/60 Superdex 200 column (GE Healthcare), which was equilibrated with the following buffer: 50 mM Tris pH 7.4, 150 mM NaCl, 5 mM MgCl<sub>2</sub>, 1 mM DTT, and 200 μM leucine. The collected protein was concentrated and immediately used in binding assays or frozen at - 80°C. Before use in any binding assays, the protein was diluted sufficiently to significantly decrease the leucine that may have remained bound through the purification steps. The control His-RagA/RagC heterodimer was purified through a similar protocol, using the Ni-NTA resin and subsequent size exclusion chromatography.

### **Purification of proteins expressed in human cells and the leucine binding assay**

4 million HEK-293T cells were plated in a 15 cm plate four days prior to the experiment. Each plate would yield the protein for one sample. Forty-eight hours after plating, the cells were transfected via the polyethylenimine method (43) with the pRK5-based cDNA expression plasmids indicated in the figures in the following amounts: 5 or 3 μg FLAG-Sestrin2; 12 μg FLAG-Rap2A; 5 μg WDR24-FLAG; 1 μg WDR24-FLAG with 4.75 μg each of Seh1L, Sec13, Mios, and WDR59; 12 μg FLAG-dSestrin (CG11299-PD); 12 μg FLAG-Sestrin1.1; 12 μg FLAG-Sestrin1.2; 12 μg FLAG-Sestrin3; 12 μg FLAG-Sestrin2 mutants (L261A, E451A, S190W) and up to 20 μg total DNA with empty-PRK5. Forty-eight hours after transfection cells were lysed as previously described. If multiple samples of the same type were represented in the experiment, the cell lysates were combined, mixed, and evenly distributed amongst the relevant tubes, to ensure equal protein amounts across samples of the same type.

Anti-FLAG immunoprecipitates were prepared as previously described, with the exception that prior to incubation with lysates, the beads were blocked by rotating in 1 μg/μl bovine serum albumin (BSA) for 20 minutes at 4°C and subsequently washed twice in lysis buffer. 30 μl of the 50/50 slurry of beads in lysis buffer was added to each of the clarified cell lysates and incubated as previously described.

For the binding assays, two tubes at a time were washed as previously indicated for immunoprecipitations. All the liquid was subsequently aspirated and a 15  $\mu$ l aliquot of proteins bound to the beads was incubated for one hour on ice in cytosolic buffer (0.1% Triton, 40 mM HEPES pH 7.4, 10 mM NaCl, 150 mM KCl, 2.5 mM MgCl<sub>2</sub>) with the appropriate amount of [3H]-labelled amino acids and cold amino acids. Tubes were flicked every five minutes. At the end of one hour, the beads were briefly spun down, aspirated dry, and rapidly washed three times with binding wash buffer (0.1% Triton, 40 mM HEPES pH 7.4, 150 mM NaCl). The beads were aspirated dry again and resuspended in 85  $\mu$ l of binding wash buffer. With a cut tip, each sample was mixed well and three 10  $\mu$ l aliquots were separately quantified using a TriCarb scintillation counter (PerkinElmer). This process was repeated in pairs for each sample, to ensure similar incubation and wash times for all samples analyzed across different experiments. For each sample, an immunoprecipitation was performed in parallel. After washing four times as previously described and once with CHAPS buffer (0.3% CHAPS, 40 mM HEPES pH 7.4), the protein was eluted in 250  $\mu$ l of CHAPS buffer with 300 mM NaCl and 1 mg/ml FLAG peptide for 1 hour at 4°C. The eluent was subsequently concentrated, quantified for protein amount using Bradford reagent, and resuspended in sample buffer. The proteins were resolved by 4-12% SDS-PAGE, and stained with SimplyBlue SafeStain.

For binding assays performed with bacterially-produced proteins, 23.6  $\mu$ g His-RagA/RagC, 23.6  $\mu$ g His-MBP-TEV-Sestrin2, or 73.6  $\mu$ g His-MBP-TEV-Sestrin2 were diluted into 500  $\mu$ l lysis buffer (50 mM Tris pH 7.4, 200 mM NaCl, 5 mM MgCl<sub>2</sub>, 0.1% CHAPS) and incubated with 15  $\mu$ l compact Ni-NTA resin as previously described. For the binding assays, two tubes were washed at a time. The Ni-NTA resin with proteins bound to it was washed one time with lysis buffer and three times with lysis buffer supplemented with 300 mM NaCl. After washing, the liquid was aspirated and the protein bound to the resin was incubated for one hour on ice with the appropriate amount of [3H]-labelled amino acids and, where indicated, cold amino acids. The tubes were flicked every five minutes. The samples were subsequently washed three times after binding with wash buffer (lysis buffer with 300 mM additional NaCl). The resin was aspirated dry and resuspended in 85  $\mu$ l of wash buffer. The samples were then well

mixed with a cut tip and 10  $\mu$ l of each was loaded into scintillation fluid in triplicate and quantified with a TriCarb Scintillation Counter. Samples performed in parallel were eluted with lysis buffer + 300 mM imidazole and analyzed by SDS-PAGE as described above.

### **Kd/Ki calculations**

Amino acid affinities to Sestrin2 were determined by first normalizing the bound [<sup>3</sup>H]-labeled amino acid concentrations across three separate binding assays performed with varying amounts of cold amino acid competition. These values were plotted and fit to a hyperbolic equation (Cheng-Prusoff equation) to estimate the IC<sub>50</sub> value. *K<sub>d</sub>* or *K<sub>i</sub>* values were derived from the IC<sub>50</sub> value using the equation:  $K_d \text{ or } K_i = IC_{50} / (1 + ([^3H]Leucine)/K_d)$ .

### ***In vitro* Sestrin2-GATOR2 dissociation assay**

HEK-293T cells stably expressing FLAG-WDR24 were starved for all amino acids for 50 minutes, lysed and subjected to anti-FLAG immunoprecipitation as described previously. The GATOR2-Sestrin2 complexes immobilized on the agarose beads were washed twice in lysis buffer with 500 mM NaCl, as previously described, and then incubated for 10 minutes in 1 mL of cytosolic buffer with the indicated concentrations of individual amino acids. The amount of GATOR2 and Sestrin2 that remained bound was assayed by SDS-PAGE and immunoblotting as described previously.

### **Thermal shift assay**

The thermal shift (protein melting) assays were performed according to the LightCycler 480 instruction manual. Briefly, for Sestrin2, 5X Sypro orange dye and Sestrin2 at 4  $\mu$ M were combined with or without leucine or arginine (at the indicated concentrations) in thermal shift buffer (100 mM Tris pH 7.4, 100 mM NaCl, and 1 mM DTT) in a volume of up to 10  $\mu$ l in one well of a LightCycler Multiwell 384-well plate. 20X

Sypro orange dye was used for the two control proteins, human choline acetyltransferase (ChAT) (at 4  $\mu$ M) or *Physconitrella patens* hydroxycinnamoyl transferase (PpHCT) (at 2.5  $\mu$ M). Each condition was tested in triplicate. The plate was subjected to a protocol in which the temperature increased from 20° to 85°C at 0.06°C/second. Fluorescence was recorded and plotted over time, and melting temperatures were calculated as described in the LightCycler 480 instruction manual. Briefly, the negative first derivative of the curve shown (change in fluorescence/change in temperature) was plotted against the temperature. The peak (i.e., lowest point on this curve) reflects the melting temperature. Each reported melting temperature is the mean  $\pm$  SD for three replicates from one experiment.

### **Generation of CRISPR/Cas9 genetically modified cells**

To generate HEK-293T cells with loss of all three Sestrins, the following sense (S) and antisense (AS) oligonucleotides encoding the guide RNAs were cloned into the pX330 vector.

sgSesn2\_S: caccgGACTACCTGCGGTTGCCCC  
sgSesn2\_AS: aaacGGGCGAACCGCAGGTAGTCC  
sgSesn3\_1S: caccgCAGCCACGATGAACCGGGG  
sgSesn3\_1AS: aaacCCCCGGTTCATCGTGGCTGc  
sgSesn1\_1S: caccgTGCATGTACCAATTCCGCAA  
sgSesn1\_1AS: aaacTTGCGGAATTGGTACATGCAc

On day one, 200,000 cells were seeded into 6 wells of a 6-well plate. Twenty-four hours post seeding, each well was transfected with 250 ng shGFP pLKO, 1  $\mu$ g of the pX330 guide construct, and 500 ng of empty pRK5 using XtremeGene9. The following day, cells were trypsinized, pooled in a 10 cm dish, and selected with puromycin to eliminate untransfected cells. Forty-eight hours after selection, the media was aspirated and replenished with fresh media lacking puromycin. The following day, cells were single cell sorted with a flow cytometer into the wells of a 96-well plate containing 150  $\mu$ l of DMEM supplemented with 30% IFS. Cells were grown for two weeks and the

resultant colonies were trypsinized and expanded. Clones were validated for loss of the relevant protein via immunoblotting.

To create the Sestrin1-3 triple null cells, Sestrin1 null cells were generated first. The same method was repeated in the Sestrin1 null cells with Sestrin2 guides and Sestrin1-2 double null cells were produced. The method was repeated for a third time with the Sestrin1-2 double null cells and a guide RNA targeting Sestrin3 to create the Sestrin1-3 triple null cells.

### **pS2 plasmid**

To produce the pS2 plasmid the 1500 base pairs upstream of the human Sestrin2 gene start site was amplified using the following primers and subsequently subcloned into the pLJC5 lentiviral vector in place of the UbC promoter.

S2\_promoter\_F: CCACCGGT TAGGTAGAATGTGATACATGTGAAAAG

S2\_promoter\_R:GCGT GTCGACGCACCACCACCACCACCCTTGTGCATCGTCA  
TCCTTGTAGTCCATGGTGGCGGTGCGCGCCAGGACCCGGTCGCGG

### **Lentivirus production and lentiviral transduction**

Lentiviruses were produced by transfection of HEK-293T cells with either pLJC5-FLAG-metap2, pLJC5-FLAG-Sestrin2 (wild-type or mutant), or pS2-FLAG-Sestrin2 (wild-type or mutant) plasmids in combination with the VSV-G envelope and CMV  $\Delta$ VPR packaging plasmids. Twenty-four hours after transfection, the media was changed to DMEM with 20% IFS. Forty-eight hours after transfection, the virus-containing supernatant was collected from the cells and passed through a 0.45  $\mu$ m filter. Target cells were plated in 6-well plates containing DMEM 10% IFS with 8  $\mu$ g/mL polybrene and infected with virus containing media. Twenty-four hours later, the media was changed to fresh media containing puromycin for selection. To obtain the equal expression levels shown in Figure 4C the pS2 plasmid was used to express wild-type Sestrin2 and Sestrin2 L261A while the pLJC5 plasmid was used to express Sestrin2 E451A and metap2.



## **Immunofluorescence assays**

Immunofluorescence assays were performed as described in (21). Briefly, 400,000 HEK-293T cells were plated on fibronectin-coated glass coverslips in 6-well tissue culture plates. Twenty-four hours later, the slides were rinsed once with PBS and fixed with 4% paraformaldehyde in PBS for 15 min at room temperature. The slides were subsequently rinsed three times with PBS and cells were permeabilized with 0.05% Triton X-100 in PBS for 5 min. After rinsing three times with PBS, cells were incubated with primary antibody in Odyssey blocking buffer for 1 hr at room temperature, rinsed three times with PBS, and incubated with secondary antibodies produced in donkey (diluted 1:400 in Odyssey blocking buffer) for 45 minutes at room temperature in the dark and washed three times with PBS. Slides were mounted on glass coverslips using Vectashield (Vector Laboratories) and cells imaged on a spinning disk confocal system (Perkin Elmer).

## **Statistical analyses**

Two-tailed t tests were used for comparison between two groups. All comparisons were two-sided, and P values of less than 0.001 were considered to indicate statistical significance.

## CHAPTER 5

Reprinted from Nature:

### **KICSTOR recruits GATOR1 to the lysosome and is necessary for nutrients to regulate mTORC1**

**Rachel L. Wolfson<sup>1,2,3,4,\*</sup>, Lynne Chantranupong<sup>1,2,3,4,\*</sup>, Gregory A. Wyant<sup>1,2,3,4</sup>, Xin Gu<sup>1,2,3,4</sup>, Jose M. Orozco<sup>1,2,3,4</sup>, Kuang Shen<sup>1,2,3,4</sup>, Kendall J. Condon<sup>1,2,3,4</sup>, Sabrina Petri<sup>5</sup>, Jibril Kedir<sup>1,2,3,4</sup>, Sonia M. Scaria<sup>1,2,3,4</sup>, Monther Abu-Remaileh<sup>1,2,3,4</sup>, Wayne N. Frankel<sup>5</sup>, and David M. Sabatini<sup>1,2,3,4</sup>**

<sup>1</sup>Whitehead Institute for Biomedical Research and Massachusetts Institute of Technology, Department of Biology, 9 Cambridge Center, Cambridge, MA 02142, USA

<sup>2</sup>Howard Hughes Medical Institute, Department of Biology, Massachusetts Institute of Technology, Cambridge, MA 02139, USA

<sup>3</sup>Koch Institute for Integrative Cancer Research, 77 Massachusetts Avenue, Cambridge, MA 02139, USA

<sup>4</sup>Broad Institute of Harvard and Massachusetts Institute of Technology, 7 Cambridge Center, Cambridge MA 02142, USA

<sup>5</sup>Department of Genetics and Development and Institute for Genomic Medicine, Columbia University Medical Center, New York, NY 10032, USA

\*These authors contributed equally to this work

Correspondence should be addressed to D.M.S.

Tel: 617-258-6407; Fax: 617-452-3566; Email: [sabatini@wi.mit.edu](mailto:sabatini@wi.mit.edu)

**Experiments in Fig. 1a were performed by L.C.**

**Analysis in Fig. 1b was performed by R.L.W.**

**Experiments in Fig. 1c-e were performed by X.G.**

**Experiments in Fig. 1g-i were performed by R.L.W.**

**Experiments in Ext. Data Fig. 1a-b were performed by G.A.W and R.L.W.**

**Experiments in Ext. Data Fig 1c were performed by R.L.W.**

**Experiments in Ext. Data Fig. 1d,f were performed by X.G.**

**Experiments in Ext. Data Fig. 1e were performed by G.A.W.**

**Experiments in Ext. Data Fig. 1g,h were performed by L.C.**

**Experiments in Ext. Data Fig. 2 were performed by K.S.**

**Experiments in Ext. Data Fig. 3a were performed by L.C.**

**Experiments in Ext. Data Fig. 3b-f were performed by R.L.W.**

**Experiments in Ext. Data Fig. 4a-c were performed by R.L.W.**

**Experiments in Ext. Data Fig. 4d were performed by G.A.W.**

**Experiments in Fig. 2a were performed by J.M.O.**

**Experiments in Fig. 2b-c were performed by G.A.W.**

**Experiments in Fig. 2 d-f were performed by R.L.W., G.A.W., and S.P.**

Experiments in Ext. Data Fig. 5a-c,f,i were performed by L.C. with help from J.K. and S.M.S.

Experiments in Ext. Data Fig. 5d were performed by X.G.

Experiments in Ext. Data Fig. 5e,g,h,j were performed by R.L.W.

Experiments in Ext. Data Fig. 6a-c were performed by R.L.W., G.A.W., and S.P.

Experiments in Fig. 3a-b were performed by X.G.

Experiments in Fig. 3c were performed by R.L.W.

Experiments in Fig. 3d were performed by R.L.W. and L.C.

Experiments in Ext. Data Fig. 6 were performed by R.L.W.

Experiments in Fig. 4a,b,d were performed by R.L.W.

Experiments in Fig. 4c were performed by G.A.W.

Experiments in Ext. Data Fig. 8 were performed by R.L.W.

Experiments in Ext. Data Fig. 9a were performed by R.L.W.

Experiments in Ext. Data Fig. 9b-d were performed by L.C.

## **Abstract**

**The mechanistic target of rapamycin complex 1 kinase (mTORC1) is a central regulator of cell growth that responds to diverse environmental signals and is deregulated in many human diseases, including cancer and epilepsy<sup>1-3</sup>. Amino acids are a key input, and act through the Rag GTPases to promote the translocation of mTORC1 to the lysosomal surface, its site of activation<sup>4</sup>. Multiple protein complexes regulate the Rag GTPases in response to amino acids, including GATOR1, a GTPase activating protein for RagA, and GATOR2, a positive regulator of unknown molecular function. Here, we identify a four-membered protein complex (KICSTOR) composed of the KPTN, ITFG2, C12orf66, and SZT2 gene products as required for amino acid or glucose deprivation to inhibit mTORC1 in cultured cells. In mice lacking SZT2, mTORC1 signaling is increased in several tissues, including in neurons in the brain. KICSTOR localizes to lysosomes; binds to GATOR1 and recruits it, but not GATOR2, to the lysosomal surface; and is necessary for the interaction of GATOR1 with its substrates, the Rag GTPases, and with GATOR2. Interestingly, several KICSTOR components are mutated in neurological diseases associated with mutations that lead to hyperactive mTORC1 signaling<sup>5-10</sup>. Thus, KICSTOR is a lysosome-associated negative regulator of mTORC1 signaling that, like GATOR1, is mutated in human disease<sup>11,12</sup>.**

To search for GATOR1-interacting proteins that may have escaped prior identification, we used the CRISPR/Cas9 system to engineer the *DEPDC5* gene in HEK-293T cells to express a FLAG-tagged version of DEPDC5, a GATOR1 component, at endogenous levels. Mass spectrometric analysis of FLAG-immunoprecipitates prepared from these cells revealed the presence of GATOR2, as well as four proteins of unknown function encoded by the *KPTN*, *ITFG2*, *C12orf66*, and *SZT2* genes and of predicted molecular weights of 48, 49, 50, and 380 kDa, respectively (Fig. 1a). As shown below, these proteins form a complex, which we named KICSTOR for KPTN, ITFG2, C12orf66, and SZT2-containing regulator of mTORC1. KICSTOR components are conserved in vertebrates but not fungi (Fig. 1b). Some non-vertebrates, like *Caenorhabditis elegans*, encode homologues of *SZT2* but not of *KPTN*, *ITFG2*, or *C12orf66*, while others, including *Drosophila melanogaster*, lack all four KICSTOR components (Fig. 1b).

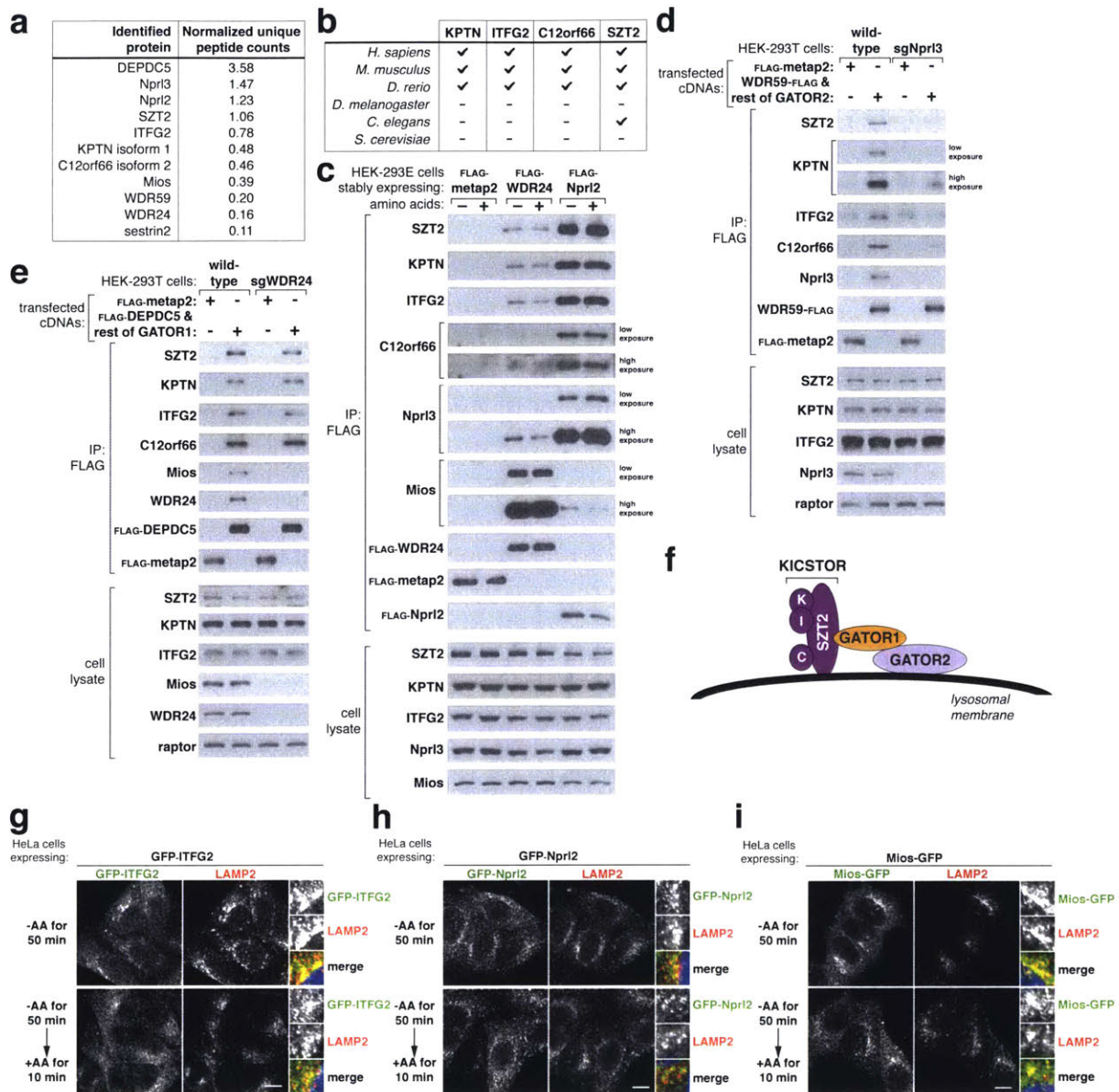


**Figure 1: The KICSTOR complex interacts with GATOR1 and localizes to lysosomes**

a) Mass spectrometric analyses identified KICSTOR-derived peptides in immunoprecipitates prepared from HEK-293T cells expressing endogenously FLAG-tagged DEPDC5.

b) Presence or absence of KICSTOR component gene orthologs in model organisms.

c) GATOR1 co-immunoprecipitates more KICSTOR than does GATOR2. Immunoprecipitates were prepared from HEK-293E cells stably expressing the indicated FLAG-tagged proteins and analyzed by immunoblotting for the indicated proteins.

- d) GATOR2 requires GATOR1 to associate with KICSTOR. Anti-FLAG immunoprecipitates were prepared from wild-type and Npr13-deficient HEK-293T cells transiently expressing the indicated cDNAs. Anti-FLAG immunoprecipitates and lysates were analyzed as in (c).
- e) GATOR1 does not require intact GATOR2 to interact with KICSTOR. Wild-type and WDR24-deficient HEK-293T cells transiently expressing the indicated cDNAs were treated and analyzed as in (c).
- f) Model proposing that the KICSTOR complex interacts with GATOR1, which in turn interacts with GATOR2. KPTN, ITFG2, and C12orf66 are indicated by the first letter of each.
- g) KICSTOR localizes to lysosomes in an amino acid independent fashion. Wild-type HeLa cells stably expressing GFP-ITFG2 were starved or starved and restimulated with amino acids for the indicated times prior to processing for immunofluorescence detection of GFP and LAMP2, a lysosomal marker. In all images, insets depict selected fields magnified 3.24X and their overlays. Scale bar represents 10  $\mu$ m.
- h) GATOR1 localizes to lysosomes regardless of amino acid levels. Npr12-deficient HeLa cells were reconstituted with GFP-Npr12 and treated and analyzed as in (g).
- i) GATOR2 localizes to lysosomes regardless of amino acid levels. Wild-type HeLa cells stably expressing Mios-GFP were treated and analyzed as in (g).

Endogenous KICSTOR was present in anti-FLAG immunoprecipitates prepared from cells expressing endogenously FLAG-tagged DEPDC5 or WDR59, a GATOR2 component (Extended Data Fig. 1a, b). Importantly, an anti-KPTN antibody co-immunoprecipitated SZT2, ITFG2, and C12orf66, as well as GATOR1 and GATOR2 components (Extended Data Fig. 1c). Amino acid starvation and stimulation of cells did not significantly affect the interactions between any complex components (Extended Data Fig. 1a, b, c). Thus, GATOR1 and GATOR2 associate with KICSTOR in an amino acid insensitive fashion.





**Extended Data Figure 1: GATOR1 and GATOR2 associate with endogenous KICSTOR components in an amino acid insensitive fashion**

a) An endogenously tagged GATOR1 component co-immunoprecipitates endogenous KICSTOR. Anti-FLAG immunoprecipitates were prepared from HEK-293T cells expressing endogenously FLAG-tagged DEPDC5, a GATOR1 component, that had been starved of amino acids for 50 min or starved and restimulated with amino acids for 10 min. Immunoprecipitates and cell lysates were analyzed by immunoblotting for the indicated proteins.

b) An endogenously tagged GATOR2 component co-immunoprecipitates endogenous GATOR1 and KICSTOR. Anti-FLAG immunoprecipitates were prepared from HEK-293T cells expressing endogenously FLAG-tagged WDR59, a GATOR2 component, and treated as in (a). Immunoprecipitates and cell lysates were analyzed by immunoblotting for the indicated proteins.

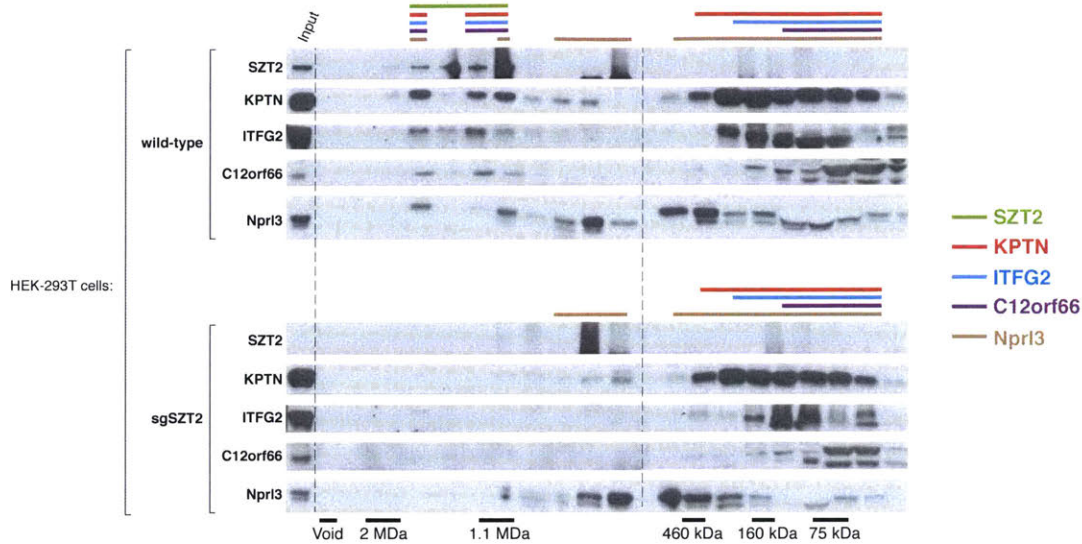
c) An anti-KPTN antibody co-immunoprecipitates endogenous components of KICSTOR, GATOR1, and GATOR2. Anti-KPTN immunoprecipitates were prepared from wild-type HEK-293T treated as in (a) and immunoprecipitates and cell lysates analyzed by immunoblotting for the indicated proteins. Anti-GSK3b immunoprecipitates were used to monitor the non-specific binding of proteins to the beads.

d) KPTN and ITFG2 form a heterodimer that requires SZT2 to associate with C12orf66. Anti-FLAG immunoprecipitates and lysates prepared from HEK-293T cells expressing the indicated cDNAs were analyzed by immunoblotting for the relevant epitope tags.

e) Loss of KICSTOR components did not have a significant effect on the expression levels of GATOR1 or GATOR2 components. HEK-293T cell clones deficient for indicated KICSTOR components or Npr13 or WDR24 were generated via the CRISPR/Cas9 system and single cell cloning. Cell lysates were analyzed by immunoblotting for the indicated proteins. DNA sequencing of the *C12orf66* gene was used to verify out of frame mutations in the genomic locus of the sgC12orf66 cells because an antibody that detects the C12orf66 protein in cell lysates is not available. The HEK-293T cell clones analyzed here were used in subsequent figures, where indicated.

- f) KPTN interacts with ITFG2 even in cells lacking other KICSTOR components. Immunoprecipitates and cell lysates prepared from wild-type, SZT2-deficient, or C12orf66-deficient HEK-293T cell clones expressing the indicated proteins were analyzed by immunoblotting.
- g) Expression levels of KPTN and ITFG2 in HEK-293T cells stably expressing the indicated sgRNAs under amino acid starved or replete conditions. Cell lysates were analyzed by immunoblotting for the levels of the indicated proteins. Raptor serves as a loading control. These same cell lines were also analyzed for phospho-S6K1 and S6K1 levels in Extended Data Fig. 5a-c.
- h) KPTN-ITFG2 does not compete with C12orf66 for associating with SZT2. HEK-293T cells expressing the indicated cDNAs were treated and analyzed as in (d).

Using HEK-293T cells transiently expressing recombinant versions of the KICSTOR components, we explored how they interact with each other. KPTN and ITFG2 associated even in the absence of the co-expression of either C12orf66 or SZT2 (Extended Data Fig. 1d), suggesting that they form a heterodimer on their own. Indeed, KPTN and ITFG2 associated in cells deficient for SZT2 or C12orf66, and loss of ITFG2 severely reduced KPTN levels and vice versa (Extended Data Fig. 1e, f, g). The KPTN-ITFG2 heterodimer co-immunoprecipitated C12orf66 only when SZT2 was also expressed and did not compete with C12orf66 for interacting with SZT2 (Extended Data Fig. 1d, h). In size-exclusion chromatography analyses of cell lysates, C12orf66, KPTN, and ITFG2 fractionated into two main pools, one that co-migrated at a very high molecular weight with SZT2 and was absent in SZT2-deficient cells, and a more abundant pool that migrated at lower molecular weights (Extended Data Fig. 2). Collectively, these results suggest that the four KICSTOR proteins form a large complex in which SZT2 serves as the link between the other three.

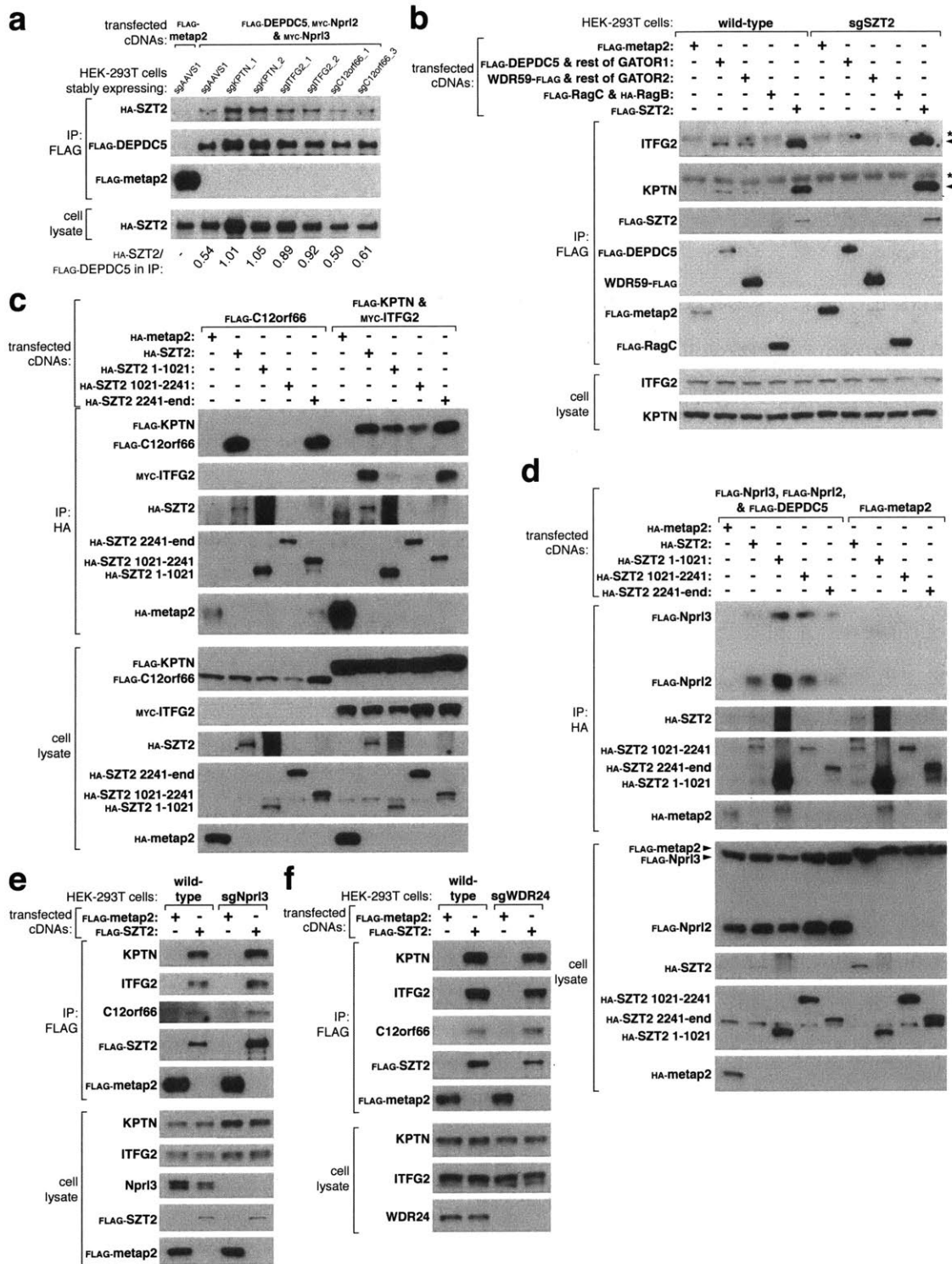


## Extended Data Figure 2: Size exclusion chromatography analysis of KICSTOR components

Lysates of wild-type or SZT2-deficient (sgSZT2) HEK-293T cells were fractionated with tandem Superose 6 size exclusion chromatography columns and the collected fractions analyzed by immunoblotting for the indicated proteins. Colored bars indicate fractions that contain the protein denoted by that color in the key. Fractions containing the molecular weight standards are indicated. Note that the C12orf66 antibody exhibits significant background when used to probe total cell lysates by immunoblotting so we are only confident that the bands in the high molecular weight fractions that disappear in the SZT2-deficient cells actually represent C12orf66.

We readily detected endogenous KICSTOR in anti-FLAG immunoprecipitates from HEK-293E cells stably expressing FLAG-tagged Npr12, a GATOR1 component, but FLAG-tagged WDR24, a GATOR2 component, co-immunoprecipitated much lower amounts of KICSTOR (Fig. 1c). Consistent with the GATOR2-KICSTOR association being indirect, loss of GATOR1 strongly reduced it (Fig. 1d), while that of GATOR2 did not significantly affect the GATOR1-KICSTOR interaction (Fig. 1e). SZT2 co-immunoprecipitated with GATOR1 even in cells lacking other KICSTOR components (Extended Data Fig. 3a) and was required for GATOR1 or GATOR2 to co-immunoprecipitate the KPTN-ITFG2 heterodimer (Extended Data Fig. 3b). Moreover,

KPTN-ITFG2, C12orf66, and GATOR1 co-immunoprecipitated three fragments of the 380 kDa SZT2 to different extents and the integrity of KICSTOR did not depend on either GATOR complex (Extended Data Fig. 3c, d, e, f). Altogether, these results suggest that KICSTOR is a distinct four-protein complex that uses its SZT2 component to interact with GATOR1, which in turn binds to GATOR2 (Fig. 1f). Consistent with this model, the very high molecular weight pool of Npr13 detected by size-exclusion chromatography was absent in SZT2-deficient cells (Extended Data Fig. 2).



**Extended Data Figure 3: SZT2 interacts with KPTN-ITFG2, C12orf66, and GATOR1**

a) SZT2 interacts with GATOR1 in the absence of other KICSTOR components. HEK-293T cells stably expressing a control sgRNA (sgAAVS1) or sgRNAs targeting the

indicated KICSTOR components were transfected with the indicated cDNAs. Anti-FLAG immunoprecipitates were prepared and analyzed, along with cell lysates, by immunoblotting for the relevant epitope tags. The ratios of the intensities of the HA-SZT2 to FLAG-DEPDC5 bands are indicated below the FLAG-DEPDC5 blot. See Extended Data Fig. 1g for the expression levels of the KICSTOR components in the cell lines used here.

b) SZT2 links the other KICSTOR components to the GATOR complexes. Anti-FLAG immunoprecipitates prepared from wild-type or SZT2-deficient HEK-293T cells expressing the indicated cDNAs were analyzed by immunoblotting for the indicated proteins. \* marks non-specific bands. See Extended Data Fig. 1e for the expression level of SZT2 in the SZT2-deficient HEK-293T cells.

c) C12orf66 interacts with SZT2 at a distinct site than KPTN-ITFG2. HEK-293T cells expressing the indicated cDNAs were analyzed as in (b).

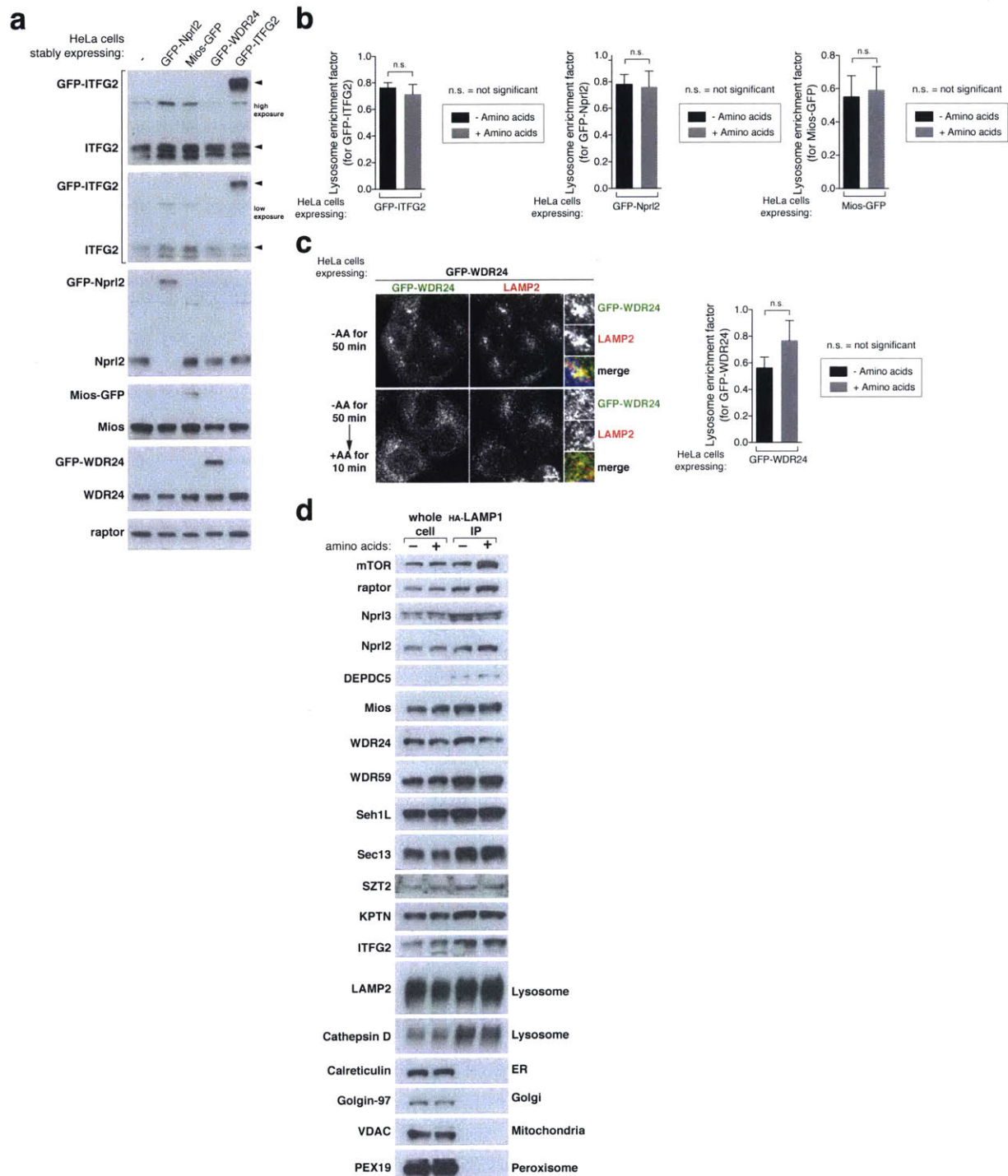
d) GATOR1 interacts with the first and second regions of SZT2. HEK-293T cells expressing the indicated cDNAs were analyzed as in (b).

e) The association of SZT2 with KPTN-ITFG2 persists in the absence of GATOR1 or (f) GATOR2. Anti-FLAG immunoprecipitates were prepared from wild-type, Nprl3-deficient, or WDR24-deficient HEK-293T cells expressing the indicated cDNAs and analyzed as in (b).

Because much of the nutrient sensing machinery upstream of mTORC1, including the Rag GTPases, localizes to the lysosomal surface<sup>4,13</sup>, we asked if KICSTOR is also there. Indeed, examination of HeLa cells expressing GFP-tagged ITFG2 (as a marker of KICSTOR) at levels 2-3 fold above the endogenous protein, revealed that KICSTOR localizes, at least in part, to lysosomes in an amino acid-insensitive fashion (Fig. 1g, and Extended Data Fig. 4a, b). The GATOR complexes have been reported to localize to the lysosome<sup>14-17</sup>, which we confirmed in HeLa cells stably expressing GFP-tagged components of GATOR1 (Nprl2) or GATOR2 (Mios and WDR24) (Fig. 1h, i and Extended Data Fig. 4a, b, c). Consistent with these results, amino acids did not affect the amounts of endogenous GATOR1, GATOR2, or KICSTOR present on immunopurified lysosomes, but, as expected, did regulate that of



mTORC1 (Extended Data Fig. 4d). The lysosomes were not contaminated with mitochondria, Golgi, ER, or peroxisomes (Extended Data Fig. 4d).



**Extended Data Figure 4: Subcellular localization of the GATOR and KICSTOR complexes**

- a) Expression levels of GFP-tagged GATOR1, GATOR2, or KICSTOR components used in the localization experiments. Npr12-deficient or wild-type HeLa cells stably expressing the indicating GFP-tagged proteins were single cell sorted for the low GFP population and single cell clones were analyzed by immunoblotting for levels of the indicated proteins.
- b) Quantitation of the imaging data in Figures 1g, h, i. Values are mean  $\pm$  standard error.
- c) Amino acids do not control the localization of GATOR2 to the lysosomal surface. Wild-type HeLa cells stably expressing GFP-tagged WDR24, a component of GATOR2, were starved or starved and restimulated with amino acids for the indicated times prior to processing for immunofluorescence detection of GFP and LAMP2. Scale bars represent 10  $\mu$ m. Quantitation of the imaging data is shown in the bar graph on the right.
- d) Amino acids do not regulate the amounts of GATOR1, GATOR2, or KICSTOR components on purified lysosomes. Lysosomes immunopurified with anti-HA beads from wild-type HEK-293T cells expressing HA-tagged LAMP1 and treated as in (c) were analyzed by immunoblotting for the levels of the indicated proteins.

Given the strong interaction between KICSTOR and GATOR1, an inhibitor of the Rag GTPases, we reasoned that KICSTOR might be required for the control of the mTORC1 pathway by amino acids. Indeed, in HEK-293T cells lacking any KICSTOR subunit, amino acid deprivation did not inhibit mTORC1 signaling, as detected by the phosphorylation of S6K1, 4E-BP1, and ULK1, or induce autophagy (Fig. 2a, b and Extended Data Fig. 1e and 5a, b, c). In HeLa cells loss of either SZT2 or ITFG2 had similar effects on S6K1 phosphorylation (Extended Data Fig. 5d, e, f). Although less is known about how glucose is sensed upstream of the Rag GTPases<sup>18,19</sup>, loss of any KICSTOR component in HEK-293T cells also rendered mTORC1 signaling insensitive to glucose starvation (Fig. 2c). Glucose did not affect the lysosomal localization of GATOR1 and serum deprivation and insulin stimulation still regulated mTORC1 in HeLa cells lacking KICSTOR components (Extended Data Fig. 5g, h, i, j).



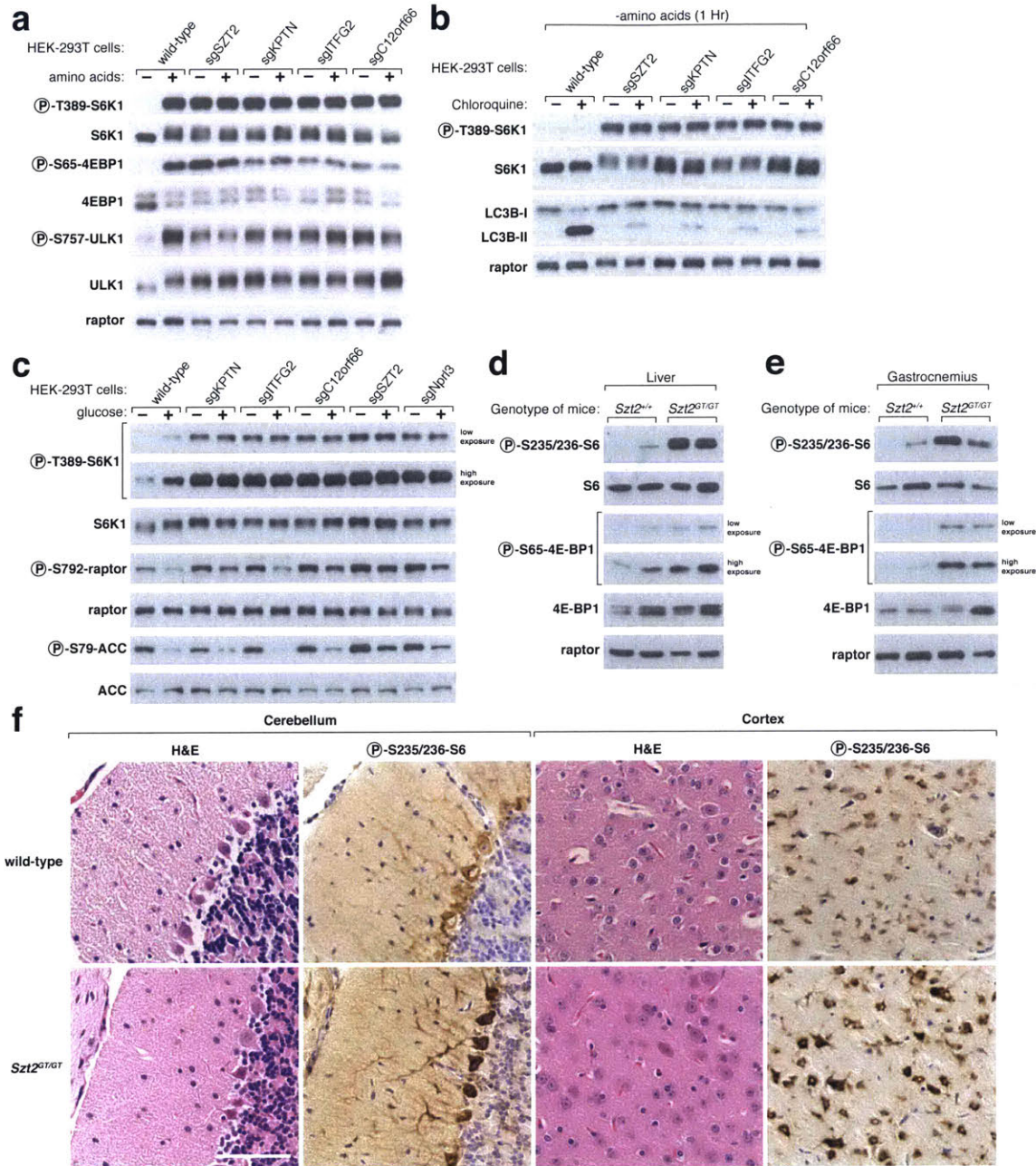
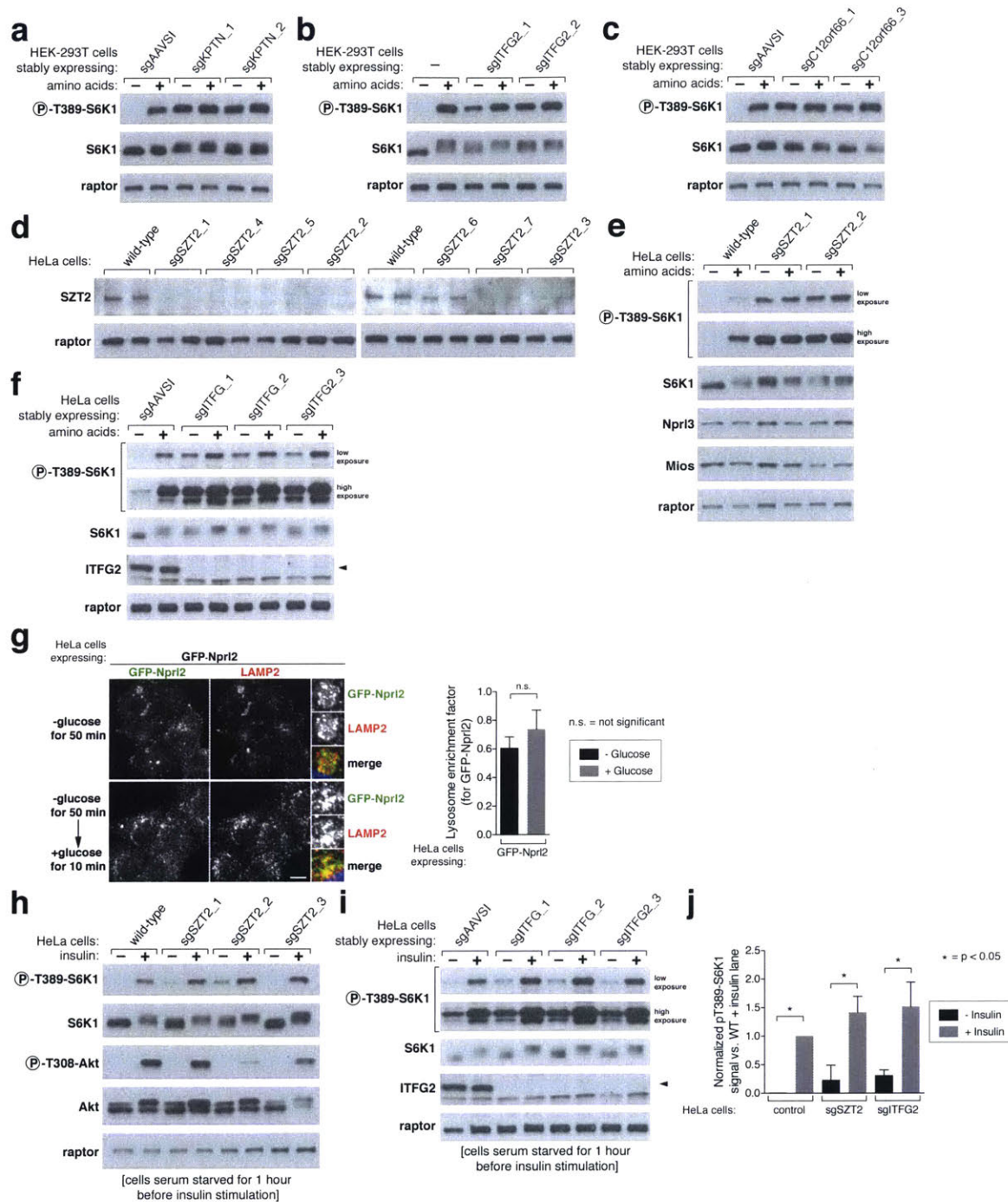


**Figure 2: Regulation of mTORC1 signaling by nutrients requires KICSTOR**

a) mTORC1 signaling is insensitive to amino acid starvation in cells lacking any KICSTOR component. HEK-293T cell clones deficient for each KICSTOR component were starved of amino acids for 50 min or starved and restimulated with amino acids for 10 min. Cell lysates were analyzed by immunoblotting for the levels and phosphorylation states of the indicated proteins. See Extended Data Fig. 1e for validation of the KICSTOR deficient cells.

- b) Activation of autophagy induced by amino acid starvation requires KICSTOR. The HEK-293T cell clones as in (a) were monitored for LC3B processing and accumulation after one hour of amino acid starvation in the absence or presence of chloroquine.
- c) mTORC1 signaling is insensitive to glucose starvation in cells lacking KICSTOR. Experiment was performed as in (a) except that cells were starved of and stimulated with glucose.
- d) SZT2 inhibits mTORC1 signaling in mouse liver. Mice with the indicated genotypes were fasted for 8 hours and liver lysates analyzed by immunoblotting for the levels and phosphorylation states of the indicated proteins. Two wild-type and two *Szt2*<sup>GT/GT</sup> mice were analyzed in this experiment and in (e).
- e) SZT2 inhibits mTORC1 signaling in the mouse gastrocnemius muscle. Mice were treated and muscle lysates analyzed as in (d).
- f) SZT2 inhibits mTORC1 signaling in mouse neurons *in vivo*. Brain sections prepared from mice treated as in (d) were analyzed by immunohistochemistry for phospho-S235/236 S6 levels and stained with hematoxylin and eosin (H&E). Equivalent regions of the cortex and cerebellum are shown for the two genotypes. Scale bar represents 40  $\mu\text{m}$ .



## Extended Data Figure 5: KICSTOR loss affects the sensitivity of the mTORC1 pathway to nutrients but not growth factors

a) CRISPR/Cas9-mediated depletion of KPTN, (b) ITFG2, or (c) C12orf66 renders mTORC1 signaling insensitive to amino acid deprivation. HEK-293T cells stably expressing the indicated sgRNAs were starved of amino acids for 50 min or starved and

restimulated with amino acids for 10 min. Cell lysates were analyzed by immunoblotting for the levels and phosphorylation states of the indicated proteins. See Extended Data Fig. 1g for the expression levels of the KICSTOR components in the cell lines used here.

d) Testing of indicated SZT2 sgRNA-treated HeLa cell clones for levels of SZT2 and raptor by immunoblotting. Note that not all clones have complete loss of the SZT2 protein.

e) mTORC1 signaling in SZT2-deficient cells is insensitive to amino acid deprivation. Indicated HeLa cell SZT2-deficient clones from (d) were treated and analyzed as in (a).

f) CRISPR/Cas9-mediated depletion of ITFG2 renders mTORC1 signaling partially insensitive to amino acid deprivation. HeLa cells stably expressing the indicated ITFG2 sgRNAs were treated and analyzed as in (a).

g) Glucose levels do not affect GATOR1 localization, as monitored by GFP-Nprl2. HeLa cells expressing GFP-Nprl2 from Figure 1h were starved of glucose for 50 min or starved and restimulated with glucose for 10 min prior to processing for immunofluorescence for GFP and LAMP2 (left). Scale bars represent 10  $\mu$ m. Quantitation of the imaging data is shown in bar graph on the right.

h) In SZT2-deficient cells mTORC1 signaling is still sensitive to serum starvation and insulin stimulation. Indicated HeLa cell SZT2-deficient clones from (d) were starved of serum for 50 min or starved of serum and restimulated with insulin for 10 min. Cell lysates were analyzed by immunoblotting for the levels and phosphorylation states of the indicated proteins.

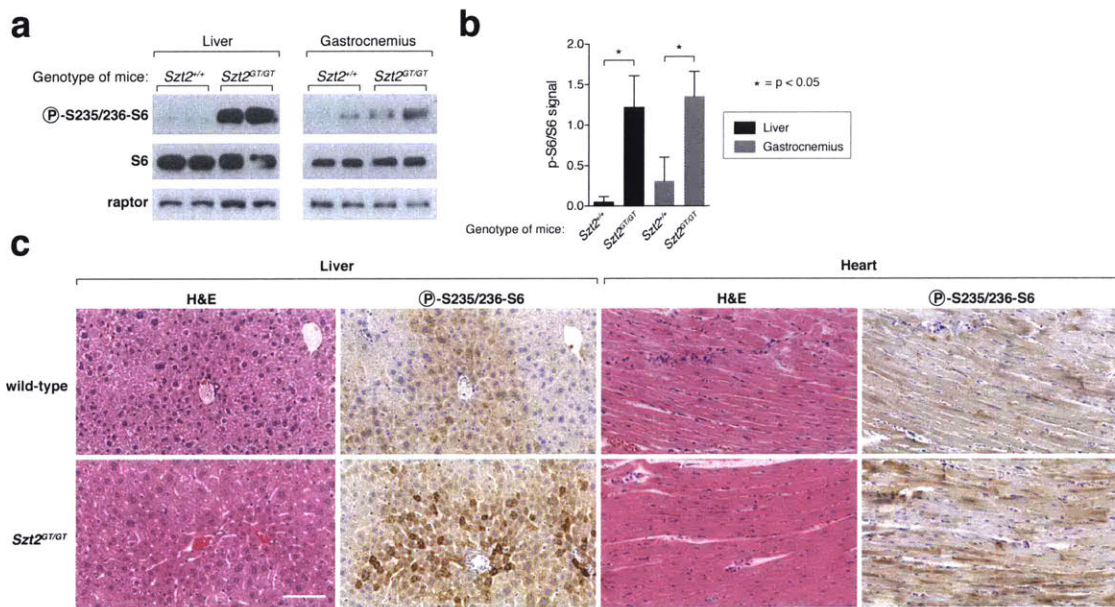
i) In cells with CRISPR/Cas9-mediated depletion of ITFG2, mTORC1 signaling is still sensitive to serum starvation and insulin stimulation. HeLa cells stably expressing the indicated ITFG2 sgRNAs were treated and analyzed as in (h).

j) Quantitation of phospho-S6K1 blots in (h) and (i). Values are mean  $\pm$  standard deviation.

To determine if KICSTOR also inhibits mTORC1 signaling *in vivo* we analyzed previously generated mice in which the *Szt2* gene was disrupted by a gene trap (*Szt2*<sup>GT/GT</sup>)<sup>20</sup>. Compared to wild-type littermates, mTORC1 signaling was increased in



the liver and skeletal muscle of fasted *Szt2* gene trap mice as assessed by the phosphorylation of S6, a substrate of S6K1, and of 4E-BP1 (Fig. 2d, e and Extended Data Fig. 6a, b). Immunohistochemical detection of phospho-S6 in tissue slices from the brain as well as liver and heart revealed increases in mTORC1 signaling in cerebellar and cortical neurons and hepatocytes and cardiomyocytes of the *Szt2<sup>GT/GT</sup>* mice (Fig. 2f and Extended Data Fig. 6c). Thus, loss of the SZT2 component of KICSTOR increases mTORC1 signaling in multiple mouse tissues *in vivo*.



### Extended Data Figure 6: Activation of mTORC1 signaling in tissues from *Szt2<sup>GT/GT</sup>* mice

- a) SZT2 inhibits mTORC1 signaling in mouse liver and muscle. Mice with the indicated genotypes were treated and analyzed by immunoblotting for the levels and phosphorylation state of S6 as in Figure 2d. The animals examined here represent an additional two animals of each genotype beyond those analyzed in Figures 2d, e.
- b) Quantitation of the ratio of phospho-S6 to S6 bands in (a) and in Figures 2d, e. Values are mean  $\pm$  standard deviation for n=4.
- c) SZT2 inhibits mTORC1 signaling in hepatocytes and cardiomyocytes *in vivo*. Liver and heart sections prepared from mice treated as in Figure 2d were analyzed by immunohistochemistry for phospho-S235/236 S6 levels and serial sections were stained

with hematoxylin and eosin (H&E). Liver image is centered over a central vein. Scale bar represents 40  $\mu\text{m}$ .

To define where KICSTOR acts in the mTORC1 pathway, we performed epistasis experiments between KICSTOR and established components of the pathway. Expression of the dominant negative Rag GTPases (RagB<sup>T54N</sup>-RagC<sup>Q120L</sup>) still inhibited mTORC1 in SZT2-deficient cells, indicating that KICSTOR is upstream of the Rag GTPases (Fig. 3a). While great overexpression of GATOR1 suppressed mTORC1 signaling in both wild-type and SZT2-deficient cells (Fig. 3a), much lower levels of GATOR1 overexpression reduced mTORC1 signaling to a lesser extent in the SZT2-deficient than wild-type cells, suggesting that GATOR1 requires SZT2 to efficiently exert its inhibitory effects (Fig. 3b). Loss of GATOR2 strongly inhibited mTORC1 signaling in wild-type cells, but did not affect the constitutive signaling of cells deficient for SZT2 (Fig. 3c) or Nprl3 (Extended Data Fig. 7a). Thus, KICSTOR, likely acting in concert with GATOR1, functions downstream of or in parallel to GATOR2 to negatively regulate Rag GTPase signaling to mTORC1. Consistent with this interpretation, loss of KICSTOR, like that of GATOR1<sup>17</sup>, was sufficient to drive mTORC1 to the lysosomal surface in cells starved of amino acids (Fig. 3d and Extended Data Fig. 7b).

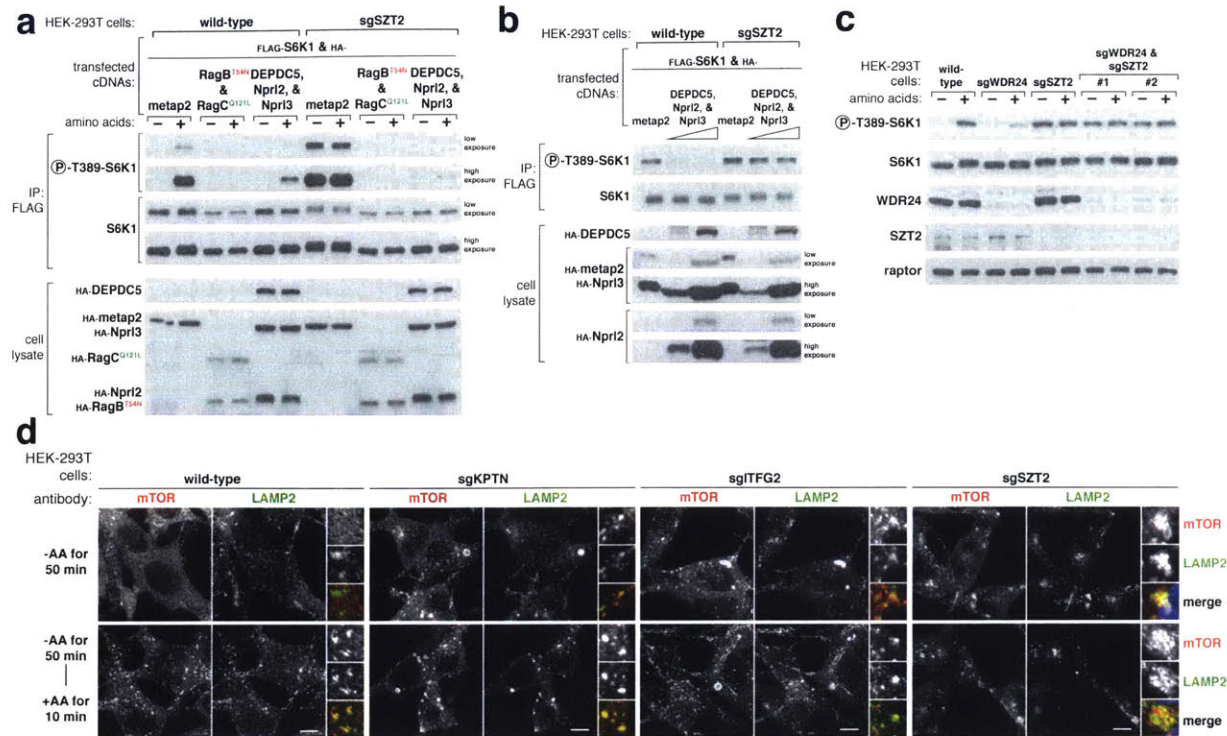


**Figure 3: KICSTOR acts upstream of the Rag GTPases**

a) KICSTOR functions upstream of the Rag GTPases. Wild-type or SZT2-deficient HEK-293Ts expressing the indicated cDNAs were starved of amino acids for 50 min or starved and restimulated with amino acids for 10 min. FLAG immunoprecipitates and cell lysates were analyzed by immunoblotting for the levels and phosphorylation states of the indicated proteins.

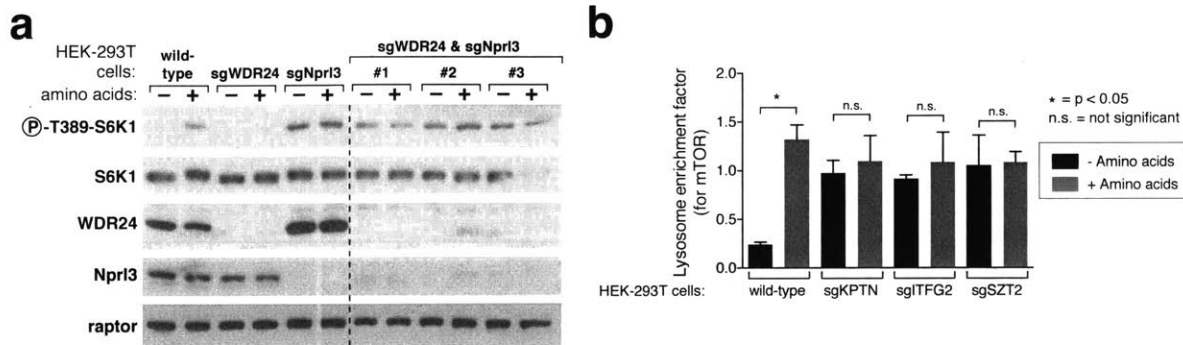
b) Modest GATOR1 overexpression inhibits mTORC1 signaling to a lesser extent in SZT2-deficient than in wild-type cells. FLAG immunoprecipitates and cell lysates prepared from cells expressing the indicated cDNAs and in amino acid replete conditions were analyzed as in (a). In this experiment 0.5 and 2.0 ng of the cDNA for each GATOR1 component was transfected while 100 ng of each was used in (a).

c) KICSTOR functions downstream of or in parallel to GATOR2. Wild-type, SZT2-deficient, or double SZT2- and WDR24-deficient HEK-293Ts were treated and analyzed as in (a).

d) Amino acid insensitive localization of mTOR to lysosomes in cells lacking KICSTOR components. Wild-type and KPTN-, ITFG2-, or SZT2-deficient HEK-293T cells were starved or starved and restimulated with amino acids for the indicated times prior to



processing for immunofluorescence detection of mTOR and LAMP2. In all images, insets depict selected fields magnified 3.24X and their overlays. Scale bars represent 10  $\mu\text{m}$ .



### Extended Data Figure 7: GATOR1, like KICSTOR, functions downstream of or parallel to GATOR2 in the mTORC1 pathway

a) GATOR1, like KICSTOR, is epistatic to GATOR2. Wild-type, WDR24-deficient, or Npr13- and WDR24-deficient HEK-293Ts were starved of amino acids for 50 min or starved and restimulated with amino acids for 10 min. Cell lysates were analyzed by immunoblotting for the indicated proteins and phosphorylation states.

b) Quantitation of the imaging data in Figure 3d. Values are mean  $\pm$  standard error.

While Ragulator tethers the Rags to the lysosomal surface<sup>13</sup>, it is unknown what recruits GATOR1 there and so we considered such a role for KICSTOR. This was the case as in cells deficient for KICSTOR, GATOR1 no longer localized to lysosomes and instead was dispersed throughout the cytoplasm (Fig. 4a, b, and Extended Data Fig. 8a). In contrast, loss of KICSTOR had little effect on the lysosomal localization of GATOR2 or the Rag GTPases (Extended Data Fig. 8b, c). In agreement with the imaging results, loss of SZT2 very strongly decreased the amount of GATOR1, but not GATOR2, on purified lysosomes (Fig. 4c). Consistent with the amino acid-insensitive lysosomal localization of mTOR in cells deficient for SZT2 (Fig. 3d), amino acid starvation did not reduce the amount of mTORC1 on lysosomes isolated from these cells (Fig. 4c). Given the importance of KICSTOR for localizing GATOR1 to lysosomes,



we reasoned that KICSTOR should be necessary for GATOR1 to interact with its substrates the Rag GTPases, as well as with GATOR2. Indeed, loss of SZT2 strongly reduced the amounts of RagA and RagC and GATOR2 that co-immunoprecipitated with GATOR1 (Fig. 4d and Extended Data Fig. 9a, b, c, d). As previously reported<sup>17</sup>, amino acid stimulation reduced the interaction of GATOR1 with the Rag GTPases in wild-type cells (Fig. 4d). Thus, KICSTOR has at least two molecular functions that can explain its loss of function phenotype: KICSTOR targets GATOR1 to the lysosomal surface where its substrates, the Rag GTPases, and its potential regulator, GATOR2, reside (Fig. 4e). KICSTOR is a large complex so it likely has additional roles in mTORC1 signaling beyond those we have defined, but the protein sequences of its components do not suggest any biochemical functions. It was not possible to ascertain if tethering of GATOR1 to the lysosomal surface bypasses the need for KICSTOR for the control of mTORC1 signaling by nutrients because the addition to any GATOR1 component, on its N- or C-terminus, of the lysosomal targeting sequence of LAMTOR1 prevented formation of GATOR1 or its interaction with GATOR2.

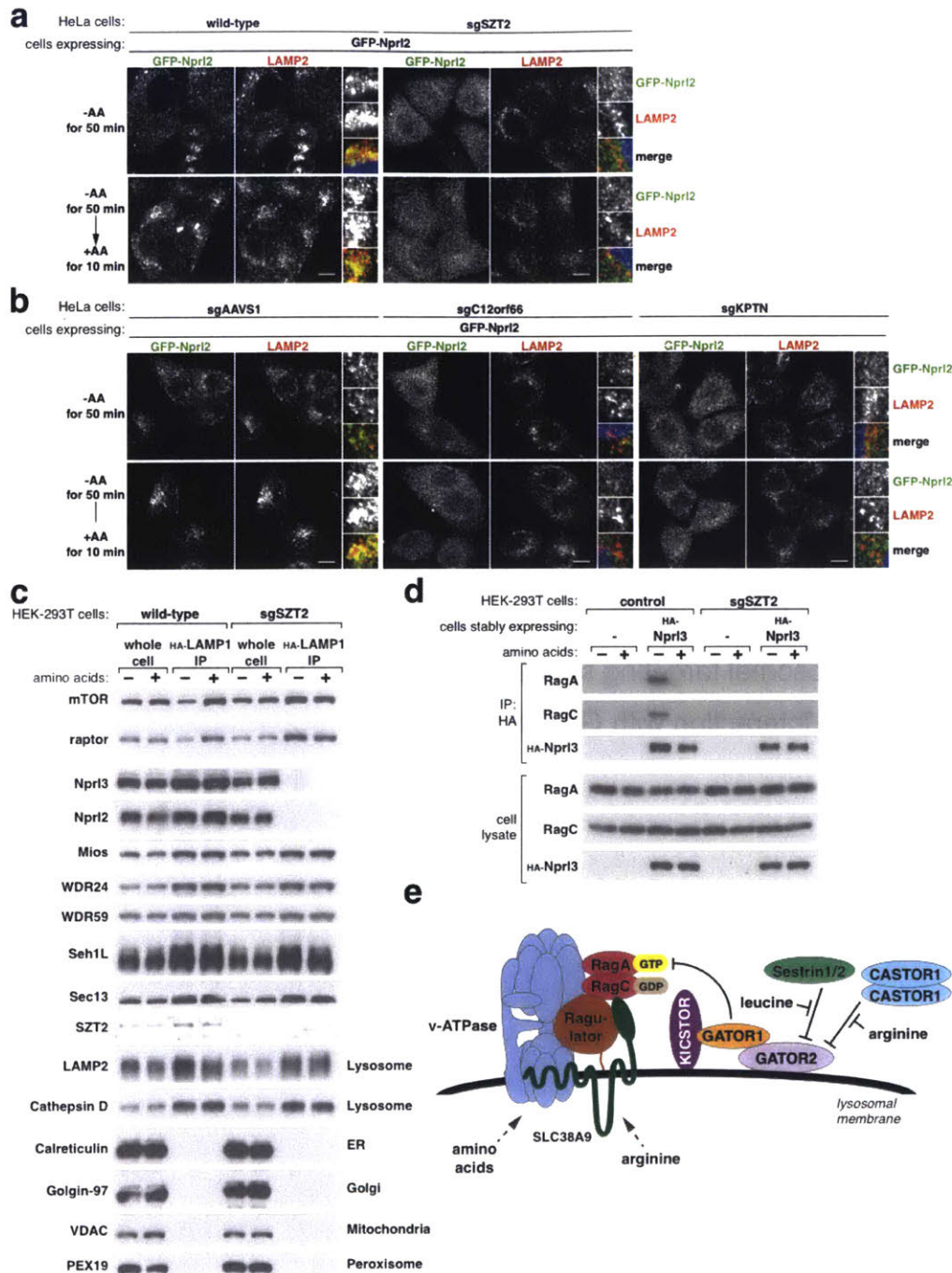


**Figure 4: The lysosomal localization of GATOR1 requires KICSTOR**

a) SZT2 loss renders GATOR1 dispersed throughout the cytoplasm. Npr12-deficient HeLa cells were reconstituted with GFP-Npr12 and subsequently modified with the CRISPR/Cas9 system to create SZT2-deficient cells expressing GFP-Npr12. These cells were starved or starved and restimulated with amino acids for the noted times prior to

the detection of GFP and LAMP2 by immunofluorescence. Insets depict selected fields magnified 3.24X and their overlays. Scale bars represent 10  $\mu$ m.

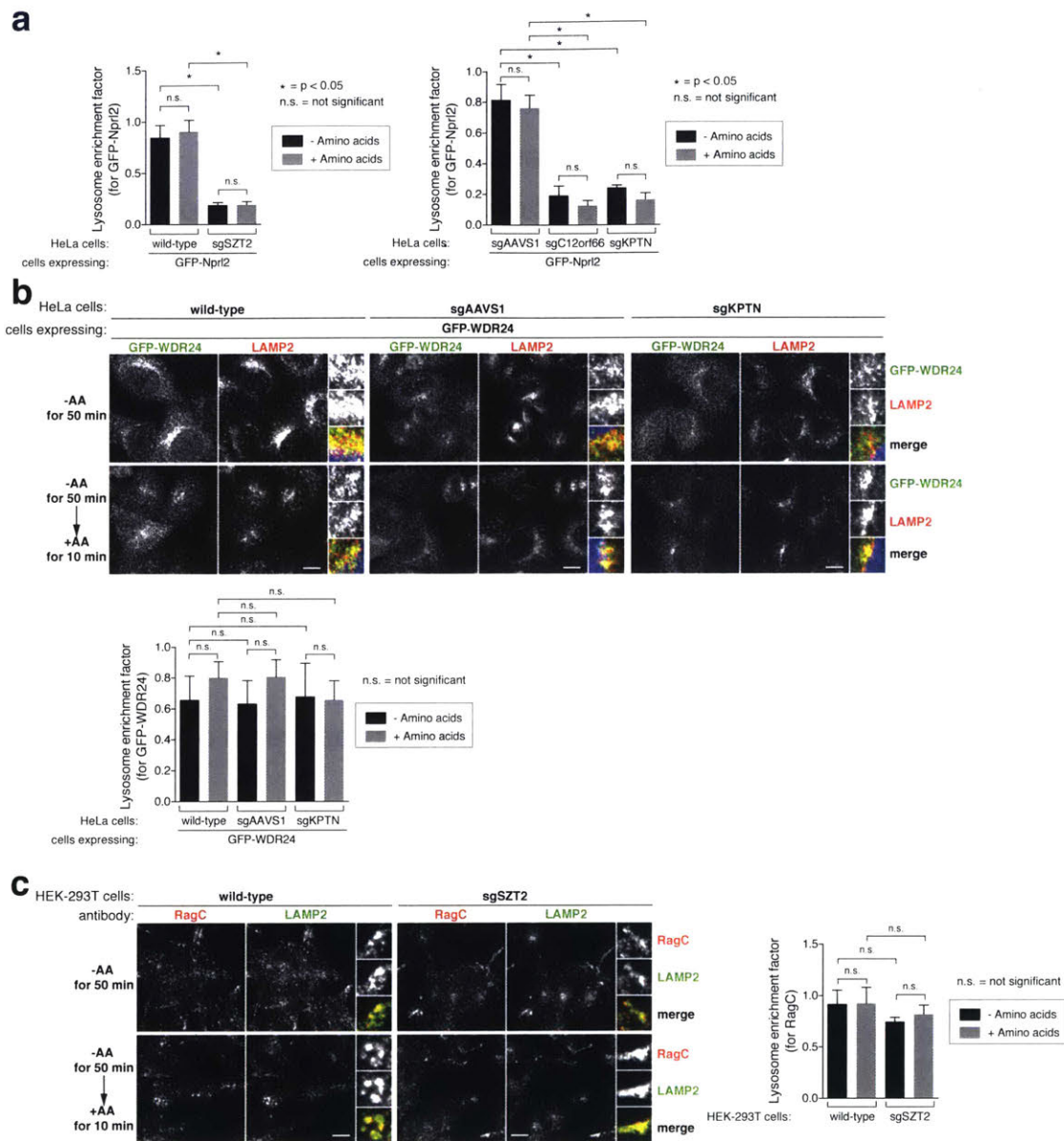
b) Loss of C12orf66 or KPTN also disrupts the localization of GATOR1 to the lysosome. Cell lines were generated, treated, and analyzed as in (a).

c) In SZT2-deficient cells, GATOR1 is not present on immunopurified lysosomes.

Lysosomes were immunopurified from wild-type or SZT2-deficient HEK-293T cells expressing HA-tagged LAMP1 and starved of and stimulated with amino acids as in (a). Lysosomes and whole cell lysates were analyzed by immunoblotting for the levels of the indicated proteins.

d) Loss of SZT2 disrupts the GATOR1-Rag GTPase interaction. Control or SZT2-deficient HEK-293T cells with or without the stable expression of HA-Npr13 were starved of amino acids for 50 min or starved and restimulated with amino acids for 10 min. Lysates and anti-HA immunoprecipitates were prepared and analyzed by immunoblotting for the levels of the indicated proteins.

e) Proposed role for KICSTOR in the nutrient sensing pathway upstream of mTORC1.

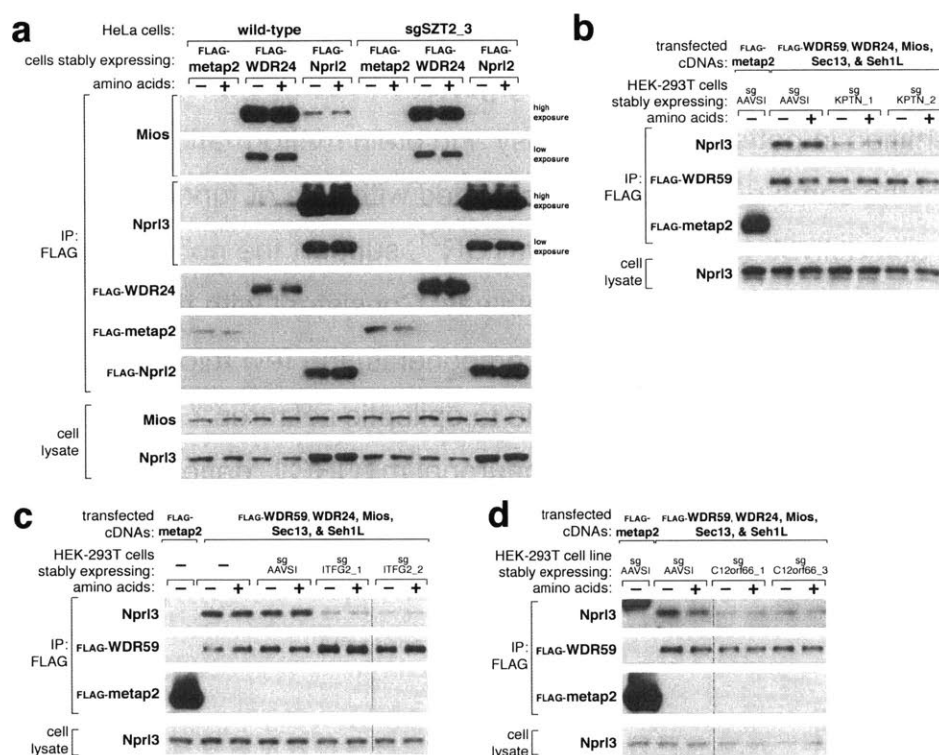


### Extended Data Figure 8: KICSTOR regulates the lysosomal localization of GATOR1 but not of GATOR2 or the Rag GTPases

a) Quantitation of the imaging data in Figures 4a, b. Values are mean  $\pm$  standard error.

b) Loss of KICSTOR components does not affect the lysosomal localization of GATOR2. GFP-WDR24 expressing HeLa cells prepared as in Extended Data Fig. 4c were subsequently modified with the CRISPR/Cas9 system to create KPTN-deficient cells. These cells as well as wild-type and sgAAVS1-treated control cells were starved or starved and restimulated with amino acids for the noted times prior to processing for the detection of GFP and LAMP2 by immunofluorescence. Insets depict selected fields

magnified 3.24X and their overlays. Scale bars represent 10  $\mu$ m. Quantitation of the imaging data is shown in the bar graph below images (mean  $\pm$  standard error).  
 c) The Rag GTPases localize to lysosomes regardless of SZT2 expression. Wild-type and SZT2-deficient HEK-293T cells were treated as in (b) prior to processing for the detection of RagC and LAMP2 by immunofluorescence. Insets depict selected fields magnified 3.24X and their overlays. Scale bars represent 10  $\mu$ m. Quantitation of the imaging data is shown in the bar graph on the right (mean  $\pm$  standard error).



### Extended Data Figure 9: Loss of KICSTOR disrupts the GATOR1-GATOR2 interaction

a) Loss of SZT2 disrupts the GATOR1-GATOR2 interaction. Anti-FLAG immunoprecipitates were prepared from wild-type or SZT2-deficient HeLa cells stably expressing the indicated cDNAs and starved of amino acids for 50 min or starved and restimulated with amino acids for 10 min. Immunoprecipitates and cell lysates were analyzed by immunoblotting for the indicated proteins.

- b) *KPTN* is necessary for the interaction of GATOR2 with GATOR1. HEK-293T cells stably expressing the indicated sgRNAs were transfected with the indicated cDNAs and subsequently treated and analyzed as in (a).
- c) *ITFG2* is also necessary for the GATOR1-GATOR2 interaction. Cells were prepared, treated, and analyzed as in (b).
- d) *C12orf66* is also necessary for the GATOR1-GATOR2 interaction. Cells were prepared, treated, and analyzed as in (b).

It will be important to understand if our findings have therapeutic implications because mutations in *KPTN* and *SZT2* and loss of the genomic locus containing *C12orf66* have been identified in patients with epilepsy and brain malformation disorders<sup>5-9</sup>. The fact that the same diseases are associated with loss of function mutations in GATOR1<sup>12</sup> and activating mutations in mTOR<sup>21</sup>, support the notion that KICSTOR is a negative regulator of the mTORC1 pathway. Consistent with the phenotypes of patients with mutations in KICSTOR components, the few mice deficient in *Szt2* that survive to adulthood are more susceptible to epileptic seizures<sup>20</sup>. If, as in mice, KICSTOR mutations in humans also activate neuronal mTORC1, patients with these mutations might benefit from inhibition of mTORC1 with drugs like rapamycin.

## References:

- 1 Laplante, M. & Sabatini, D. M. mTOR Signaling in Growth Control and Disease. *Cell* **149**, 274-293, doi:10.1016/j.cell.2012.03.017 (2012).
- 2 Dibble, C. C. & Manning, B. D. Signal integration by mTORC1 coordinates nutrient input with biosynthetic output. *Nature Cell Biology* **15**, 555-564, doi:10.1038/ncb2763 (2013).
- 3 Jewell, J. L., Russell, R. C. & Guan, K.-L. Amino acid signalling upstream of mTOR. *Nat. Rev. Mol. Cell Biol.* **14**, 133-139 (2013).
- 4 Sancak, Y. *et al.* The Rag GTPases Bind Raptor and Mediate Amino Acid Signaling to mTORC1. *Science* **320**, 1496-1501, doi:10.1126/science.1157535 (2008).
- 5 Basel-Vanagaite, L. *et al.* Biallelic SZT2 mutations cause infantile encephalopathy with epilepsy and dysmorphic corpus callosum. *Am. J. Hum. Genet.* **93**, 524-529 (2013).
- 6 Venkatesan, C., Angle, B. & Millichap, J. J. Early-life epileptic encephalopathy secondary to SZT2 pathogenic recessive variants. *Epileptic Disord* **18**, 195-200 (2016).
- 7 Baple, E. L. *et al.* Mutations in KPTN cause macrocephaly, neurodevelopmental delay, and seizures. *Am. J. Hum. Genet.* **94**, 87-94 (2014).
- 8 Pajusalu, S., Reimand, T. & Õunap, K. Novel homozygous mutation in KPTN gene causing a familial intellectual disability-macrocephaly syndrome. *Am. J. Med. Genet. A* **167A**, 1913-1915 (2015).
- 9 Mc Cormack, A. *et al.* 12q14 Microdeletions: Additional Case Series with Confirmation of a Macrocephaly Region. *Case Rep Genet* **2015**, 192071 (2015).
- 10 Crino, P. B. mTOR: A pathogenic signaling pathway in developmental brain malformations. *Trends Mol Med* **17**, 734-742 (2011).
- 11 D'Gama, A. M. *et al.* Mammalian target of rapamycin pathway mutations cause hemimegalencephaly and focal cortical dysplasia. *Ann. Neurol.* **77**, 720-725 (2015).
- 12 Baldassari, S., Licchetta, L., Tinuper, P., Bisulli, F. & Pippucci, T. GATOR1 complex: the common genetic actor in focal epilepsies. *J. Med. Genet.* **53**, 503-510 (2016).
- 13 Sancak, Y. *et al.* Regulator-Rag Complex Targets mTORC1 to the Lysosomal Surface and Is Necessary for Its Activation by Amino Acids. *Cell* **141**, 290-303, doi:10.1016/j.cell.2010.02.024 (2010).
- 14 Wei, Y. & Lilly, M. A. The TORC1 inhibitors Npr12 and Npr13 mediate an adaptive response to amino-acid starvation in Drosophila. *Cell Death Differ.* **21**, 1460-1468 (2014).
- 15 Wei, Y. *et al.* TORC1 regulators Iml1/GATOR1 and GATOR2 control meiotic entry and oocyte development in Drosophila. *Proceedings of the National Academy of Sciences* **111**, E5670-5677 (2014).
- 16 Cai, W., Wei, Y., Jarnik, M., Reich, J. & Lilly, M. A. The GATOR2 Component Wdr24 Regulates TORC1 Activity and Lysosome Function. *PLoS Genet.* **12**, e1006036 (2016).



- 17 Bar-Peled, L. *et al.* A Tumor suppressor complex with GAP activity for the Rag GTPases that signal amino acid sufficiency to mTORC1. *Science* **340**, 1100-1106 (2013).
- 18 Efeyan, A. *et al.* Regulation of mTORC1 by the Rag GTPases is necessary for neonatal autophagy and survival. *Nature* **493**, 679-683 (2013).
- 19 Kalender, A. *et al.* Metformin, Independent of AMPK, Inhibits mTORC1 in a Rag GTPase-Dependent Manner. *Cell Metabolism* **11**, 390-401, doi:10.1016/j.cmet.2010.03.014 (2010).
- 20 Frankel, W. N., Yang, Y., Mahaffey, C. L., Beyer, B. J. & O'Brien, T. P. Szt2, a novel gene for seizure threshold in mice. *Genes Brain Behav.* **8**, 568-576 (2009).
- 21 Baulac, S. mTOR signaling pathway genes in focal epilepsies. *Prog. Brain Res.* **226**, 61-79 (2016).
- 22 Kim, D. H., Sarbassov, D. D., Ali, S. M., King, J. E. & Latek, R. R. mTOR interacts with raptor to form a nutrient-sensitive complex that signals to the cell growth machinery. *Cell* (2002).
- 23 Boussif, O. *et al.* A versatile vector for gene and oligonucleotide transfer into cells in culture and in vivo: polyethylenimine. *Proceedings of the National Academy of Sciences of the United States of America* **92**, 7297-7301 (1995).
- 24 Tsun, Z.-Y. *et al.* The Folliculin Tumor Suppressor Is a GAP for the RagC/D GTPases That Signal Amino Acid Levels to mTORC1. *Molecular cell* **52**, 495-505, doi:10.1016/j.molcel.2013.09.016 (2013).
- 25 Zoncu, R. *et al.* mTORC1 Senses Lysosomal Amino Acids Through an Inside-Out Mechanism That Requires the Vacuolar H<sup>+</sup>-ATPase. *Science* **334**, 678-683, doi:10.1126/science.1207056 (2011).
- 26 Petit, C. S., Rocznik-Ferguson, A. & Ferguson, S. M. Recruitment of folliculin to lysosomes supports the amino acid-dependent activation of Rag GTPases. *The Journal of Cell Biology* **202**, 1107-1122 (2013).
- 27 Schindelin, J. *et al.* Fiji: an open-source platform for biological-image analysis. *Nat. Methods* **9**, 676-682 (2012).
- 28 Yilmaz, Ö. H. *et al.* mTORC1 in the Paneth cell niche couples intestinal stem-cell function to calorie intake. *Nature*, doi:10.1038/nature11163 (2012).



## **Acknowledgements**

We thank all members of the Sabatini Lab for helpful insights. We thank Kara McKinley and Iain Cheeseman for generously providing the retroviral GFP constructs used in this work, Connie Mahaffey for technical support with the mouse experiments, and Jianxin Xie from Cell Signaling Technology, Inc. for generously providing the DEPDC5, Mios, Npr12, WDR24, WDR59, C12orf66, Seh1L, and SZT2 antibodies. D.M.S. is a founder, consultant, and shareholder of Navitor Pharmaceuticals, Inc., which is targeting the amino acid sensing pathway for therapeutic benefit. R.L.W., L.C., and J.M.O. are shareholders of Navitor Pharmaceuticals. R.L.W., L.C., J.M.O., D.M.S., and the Whitehead Institute have filed two provisional patents that relate to amino acid sensing by the mTOR pathway. This work was supported by grants from the NIH to D.M.S. (R01 CA103866 and R37 AI47389) and W.N.F. (R37 NS031348), Department of Defense (W81XWH-07-0448) to D.M.S., and fellowship support from the NIH to R.L.W. (T32 GM007753 and F30 CA189333), L.C. (F31 CA180271), and J.M.O. (T32 GM007753 and F30 CA210373), from NSF to K.J.C. (2016197106), from the National Defense Science & Engineering Graduate Fellowship (NDSEG) Program to G.A.W., from the Life Sciences Research Foundation to K.S. (Pfizer fellow), from the EMBO Long-Term Fellowship to M.A.R., and from the Paul Gray UROP Fund to S.M.S. (3143900). D.M.S. is an investigator of the Howard Hughes Medical Institute.

## **Author Contributions**

R.L.W., L.C., and D.M.S. formulated the research plan and interpreted experimental results. R.L.W. and L.C. designed and performed most experiments with assistance from G.A.W., X.G., J.M.O., K.S., K.J.C., J.K., S.M.S., and M.A.R. X.G. undertook the epistasis experiments, G.A.W. those using purified lysosomes, J.M.O. those involving glucose signaling, and K.S. those using size exclusion chromatography. S.P. and W.N.F. generated the *Szt2* gene trap mice and harvested tissues, which were analyzed by R.L.W. and G.A.W. R.L.W. and D.M.S. wrote the manuscript and all authors edited it.

## Methods

### Materials

Reagents were obtained from the following sources: antibodies to LAMP2 (sc-18822), ITFG2 (SC 134686), and HRP-labeled anti-mouse and anti-rabbit secondary antibodies from Santa Cruz Biotechnology; the antibody to PEX19 (ab137072) from Abcam; the antibody to raptor from EMD Millipore (2818718); the antibody to Sec13 from Gene Tex (GTX 101055); antibodies to phospho-T389 S6K1 (9234), S6K1 (2708), phospho-S235/236 S6 (2211), S6 (2217), phospho-S65 4E-BP1 (9451), 4E-BP1 (9644), phospho-757 ULK1 (6888), ULK1 (8054), phospho-792-raptor (2083), phospho-79-ACC (3661), ACC (3662), phospho-T308-Akt (4056), Akt (4691), LC3B (2775), mTOR (2983), RagC (3360), Mios (13557), VDAC (4661), Calreticulin (12238), Golgin-97 (13192), Cathepsin D (2284), and the myc (2278) and FLAG (2368) epitopes from Cell Signaling Technology (CST); antibodies to the HA epitope from CST (3724) and Bethyl laboratories (A190208A); antibody to KPTN from ProteinTech (16094-1AP); antibody to Nprl3 from Sigma (HPA0011741). RPMI, FLAG M2 affinity gel, and amino acids from Sigma Aldrich; DMEM from SAFC Biosciences; XtremeGene9 and Complete Protease Cocktail from Roche; Alexa 488 and 568-conjugated secondary antibodies; Inactivated Fetal Bovine Serum (IFS) from Invitrogen; and amino acid-free RPMI from US Biologicals. Jianxin Xie (Cell Signaling Technology) generously provided the DEPDC5, Mios, Nprl2, WDR24, WDR59 (53385), C12orf66, Seh1L, and SZT2 antibodies. The C12orf66 and SZT2 antibodies are bleeds. At the beginning of this project we also used an antibody to SZT2 from Abcam (SZT2 blots in Fig. 1c and Extended Data Fig. 5d), but it has since been discontinued and is no longer available.

### Cell lines and tissue culture

HEK-293T, HEK-293E, and HeLa cells were cultured in DMEM 10% IFS (inactivated fetal bovine serum) supplemented with 2 mM glutamine. All cell lines were maintained at 37°C and 5% CO<sub>2</sub>. All cell lines were obtained from ATCC (American

Type Culture Collection) and validated and tested for mycoplasma.

### **Cell lysis, immunoprecipitations, transfections, and lysosomal purifications**

Cells were rinsed once with ice-cold PBS and lysed immediately with Triton lysis buffer (1% Triton, 10 mM  $\beta$ -glycerol phosphate, 10 mM pyrophosphate, 40 mM Hepes pH 7.4, 2.5 mM  $MgCl_2$  and 1 tablet of EDTA-free protease inhibitor [Roche] (per 25 ml buffer). The cell lysates were clarified by centrifugation at 13,000 rpm at 4°C in a microcentrifuge for 10 minutes. For anti-FLAG-immunoprecipitations, the FLAG-M2 affinity gel was washed with lysis buffer 3 times. 30  $\mu$ l of a 50% slurry of the affinity gel was then added to cleared cell lysates and incubated with rotation for 2 hours at 4°C. The beads were washed 3 times with lysis buffer containing 500 mM NaCl. Immunoprecipitated proteins were denatured by the addition of 50  $\mu$ l of sample buffer and boiling for 5 minutes as described<sup>22</sup>, resolved by 8%–16% SDS-PAGE, and analyzed by immunoblotting.

For transfection experiments in HEK-293T cells, 2 million cells were plated in 10 cm culture dishes. Twenty-four hours later, cells were transfected via the polyethylenimine method<sup>23</sup> with the pRK5-based cDNA expression plasmids indicated in the figures. The total amount of plasmid DNA in each transfection was normalized to 5  $\mu$ g with empty pRK5. Thirty-six hours after transfection, cells were lysed as described above.

For experiments which required amino acid starvation or restimulation, cells were treated as previously described<sup>24</sup>. Briefly, cells were incubated in amino acid free RPMI for 50 minutes and then stimulated with amino acids for 10 minutes. The amino acid mixture used was previously described<sup>17</sup>. For glucose starvation, cells were incubated in RPMI media lacking glucose but containing amino acids and dialyzed serum for 50 minutes, followed by a 10-minute restimulation with 5 mM D-Glucose. For insulin stimulation experiments, cells were incubated in RPMI without serum for 50 minutes and restimulated with 1 mg/ml insulin for 10 minutes.

Lysosomes were purified via immunopurification from wild-type or engineered HEK-293T cells stably expressing HA-RFP-LAMP1 as previously described<sup>25</sup>.

### **Identification of KICSTOR by immunoprecipitation followed by mass spectrometry**

Immunoprecipitates from HEK-293T cells expressing endogenously tagged 3xFLAG-DEPDC5 were prepared using Triton lysis buffer. Proteins were eluted with the FLAG peptide (sequence DYKDDDDK) from the FLAG-M2 affinity gel, resolved on 4-12% NuPage gels (Invitrogen), and stained with simply blue stain (Invitrogen). Each gel lane was sliced into 10-12 pieces and the proteins in each gel slice digested overnight with trypsin. The resulting digests were analyzed by mass spectrometry as described<sup>4</sup>. Peptides corresponding to KICSTOR components were detected in the FLAG-DEPDC5 immunoprecipitates, while no peptides were detected in negative control immunoprecipitates of FLAG-metap2.

### **Evolutionary and domain analysis of the KICSTOR components**

To assess the conservation of the proteins in the KICSTOR complex, analysis was performed using the PHMMER software (<https://www.ebi.ac.uk/Tools/hmmer/search/phmmer>).

### **Generation of cells with loss of function mutations in GATOR2, GATOR1, or KICSTOR components**

To generate HEK-293T or HeLa cells with reduced expression of GATOR2, GATOR1, or KICSTOR components, sense (S) and antisense (AS) oligonucleotides encoding the following single guide RNAs (sgRNAs) were cloned into the pX330 vector. Cells treated with the sgRNA targeting the AAVS1 locus served as negative control cells.

sgAAVS1\_S: caccgTCCCCTCCACCCCACAGTG  
sgAAVS1\_AS: aaacCACTGTGGGGTGGAGGGGAc

sgSZT2\_1S: caccgGAAGCAGCCCGCCTAAGCAG  
sgSTZ2\_1AS: aaacGAAGCAGCCCGCCTAAGCAGc

sgSZT2\_2S: caccgGTGGCAGCCAGATGAACCAG  
sgSTZ2\_2AS: aaacCTGGTTCATCTGGCTGCCACc

sgSZT2\_3S: caccgAACACGGGTGGAAGTGACGA  
sgSTZ2\_3AS: aaacTCGTCACTTCCACCCGTGTTc

sgWDR24\_1S: caccgACCCAGGGCTGTGGTCACAC  
sgWDR24\_1AS: aaacTCAGGAGTACTCGCAGAGGTc

sgNprl3\_1S: caccGGCTTTCAGGCTCCGTTCGA  
sgNprl3\_1AS: aaacTCGAACGGAGCCTGAAAGCC

sgKPTN\_1S: caccgATCACATCAGTAAACATGAG  
sgKPTN\_1AS: aaacCTCATGTTTACTGATGTGATc

sgITFG2\_1S: caccgACCCAGGGCTGTGGTCACAC  
sgITFG2\_1AS: aaacGTGTGACCACAGCCCTGGGTc

sgC12orf66\_3S: caccgGGCTAAGGACAATGTGGAGA  
sgC12orf66\_3AS: aaacTCTCCACATTGTCCTTAGCCc

On day one, 200,000 HEK-293T cells were seeded into 6 wells of a 6-well plate. Twenty-four hours post seeding, each well was transfected with 250 ng shGFP pLKO, 1 ug of the pX330 guide construct, 0.5 ug of empty pRK5 using XtremeGene9. The

following day, cells were trypsinized, pooled in a 10 cm dish, and selected with puromycin to eliminate untransfected cells. Forty-eight hours after selection, the media was aspirated and replenished with fresh media lacking puromycin. The following day, cells were single cell sorted with a flow cytometer into the wells of a 96-well plate containing 150 ul of DMEM supplemented with 30% IFS.

For HeLa cells, on day one 1 million cells were plated into a 10 cm dish. Twenty-four hours later, the cells were transfected with 1 ug pLJM1 GFP and 300 ng of the pX330 guide construct using XtremeGene9. Selection with puromycin was started the following day to eliminate untransfected cells. Forty-eight hours after selection, the media was aspirated and replenished with fresh media lacking puromycin and the cells were single cell sorted as described above. Cells were grown for two weeks and the resultant colonies were trypsinized and expanded. Cell clones were validated for reduced expression of the relevant proteins via immunoblotting (SZT2, KPTN, ITFG2, Nprl3, WDR24) or by confirming that the targeted exon contains out of frame mutations via genomic DNA sequencing (*C12orf66*). Most of the cell clones we generated likely do not express the targeted proteins, but because there is the possibility that some expression remains below the limit of detection of the available antibodies, we do not label the clones as null. We suspect that the cell clone generated with the sgRNA targeting the *WDR24* gene expresses a very low amount of the WDR24 protein that is below the limit of detection of the available antibody.

To generate HEK-293T or HeLa cells stably expressing the indicated sgRNAs, the following oligonucleotides were cloned into the pLenti viral vectors:

sgAAVS1\_S: caccgTCCCCTCCACCCCACAGTG

sgAAVS1\_AS: aaacCACTGTGGGGTGGAGGGGAc

sgKPTN\_1S: caccgGCGCAACGGACAAGGCCCCG

sgKPTN\_1AS: aaacCGGGGCCTTGTCCGTTGCGCc

sgKPTN\_2S: caccgGCAGAGCAATGTGTACGGGC

sgKPTN\_2AS: aaacGCCCCGTACACATTGCTCTGCc

sgKPTN\_3S: caccgGAGCACCTTGCCTTTAAGGG

sgKPTN\_3AS: aaacCCCTTAAAGGCAAGGTGCTCc

sgKPTN\_6S: caccgGTCAAGGTTGTACTIONCAGAGC

sgKPTN\_6AS: aaacGCTCTGAGTACAACCTTGACc

sgITFG2\_1S: caccgGGTGGGAGACACCAGCGGGA

sgITFG2\_1AS: aaacTCCCGCTGGTGTCTCCACCCc

sgITFG2\_2S: caccgGAAGTTAAATGAACTGGTGG

sgITFG2\_2AS: aaacCCACCAGTTCATTTAACTTCc

sgITFG2\_3S: caccgAAAATGATGACAGTCGGCCA

sgITFG2\_3AS: aaacTGGCCGACTGTCATCATTTTc

sgC12orf66\_1S: caccgCGAGAGGCCAACAAGAGCGC

sgC12orf66\_1AS: aaacGCGCTCTTGTGGCCTCTCGc

sgC12orf66\_3S: caccgGGCTAAGGACAATGTGGAGA

sgC12orf66\_3AS: aaacTCTCCACATTGTCCTTAGCCc

To generate the lentiviruses, on day one 750,000 HEK-293T cells were seeded in a 6 well plate in DMEM supplemented with 20% inactivated fetal bovine serum (IFS). Twenty-four hours later, the cells were transfected with the above sgRNA pLenti encoding plasmids alongside the Delta VPR envelope and CMV VSV-G packaging plasmids using XtremeGene9 transfection reagent. Twelve hours post transfection, the spent media was aspirated and replaced with 2 ml fresh media. Virus-containing supernatants were collected 36 hours after replacing media and passed through a 0.45

micron filter to eliminate cells. One million HEK-293T or HeLa cells in the presence of 8 µg/ml polybrene (Millipore) were infected with 250 µl of virus for each construct in 1 ml total volume of media and then spun at 2,200 rpm for 45 minutes at 37°C. Forty-eight hours after selection, cells were trypsinized and selected with 1 µg/ml puromycin and seeded on the 10<sup>th</sup> day for signaling experiments, as described. Cell lines were validated for reduced expression of the relevant proteins via immunoblotting (KPTN, ITFG2) or by confirming that the targeted exon contains out of frame mutations via genomic DNA sequencing (*C12orf66*).

### **Generation of cells expressing endogenously FLAG-tagged WDR59 or DEPDC5**

To insert an N-terminal 3xFLAG tag into the *WDR59* or *DEPDC5* genes, 200,000 HEK-293T cells were seeded into 6 wells of a 6 well plate. Twenty-four hours later, each well was transfected with the following constructs: 250 ng shGFP pLKO (to provide transient puromycin resistance), 1000 ng of the indicated single guide RNA (sgRNA), 500 ng of the indicated single stranded DNA oligos, and 5.25 ul XtremeGene9 transfection reagent.

Single stranded DNA oligos used for homologous recombination:

WDR59:

```
CTAGCTCACCTGGGAGTCACGGA ACTCTACAACCACGTTTTTCGCTGCTCCA  
TCTTGCAGCGCCTGCGGCCGCCTTGTCATCGTCATCCTTGTAATCAATGTCA  
TGATCTTTATAATCACCGTCATGGTCTTTGTAGTCCATCTCCCCCGCCCGGC  
CGCCGCGGCCCCAGGACGGCGCCCTCCCACCCCGCCGTCCCCAGT
```

DEPDC5:

```
GGAGGCAAGATGACTTCTCTGCCCAAGCTTGGAACAGCTAAAGGGAAAAA  
CAGTGCAAGATGGACTACAAAGACCATGACGGTGATTATAAAGATCATGACA
```



TTGATTACAAGGATGACGATGACAAGGCGGCCGCAGGCCGTACGACGAAA  
GTCTACAAACTCGTCATCCACAAGAAGGGCTTTGGGGGCAGTGGTCA

sgRNAs cloned into pX330:

WDR59 sense: caccgCGGGGAGATGGCGGCGCGA

WDR59 antisense: aaacTCGCGCCGCCATGTCCCCCGc

DEPDC5 sense: caccgTGCAAGATGAGAACAACAA

DEPDC5 antisense: aaacTTGTTGTTCTCATCTTGCAc

Forty-eight hours after transfection, the media was removed from cells and replaced with fresh media supplemented with 2 ug/ml of puromycin. The following day, cells were trypsinized, pooled, and replated into 10 cm plates in media containing puromycin. Twenty-four hours later, the cell media was changed to fresh media lacking puromycin. Forty-eight hours later, cells were single cell sorted into 96 well plates in 150 ul of cell media.

Following two weeks of growth, individual clones were expanded. To identify clones containing a 3xFLAG tag incorporated into the endogenous gene, genomic DNA was extracted from each clone using QuickExtract DNA solution (Epicentre) as described<sup>26</sup>. The primers indicated below were used to amplify the genomic region surrounding the insertion site, PCR products were subcloned into pRK5, and plasmids were subsequently submitted for sequencing. Validated clones were tested for their response to amino acid starvation and stimulation compared to wild type HEK-293T cells to verify that incorporation of the epitope tag did not alter mTORC1 signaling.

Genomic PCR primers:

WDR59\_F: TCCACTCGGCCTCTAGCTCA

WDR59\_R: GAGGGCGTGCCTGTTTGTG

DEPDC5\_F: TTCCGAGAGTCACTTGGCAC  
DEPDC5\_R: AGTCGCCTGTTTAGCCTCAAT

### **Generation of cells stably expressing cDNAs**

For the GFP-tagged cDNAs, the indicated GATOR1, GATOR2, and KICSTOR components were cloned into the N-terminal GFP retroviral vector pIC242 or the C-terminal GFP retroviral vector KG371 in the case of Mios. For retrovirus production, 750,000 HEK-293T cells were seeded on Day 1 into a 6 well plate and were transfected 18-24 hours later with 1 ug of pIC242 or KG371 construct, gag/pol and the CMV VSV-G packaging plasmids using the XtremeGene9 transfection reagent. Twelve hours later the media was changed to fresh DMEM with 20% IFS, followed by collection of the virus 36 hours after transfection. The virus was filtered through a 0.45 um filter and added, with polybrene, to the appropriate HeLa cells in a 6 well plate (500,000 cells per well). Twelve hours later the media was changed to fresh media. Finally, twenty-four hours after infection the cells were trypsinized and plated into a 10 cm plate in the presence of 1 ug/ul blasticidin for three days. The following day, low expressing GFP cells were single cell sorted with a flow cytometer into the wells of a 96-well plate containing 150 ul of DMEM supplemented with 30% IFS. Cells were grown for two weeks and the resultant colonies were trypsinized and expanded. Clones were validated for expression of the relevant protein via immunoblotting. To generate HeLa cells deficient in KICSTOR and expressing GFP-tagged GATOR1 or GATOR2 components, the protocol for CRISPR/Cas9 modification of HeLa cells described previously was used, and the cells were subjected to a second round of cell sorting.

The lentiviral expression plasmids used were: pLJM1-FLAG-metap2, pLJM1-FLAG-WDR24, pLJM1-FLAG-Npr12, and pLJC5-HA-Npr13 for the interaction experiments and pLJM1-HA-RFP-LAMP1 for the lysosomal immunopurifications. Lentiviruses were produced by transfection of HEK-293T cells with the above plasmids

in combination with VSV-G envelope and CMV  $\Delta$ VPR 8 packaging plasmids. Twenty-four hours after transfection, the media was changed to DMEM with 20% IFS. Forty-eight hours after transfection, the virus-containing supernatant was collected from the cells and passed through a 0.45  $\mu$ m filter. Target cells were plated in 6-well plates containing DMEM 10% IFS with 8  $\mu$ g/mL polybrene and infected with virus containing media. Twenty-four hours later, the media was changed to fresh media containing puromycin for selection.

### **Immunofluorescence assays**

Immunofluorescence assays were performed as described previously<sup>13</sup>. Briefly, 300,000 HEK-293T or 150,000 HeLa cells were plated on fibronectin-coated glass coverslips in 6-well tissue culture plates. Twenty-four hours later, the slides were rinsed with PBS once and fixed for 15 minutes with 4% paraformaldehyde in PBS at room temperature. The slides were rinsed three times with PBS and cells were permeabilized with 0.05% Triton X-100 in PBS for 5 minutes. After rinsing three times with PBS, the slides were blocked for 1 hour in Odyssey blocking buffer, and then incubated with primary antibody in Odyssey blocking buffer for 1 hour at room temperature, rinsed three times with PBS, and incubated with secondary antibodies produced in donkey (diluted 1:1000 in Odyssey blocking buffer) for 45 minutes at room temperature in the dark and washed three times with PBS. The primary antibodies used were directed against GFP (Rockland Immunochemicals; 1:500 dilution), LAMP2 (Santa Cruz Biotechnology; 1:300 dilution), mTOR (CST; 1:100-1:300 dilution), and RagC (CST; 1:100 dilution). Slides were mounted on glass coverslips using Vectashield (Vector Laboratories) containing DAPI.

Images were acquired on a Zeiss AxioVert200M microscope with a 63X oil immersion objective and a Yokogawa CSU-22 spinning disk confocal head with a Borealis modification (Spectral Applied Research/Andor) and a Hamamatsu Orca-ER CCD camera. The MetaMorph software package (Molecular Devices) was used to

control the hardware and image acquisition. Images were captured in the Cy3, Cy5, and DAPI channels. Although the DAPI channel is not shown in the main images, it is in the insets as a blue signal.

For quantitative analyses, the raw image files were opened in the Fiji software package<sup>27</sup> and a maximum intensity projection of a z-stack of ~6-8 contiguous focal planes (~0.5  $\mu\text{m}$  each) was used. In each cell analyzed, a cytoplasmic region of interest containing lysosomes (high LAMP2 signal) was chosen and in this area the mean fluorescence intensities (MFIs) of the Cy5 (LAMP2) and Cy3 channels (GFP, mTOR, or RagC) were measured. In the same cell an equivalently sized area in a region of the cytoplasm not containing lysosomes (low LAMP2 signal) was chosen and the MFIs of the Cy5 and Cy3 channels were also measured in this area. For each channel, the MFI of the non-lysosomal area was subtracted from that of the lysosomal area. The value obtained for the Cy3 channel was then divided by the analogous value for the Cy5 channel to give the lysosomal enrichment factor shown in the bar graphs in the figures. A lysosomal enrichment factor close to 1 indicates that the Cy3 signal was enriched in a region of the cell containing lysosomes over one that does not. A lysosomal enrichment factor closer to 0 indicates that the Cy3 signal was not enriched at the lysosomes, indicating no specific co-localization with the Cy5 signal. For each condition studied, images of at least 3 distinct fields were captured and within each 2-5 cells were analyzed as described above so that at least 10 cells were analyzed per condition. The mean lysosomal enrichment factor was calculated for each field analyzed, and the mean of the means of these fields is shown (bar graphs show mean  $\pm$  standard error of the mean). In our experiments, the MFIs in the Cy3 and Cy5 channels were of similar magnitudes and so we obtained equivalent results regarding lysosomal co-localization whether we subtracted or divided the MFIs of the two areas in calculating the lysosomal enrichment factors. Two-tailed *t* tests were used for comparisons between conditions. All comparisons were two-sided, and *p*-values < 0.05 were considered significant. Variance was similar across groups.

### **Analysis of mTORC1 signaling in *Szt2*<sup>GT/GT</sup> mice**

Previously described homozygous 129S1.129P2-*Szt2*<sup>Gt(XH662)Byg</sup>/*Szt2*<sup>Gt(XH662)Byg</sup> (hereafter *Szt2*<sup>GT/GT</sup>) and wild-type mice<sup>20</sup> of 1-5 months in age were fasted for 8 hours beginning at 7 am. A total of 8 mice were used across experiments – four wild-type females, three *Szt2*<sup>GT/GT</sup> females and one *Szt2*<sup>GT/GT</sup> male. Sample size was determined based on variation in mTORC1 signaling observed in wild-type mice. Mice were sacrificed and the liver, gastrocnemius muscle, heart, and brain were harvested. Portions of the liver and muscle were analyzed by immunoblotting for phospho-S235/236 S6, S6, phospho-S65 4E-BP1, and 4E-BP1 levels as described<sup>18</sup> except that tissues were disrupted with a homogenizer instead of a sonicator. Small portions of the liver, heart, and brain were fixed in formalin and processed for phospho-S235/236 S6 immunohistochemistry as described<sup>28</sup>. All mice were housed in a barrier facility with standard 12-h light/dark cycle. Food and water were available *ad libitum* until the 8-hour fast. Animal studies were performed under AAALAC and NIH guidelines and were approved by institutional animal care and use committee (IACUC). No randomization or blinding was performed.

### **Size exclusion chromatography**

A confluent 15 cm plate of wild-type or SZT2-deficient HEK-293T cells (~40 x 10<sup>6</sup> cells) was lysed in a CHAPS-containing buffer (50 mM NaHEPES, 100 mM NaCl, 2 mM MgCl<sub>2</sub>, 2 mM DTT, and 0.3% CHAPS). The lysate was cleared by ultracentrifugation at 100,000 xg for 30 minutes, to completely remove non-lysed cells and insoluble aggregates. The cleared lysate was normalized to a protein concentration of 3 mg/ml, and 1 ml of it was loaded onto a tandem Superose 6 gel filtration column. The elutant was fractionated and the proteins in each fraction were precipitated separately with trichloroacetic acid (TCA). The precipitants were collected by centrifugation and washed twice with acetone to remove residual TCA. The protein pellets were re-dissolved in 2xSDS loading buffer. Equal amounts of each were separated by 8% SDS-PAGE and analyzed by immunoblotting for indicated antibodies.

## **Data availability statement**

No large-scale datasets were generated or analysed during the current study. Plasmids that were generated are available on Addgene.

## CHAPTER 6

### Future Directions and Discussion

mTORC1 is a master regulator of cell growth that is regulated by a diverse set of environmental signals, including nutrient levels. Deregulation of the mTORC1 signaling pathway is associated with multiple human diseases, including cancer and epilepsy. Over the past decade, the work of our lab and others have helped to identify many key players involved in relaying amino acid availability to mTORC1, but many questions remain.

### The role of RagC mutations in follicular lymphoma tumorigenesis

In this thesis, we identify mTORC1-activating, recurrent mutations in *RRAGC*, which encodes the RagC GTPase, an important regulator of mTORC1 in response to amino acids (Okosun et al., 2016). These mutations increase RagC binding to raptor, and, when overexpressed, render cells partially insensitive to amino acid deprivation. Further, we biochemically characterize how the mutations in RagC affect its nucleotide binding, uncovering two classes of mutants. One class has a significantly decreased affinity for GTP, with a preference for binding GDP over GTP. This class of mutants likely activates the pathway by rendering RagC GDP-loaded (and thereby in its “active” conformation) or by affecting its affinity for its potential GEF (although such a modulator of RagC has not yet been discovered). The other class of mutants biases the RagC nucleotide affinity for GDP without an overall decrease in affinity for GTP in comparison to wild-type RagC. Whether this increased affinity for GDP would be enough to modulate raptor binding *in vivo*, however, is unclear, as intracellular GTP concentrations are 10-20 times higher than GDP concentrations (Proud, 1986).

While these studies identify two separate potential mechanisms for how RagC mutants activate mTORC1 signaling, more work is needed to understand the exact mechanisms through which they act. Additionally, although the fact that the mutations in *RRAGC* exist in the dominant clone and are stable throughout disease progression is

consistent with RagC acting as a driver of oncogenesis, further work is needed to uncover if this is indeed the case. For example, classic cancer studies such as those showing that mutant RagC overexpression can stimulate transformation and proliferation in primary cells are necessary. Further, creating mouse models in which these recurrent mutations in RagC can be induced in B-lymphocytes, the progenitor cells for follicular lymphoma, and analyzing the resulting phenotype would further prove that RagC is indeed acting as an oncogene in these follicular lymphoma patients. The activating nature of these mutations and the fact that they only occur in a heterozygous manner in the tumor cells are consistent with RagC acting as an oncogene, but further work is needed to establish its role as such.

Another interesting question is why these mutations were not observed in RagA, the constitutive binding partner of RagC. One hypothesis could be that RagB, which is highly similar to and functionally redundant with RagA, may also be expressed, along with RagA, in these cells, and thus mutations in either one of these may not be enough to overcome the wild-type protein present. However, further work will be needed to clarify why these mutations only occur in RagC.

Finally, these mutations in RagC in follicular lymphoma patients suggest that treatment with mTOR inhibitors may be effective therapy for this disease. First, cell culture studies in which the sensitivity to mTOR inhibitors of cell lines harboring these mutations is measured are needed. If indeed the cells are more sensitive to these treatments, eventually clinical trials could be performed in follicular lymphoma patients who, by sequencing, are shown to harbor these mutations in their tumors. The discovery of these mTORC1-activating, recurrent mutations in *RRAGC* in follicular lymphoma further suggests the importance of the nutrient sensing pathway in tumorigenesis, and indicates a promising set of therapies that may be effective for these patients.

### **Amino acid sensing by the mTORC1 pathway**

Our characterization of Sestrin2 as a leucine sensor for the mTORC1 pathway represents an exciting advance in the field. First, the identify of the leucine sensor had



been long sought, and now a variety of interesting questions remain to further understand how amino acids are sensed. In addition, Sestrin2 was the first bona fide amino acid sensor identified for the mTORC1 pathway, and thus our characterization set a paradigm for future studies.

It had long been recognized that the pathway is sensitive to multiple amino acids, including principally leucine and arginine. How these distinct amino acids were directly sensed remained a mystery for many years: was there one amino acid sensor that non-specifically bound to these separate classes of amino acids, or were there multiple sensors? Now, with the identification of SLC38A9 as a putative lysosomal arginine sensor, and Sestrin1/2 and CASTOR1 as cytosolic leucine and arginine sensors, respectively, it's clear that multiple separate sensors are coordinating mTORC1 activity in response to the various amino acid inputs (Chantranupong et al., 2016; Saxton et al., 2016a; Saxton et al., 2016b; Wang et al., 2015; Wolfson et al., 2016). Do other amino acid sensors exist? Perhaps different tissues are sensitive to distinct amino acids, and thus the expression of various sensors may vary across the body. Similarly, how the lysosomal and cytosolic inputs to these various amino acid sensors are coordinated remains unknown.

The identification of Sestrin2 as a leucine-binding protein allowed for our characterization of its affinity for leucine and other similar amino acids. As mentioned previously, Sestrin2 binds leucine with an affinity of ~20  $\mu$ M, which is similar to that of another cytosolic leucine-binding protein, LRS, which binds leucine with an affinity of ~45  $\mu$ M (Chen et al., 2011). Although this implies that the affinity of Sestrin2 for leucine is reasonable, to fully understand how amino acids are sensed it is essential to identify how amino acid concentrations in cells and *in vivo* fluctuate in response to environmental changes.

Recent advances in mass spectrometry have allowed for the accurate measurement of various metabolites. Using these metabolomics approaches it's now possible to rapidly isolate mitochondria and probe the concentrations of small molecules, including amino acids, within this organelle (Chen et al., 2016). While whole cell concentrations of metabolites can be measured as well, measuring the cytosolic amino acid concentrations presents a unique challenge, as estimating the cytosolic

volume is non-trivial. In addition, amino acids can exist in both free and bound pools within the cell, and those that are bound (specifically or non-specifically to proteins, lipids, or other molecules) are not available to bind to the amino acid sensors. However, both the free and bound pools would be measured by metabolomics, and thus accurately estimating the concentration of amino acids that are free and available to bind to the amino acid sensors remains a significant challenge. Finally, while it is clear how plasma amino acid concentrations fluctuate with changes in diet (Stegink et al., 1991; Stein and Moore, 1954), how the levels of these metabolites within tissues and within cells *in vivo* fluctuate is unknown.

### **Understanding the mechanism through which the Sestrins inhibit GATOR2**

Under leucine deprivation conditions, Sestrin2, a negative regulator of the mTORC1 pathway, binds GATOR2 and likely inhibits its function (Chantranupong et al., 2014; Wolfson et al., 2016). The mechanism through which Sestrin2 inhibits the pathway, however, awaits the characterization of the molecular function of GATOR2. It's clear that GATOR2 is a positive regulator of the pathway, as loss of its components render the mTORC1 pathway inhibited regardless of amino acid availability (Bar-Peled et al., 2013). Further, GATOR2 is epistatic to GATOR1 implying that it functions either upstream or parallel to its interacting partner. Interestingly, our recent work characterizing KICSTOR reveals that GATOR1 but not GATOR2 localization to the lysosomal surface is disrupted in cells deficient for KICSTOR components, implying that GATOR2 is targeted to the lysosomal surface in a separate process from that of GATOR1 (Wolfson et al, 2017). Understanding how GATOR2 is targeted to this compartment may reveal other interacting partners of this complex within the pathway, perhaps giving insight into its molecular function.

### **Regulation and function of the KICSTOR complex**

Our identification of a four-membered protein complex that targets GATOR1 to the lysosomal surface and is a negative regulator of the nutrient sensing pathway raises

many unanswered questions. Consistent with its role as a scaffold, one component of the complex, SZT2, which links the other three to GATOR1, is ~380 kilodaltons. However, while the other three components also seem necessary for the lysosomal targeting of GATOR1, these proteins are each only ~50 kilodaltons, and likely do not act as large scaffolding proteins on the lysosomal surface, like SZT2. Thus, it's intriguing to hypothesize that perhaps these proteins serve some other role in the pathway, as well. Sequence analysis, however, does not reveal any obvious domains, and so further work will be needed to uncover if members of the KICSTOR complex have any function beyond targeting GATOR1 to the lysosomal surface.

In addition, while loss of KICSTOR renders cells insensitive to amino acid or glucose, but not growth factor, deprivation, whether any of these nutrient inputs feeds in specifically upstream of KICSTOR is unknown. How is the KICSTOR complex regulated? Are there other inputs, beyond nutrient deprivation, that regulate this complex? IP/MS analysis of this complex may reveal interesting interacting partners, and could help to elucidate how and if KICSTOR is regulated.

### **mTOR inhibitors as therapy for epilepsy patients**

Families with mutations in either *SZT2* or *KPTN* or loss of the genomic locus containing *C12orf66* are prone to develop seizures or brain malformation disorders (Baple et al., 2014; Basel-Vanagaite et al., 2013; Mc Cormack et al., 2015; Venkatesan et al., 2016). Our work identifying KICSTOR as an mTORC1 regulator hints that these patients may be experiencing epilepsy due to deregulation of mTORC1 signaling in neurons. This is consistent with many other regulators of the mTORC1 pathway that are mutated in epilepsy and brain malformation disorders, including GATOR1 (Baulac, 2016). Further, we show that mTORC1 signaling is indeed increased in neurons in the brains of mice in which *Szt2* is disrupted by a gene-trap. This work implies that rapalogs or other mTOR inhibitors may be effective therapies for epilepsy patients that harbor mutations in KICSTOR components. Additionally, sequencing efforts in patients with these disorders may identify more patients with KICSTOR mutations, including in sporadic disease.

## References

- Baple, E.L., Maroofian, R., Chioza, B.A., Izadi, M., Cross, H.E., Al-Turki, S., Barwick, K., Skrzypiec, A., Pawlak, R., Wagner, K., *et al.* (2014). Mutations in KPTN cause macrocephaly, neurodevelopmental delay, and seizures. *Am J Hum Genet* 94, 87-94.
- Bar-Peled, L., Chantranupong, L., Cherniack, A.D., Chen, W.W., Ottina, K.A., Grabiner, B.C., Spear, E.D., Carter, S.L., Meyerson, M., and Sabatini, D.M. (2013). A Tumor suppressor complex with GAP activity for the Rag GTPases that signal amino acid sufficiency to mTORC1. *Science* 340, 1100-1106.
- Basel-Vanagaite, L., Hershkovitz, T., Heyman, E., Raspall-Chaure, M., Kakar, N., Smirin-Yosef, P., Vila-Pueyo, M., Kornreich, L., Thiele, H., Bode, H., *et al.* (2013). Biallelic SZT2 mutations cause infantile encephalopathy with epilepsy and dysmorphic corpus callosum. *Am J Hum Genet* 93, 524-529.
- Baulac, S. (2016). mTOR signaling pathway genes in focal epilepsies. *Prog Brain Res* 226, 61-79.
- Chantranupong, L., Scaria, S.M., Saxton, R.A., Gygi, M.P., Shen, K., Wyant, G.A., Wang, T., Harper, J.W., Gygi, S.P., and Sabatini, D.M. (2016). The CASTOR Proteins Are Arginine Sensors for the mTORC1 Pathway. *Cell* 165, 153-164.
- Chantranupong, L., Wolfson, R.L., Orozco, J.M., Saxton, R.A., Scaria, S.M., Bar-Peled, L., Spooner, E., Isasa, M., Gygi, S.P., and Sabatini, D.M. (2014). The Sestrins interact with GATOR2 to negatively regulate the amino-acid-sensing pathway upstream of mTORC1. *Cell Rep* 9, 1-8.
- Chen, W.W., Freinkman, E., Wang, T., Birsoy, K., and Sabatini, D.M. (2016). Absolute Quantification of Matrix Metabolites Reveals the Dynamics of Mitochondrial Metabolism. *Cell* 166, 1324-1337.e1311.
- Chen, X., Ma, J.-J., Tan, M., Yao, P., Hu, Q.-H., Eriani, G., and Wang, E.-D. (2011). Modular pathways for editing non-cognate amino acids by human cytoplasmic leucyl-tRNA synthetase. *Nucleic acids research* 39, 235-247.
- Mc Cormack, A., Sharpe, C., Gregersen, N., Smith, W., Hayes, I., George, A.M., and Love, D.R. (2015). 12q14 Microdeletions: Additional Case Series with Confirmation of a Macrocephaly Region. *Case Rep Genet* 2015, 192071.
- Okosun, J., Wolfson, R.L., Wang, J., Araf, S., Wilkins, L., Castellano, B.M., Escudero-Ibarz, L., Al Seraihi, A.F., Richter, J., Bernhart, S.H., *et al.* (2016). Recurrent mTORC1-activating RRAGC mutations in follicular lymphoma. *Nat Genet* 48, 183-188.
- Proud, C. (1986). Guanine nucleotides, protein phosphorylation and the control of translation. *Trends in Biochemical Sciences*.

Saxton, R.A., Chantranupong, L., Knockenhauer, K.E., Schwartz, T.U., and Sabatini, D.M. (2016a). Mechanism of arginine sensing by CASTOR1 upstream of mTORC1. *Nature* 536, 229-233.

Saxton, R.A., Knockenhauer, K.E., Wolfson, R.L., Chantranupong, L., Pacold, M.E., Wang, T., Schwartz, T.U., and Sabatini, D.M. (2016b). Structural basis for leucine sensing by the Sestrin2-mTORC1 pathway. *Science* 351, 53-58.

Stegink, L.D., Filer, L.J., Brummel, M.C., Baker, G.L., Krause, W.L., Bell, E.F., and Ziegler, E.E. (1991). Plasma amino acid concentrations and amino acid ratios in normal adults and adults heterozygous for phenylketonuria ingesting a hamburger and milk shake meal. *Am J Clin Nutr* 53, 670-675.

Stein, W.H., and Moore, S. (1954). The free amino acids of human blood plasma. *J Biol Chem* 211, 915-926.

Venkatesan, C., Angle, B., and Millichap, J.J. (2016). Early-life epileptic encephalopathy secondary to SZT2 pathogenic recessive variants. *Epileptic Disord* 18, 195-200.

Wang, S., Tsun, Z.-Y., Wolfson, R.L., Shen, K., Wyant, G.A., Plovanich, M.E., Yuan, E.D., Jones, T.D., Chantranupong, L., Comb, W., *et al.* (2015). Metabolism. Lysosomal amino acid transporter SLC38A9 signals arginine sufficiency to mTORC1. *Science* 347, 188-194.

Wolfson, R.L., Chantranupong, L., Saxton, R.A., Shen, K., Scaria, S.M., Cantor, J.R., and Sabatini, D.M. (2016). Sestrin2 is a leucine sensor for the mTORC1 pathway. *Science* 351, 43-48.

Wolfson, R.L., Chantranupong, L., Wyant, G.A., Gu, X., Orozco, J.M., Shen, K., Condon, K.J., Petri, S., Kedir, J., Scaria, S.M., Abu-Remaileh, M., Frankel, W.N., and Sabatini, D.M. (2017). KICSTOR recruits GATOR1 to the lysosome and is necessary for nutrients to regulate mTORC1. *Nature*, in press.